ESTIMATING FOREST ATTRIBUTES FROM SPHERICAL IMAGES

by

Haozhou WANG

Bachelor of Ecology, Nanjing Forestry University, 2017

A Thesis Submitted in Partial Fulfillment
of the Requirements for the Degree of

Master of Science in Forestry

in the Graduate Academic Unit of Faculty of Forestry and Environmental Management

This thesis is accepted by the
Dean of Graduate Studies

THE UNIVERSITY OF NEW BRUNSWICK

December, 2019

Abstract

Forest attribute estimation is fundamental in forest inventory and management, but is often time-consuming and labor intensive using traditional measurement methods. A consumer-level spherical camera (Ricoh Theta S) which can obtain panoramic photos from single exposures controlled by a smart phone, shows great potential to make forest inventories more efficient. In this study, the spherical camera was used in estimating stand basal area, canopy structural fractions, and individual tree diameters and heights. Our results showed good correspondence (high r^2 and low rMSE) between image measured values and field measured values in most cases by linear regression. Potential factors which may affect image estimation also were analyzed. We believe this low-cost system could make some contributions to forest operations and more efficient forest management.

Acknowledgement

A long time and many detours were taken that brought me to this point. I believe the project could have more depth if less time was wasted at various twists, however, without these twists, fewer lessons would have been learned during my graduate studies. Thanks to the UNB/NFU 3+1+1 program for providing me a chance to accomplish my graduate studies in Canada. What is more, this project would not be accomplished without the help of some individuals. First of all, I would like to thank Dr. John Kershaw who got me started, patiently and responsibly guided the whole journey of this project. Specially, I would like to thank Dr. Lavigne Mike who funded me through my toughest two seasons. Also, Dr. Lloyd Waugh and Jae Ogilvie who served on my committee, and Goodine Gretta who helped me with image processing and technical problems. Thank you to my lab mates and field assistant students who helped me collect field measurement data in Newfoundland and the Noonan Research Forest: Ting-Ru Yang, Yung-Han Hsu, Yang Zhan, Yingbing Chen, Wushuang Li, Shun-Ying Chen, Xu Ma, and Emily Loretta Nicholson. Also, Zizhen Gao, Rongrong Gu, Luji Xiong, Xu Gong, Tiancheng Wu in the neighboring wood tech lab, as well as other friends in Fredericton who supported me a lot in my local life. Finally, I would like to thank my parents, Shiquan Wang and Chunyan Feng, for their understanding, patience, and economic support during my graduate studies.

Funding for this project was provided in part by the National Science and Engineering Research Council of Canada, Discovery Grants program, the Province of Newfoundland and Labrador Centre for Forest Science and Innovation Contribution

Agreement, and the New Brunswick Innovation Foundation Research Assistant's Initiative and Graduate Scholarships programs.

Table of Contents

List of Tables

List of Figures

List of Abbreviations

AA	Average accuracy
BA	Basal area, the cross-sectional area of tree trunk at breast height
BAF	Basal area factor
BC	Blue channel in RGB color space
BPF	Plant fraction by blue-channel classification algorithms
CFF	Foliage fraction by cylindrical approach (in Chapter 3)
CPF	Plant fraction by cylindrical approach (in Chapter 3)
CWF	Wood fraction by cylindrical approach (in Chapter 3)
DBH	Individual tree stem diameter at breast height (1.3m)
DSP	Digital sample point
EVI	Enhanced vegetation index
FBA	Field basal area
GF	Gap fraction
GPS	Global positioning system
HFF	Foliage fraction by hemispherical approach (in Chapter 3)
HPF	Plant fraction by hemispherical approach (in Chapter 3)
HWF	Wood fraction by hemispherical approach (in Chapter 3)
HPS	Horizontal point sampling
HSV	Hue, saturation, brightness (value) color space
HT	The total height of tree
LAI	Leaf area index
LiDAR	Light detection and ranging
LME	Linear mixed effect (models)
LOWESS	Locally weighted scatterplot smoothing
NDVI	Normalized difference vegetation index
NL	Newfoundland
NRF	Noonan Research Forest
OA	Overall accuracy
PA_i	Producer's accuracy of class *i*
PAI	Plant area index
PBA	Photo basal area
PF	Plant fraction
RAW	Raw image file (minimally processed data from the camera sensor)
RGB	Red, green, blue color space
rMSE	Root mean square error
SAVI	Soil-adjusted vegetation index
SfM	Structure from Motion
SI	The International system of units
TF	Tree factor or expansion factor
TLS	Terrestrial laser scanner
UAV	Unmanned aerial vehicles
VPS	Vertical point sampling

Chapter 1: General Introduction

1.1 Background

Forests are the dominant terrestrial ecosystem on Earth and account for over three quarters of the gross primary productivity of the biosphere and about 80% of plant biomass (Pan et al. 2013). They provide several ecosystem services including watershed protection, soil structure maintenance, and global carbon storage (Chazdon 2008). Due to the importance of forests, estimating complex forest conditions using easily-measured tree attributes is critical to forest inventory and management.

1.2 Tree Parameters

1.2.1 Individual tree parameters

Individual tree attributes are of great importance, because they are often the fundamental measures of area-based attribute estimates such as total volume and biomass which are difficult or even impossible to measure directly. Individual tree attributes often include age, stem diameter (cross-sectional areas), total height, merchantable height, main stem form, and crown parameters (Kershaw et al. 2016). Typically diameter at breast height (DBH; breast height (BH) = 1.3m) and total height (HT) are the most common individual tree attributes measured (Avery and Burkhart 2002), and are the fundamental parameters used in allometric equations to estimate biomass, volume, or carbon (Lambert et al. 2005, Xing et al. 2005, Zianis et al. 2005).

The definition of *tree diameter* is a straight line that passes through the tree center and meets each end of the tree bark (Kershaw et al. 2016). This attribute is important due to the ability to directly measure and the ability to derive other parameters such as cross-sectional area (basal area, BA), surface area, and trunk volume (Kershaw et al. 2016). Though which diameters should be measured vary with different circumstance, the diameter at breast height (1.3 m in SI units or 4.5 ft in imperial units) is widely used in North America (Kershaw et al. 2016). Traditionally, this attribute can be easily measured by contact dendrometers (Fig 1.1.a-d) such as diameter tape, Biltmore stick, calipers, and sector fork (Jackson 1911, Bower and Blocker 1966, Kershaw et al. 2016). Clark et al. (2000a) comprehensively reviewed various diameter measurement tools and their associated accuracies. In this review, he also pointed out that although these tools are very handy and have been widely used among researchers and forest managers, the reliability and subjectivity effects should be taken into consideration for large-scale inventory work.

Tree height has several definitions, including total height, bole height, merchantable height, stump height, and so on (Kershaw et al. 2016). Total height, which is defined as the vertical distance from the tip of tree to the ground, is commonly used. Traditionally, total height is measured from the ground based on similar triangles or trigonometry (Kershaw et al. 2016). Based on these principles, instruments such as the hypsometer, clinometer, and altimeter (Fig 1.1.e-i) accompanied with a measuring tape for horizontal distance were used in field measurement (Pardé 1955, Wesley 1956, Curtis and Bruce 1968, Iles and Fall 1988, Kershaw et al. 2016). But with the development of technology, several advanced electronic hypsometers (Fig 1.1.j) which use laser or ultrasonic sound waves to measure distances precisely are available with the disadvantage of a high price (US$800-US$3000) and bulkiness (Kershaw et al. 2016).

1.2.2 Stand structure parameters

Stand-level attributes such as basal area per ha, volume per ha, and biomass per ha are usually estimated by summing individual tree values and applying the appropriate expansion factors to scale from plot to per unit area (Kershaw et al. 2016). For stand crown and canopy measurement, attributes such as crown closure, canopy cover, and leaf area index are often measured at the stand level rather than summarized from individual tree measurements (Kershaw et al. 2016).

Stand basal area, defined as the sum of individual tree cross-sectional areas, is one of the most common stand-level parameters estimated in most forest inventories (Iles 2003, Kershaw et al. 2016). Basal area is often expressed at breast height, and is an important measure of stand density that incorporates tree size as well as number (Kershaw et al. 2016). It is a fundamental component of volume and biomass calculations (Iles 2003, Jenkins et al. 2003, Lambert et al. 2005, Slik et al. 2010) and is an important stand characteristic for forest growth models (Opie 1968, Lootens et al. 2007, Weiskittel et al. 2011). Stand basal area can be derived by summarizing the DBH of all trees in fixed-area plots, or can be calculated using horizontal point sampling by counting the numbers of trees that subtend a projected horizontal angle and multiplying by a constant without measuring any DBHs (Kershaw et al. 2016). Horizonal point sampling typically uses tools such as an angle gauge, relascope, or prism (Fig 1.2.a-c) to decide which trees are counted. The theory of this sampling method will be discussed in Section 1.3.2.

There are several canopy attributes such as gap fraction, canopy cover, canopy closure, canopy openness, and so on. These attributes are similar but slightly different concepts that need to be clarified (Gonsamo et al. 2013).

Gap fraction (GF, or P_0), defined as "the area fraction of open sky not obstructed by canopy elements over the limited area defined by specific view zenith (θ) and azimuth (Φ) angles" (Gonsamo et al. 2013), The key point of the GF definition is the limited area fraction defined by specific view angles. Commonly, the GF or P_0 should include two subscripts: GF (θ, Φ) or P_0 (θ, Φ). When the azimuth angle is not given, GF (θ) or P_0 (θ) represent the gap proportion in a narrow ring area at that zenith angle (Jonckheere et al. 2005, Pekin and MacFarlane 2009).

Canopy cover is the proportion of canopy elements vertically projected onto the ground (Gonsamo et al. 2013). This measurement is easy to measure from a vertical direction, and is commonly measured using satellite, airborne, or unmanned aerial vehicle (UAV) images.

Canopy openness is defined as "the area fraction of the sky hemisphere (180°) that is unobstructed by canopy elements when viewed from a single point" (Gonsamo et al. 2013). The key point of canopy openness is the full sky hemisphere (180°). Canopy openness can be simply calculated from the sky pixels versus total pixel numbers in classified binary images.

Canopy closure, defined as the complement of canopy openness (1 – canopy openness), ideally it is expressed using the whole hemisphere, however, closure measurements are often restricted by selected zenith angles because horizon gaps and canopy elements are hard to measure (Gonsamo et al. 2013). Canopy closure often is the same definition as *plant fraction*, which is used in this study, and a restricted zenith angle of 57.5° is often used. Lemmon (1956, 1957) first developed a method to measure plant fraction using a spherical densiometer (Fig 1.2.d) which is a curved mirror with a grid, and counting the number of grids containing plants divided by the total grid number. Photographic techniques with high-quality digital images provide a much more accurate and repeatable measure than traditional grid counting (Kershaw et al. 2016). This image-based method is sensitive to thresholding which separates the image pixels into sky and other components.

Leaf area index (LAI) is the total foliage area (one-sided projection area) in a unit area (Kershaw et al. 2016), the units are $m^2 \cdot m^{-2}$ or $m^2 \cdot ha^{-1}$. This parameter shows a strong linear relationship with stem wood and total biomass production (Waring et al. 1981, Oren et al. 1987, Vose and Allen 1988). The direct method to estimate LAI requires destructive sampling: felling individual trees and weighing the foliage in lab (Kershaw et al. 2016). This method is not only labor intensive, but also has effects on the remaining stand. Indirect methods such as allometric regression relationships, litterfall traps (Fig 1.2.e), and indirect noncontact methods have theoretical, practical, or methodological challenges (Larsen and Kershaw 1990, Weiss et al. 2004, Jonckheere et al. 2004). Alternatively, hemispherical photographic methods (Fig 1.2.f) are widely used in forest LAI estimates (MacFarlane et al. 2007a, Liu et al. 2013, Fournier and Hall 2017). These methods employ simple models of forest canopy radiation transfer, along with image processing and the relationship between gap fraction and zenith angle to estimate LAI (Rich 1990, Weiss et al. 2004).

1.3 Sampling Strategies for Parameters

Measuring the attributes of all individual trees in a stand or forest area should be the most accurate method to evaluate forest conditions, ideally. However, obviously, it is quite labor intensive and time consuming, also it is not applicable for large scale forest inventories. The most common practice is using *sample plots*, which are defined as the units for recording information and measurements (Kershaw et al. 2016). Basic sampling strategies can be divided into two main categories: equal probability and variable probability.

1.3.1 Equal probability

The most common sample plot has been a unit of fixed area for many years, and these fixed-area sampling units are often small areas of square, rectangular, circular, or triangular shape (Kershaw et al. 2016). A plot center is set in a forest, and based on this center, a boundary of fixed-area, shape, and orientation determined. Each tree meeting some defined height or diameter criteria included within the boundary is selected and measured.

Alternatively, each tree can be thought to have its own inclusion zone which is the same size, shape, and orientation as the fixed-area boundary, just centered on each tree. A sample point (plot center) is set in the forest, and those trees whose inclusion zones include the plot center are selected and measured (Fig 1.3.a&b). In this procedure, the probability of selection is the same for all individual trees because their inclusion zones are all the same size (Kershaw et al. 2016), and therefore, their probabilities of selection are equal.

Circular plots, which use a radius as a single dimension to define the boundary, have been widely used (Kershaw et al. 2016). In this plot type, the inclusion zone of each individual tree has the same radius as the plot radius (Fig 1.3.a). The main advantages of circular plots are: 1) The length of boundary is the minimum of all shapes with the same area. It implies fewer decisions to judge trees near the boundary. 2) Unlike rectangle or strip plots, circular plots have no predetermined orientation. and 3) They are the simplest for correcting slopover bias, which caused by the inclusion zone of one tree partly falls outside the plot center. The main disadvantage is the difficulties associated with carefully determining distances from trees to plot center without the assistance of modern ultrasonic or laser distance measuring tools (Kershaw et al. 2016). Unlike circular plots, *square or rectangular plots* are much easier to decide in or out due to the straight-line boundary, also these straight boundaries can be easily marked by compass and tape (Kershaw et al. 2016). But laying out the plot corners and boundaries carefully and the orientation effects should be taken into consideration when analyzing bias (Kershaw et al. 2016).

The fixed-area plot also has limitations. Normally, in the east coast of the North America, there are many more small trees than large ones in natural forests. Due to the equal probability, there tends to be many small trees selected in this sampling method. However, compared with large trees, when measuring volume, biomass, or carbon storage, small trees are less proportionally of lower influence or consequence, but are measured many more times than large trees (Kershaw et al. 2016). To solve this problem, different sizes of plots for different sized vegetation can be used. For example, Van Den Meersschaut and Vandekerkhove (2000) used four concentric circular plots with 4 different areas to measure: seedlings (16 m^2), shrubs (64 m^2), living trees (255 m^2), dead trees (1018 m^2), and lesser vegetation and lying deadwood (16 m$\times$16 m). While this is still considered fixed area plot sampling, it is really an intermediate step between equal probability sampling and variable probability sampling (Section 1.3.2) and can be quite cumbersome to implement in the field.

1.3.2 Variable probability

While using concentric plots is one method to solve the problem of oversampling certain classes of vegetation, using a sampling procedure in which the probability of selecting a tree depends on some tree character (e.g. DBH or HT) is also possible (Kershaw et al. 2016). In this situation, larger trees have larger inclusion zones while smaller trees have smaller zones (Fig 1.3.c), which means, the probability of selecting a tree is proportional to its size (Kershaw et al. 2016). Variable probability is a very efficient sampling scheme; however, because there is high variance in counts of trees between points, sample sizes are often much higher than when using fixed area plots (Iles 2003, Kershaw et al. 2016, Yang et al. 2017). As a result, various subsampling schemes have been developed to reduce the point and tree measurements (Grosenbaugh 1963a, Iles 2003, Marshall et al. 2004, Yang et al. 2017). Variable probability selection can be applied to trees, sample points, and even stands (Kershaw et al. 2016); however, one of the limitations of variable probability sampling is identification of an appropriate covariate for selection (Hsu et al. In Review).

Horizontal Point Sampling, is the most used application of variable probability sampling and was originally developed by Bitterlich (1947). It is also called *angle count sampling* because an angle is used to select trees proportional to their basal area (Bitterlich 1947, 1984). In this method, the observer occupies the point (plot center) and a horizontal angle (often created by tools shown in Fig 1.2.a-c) is projected towards each tree at DBH level (Fig 1.4.a). All trees that are as large as or larger than the projected horizontal angles are counted.

1.3.3 Stand basal area estimates by variable probability

In most forest inventory data analyses, measurements are summarized and divided by the total plot size to express values on a per unit area basis (Kershaw et al. 2016). The ratio of each selected tree scaled to per unit area measurement is called the tree factor or expansion factor (Kershaw et al. 2016). For each tree:

$$TF_i = \frac{Unit\ Area}{Inclusion\ zone\ area_i} \tag{1.1}$$

where TF$_i$ is the tree factor of sample tree *i*, unit area is 10000 m^2, inclusion zone area$_i$ is the inclusion zone area of sample tree *i* in the same units as Unit Area.

Tree factor can then be used to expand specific tree attributes (Attribute Factor, XF$_i$) to stand or forest level attributes by simply multiplying the value of that attributes (X$_i$) by tree factor (TF$_i$):

$$XF_i = X_i \cdot TF_i \tag{1.2}$$

The stand attribute value equals the sum of all selected trees:

$$X_{stand} = \sum_{i=1}^{n} XF_i = \sum_{i=1}^{n} X_i \cdot TF_i \tag{1.3}$$

e.g. Stand Basal Area

$$BA_{stand} = \sum_{i=1}^{n} BAF_i = \sum_{i=1}^{n} BA_i \cdot TF_i \tag{1.4}$$

Combined with Eq. (1.1):

$$BA_{stand} = \sum_{i=1}^{n} BA_i \cdot \frac{Unit\ Area}{Inclusion\ Zone\ Area_i}$$

Individual tree, basal area is calculated using (Fig 1.4.c):

$$BA_i = \pi \cdot r_i^2 \tag{1.5}$$

where the r*i* is the radius of tree trunk at breast height and equals half of DBH.

The relationship between inclusion zone area and horizontal angle (θ) is shown in Fig 1.4.c:

$$\frac{r_i}{R_i} = \sin\left(\frac{\theta}{2}\right) \Rightarrow R_i = \frac{r_i}{\sin\left(\frac{\theta}{2}\right)} \tag{1.6}$$

where R*i* is the radius of the inclusion zone for a specific tree.

So, combined with Eq. (1.5) and Eq. (1.6), stand basal area equals

$$BA_{stand} = \sum_{i=1}^{n} (\pi \cdot r_i^2) \cdot \frac{10000\ m^2}{\pi \cdot R_i^2} = \sum_{i=1}^{n} \pi \cdot r_i^2 \cdot \frac{10000\ m^2}{\pi \cdot \frac{r_i^2}{\sin^2\left(\frac{\theta}{2}\right)}} = \sum_{i=1}^{n} 10000\ m^2 \cdot \sin^2\left(\frac{\theta}{2}\right)$$

Since the projected horizontal angle (θ) is constant, BAF*i* which equals $10000\ m^2 \cdot \sin^2(\frac{\theta}{2})$ is constant. Thus, the stand basal area is estimated by counting the number of selected trees and multiplying by BAF*i*. No tree measurements are required to estimate stand basal area per ha (Kershaw et al. 2016).

1.4 Remote Sensing Technologies

1.4.1 Above canopy remote sensing

Above canopy remote sensing techniques, e.g. satellite, manned aircraft, and unmanned aerial vehicles (UAV), are applied in forest inventory to save time and workloads for large-scale investigations.

Satellite remote sensing is a mature technology for large scale investigation, it can be applied for estimating biomass, leaf area, land-cover classification, and deforestation monitoring (Tucker et al. 1985, Running et al. 1986, Skole and Tucker 1993, Lu 2006, Jin et al. 2014). The most common method for these applications is using different vegetation indices such as normalized difference vegetation index (NDVI), soil-adjusted vegetation index (SAVI), enhanced vegetation index (EVI), and so on to represent plant or environmental conditions (Major et al. 1990, Nagler et al. 2005). However, limited by the low spatial resolution, cloud contamination, and overpass period, it is difficult for conventional satellite remote sensing techniques to estimate individual tree information which match with the detailed data measured during ground investigations (Turner et al. 2012).

Airborne remote sensing has been developed for many years (Reeves 1936, Colwell 1964). Airborne images are no longer limited to sensors in the visible spectrum, but also can use infrared, laser (LiDAR), ultrasonic (radar), and even hyperspectral (Kasischke et al. 1997, Asner et al. 2007, Smith et al. 2010). Several attributes such as canopy height (Paine and Kiser 2012), species detection (Junttila and Kauranne 2012), canopy diversity (Asner and Martin 2009, Asner et al. 2017), and above ground biomass (Lefsky et al.

2002, Meyer et al. 2013, Hayashi et al. 2015) can be estimated using this technology. However, manned aircraft is limited by flight route control in some areas and the sensors often have a very high investment cost, thus high costs for airborne imaging.

This big challenge is partially resolved by *unmanned aerial vehicle* (UAV) *remote sensing*, which is an emerging tool to provide timely, lower-cost, and high resolution means of investigation (Anderson and Gaston 2013). Several studies demonstrate the possibility of using high resolution UAV images to extract individual tree heights and crown coverages by structure from motion (SfM) techniques (Turner et al. 2012, Dandois and Ellis 2013, Wallace et al. 2016). Also the vegetation structure and functional properties can be extracted to explore biodiversity (Getzin et al. 2011, Hoffmann et al. 2016). However, many of these approaches require high-performance-computers for indoor 3D point cloud reconstruction and data analysis, driving up the costs and time required to complete inventories. The canopy makes extracting tree trunk attributes hard when using visible spectrum sensors. Though radio and laser sensor techniques make penetration of canopies easier (Wallace et al. 2016, Asner et al. 2017), the high prices of these sensors limit wide spread use. Also, the scale at which a UAV sample can be efficiently processed is generally too small for a woodlot-scale inventory.

Above canopy remote sensing has saved a large amount of labor and makes large scale forest investigations possible. However, collecting under canopy forest attributes data for validation cannot be avoided.

1.4.2 Below canopy remote sensing

For under canopy data collection, there are also some novel indirect optical remote sensing tools. Some of the simpler tools were introduced in Section 1.2, some other self-made and minority instruments such as TRAC and MVI (for PAI/LAI measurement), DEMON (for beam transmission), spherical densiometer (for forest canopy parameters), and Moosehorn (for crown closure) are seldomly used in practice (Seidel et al. 2011). The most popular optical methods includes hemispherical (fisheye) cameras (MacFarlane et al. 2007b, Jonckheere et al. 2009, Brandão et al. 2016), laser scanners (Lefsky et al. 2002, Seidel et al. 2012, Hayashi et al. 2015), and digital cameras (Lati et al. 2011, Maynard et al. 2014, Inoue et al. 2015).

Hemispherical photographs have been used to estimate crown and canopy parameters, such as gap fraction, foliage cover, and leaf area index for many years (Demarez et al. 2008, Zhao et al. 2012). Though many software and algorithms have been developed to analyze fisheye images (van Gardingen et al. 1999, Lang and Yueqin 1986, Montes et al. 2007, Seidel et al. 2011), the high price of traditional hemispherical cameras make consumer-grade digital cameras more and more popular for different aspects of forest measuring (Frazer et al. 2001).

Terrestrial (ground-based) laser scanner (TLS) is an optical method which has the ability to record 3D point cloud information of the forest structure. Several studies have used this novel tool to estimate biomass and canopy metrics (Hilker et al. 2010, Holopainen et al. 2011, Wallace et al. 2017). Directly using the point cloud 3D information to calculate biomass by counting plant voxel volume is another approach (Seidel et al. 2012). However, the high price of laser scanners (50 to 80 times the price of a fisheye camera) (Seidel et al. 2011) accompanied by the long scanning times, difficulties in analyzing point clouds, and high computer hardware performance requirements significantly limits wide spread use.

Using *consumer-grade digital cameras* to extract tree attributes has been developed over decades including measuring upper stem diameters (Grosenbaugh 1963b), heights (Clark et al. 2000b), and even generating 3D stem models (Larsen 2006, Mokroš et al. 2018). These studies pay more attention to photographing single trees, which is not so useful for estimating attributes of a large cluster of trees (Perng et al. 2018). Merging 360 degrees photos into panoramic images to get cluster attributes such as basal area is a method reported by many researchers (Fastie 2010, Dick et al. 2010), but it only contains horizontal information and sloped terrain makes the center of image not exactly breast height (Perng et al. 2018).

The new 360° spherical cameras offer an inexpensive option for obtaining inventory covariates and potentially obtaining direct stand and tree measurements. The compact size of a spherical camera makes it an easy-to-use tool in the forest and can be moved through the canopy to obtain structural estimates more easily than traditional fisheye cameras and other digital cameras.

1.5 Objectives

This project has three main objectives. The first one will use the horizontal part of spherical images to extract stand basal area. The second part will extract forest canopy attributes in the vertical projection of spherical images. The last objectives will be to extract individual tree attributes from two spherical images taken at different heights. The specific objectives are as follows:

1. Using spherical images for image-based angle count sampling to estimate stand basal area and analyze effects of potential vegetation and stand structure factors that might limit generalization of this techinique.

2. Developing a novel HSV classification threshold to classify transformed or original spherical images and to estimates plant fractions, stem fractions, foliage fractions, etc. and compare the results with traditional fisheye classification algorithm (blue channel classification).

3. Using paired spherical images at two different heights, to extract individual tree DBH and height; the results will be compared with field measurements obtained in an urban setting and across an early spacing trial for a real forest comparison.

A framework that enables using spherical images to extract common forest attributes will be developed in this project. The outcomes include several applications for Microsoft windows for each objective respectively. This framework will provide the opportunity to increase the efficiency in the field, reduce measurement errors and ensure data consistency in long-term investigations.

1.6 Thesis Structure

The structure of this thesis is around five chapters to cover the objectives mentioned above. This chapter (Chapter 1) is a general introduction chapter. Chapter 2, *Estimating Forest Basal Area from Spherical Images* demonstrates how spherical images can be used to conduct horizontal point sampling for stand basal area attributes (Chapter 2 is accepted for publication in Mathematical and Computational Sciences in Forestry and Natural Resources). Chapter 3, *Plant Fraction Calculation from Spherical Images by HSV Color Space* demonstrates how spherical images can be used to estimate fisheye camera attributes in an automatic way. Chapter 4, *Estimating Individual Tree Diameters and Heights with Spherical Images* demonstrates how spherical images can be used to extract individual tree attributes. The concluding Chapter 5 summarizes the results of this project and future developments to extend the project direction.

1.7 References

Anderson, K., and K. J. Gaston. 2013. Lightweight unmanned aerial vehicles will revolutionize spatial ecology. Frontiers in Ecology and the Environment 11:138–146.

Asner, G. P., D. E. Knapp, T. Kennedy-Bowdoin, M. O. Jones, R. E. Martin, J. Boardma, and C. B. Field. 2007. Carnegie Airborne Observatory: in-flight fusion of hyperspectral imaging and waveform light detection and ranging for three-dimensional studies of ecosystems. Journal of Applied Remote Sensing 1(1):013536.

Asner, G. P., and R. E. Martin. 2009. Airborne spectranomics: mapping canopy chemical and taxonomic diversity in tropical forests. Frontiers in Ecology and the Environment 7:269–276.

Asner, G. P., R. E. Martin, D. E. Knapp, R. Tupayachi, C. B. Anderson, F. Sinca, N. R. Vaughn, and W. Llactayo. 2017. Airborne laser-guided imaging spectroscopy to map forest trait diversity and guide conservation. Science 355:385–389.

Avery, T. E., and H. E. Burkhart. 2002. Forest measurements. Fifth. McGraw-Hill, New York.

Bitterlich, W. 1947. Die winkelzählmessung (Measurement of basal area per hectare by means of angle measurement.). Allgemeine Forst- und Holzwirtschaftliche Zeitung 58:94–96.

Bitterlich, W. 1984. The relascope idea: Relative measurements in forestry. First. CAB International, Slough, England.

Bower, D. R., and W. W. Blocker. 1966. Accuracy of bands and tape for measuring diameter increments. Journal of Forestry 64:21–22.

Brandão, Z. N., J. H. Zonta, Z. N. Brandão, and J. H. Zonta. 2016. Hemispherical photography to estimate biophysical variables of cotton. Revista Brasileira de Engenharia Agrícola e Ambiental 20:789–794.

Chazdon, R. L. 2008. Beyond Deforestation: Restoring Forests and Ecosystem Services on Degraded Lands. Science 320:1458–1460.

Clark, N. A., R. H. Wynne, and D. L. Schmoldt. 2000a. A review of past research on dendrometers. Forest Science 46:570–576.

Clark, N. A., R. H. Wynne, D. L. Schmoldt, and M. Winn. 2000b. An assessment of the utility of a non-metric digital camera for measuring standing trees. Computers and Electronics in Agriculture 28:151–169.

Colwell, R. N. 1964. Aerial Photography - a Valuable Sensor for the ScientistT. American Scientist 52:17–49.

Curtis, R. O., and D. Bruce. 1968. Tree heights without a tape. Journal of Forestry 66:60–61.

Dandois, J. P., and E. C. Ellis. 2013. High spatial resolution three-dimensional mapping of vegetation spectral dynamics using computer vision. Remote Sensing of Environment 136:259–276.

Demarez, V., S. Duthoit, F. Baret, M. Weiss, and G. Dedieu. 2008. Estimation of leaf area and clumping indexes of crops with hemispherical photographs. Agricultural and Forest Meteorology 148:644–655.

Dick, A. R., J. A. Kershaw, and D. A. MacLean. 2010. Spatial Tree Mapping Using Photography. Northern Journal of Applied Forestry 27:68–74.

Fastie, C. L. 2010. Estimating stand basal area from forest panoramas. Proceedings of the Fine International Conference on Gigapixel Imaging for Science. Carnegie Mellon University, Pittsburg, PA. 4(8).

Fournier, R. A., and R. J. Hall, editors. 2017. Hemispherical Photography in Forest Science: Theory, Methods, Applications. Springer Netherlands.

Frazer, G. W., R. A. Fournier, J. A. Trofymow, and R. J. Hall. 2001. A comparison of digital and film fisheye photography for analysis of forest canopy structure and gap light transmission. Agricultural and Forest Meteorology 109:249–263.

van Gardingen, P. R., G. E. Jackson, S. Hernandez-Daumas, G. Russell, and L. Sharp. 1999. Leaf area index estimates obtained for clumped canopies using hemispherical photography. Agricultural and Forest Meteorology 94:243–257.

Getzin, S., K. Wiegand, and I. Schöning. 2011. Assessing biodiversity in forests using very high-resolution images and unmanned aerial vehicles. Methods in Ecology and Evolution 3:397–404.

Gonsamo, A., P. D'odorico, and P. Pellikka. 2013. Measuring fractional forest canopy element cover and openness – definitions and methodologies revisited. Oikos 122:1283–1291.

Grosenbaugh, L. R. 1963a. Some suggestions for better sample–tree measurement. Proceedings of the 1963 Society of American Foresters National Convention. Society of American Foresters. pp 36–42.

Grosenbaugh, L. R. 1963b. Optical dendrometers for out-of-reach diameters: A conspectus and some new theory. Forest Science Monographs 4(48).

Hayashi, R., J. A. Kershaw Jr., and A. R. Weiskittel. 2015. Evaluation of alternative methods for using LiDAR to predict aboveground biomass in mixed species and structurally complex forests in northeastern North America. Mathematical and Computational Forestry and Natural Resources Sciences 7:49–65.

Hilker, T., M. van Leeuwen, N. C. Coops, M. A. Wulder, G. Newnham, D. L. B. Jupp, and D. S. Culvenor. 2010. Comparing canopy metrics derived from terrestrial and airborne laser scanning in a Douglas-fir dominated forest stand. Trees, Structure and Function 24:819–832.

Hoffmann, H., R. Jensen, A. Thomsen, H. Nieto, J. Rasmussen, and T. Friborg. 2016. Crop water stress maps for an entire growing season from visible and thermal UAV imagery. Biogeosciences 13:6545–6563.

Holopainen, M., M. Vastaranta, V. Kankare, M. Räty, M. Vaaja, X. Liang, X. Yu, J. Hyyppä, H. Hyyppä, R. Viitala, and S. Kaasalainen. 2011. Biomass Estimation of Individual Trees Using STEM and Crown Diameter Tls Measurements. ISPRS -

International Archives of the Photogrammetry, Remote Sensing and Spatial Information Sciences 3812:91–95.

Hsu, Y.-H., T.-R. Yang, and Y. Chen. In Review. Sampling to correct LiDAR-assisted forest inventories. Forest Science.

Iles, K. 2003. A sampler of inventory topics. 2nd edition. Kim Iles and Associates, Nanaimo, BC.

Iles, K., and M. Fall. 1988. Can an angle gauge really evaluate “borderline trees” accurately in variable plot sampling? Canadian Journal of Forest Research 18:776–783.

Inoue, T., S. Nagai, H. Kobayashi, and H. Koizumi. 2015. Utilization of ground-based digital photography for the evaluation of seasonal changes in the aboveground green biomass and foliage phenology in a grassland ecosystem. Ecological Informatics 25:1–9.

Jackson, A. 1911. The Biltmore stick and its use on national forests. Journal of Forestry 9:406–411.

Jenkins, J. C., D. C. Chojnacky, L. S. Heath, and R. A. Birdsey. 2003. National scale biomass estimators for United States tree species. Forest Science 49:12–35.

Jin, Y., X. Yang, J. Qiu, J. Li, T. Gao, Q. Wu, F. Zhao, H. Ma, H. Yu, and B. Xu. 2014. Remote Sensing-Based Biomass Estimation and Its Spatio-Temporal Variations in Temperate Grassland, Northern China. Remote Sensing 6:1496–1513.

Jonckheere, I., L. Comita, J. Thompson, J. Zimmerman, M. Uriarte, and P. Coppin. 2009. Exploration of in-situ light and biomass estimation by digital hemispherical photography in tropical forests. 11, Page 12447.

Jonckheere, I., S. Fleck, K. Nackaerts, B. Muys, P. Coppin, M. Weiss, and F. Baret. 2004. Review of methods for in situ leaf area index determination: Part I. Theories, sensors and hemispherical photography. Agricultural and Forest Meteorology 121:19–35.

Jonckheere, I. G. C., B. Muys, and P. R. Coppin. 2005. Derivative analysis for in situ high dynamic range hemispherical photography and its application in forest stands. IEEE Geoscience and Remote Sensing Letters 2:296–300.

Junttila, V., and T. Kauranne. 2012. Evaluating the robustness of plot databases in species-specific light detection and ranging-based forest inventory. Forest Science 58:311–325.

Kasischke, E. S., J. M. Melack, and M. C. Dobson. 1997. The use of imaging radars for ecological applications—A review. Remote Sensing of Environment 59:141–156.

Kershaw, J. A., Jr., M. J. Ducey, T. W. Beers, and B. Husch. 2016. Forest Mensuration. 5th edition. Wiley/Blackwell, Hobokin, NJ.

Lambert, M.-C., C.-H. Ung, and F. Raulier. 2005. Canadian national tree aboveground biomass equations. Canadian Journal of Forest Research 35:1996–2018.

Lang, A. R. G., and X. Yueqin. 1986. Estimation of leaf area index from transmission of direct sunlight in discontinuous canopies. Agricultural and Forest Meteorology 37:229–243.

Larsen, D. R., and J. A. Kershaw Jr. 1990. The measurement of leaf area. Techniques in Forest Tree Ecophysiology. Lassoie, J. and T. Hinkley (eds.). CRC Press, Boca Raton, FL. pp. 465–475.

Larsen, D. R. 2006. Development of a photogrammetric method of measuring tree taper outside bark. Gen. Tech. Rep. SRS-92. Asheville, NC: U.S. Department of Agriculture, Forest Service, Southern Research Station. pp. 347-350.

Lati, R. N., S. Filin, and H. Eizenberg. 2011. Robust Methods for Measurement of Leaf-Cover Area and Biomass from Image Data. Weed Science 59:276–284.

Lefsky, M. A., W. B. Cohen, D. J. Harding, G. G. Parker, S. A. Acker, and S. T. Gower. 2002. Lidar remote sensing of above-ground biomass in three biomes. Global Ecology and Biogeography 11:393–399.

Lemmon, P. E. 1956. A spherical densiometer for estimating forest overstory density. Forest Science 2:314–320.

Lemmon, P. E. 1957. A new instrument for measuring over-story density. Journal of Forestry 55:667–669.

Liu, C., S. Kang, F. Li, S. Li, and T. Du. 2013. Canopy leaf area index for apple tree using hemispherical photography in arid region. Scientia Horticulturae 164:610–615.

Lootens, J. R., D. R. Larsen, and S. R. . Shifley. 2007. Height-diameter equations for 12 upland species in the Missouri Ozark Highlands. Northern Journal of Applied Forestry 24:1149–152.

Lu, D. 2006. The potential and challenge of remote sensing-based biomass estimation. International Journal of Remote Sensing 27:1297–1328.

MacFarlane, C., S. K. Arndt, S. J. Livesley, A. C. Edgar, D. A. White, M. A. Adams, and D. Eamus. 2007a. Estimation of leaf area index in eucalypt forest with vertical foliage, using cover and fullframe fisheye photography. Forest Ecology and Management 242:756–763.

MacFarlane, C., A. Grigg, and C. Evangelista. 2007b. Estimating forest leaf area using cover and fullframe fisheye photography: Thinking inside the circle. Agricultural and Forest Meteorology 146:1–12.

Major, D. J., F. Baret, and G. Guyot. 1990. A ratio vegetation index adjusted for soil brightness. International Journal of Remote Sensing 11:727–740.

Marshall, D. D., K. Iles, and J. F. Bell. 2004. Using a large-angle gauge to select trees for measurement in variable plot sampling. Canadian Journal of Forest Research 34:840–845.

Maynard, D. S., M. J. Ducey, R. G. Congalton, J. Kershaw, and J. Hartter. 2014. Vertical point sampling with a digital camera: Slope correction and field evaluation. Computers and Electronics in Agriculture 100:131–138.

Meyer, V., S. S. Saatchi, J. Chave, J. Dalling, S. Bohlman, G. A. Fricker, C. Robinson, and M. Neumann. 2013. Detecting tropical forest biomass dynamics from repeated airborne Lidar measurements. Biogeosciences 10:5421–5438.

Mokroš, M., J. Výbošťok, J. Tomaštík, A. Grznárová, P. Valent, M. Slavík, and J. Merganič. 2018. High Precision Individual Tree Diameter and Perimeter Estimation from Close-Range Photogrammetry. Forests 9(696).

Montes, F., P. Pita, A. Rubio, and I. Cañellas. 2007. Leaf area index estimation in mountain even-aged Pinus silvestris L. stands from hemispherical photographs. Agricultural and Forest Meteorology 145:215–228.

Nagler, P. L., R. L. Scott, C. Westenburg, J. R. Cleverly, E. P. Glenn, and A. R. Huete. 2005. Evapotranspiration on western U.S. rivers estimated using the Enhanced Vegetation Index from MODIS and data from eddy covariance and Bowen ratio flux towers. Remote Sensing of Environment 97:337–351.

Opie, J. E. 1968. Predictability of Individual Tree Growth Using Various Definitions of Competing Basal Area. Forest Science 14:314–323.

Oren, R., R. H. Waring, S. G. Stafford, and J. W. Barrett. 1987. Twenty-four years of ponderosa pine growth in relation to canopy leaf area and understory competition. Forest Science 33:538–547.

Paine, D. P., and J. D. Kiser. 2012. Aerial photography and image interpretation. 3rd edition. Wiley, New York.

Pan, Y., R. A. Birdsey, O. L. Phillips, and R. B. Jackson. 2013. The Structure, Distribution, and Biomass of the World's Forests. Annual Review of Ecology, Evolution, and Systematics 44:593–622.

Pardé, J. 1955. Le mouvement forestier à l'étranger. Un dendromètre pratique : le Dendromètre Blume-Leiss (The forest movement abroad. A practical dendrometer: the dendrometer Blume-Leiss). Revue Forestière Française 7:207–210.

Pekin, B., and C. MacFarlane. 2009. Measurement of Crown Cover and Leaf Area Index Using Digital Cover Photography and Its Application to Remote Sensing. Remote Sensing 1:1298–1320.

Perng, B.-H., T. Y. Lam, and M.-K. Lu. 2018. Stereoscopic imaging with spherical panoramas for measuring tree distance and diameter under forest canopies. Forestry: An International Journal of Forest Research 91:662–673.

Rich, P. M. 1990. Characterizing plant canopies with hemispherical photographs. Remote Sensing Reviews 5:13–29.

Reeves, D. M. 1936. Aerial Photography and Archaeology. American Antiquity 2:102–107.

Running, S. W., D. L. Peterson, M. A. Spanner, and K. B. Teuber. 1986. Remote sensing of coniferous forest leaf area. Ecology 67:273–276.

Seidel, D., S. Fleck, and C. Leuschner. 2012. Analyzing forest canopies with ground-based laser scanning: A comparison with hemispherical photography. Agricultural and Forest Meteorology 154–155:1–8.

Seidel, D., S. Fleck, C. Leuschner, and T. Hammett. 2011. Review of ground-based methods to measure the distribution of biomass in forest canopies. Annals of Forest Science 68:225–244.

Skole, D., and C. Tucker. 1993. Tropical deforestation and habitat fragmentation in the Amazon: Satellite data from 1978 to 1988. Science 260:1905–1910.

Slik, J. W. F., S.-I. Aiba, F. Q. Brearley, C. H. Cannon, O. Forshed, K. Kitayama, H. Nagamasu, R. Nilus, J. Payne, G. Paoli, A. D. Poulsen, N. Raes, D. Sheil, K. Sidiyasa, E. Suzuki, and J. L. C. H. van Valkenburg. 2010. Environmental correlates of tree biomass, basal area, wood specific gravity and stem density gradients in Borneo's tropical forests. Global Ecology and Biogeography 19:50–60.

Smith, A. M. S., M. J. Falkowski, A. T. Hudak, J. S. Evans, A. P. Robinson, and C. M. Steele. 2010. A cross-comparison of field, spectral, and lidar estimates of forest canopy cover. Canadian Journal of Remote Sensing 36:447–459.

Tucker, C. J., J. R. Townshend, and T. E. Goff. 1985. African land-cover classification using satellite data. Science 227:369–375.

Turner, D., A. Lucieer, and C. Watson. 2012. An automated technique for generating georectified mosaics from ultra-high resolution unmanned aerial vehicle (UAV) imagery, based on structure from motion (SfM) point clouds. Remote Sensing 4:1392–1410.

Van Den Meersschaut, D., and K. Vandekerkhove. 2000. Development of a stand–scale forest biodiversity index based on the State forest inventory. Integrated tools for natural resources inventories in the 21st century. Proceedings. USDA, Forest Service, North Central Forest Experiment Station General Techinal Report GTR-NC-212. pp. 340–347.

Vose, J. M., and H. L. Allen. 1988. Leaf area, stemwood growth, and nutrition relationships in loblolly pine. Forest Science 34:547–563.

Wallace, L., S. Hillman, K. Reinke, and B. Hally. 2017. Non-destructive estimation of above-ground surface and near-surface biomass using 3D terrestrial remote sensing techniques. Methods in Ecology and Evolution 8:1607–1616.

Wallace, L., A. Lucieer, Z. Malenovskỳ, D. Turner, and P. Vopěnka. 2016. Assessment of Forest Structure Using Two UAV Techniques: A Comparison of Airborne Laser Scanning and Structure from Motion (SfM) Point Clouds. Forests 7(62).

Waring, R. H., K. Newman, and J. Bell. 1981. Efficiency of tree crowns and stemwood production at different canopy leaf densities. Forestry 54:129–137.

Weiskittel, A. R., D. W. Hann, J. A. Kershaw Jr., and J. K. Vanclay. 2011. Forest Growth and Yield Modeling. 2nd edition. Wiley/Blackwell, New York.

Weiss, M., F. Baret, G. J. Smith, I. Jonckheere, and P. Coppin. 2004. Review of methods for in situ leaf area index (LAI) determination: Part II. Estimation of LAI, errors and sampling. Agricultural and Forest Meteorology 121:37–53.

Wesley, R. 1956. Measuring the height of trees. Park Administration 21:80–84.

Xing, Z., C. P.-A. Bourque, D. E. Swift, C. W. Clowater, M. Krasowski, and F.-R. Meng. 2005. Carbon and biomass partitioning in balsam fir (Abies balsamea). Tree Physiology 25:1207–1217.

Yang, T.-R., Y.-H. Hsu, J. A. Kershaw, E. McGarrigle, and D. Kilham. 2017. Big BAF sampling in mixed species forest structures of northeastern North America: influence of count and measure BAF under cost constraints. Forestry: An International Journal of Forest Research 90:649–660.

Zhao, D., D. Xie, H. Zhou, H. Jiang, and S. An. 2012. Estimation of Leaf Area Index and Plant Area Index of a Submerged Macrophyte Canopy Using Digital Photography. PLOS ONE 7(12):e51034.

Zianis, D., P. Muukkonen, R. Mäkipää, and M. Mencuccini. 2005. Biomass and stem volume equations for tree species in Europe. Silva Fennica Monographs 4(63).

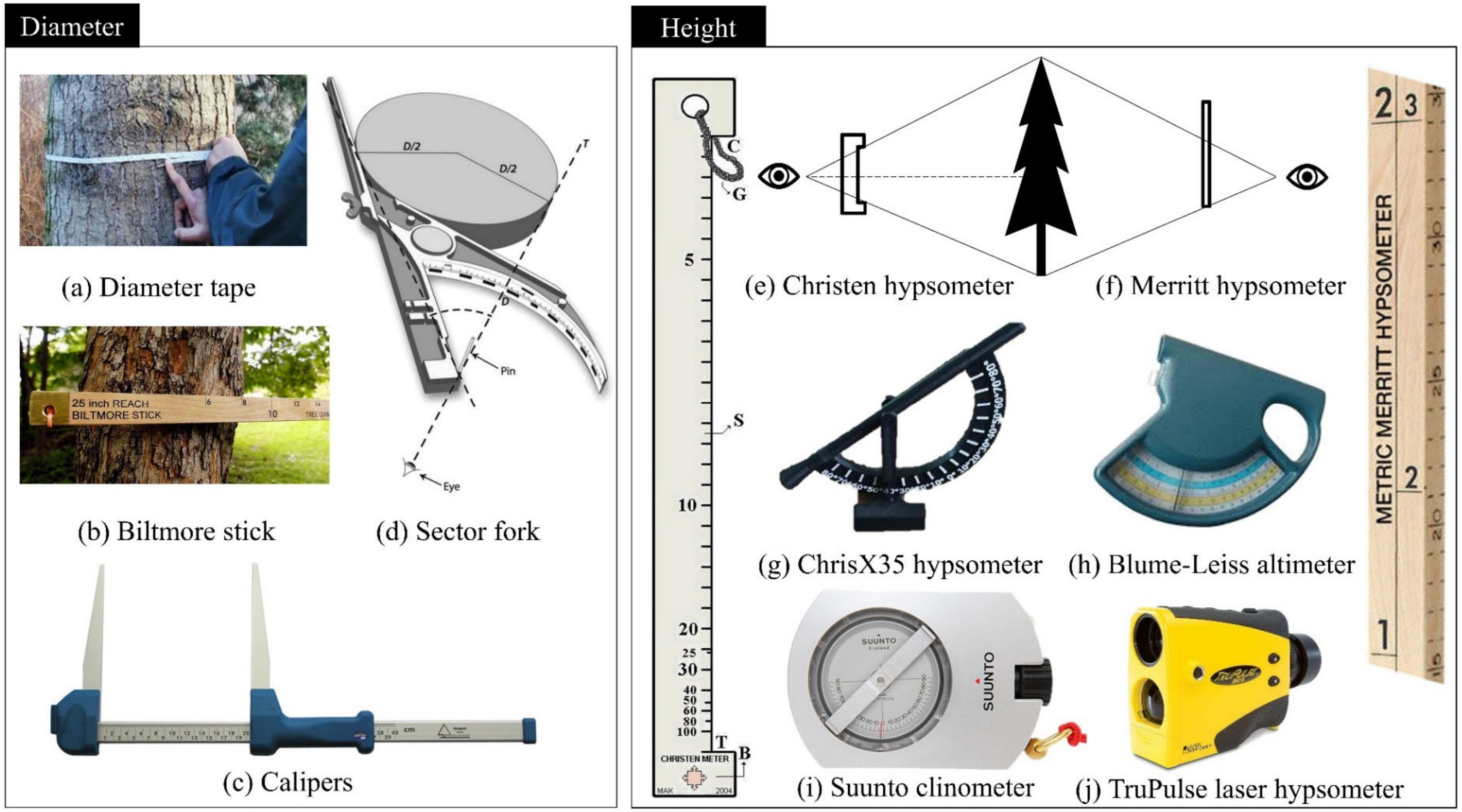

Fig 1.1: Tools used in individual tree diameter and height measurements

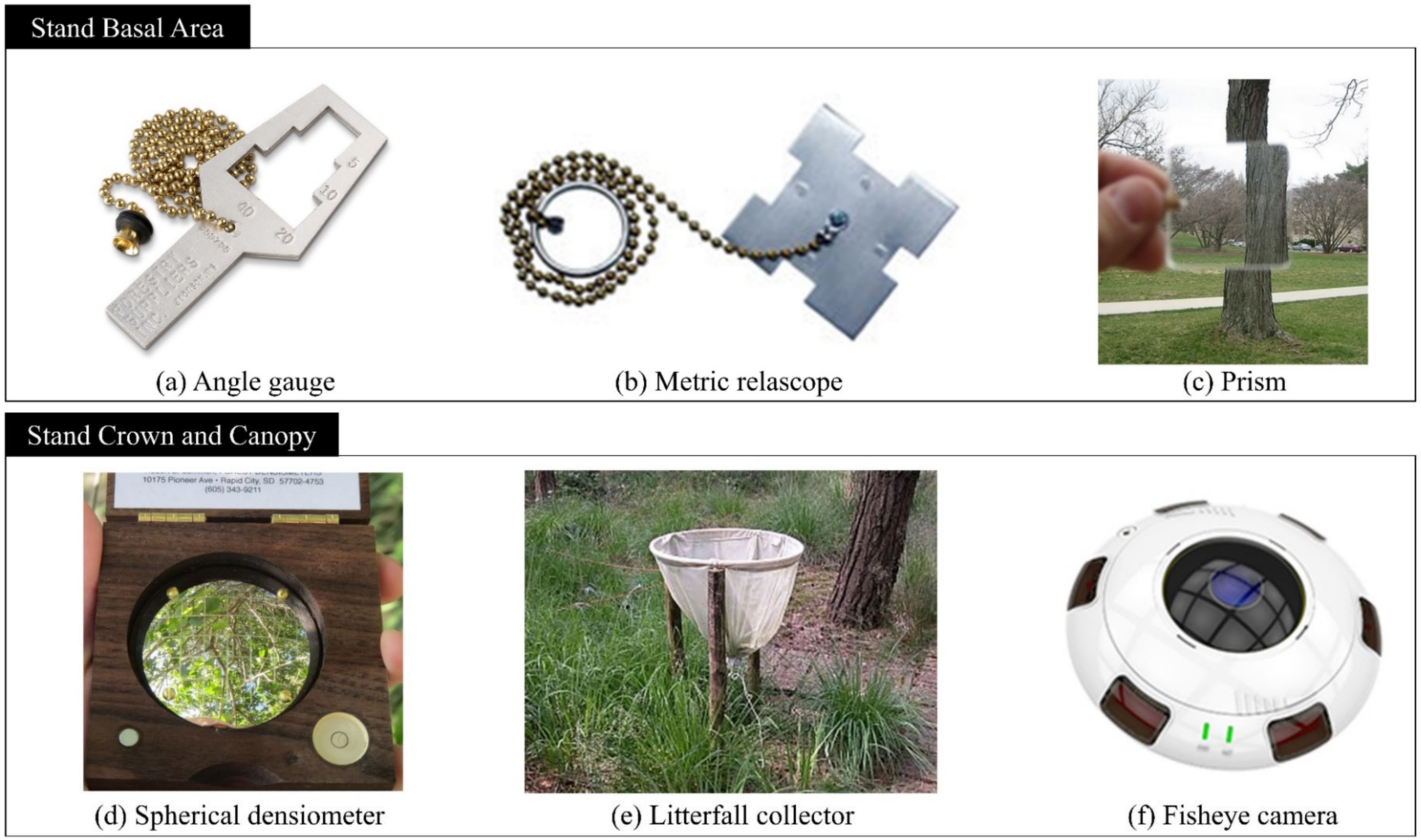

Fig 1.2: Tools used in stand level attributes measurements

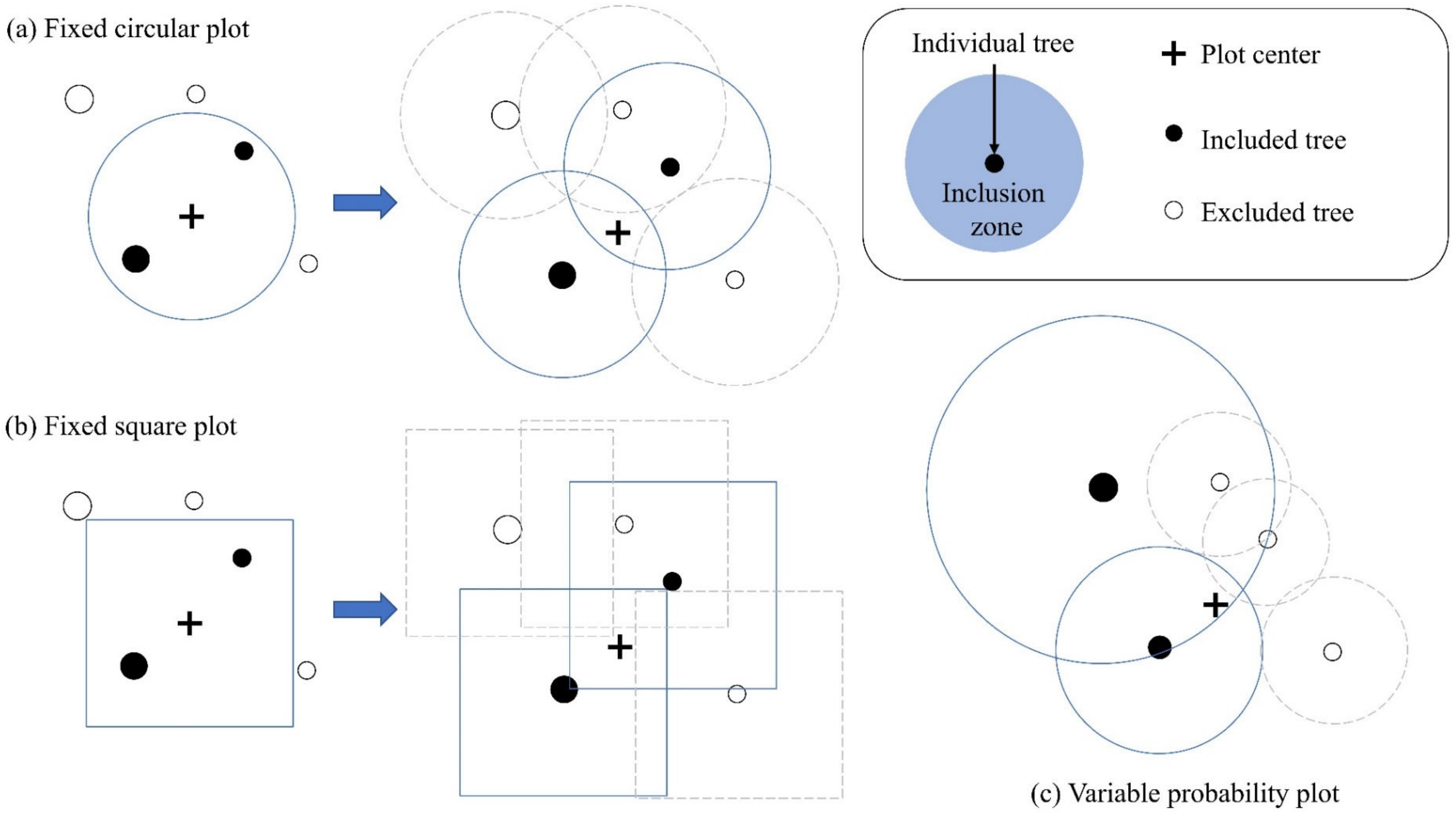

Fig 1.3: Equal probability and variable probability sampling design

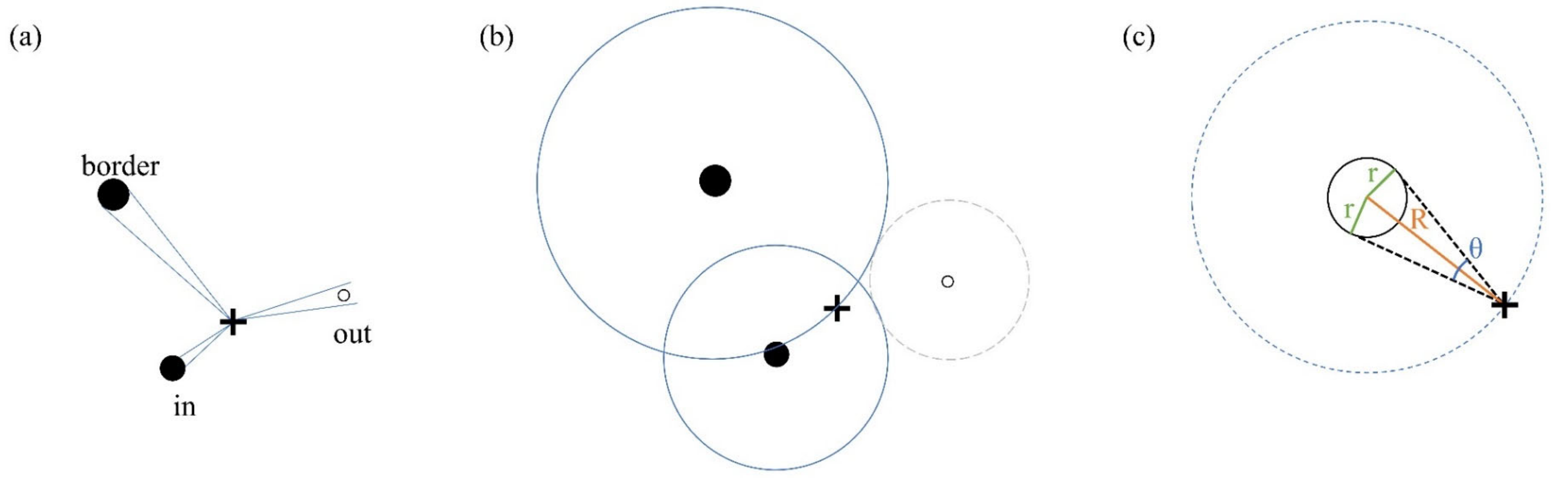

Fig 1.4: Selection of trees in horizontal point sampling (angle gauge sampling) (a) three status of trees based on projected angle (b) the inclusion zone of each individual tree (c) the relationship between trunk diameter and inclusion zone radius.

Chapter 2: Estimating Forest Basal Area from Spherical Images

2.1 Introduction

Forests are the dominant terrestrial ecosystem on Earth and account for three quarters of the gross primary productivity of the biosphere and about 80% of plant biomass (Pan et al., 2013). In addition to ecosystem services like watershed protection and carbon storage (Chazdon, 2008), the other economic and social products provided by forests are of great interest to land owners and forest managers (Gillis, 1990; Christensen et al., 1996). To satisfy the multiple demands from forests, advanced tools used to collect data efficiently are required for making good forest management decisions (Clutter et al., 1983; Baskerville, 1986; Bettinger et al., 2017). Therefore, coupling advanced technology with traditional forest inventories to save costs and time, and to improve accuracy of estimates, are of great importance (Husch, 1980; Iles, 2003; Kershaw et al., 2016).

Forest inventories typically collect measurements on individual trees (e.g., species, diameter at breast height, and total height) and use these measures to estimate stand-level parameters such as density, volume, and biomass (Kershaw et al., 2016). Stand basal area, defined as the sum of individual tree cross-sectional areas, is one of the most common stand-level parameters estimated in most forest inventories (Iles, 2003; Kershaw et al., 2016). Basal area is often expressed at breast height (1.3 m in SI and 4.5 ft in the Imperial system). Basal area is an important measure of stand density that incorporates tree size as well as number (Kershaw et al., 2016). It is a fundamental component of volume and biomass calculations (Iles, 2003; Jenkins et al., 2003; Lambert et al., 2005;

Slik et al., 2010; Kershaw et al., 2016) and is an important stand characteristic for forest growth models (Opie, 1968; Lootens et al., 2007; Weiskittel et al., 2011).

When using fixed-area sampling units, basal area is calculated from individual tree diameter measurements (Kershaw et al., 2016), which can be a time consuming endeavor depending upon tree density and sampling unit size. Angle count sampling (Bitterlich, 1947, 1984; Iles, 2003), or horizontal point sampling as it is commonly known (Grosenbaugh, 1952; Bitterlich, 1984; Iles, 2003; Kershaw et al., 2016), is an alternative method that measures basal area by counting trees that subtend (i.e., appear as large or larger than) a projected angle and multiplying by the basal area expansion factor (BAF). The ability to estimate basal area by counting trees makes angle count sampling a very efficient sampling approach (Bitterlich, 1984; Iles, 2003; Marshall et al., 2004; Kershaw et al., 2016; Yang et al., 2017).

DeCourt (1956) was the first to recognized that it was possible to conduct angle count sampling using photographs. Grosenbaugh (1963) hinted at this application but did not develop the technique very deeply. Because of the time and costs associated with film-based imagery, photo-based angle count sampling was not developed any further until the work by Stewart (2004) who proposed photo-based angle count sampling using 8 directional photos and developed methods to correct for image distortion near the photo edges. Dick (2012) using panoramic stitching software, merged 24 images into a single panorama image and eliminated the need for distortion correction. By defining an angle gauge in terms of pixels, Dick (2012) developed a simple photographic angle count method implemented in ArcGIS (ESRI, Redlands, CA). Independently, Fastie (2010) merged 504 images into an ultra-high resolution panorama to estimate basal area. Given that angle count sampling was already an extremely efficient inventory system in the field, these approaches for photo-based sampling were more curiosities than operational developments.

The main advantage of the photo-based method was that basal area estimates could potentially be extracted from archive photos (Stewart et al., 2004). However, photo-based approaches also suffered from potential under-estimation bias due to occluded (hidden) trees (Dick et al., 2010; Zasada et al., 2013). In addition to the hidden trees, other potential impacts such as understory vegetation, counting dead trees, image resolution, and user errors were not systematically explored in these previous studies.

Digital technology continues to advance rapidly, and stitching packages are now available on many smart phones. In addition, the recent development of consumer-grade spherical cameras opens the opportunity to obtain panoramic photos from single exposures controlled by a smart phone. The ability to rapidly obtain panoramic photos and develop onboard processing creates an opportunity to revisit the photo-based angle count sampling idea. The goal of this study was to develop an open-source software package that implements angle count sampling using spherical photos taken from a Ricoh Theta S, which is a relatively inexpensive consumer-grade camera. The specific objectives were: (1) to derive the geometry of applying the angle-count sampling idea to spherical images to obtain basal area estimates, (2) to assess the precision and accuracy of this approach compared to traditional field measured data, (3) to assess the inter-observer variability in implementing this approach, and (4) to assess the effects of understory tree density on the photo-based estimates.

2.2 Methods and Materials

2.2.1 Study sites

Data for this study come from two different studies. The first study was three early spacing trials located in western Newfoundland (NL). The NL sites were located in the Boreal Forest region (Rowe, 1972) and were dominated by balsam fir (*Abies balsamea*) with some black spruce (*Picea mariana*) and other boreal species. The trials were established in the early 1980's. At each site, there were three replicates of five thinning spacing treatments: Control (no spacing), 1.2m, 1.8m, 2.4m, and 3.0m average spacing.

The second study was located on the Noonan Research Forest (NRF) in central New Brunswick, Canada, managed by the University of New Brunswick. The NRF was located in the Acadian Forest region (Rowe, 1972), and was composed of a variety of stand types from relatively pure coniferous stands to mixed hardwood-softwood stands. A permanent 100m by 100m inventory sample grid was overlaid on the NRF in 1999. The 83 grid intersections within the Femelschlag Research Study were used in this study.

2.2.2 Data collection

2.2.2.1 Field data

Only the most recent measurements of the 45 NL plots (3 trials × 5 treatments/trial × 3 replicates/treatment) were used in this study (Table 2.1). The plot radii were: Control (no spacing) = 5.2m; 1.2m spacing = 7.2m; 1.8m spacing = 10.4m; 2.4m spacing = 15.0m; and 3.0m spacing = 18.0m). Plot sizes varied by treatment with the goal to have approximately 100 trees per plot at the initial measurement. On each plot, all trees taller than 1.3m were measured for diameter at breast height (DBH, 1.3m above ground, nearest 0.1cm) and total height (nearest 0.1m). Field basal area (FBA, m^2/ha) was calculated using:

$$\mathrm{FBA} = \mathrm{ExpF} \times \sum_{i=1}^{n} \left(\pi \left(\frac{DBH_i}{200} \right)^2 \right) \tag{2.1}$$

where ExpF is the plot expansion factor ($\mathrm{ExpF} = 10000/\pi R^2$; R is plot radius in meters).

On the NRF sample points, a 2 M BAF (basal area factor; i.e., each tree tallied represented 2 m^2/ha basal area) angle count sample was conducted centered at the 83 grid intersections in summer 2018. All trees that subtended the projected angle were counted and FBA (m^2/ha) was calculated by multiplying the number of count trees by the BAF (2 in this case). In addition, those trees with DBHs smaller than 6 cm were tallied as understory trees by height status (less than or greater than 1.3m tall) on a 4m radius plot centered on the grid intersections. Species and status (live or dead) also were recorded for all understory trees.

2.2.2.2 Digital sample points

For each NL sample plot, three digital sample locations were established at half the plot radius along azimuths of 120°, 240°, and 360° relative to plot center (Fig. 2.1.a). On the NRF sample points, only one digital sample location was established at the grid intersection (Fig. 2.1.a).

A Ricoh Theta S (Ricoh Imaging Company, LTD., 2016) spherical camera was used to capture spherical images. A single spherical image was captured at 1.6m above the ground at each digital sampling point (Fig. 2.1.b) and downloaded to a smart phone. . Though the spherical camera records a 360° spherical image, the spherical image is projected into a 2D digital image using cylindrical projection. In this projection system, the vertical coordinate in the 2D image and related vertical angle (latitude) in spherical coordinates are always consistent no matter how far an object is from horizontal center. The image resolution was 5376 pixels in width and 2688 pixels in height.

2.2.3 Image processing software

Angle count sampling (Bitterlich, 1947, 1984) is a sampling method that uses a horizontally projected angle to select trees for inclusion in the sample (Fig. 2.2.a). A basal area expansion factor (BAF) is derived from the sampling geometry associated with a tree that is at its limiting distance (Fig. 2.2.b). Angle count sampling is a form of sampling with variable probability and is an application of selecting sample trees based on probability proportional to size (Grosenbaugh, 1958; Kershaw et al., 2016). Basal area per ha is obtained by counting selected trees and multiplying by the BAF (Bitterlich, 1947; Kershaw et al., 2016). The key point to apply this sampling method on a spherical image is determining which trees in an image should be counted or not. In this study, two different methods for photo angle count sampling were developed and compared.

2.2.3.1 Edge marking method

In this method, the horizontal angle of each individual tree trunk at breast height (1.3m) in the image was determined (Fig. 2.2.b). This was accomplished by having the user mark the edges of each tree on the image (Fig. 2.3.a). The width of each tree trunk was used to calculate the maximum BAF threshold (maxBAF) at “border” tree condition using the following equation:

$$\text{maxBAF} = \left(100 \cdot \sin\left(\frac{TW}{PW} \cdot 360°\right)\right)^2 \tag{2.2}$$

where TW was the pixel width of the marked tree; and PW was the total width of the spherical image (PW = 5376 in this study).

By calculating maxBAF, the number of count trees was simply the number of marked trees where maxBAF ≥ desired BAF, and photo basal area (PBA, m^2/ha) was:

$$\text{PBA} = \text{BAF} * \text{count}(\text{maxBAF} \geq \text{BAF}) \tag{2.3}$$

2.2.3.2 Target count method

This method was similar to the field angle gauge process. The camera projected a horizontal angle based on the given BAF toward each tree (Fig. 2.3.b). To better visualize the cross-sectional angles of leaning trees, an octagon shaped target was used as the target threshold. A tree equal to or greater than the octagon target in size was marked as an “in” tree, otherwise that tree was an “out” tree and not counted. The PBA of this image was equal to the given BAF multiplied by the count of “in” trees.

2.2.3.3 Software implementation

An open source software package, Panorama2BasalArea, was developed in Python 3.6 (Guido, 2018) to implement the angle count sampling workflows described above. It included the plot photo management, tree trunk edge marking and octagon threshold counting, individual tree management, and PBA data export (Fig. 2.3). When using the edge marking method, a reference scale bar was provided. Trees which were narrower than the reference scale bar (BAF=1) were ignored to reduce the workload associated with edge marking (Fig. 2.3.a). For the target marking method, a reference octagon scaled to a given BAF was provided. Only those trees equal to or larger than the reference octagon were marked (Fig. 2.3.b). The source code for this software package can be downloaded from: https://github.com/HowcanoeWang/Panorama2BasalArea. It was also packaged as an executable app for Windows platforms: https://github.com/HowcanoeWang/Panorama2BasalArea/releases.

2.2.4 Data analysis

2.2.4.1 Influence of number of digital sample points

Hidden trees blocked by closer trees or understory vegetation create a potential for underestimating PBA. One possible way to deal with the hidden tree problem was to use multiple sample points in one plot. While hidden trees result in underestimation, errors in marking tree edges and judging octagon thresholds could result in over- or under-estimation relative to field basal area (FBA). To test the influence of multiple digital sample points and the effects of two tree marking methods on PBA estimates, three separate analyses were undertaken: 1) PBA estimated from one center digital sample point on the 83 NRF sample points; 2) PBA estimated on the NL plots using three individual (off-center) digital sample points; and 3) PBA estimated from the average of the three digital sample points on each NL plot. For each analysis, a simple linear regression was fitted to the FBA – PBA data:

$$\text{FBA} = b_0 + b_1 \cdot \text{PBA} \tag{2.4}$$

If PBA was the same as FBA, then $b_0 = 0$ and $b_1 = 1$. The resulting parameter estimates were tested for these values using t-tests and Bonferroni-adjusted alpha levels (Zar, 2009).

2.2.4.2 Influence of choice of BAF

As BAF increases, the distance a tree of a certain diameter can be from plot center decreases (Fig. 2.2). The expected number of count trees also decreases. Both factors should result in a lower probability of hidden trees (i.e., fewer hidden trees). On the other hand, as photo BAF increases so does variation between sample points. The trade-off becomes one of under-estimation versus increased sampling error. The optimal compromise is to use a BAF that reduces the number of hidden trees without appreciably increasing sample variation. To test this idea, BAFs ranging from 2 to 15 were applied to calculate PBA and compared to FBA using the edge marking method (edge marking was used because the user only needs to mark trees once and all BAFs can be determined, target counting requires multiple runs through the images). The difference between FBA and PBA were compared using bean plots, and variance and bias were visually analyzed.

2.2.4.3 Inter-observer variation

To examine inter-observer variability, 15 images from the three NL sites (one replicate from each trial) and 5 images from the NRF plots were selected as testing images. These 20 images were used for the edge marking method. For the target count method, horizontally mirrored images were used. In total, there were 40 test images given to 7 individuals. Everyone had different random orders for these images. The volunteers were trained how to use the software in both modes and then marked each image in the order given. Inter-Observer differences between PBA and FBA at BAF=2 for both modes were tested using linear mixed effects (LME) models. The fixed effects were PBA (covariate) and marking mode, and random effects were observer and image order.

2.2.4.4 Effects of understory density

Understory vegetation may limit sight distances in the field as well as in photos. In the field there are a variety of techniques the field observers can use to determine count trees when visibility is low. On photos, these options are not available. To test whether understory vegetation influenced PBA estimates, the difference between FBA and PBA (FBA – PBA) was graphed versus understory density and a locally weighted scatterplot smoothing (LOWESS) regression was used to assess trends in differences over understory density. Understory density was separated into two height classes: HT $\leq$ 1.3m and HT > 1.3m and evaluated by height class and total understory density.

2.3 Results

2.3.1 Influence of different digital sample locations

Fig. 2.4 shows the relationship between FBA and PBA by tree marking method and digital sample location type. With the exception of edge marking with three individual digital sampling points (Table 2.2 (e)), all slope coefficients (b_1) were not significantly different from 1.0, indicating that photo bias does not increase with increasing basal area. Results were not so consistent when examining the intercept terms. For both marking methods, when using a single digital sample location at plot center (Table 2.2 (a) and (d)), the intercept values were significantly different from 0 and almost double the intercept values (b_0) obtained using multiple digital sampling points. For the multiple digital sampling points, only the intercept term for edge marking was significantly different from 0 (Table 2.2 (e)). Both intercepts for the average of three digital sampling points were negative, though not significantly different from 0 (Table 2.2 (c) and (f)).

In terms of goodness of fit, the edge marking techniques generally had higher r^2 values and lower root mean square error (rMSE) values, indicating a stronger linear relationship between FBA and PBA (Table 2.2). All regressions indicate an under-estimation of FBA, except at the very lowest FBA values, when averaging across multiple digital sampling points. Under-estimation was consistent with the hypothesis of visibility bias resulting from occluded (hidden or missing) "in" trees. It was expected that the visibility bias would increase with increasing FBA; however, that was not generally observed in this study (Table 2.2 and Fig. 2.4).

2.3.2 Effects of BAF choice

It was hypothesized that increasing BAF would result in fewer hidden trees and less user error in marking edges and that PBA would become closer to FBA; however, that was not what was observed in this study. Fig. 2.5 shows the effects of increasing BAFs on PBA estimation. For the NRF plots, the mean differences between FBA and PBA decreased slightly, but remained positive (underestimation) across all levels of BAF. For the NL plots, the deviations decreased, but were essentially 0 across all levels of BAF. The NRF only had one center digital sample location while NL had three sample locations (Fig. 2.1.a). The additional digital sample points capture a greater range of the plot variation and reduces the effects of hidden trees. One issue noted on several of the

NRF plots was the presence of a tree very close to plot center. Large trees can block significant view angles on plots. Increasing BAF does not compensate for these situations. One the other hand, multiple digital sample locations minimized these effects by locating the camera at different positions within the plot.

For both NRF and NL sites, variation in the differences between FBA and PBA increased with increasing BAF (Fig. 2.5). Smaller plots are inherently more variable, and this was an expected outcome. It was expected that there would be an optimal BAF that minimized differences without substantial increases in variation. This was not observed in this study. It should be noted that this inference was only based on edge marking method because of the ease of changing BAF (edges only have to be marked once and all BAFs could be determined). Results for target counting were not undertaken because counts would have to be made independently for each BAF tested requiring a significant increase in image processing time.

2.3.3 Inter-observer consistency

Comparisons between FBA and PBA across the seven volunteers are shown in Fig. 2.6. Most users consistently underestimated FBA with both marking methods, with edge marking resulting in greater underestimation than target counting (Fig. 2.6. Column 1). While differences between users were observed (Fig. 2.6. Columns 2-7), on average, user estimates were comparable (i.e., LOWESS lines were very close to the 1:1 line). Target counting was generally more consistent than edge marking among different users and generally resulted in similar estimates across users (Fig. 2.6).

Fig. 2.7 shows the two plots with the least and greatest deviations between users. For the least plot, though different users did not mark exactly the same points across different trees, the edge positions, as well as the dark gray targets for “in” trees, were almost the same across users. The simple forest structure facilitates tree marking and results in lower variability between users. However, it was a different story for the plot with the greatest deviations. Neither the “out” trees nor the “in” trees have similar positions. Trees were very dense and diameters smaller, resulting in many “border” trees – small deviations in edge marking resulted in changes in “in” and “out” status. This problem was further compounded by the fact that edges of each tree were difficult to distinguish.

To statistically assess the effects of tree marking methods, different users, and image order (i.e., familiarity with using software), a linear mixed effects (LME) model was fitted to the data. The full model was:

$$\mathrm{FBA} = \mathrm{PBA} + \mathrm{Marking} + (\mathrm{User}) + (\mathrm{Order}) + \mathrm{e} \qquad (2.5)$$

where () indicate random effects. A backwards selection method was used to test significance of random effects. For the full model, the standard deviations associated with the random effects were: 2.1879 for User and 0.7292 for Order (residual standard error was 3.7051). The model was refitted with Order excluded and a log likelihood test performed. The p-value associated with dropping Order was 0.926, indicating that image order was not a significant random effect influencing deviations from FBA. Similarly, User was subsequently dropped, and the p-value was 0.081. So, while more significant than image order, differences between users were still not significant at $\alpha = 0.05$. The final reduced model only included the fixed effects PBA (covariate) and Marking (method). Both factors were significant: PBA ($p<0.001$) and Marking ($p<0.01$). The root Mean

Square Error was 10.6129 and the F value associated with PBA was 320.87 ($p < 0.001$) and for Marking Method was 9.913 ($p = 0.002$).

2.3.4 Understory density effects

Effects of understory density on PBA estimates for the NRF plots are shown in Fig. 2.8. Based on the LOWESS trend lines, understory density did not pose a large visibility bias in this study. Except for a single plot with very high understory density (> 30000 trees per ha), the trend lines remained around 15 m^2/ha, indicating little impact of understory density on FBA. The value of 15 is very close to the intercept coefficient estimated above (Table 2.2) and the results here show that the variation in FBA - PBA (Fig. 2.8) was not due to understory vegetation.

2.4 Discussion

Our results show that spherical images from a consumer-grade 360° camera can efficiently and effectively estimate basal area using photo-based angle-count sampling. While underestimation was consistently observed, the trend did not appear to be related to the amount of basal area per ha present, understory vegetation, nor inter-user variability. As a result, underestimation could be easily corrected using some form of double sampling (Dai, 2018, p. 30; Dick, 2012) with ratio correction.

In this study, two photo processing methods were used: the edge marking method and the octagon target counting method. The resulting PBA estimates were acceptable for both methods. The advantage of edge marking was that different BAFs can be assessed without remarking, but this is generally only useful for big BAF sampling (Bell et al., 1983; Iles, 2003; Marshall et al., 2004) or for research situations where one is interested in effects of different BAFs (as in this study). All users in this study felt the target counting was more familiar (more similar to the process they used in the field) and more repeatable than edge marking. Difficulties recognizing tree edges, especially in dense forest conditions, along with twice the number of mouse clicks for each tree could potentially cause higher user errors. The octagon target count method avoided potential edge marking errors and only required one click; however, repeated marking for different BAFs would be required.

It was expected that visibility bias would increase with increasing basal area because of an increasing number of hidden trees. This was not observed in this study. There are several potential explanations for this result. First, and most likely, the results obtained here were the compensatory effects of underestimation caused by hidden trees coupled with overestimation caused by increased user error as field basal area increased. In this study, the plots with the highest basal areas were generally composed of very dense small stems, especially on the NL sites. With many small trees in an image it can be difficult to distinguish multiple overlapping small trees from one larger individual tree. With the edge marking method, it can be very difficult to clearly see the tree edges as well due to the resolution and exposure conditions (Fig. 2.7.b). Secondly, the plots with very high basal areas also had a significant number of dead trees present. While care was exercised to determining live/dead and avoid marking dead trees, this could have increased counts on the higher basal area plots. Both factors may have also contributed to the lack of improvement in PBA estimates with increasing BAF.

Multiple digital sampling locations within plots greatly decreased effects of hidden trees and any user errors. In several individual images there were nearby tree trunks which occluded large portions of the plot radial view. The potential for hidden trees in these situations was quite large. The multiple digital sample locations minimize this issue by providing multiple plot viewpoints as well as capturing more of the local spatial variability. Hidden trees cannot be observed using any remote sensing technique and is a tough problem to deal with (Ducey and Kershaw, 2011; Ducey and Astrup, 2013; Zasada et al., 2013). When carrying out field measured angle count sampling, it is possible for the observer to lean left and right or even slightly change location to identify hidden trees. Distances from plot center and diameters of hidden trees also can be measured to determine if hidden trees are count trees or not. This is not possible with photographic or other remote sensing methods (Fastie, 2010). Building a model to correct for hidden tree effects can be very complex and should take into account stand density, distance from tree to sensor, the thickness of each tree trunk, and so on (Zasada et al., 2013). Such model-based approaches are inherently more variable and require substantial field data to calibrate (Ducey and Astrup, 2013). A simpler method is to use double sampling with ratio correction (Dick, 2012; Dai, 2018) or some form of distance sampling correction (Kershaw, 2010). We have shown another alternative, which is to simply add additional digital sampling locations within a plot, which is often the solution employed with terrestrial LiDAR scanning (Seidel et al., 2012; Wallace et al., 2017). Limiting plot size (or in this case increasing BAF) is another way to decrease effects of hidden trees (Dick et al., 2010; Zasada et al., 2013); however, this did not seem to be effective in this study. While multiple digital sample locations improve PBA estimation, it greatly increases field acquisition time. Given that angle count sampling is already an efficient method to implement in the field, multiple images would most likely require more field effort.

Double sampling with ratio correction is most likely to be the most efficient method for dealing with hidden trees (Dick, 2012; Dai, 2018).

It is very important to determine an appropriate BAF for angle-count sampling (Bitterlich, 1984; Iles, 2003; Yang et al., 2017). Choice of BAF greatly influences variability, which in turn, influences sample size requirements, numbers of trees counted per plot, and ultimately inventory costs (Iles, 2012; Yang et al., 2017). We found that BAF could be increased to about 5 without substantially increasing variability. Yang et al. (2017) obtained similar results for the entire NRF. The increased BAF had the added effect of slightly reducing visibility bias, thus a trade-off between visibility bias and plot variation needs to be consider when implementing photo-based angle count sampling.

In this study understory vegetation did not seem to influence visibility bias. Concerns about effects of understory vegetation has been mentioned by many photo-based forest inventory studies (Stewart, 2004; Dick et al., 2010; Fastie, 2010; Perng et al., 2018), but none of these studies verified this effect experimentally. We found that different understory tree densities had no significant impact on the differences between FBA and PBA. This was contrary to our expectations. A possible explanation for this phenomenon is that most of the understory vegetation in the study plots were shorter than 1.3m in height. Additional advantages in our study include very flat terrain and the ability to view up the stem and visualize stem size when taller understory vegetation blocked the view.

Variability between different users is a very important consideration when choosing measurement methods. While a few photo forest mensuration studies have shown that they can achieve small differences between field measured data and photo measured data (Clark et al., 2000; Fastie, 2010; Rodríguez-García et al., 2014), none, to our knowledge, have systematically tested the repeatability and reproducibility among different users. Our repeatability test given by seven volunteers showed: 1) Random effects of image processing order (familiarity of software) and different users did not have significant impacts on photo estimation; 2) the denser the plot, the more differences between users due to manual identification and selection by mouse clicking; and 3) using octagon target counts did not require identifying tree edges and resulted in lower underestimation than edge marking.

Many studies have focused on individual tree measurements, then summarizing these measures into stand level attributes. Some studies use scale tags placed on each tree or measured field distances and slopes (Dick et al. 2010, Lu et al. 2019). These methods require measuring or tagging individual trees which is time-consuming and costly and/or require multiple images for each tree of interest (Stewart et al. 2004, Perng et al. 2018). These techniques have limited benefit for improving inventory efficiency. In addition, errors resulting from stitching several digital photos together cannot be avoided (Fastie 2010, Dick et al. 2010, Perng et al. 2018, Lu et al. 2019). Structure from Motion (SfM) is an "automatic" merging technology which enables 3D reconstruction from photo series without actual measurements (Snavely et al. 2008). Several studies have used this technique to reconstruct individual tree stems (Miller et al. 2015, Surový et al. 2016, Mokroš et al. 2018), or to develop stand level point clouds (Liang et al. 2014, 2015, Forsman et al. 2016, Liu et al. 2018). However, this automatic technology requires obtaining a large number of photos (Berveglieri et al. 2017a, Liu et al. 2018) and high performance computers and complex algorithms to conduct analysis (Belton et al. 2013, Liang et al. 2015, Mulverhill et al. 2019). In addition, the points clouds require subsequent measurement to produce the tree and stand attributes. We simply extract the stand-level basal area directly from the photos.

The method we proposed here has several advantages. First, using a consumer-grade spherical camera is a very cost-effective (around $400 CDN) and time-effective (less than 1 minute per photo) method. The image is automatically merged in the camera eliminating the often time-consuming task of acquiring and stitching multiple photos from different view radii (Dick et al., 2010; Fastie, 2010) or placing reference scale objects in the field (Dean, 2003; Varjo et al., 2006; Perng et al., 2018). Keeping permanent digital records for forest plots provides the opportunity for making new retrospective measurements, this aspect is likely to become more advantageous as novel technology develops in future (Iles, 1994). Finally, quantification of differences among users is difficult to assess and correct with most field measurement techniques. The software developed here keeps a record of individual markings (Fig. 2.7) that could be used as a comparison reference for correcting photo-based samples.

This study also had some limitations. The camera elevation was not exactly at the definition of breast height (1.3 m). When selecting tree trunks for marking and estimating basal area at breast height, we used the equatorial plane of the spherical camera rather than calculating 1.3m height on tree trunks based on stereoscopic principles (Rodríguez-García et al., 2014; Sánchez-González et al., 2016; Perng et al., 2018). The spherical image is merged by two hemispherical lenses, the joint region can sometimes be fuzzy or blurred which makes tree trunk identification more difficult. Variable sunlight conditions can result in inconsistent exposure levels across the spherical image. Underexposure makes trunks in the far distance dark and hard to distinguish while overexposure flashes out trunk edges. Our terrain was relatively flat. In steeper terrain, methods for identifying breast height on trees will be required. This is a more complicated problem than is currently implemented in our software, Finally, all images were marked manually. It is quite easy to have user errors and can be time consuming in the lab. Automatic image processing and 3D reconstruction is a rapidly developing area (Hapca et al., 2007). It may prove feasible to automatize the process described here by applying computer vision and developing algorithms similar to our manual selection methods (Sánchez-González et al., 2016; Berveglieri et al., 2017). Another possibility is to use Structure from Motion (SfM) techniques (Snavely et al., 2008) to obtain point clouds from different camera views (Liang et al., 2014; Forsman et al., 2016; Surový et al., 2016; Mokroš et al., 2018); however, point cloud development obviates the simplicity of the methods developed here – other than clicking trees, no measurements were required.

2.5 Conclusion

Spherical photos are suitable for estimating stand basal area based on modified angle-count sampling methods. Adding multiple digital sample locations can decrease effects of visibility bias. Careful selection of BAF can somewhat reduce visibility bias without substantially increasing variation. Variability among different users did not seem to be a significant problem with implementing photo angle counts. Though limited by occasionally fuzzy joint regions and extreme sunlight conditions, this novel method could still be a cost-effective and efficient method to increase field sample sizes and to provide permanent forest records for future use. Effects of understory vegetation and sloping terrain needs to be examined beyond the range of conditions encountered in this study.

Future research should focus on other forest attribute extraction such as height and diameter and automatic image processing.

2.6 Acknowledgements

Funding for this project was provided in part by the National Science and Engineering Research Council of Canada, Discovery Grants program, the Province of Newfoundland and Labrador Centre for Forest Science and Innovation Contribution Agreement, and the New Brunswick Innovation Foundation Research Assistants Initiative and Graduate Scholarships programs. The authors also thank the lab mates, collaborators, and summer field crew who helped make this project possible: Emily Loretta Nicholson, UNB; Dr. Mike Lavigne, Gretta Goodine, and Rodney Foster, Atlantic Forestry Research Centre, Natural Resources Canada; We also thank Yang Zhan, Wushuang Li, Shun-Ying Chen, and Yunjia Dai for their volunteer work for software testing and inter-observer error analysis.

2.7 References

Baskerville, G. 1986. Understanding forest management. Forestry Chronicle 62:339–347.

Bell, J. F., K. Iles, and D. Marshall. 1983. Balancing the ratio of tree count-only sample points and VBAR measurements in variable plot sampling.Bell J.F. and Atterbury, T. (eds.). Proceedings: Renewable Resource Inventories for Monitoring Changes and Trends. College of Forestry, Oregon State University, Corvallis, OR. pp. 699–702.

Belton, D., S. Moncrieff, and J. Chapman. 2013. Processing tree point clouds using Gaussian Mixture Models. ISPRS Annals of Photogrammetry, Remote Sensing and Spatial Information Sciences. Copernicus GmbH, Antalya, Turkey. pp. 43–48.

Berveglieri, A., A. Tommaselli, X. Liang, and E. Honkavaara. 2017a. Photogrammetric measurement of tree stems from vertical fisheye images. Scandinavian Journal of Forest Research 32:737–747.

Berveglieri, A., A. M. G. Tommaselli, X. Liang, and E. Honkavaara. 2017b. Vertical Optical Scanning with Panoramic Vision for Tree Trunk Reconstruction. Sensors 17(2791).

Bettinger, P., K. Boston, J. Siry, and D. Grebner. 2017. Forest Management and Planning. 2nd edn. Academic Press, San Diego, CA.

Bitterlich, W. 1947. Die winkelzählmessung (Measurement of basal area per hectare by means of angle measurement.). Allgemeine Forst- und Holzwirtschaftliche Zeitung 58:94–96.

Bitterlich, W. 1984. The relascope idea: Relative measurements in forestry. First. CAB International, Slough, England.

Chazdon, R. L. 2008. Beyond Deforestation: Restoring Forests and Ecosystem Services on Degraded Lands. Science 320:1458–1460.

Christensen, N. L., A. M. Bartuska, J. H. Brown, S. Carpenter, C. D'Antonio, R. Francis, J. F. Franklin, J. A. MacMahon, R. F. Noss, D. J. Parsons, C. H. Peterson, M. G. Turner, and R. G. Woodmansee. 1996. The report of the Ecological Society of America committee on the scientific basis for ecosystem management. Ecological Applications 6:665–691.

Clark, N. A., R. H. Wynne, D. L. Schmoldt, and M. Winn. 2000. An assessment of the utility of a non-metric digital camera for measuring standing trees. Computers and Electronics in Agriculture 28:151–169.

Clutter, J. L., J. C. Fortson, L. V. Pienaar, G. H. Brister, and R. L. Bailey. 1983. Timber management. A quantitative approach. First. John Wiley & Sons, New York.

Dai, X. 2018. Bias correction in panoramic photo-based angle count sampling. Unpub. BScF Honors, University of New Brunswick, Fredericton, NB, Canada.

Dean, C. 2003. Calculation of wood volume and stem taper using terrestrial single-image close-range photogrammetry and contemporary software tools. Silva Fennica 37:359–380.

DeCourt, N. 1956. Utilisation de la photographie pour mesurer les surfaces terrières (The use of photography for measuring basal area). Revue Forestière Française 8:505–507.

Dick, A. R. 2012. Forest inventory using a camera: Concept, field implementation and instrument development. Unpublished MScF Thesis, University of New Brunswick, Fredericton, NB, Canada.

Dick, A. R., J. A. Kershaw, and D. A. MacLean. 2010. Spatial Tree Mapping Using Photography. Northern Journal of Applied Forestry 27:68–74.

Ducey, M. J., and R. Astrup. 2013. Adjusting for nondetection in forest inventories derived from terrestrial laser scanning. Canadian Journal of Remote Sensing 39:410–425.

Ducey, M. J., and J. A. Kershaw. 2011. Vertical Point Sampling with a Camera. Northern Journal of Applied Forestry 28:61–65.

Fastie, C. L. 2010. Estimating stand basal area from forest panoramas. Page 8 Proceedings of the Fine International Conference on Gigapixel Imaging for Science. Carnegie Mellon University, Pittsburg, PA.

Forsman, M., N. Börlin, and J. Holmgren. 2016. Estimation of Tree Stem Attributes Using Terrestrial Photogrammetry with a Camera Rig. Forests 7(61).

Gillis, A. M. 1990. The New Forestry. BioScience 40:558–562.

Grosenbaugh, L. R. 1952. Plotless timber estimates--New, fast, easy. Journal of Forestry 50:32–37.

Grosenbaugh, L. R. 1958. Point-sampling and line-sampling: Probability theory, geometric implications, synthesis. Page 34. Occasional Paper, USDA Forest Service, Southern Forest Experiment Station.

Grosenbaugh, L. R. 1963. Optical dendrometers for out-of-reach diameters: A conspectus and some new theory. Forest Science Monographs 4(48).

Guido, van R. 2018. Python (programming language). Python Software Foundation, US. Url: https://docs.python.org/3.6/reference/index.html. Last Accessed 12-11-2018.

Hapca, A. I., F. Mothe, and J.-M. Leban. 2007. A digital photographic method for 3D reconstruction of standing tree shape. Annals of Forest Science 64:631–637.

Husch, B. 1980. How to determine what you can afford to spend on inventories. IUFRO Workshop on Arid Land Resource Inventories. USDA, Forest Service, Washington Office, General Technical Report WO-28, La Paz, Mexico. pp. 98–102

Iles, K. 1994. Directions in Forest Inventory. Journal of Forestry 92:12–15.

Iles, K. 2003. A sampler of inventory topics. 2nd edition. Kim Iles and Associates, Nanaimo, BC.

Iles, K. 2012. Some Current Subsampling Techniques in Forestry. Mathematical & Computational Forestry & Natural Resource Sciences 4(2).

Jenkins, J. C., D. C. Chojnacky, L. S. Heath, and R. A. Birdsey. 2003. National scale biomass estimators for United States tree species. Forest Science 49:12–35.

Kershaw, J. A., Jr. 2010. Correcting for visibility bias in photo point samples. Stockbridge, MA.

Kershaw, J. A., Jr., M. J. Ducey, T. W. Beers, and B. Husch. 2016. Forest Mensuration. 5th edition. Wiley/Blackwell, Hobokin, NJ.

Lambert, M.-C., C.-H. Ung, and F. Raulier. 2005. Canadian national tree aboveground biomass equations. Canadian Journal of Forest Research 35:1996–2018.

Liang, X., A. Jaakkola, Y. Wang, J. Hyyppä, E. Honkavaara, J. Liu, and H. Kaartinen. 2014. The Use of a Hand-Held Camera for Individual Tree 3D Mapping in Forest Sample Plots. Remote Sensing 6:6587–6603.

Liang, X., Y. Wang, A. Jaakkola, A. Kukko, H. Kaartinen, J. Hyyppä, E. Honkavaara, and J. Liu. 2015. Forest Data Collection Using Terrestrial Image-Based Point Clouds From a Handheld Camera Compared to Terrestrial and Personal Laser Scanning. IEEE Transactions on Geoscience and Remote Sensing 53:5117–5132.

Liu, J., Z. Feng, L. Yang, A. Mannan, T. U. Khan, Z. Zhao, and Z. Cheng. 2018. Extraction of Sample Plot Parameters from 3D Point Cloud Reconstruction Based on Combined RTK and CCD Continuous Photography. Remote Sensing 10(1299).

Lootens, J. R., D. R. Larsen, and S. R. . Shifley. 2007. Height-diameter equations for 12 upland species in the Missouri Ozark Highlands. Northern Journal of Applied Forestry 24:1149–1152.

Lu, M.-K., T. Y. Lam, B.-H. Perng, and H.-T. Lin. 2019. Close-range photogrammetry with spherical panoramas for mapping spatial location and measuring diameters of trees under forest canopies. Canadian Journal of Forest Research 49:865–874.

Marshall, D. D., K. Iles, and J. F. Bell. 2004. Using a large-angle gauge to select trees for measurement in variable plot sampling. Canadian Journal of Forest Research 34:840–845.

Miller, J., J. Morgenroth, and C. Gomez. 2015. 3D modelling of individual trees using a handheld camera: Accuracy of height, diameter and volume estimates. Urban Forestry & Urban Greening 14:932–940.

Mokroš, M., J. Výbošťok, J. Tomaštík, A. Grznárová, P. Valent, M. Slavík, and J. Merganič. 2018. High Precision Individual Tree Diameter and Perimeter Estimation from Close-Range Photogrammetry. Forests 9(696).

Mulverhill, C., N. C. Coops, P. Tompalski, C. W. Bater, and A. R. Dick. 2019. The utility of terrestrial photogrammetry for assessment of tree volume and taper in boreal mixedwood forests. Annals of Forest Science 76(83).

Opie, J. E. 1968. Predictability of Individual Tree Growth Using Various Definitions of Competing Basal Area. Forest Science 14:314–323.

Pan, Y., R. A. Birdsey, O. L. Phillips, and R. B. Jackson. 2013. The Structure, Distribution, and Biomass of the World's Forests. Annual Review of Ecology, Evolution, and Systematics 44:593–622.

Perng, B.-H., T. Y. Lam, and M.-K. Lu. 2018. Stereoscopic imaging with spherical panoramas for measuring tree distance and diameter under forest canopies. Forestry: An International Journal of Forest Research 91:662–673.

Ricoh Imaging Company, LTD. 2016. Rioch Theta S 360 video camera. http://www.ricoh-imaging.co.jp/english/products/theta_s/. Last Accessed 26-08-2016.

Rodríguez-García, C., F. Montes, F. Ruiz, I. Cañellas, and P. Pita. 2014. Stem mapping and estimating standing volume from stereoscopic hemispherical images. European Journal of Forest Research 133:895–904.

Rowe, J. S. 1972. Forest Regions of Canada. Publication, Fisheries and Environment Canada, Canadian Forest Service, Headquarters, Ottawa. 172 p.

Sánchez-González, M., M. Cabrera, P. J. Herrera, R. Vallejo, I. Cañellas, and F. Montes. 2016. Basal Area and Diameter Distribution Estimation Using Stereoscopic Hemispherical Images. Photogrammetric Engineering & Remote Sensing 82:605–616.

Seidel, D., S. Fleck, and C. Leuschner. 2012. Analyzing forest canopies with ground-based laser scanning: A comparison with hemispherical photography. Agricultural and Forest Meteorology 154–155:1–8.

Slik, J. W. F., S.-I. Aiba, F. Q. Brearley, C. H. Cannon, O. Forshed, K. Kitayama, H. Nagamasu, R. Nilus, J. Payne, G. Paoli, A. D. Poulsen, N. Raes, D. Sheil, K. Sidiyasa, E. Suzuki, and J. L. C. H. van Valkenburg. 2010. Environmental correlates of tree biomass, basal area, wood specific gravity and stem density gradients in Borneo's tropical forests. Global Ecology and Biogeography 19:50–60.

Snavely, N., S. M. Seitz, and R. Szeliski. 2008. Modeling the World from Internet Photo Collections. International Journal of Computer Vision 80:189–210.

Stewart, B. 2004, August. Using a camera as an angle gauge in angle-count sampling. MF Thesis, The University of Georgia.

Stewart, B., C. J. Cieszewski, and M. Zasada. 2004. Use of a camera as an angle-gauge in angle-count sampling. Second International Conference on Forest Measurements and Quantitative Methods and Management. Warnell School of Forestry and Natural Resources, University of Georgia, Athens, GA. pp. 375–380

Surový, P., A. Yoshimoto, and D. Panagiotidis. 2016. Accuracy of Reconstruction of the Tree Stem Surface Using Terrestrial Close-Range Photogrammetry. Remote Sensing 8:123.

Varjo, J., H. Henttonen, J. Lappi, J. Heikkonen, and J. Juujärvi. 2006. Digital horizontal tree measurements for forest inventory. Working papers of the Finnish Forest Research Institute 40(23).

Wallace, L., S. Hillman, K. Reinke, and B. Hally. 2017. Non-destructive estimation of above-ground surface and near-surface biomass using 3D terrestrial remote sensing techniques. Methods in Ecology and Evolution 8:1607–1616.

Weiskittel, A. R., D. W. Hann, J. A. Kershaw Jr., and J. K. Vanclay. 2011. Forest Growth and Yield Modeling. 2nd edition. Wiley/Blackwell, New York.

Yang, T.-R., Y.-H. Hsu, J. A. Kershaw, E. McGarrigle, and D. Kilham. 2017. Big BAF sampling in mixed species forest structures of northeastern North America:

influence of count and measure BAF under cost constraints. Forestry: An International Journal of Forest Research 90:649–660.

Zar, J. H. 2009. Biostatistical analysis. 5th edition. Pearson, New York.

Zasada, M., K. Stereńczak, W. M. Dudek, and A. Rybski. 2013. Horizon visibility and accuracy of stocking determination on circular sample plots using automated remote measurement techniques. Forest Ecology and Management 302:171–177.

Table 2.1: Average stand-level estimates (standard errors in parentheses) by trial and treatment for the 3 early spacing trials located with western Newfoundland.

Trial	Year	Treatment	Stand-Level Averages (Standard Errors)							
			Trees (num/ha)		Basal Area (m^2/ha)		DBH (cm)		Total Height (m)	
Cormack	2013	Control (no spacing)	9974	(1807)	62.39	(6.26)	8.97	(0.42)	9.21	(0.92)
		1.2m spacing	6239	(740)	49.94	(9.49)	10.14	(1.60)	8.86	(1.63)
		1.8m spacing	2978	(433)	34.41	(10.88)	12.07	(1.64)	8.73	(1.61)
		2.4m spacing	1432	(168)	32.38	(3.81)	16.98	(0.59)	10.62	(0.54)
		3.0m spacing	965	(62)	21.54	(0.92)	16.86	(0.18)	9.62	(0.23)
Pasadena	2013	Control (no spacing)	6112	(2049)	61.04	(9.36)	11.52	(1.27)	9.83	(0.82)
		1.2m spacing	3616	(863)	67.22	(5.07)	15.59	(1.95)	11.37	(1.38)
		1.8m spacing	2611	(309)	53.59	(7.29)	16.16	(0.16)	10.81	(0.43)
		2.4m spacing	1793	(545)	46.18	(10.12)	18.26	(0.86)	11.35	(0.29)
		3.0m spacing	1111	(61)	36.88	(3.04)	20.55	(0.58)	11.60	(0.33)
Roddickton	2017	Control (no spacing)	12775	(2101)	73.19	(8.06)	8.59	(0.88)	7.07	(0.62)
		1.2m spacing	4987	(1066)	54.62	(4.61)	11.94	(1.47)	8.28	(1.28)
		1.8m spacing	2927	(247)	40.58	(2.86)	13.30	(0.50)	7.94	(0.25)
		2.4m spacing	2119	(253)	40.40	(9.13)	15.50	(0.85)	8.74	(0.67)
		3.0m spacing	1253	(87)	31.25	(2.21)	17.83	(0.41)	9.12	(0.35)

Table 2.2: Simple linear regression results for field basal area versus photo basal area by digital sample point type. The linear model is FBA=b0 + b1*PBA, if PBA is the same as FBA, then b0=0 and b1=1

Photo marking mode	Digital sample points type	Parameters	Estimate	Standard Error	p-value	r2	rMSE
Target Counting	(a) One center estimate	b_0	19.74	3.85	<0.001	0.41	9.27
		b_1	0.84	0.11	0.150		
	(b) Three individual estimates	b_0	4.44	3.08	0.152	0.61	9.66
		b_1	0.99	0.06	0.868		
	(c) Mean of three estimates	b_0	-5.22	4.79	0.282	0.75	7.77
		b_1	1.21	0.11	0.063		
Edge Marking	(d) One center estimate	b_0	15.69	4.09	<0.001	0.44	9.00
		b_1	0.83	0.10	0.093		
	(e) Three individual estimates	b_0	7.34	2.91	0.013	0.60	9.72
		b_1	0.88	0.06	0.048		
	(f) Mean of three estimates	b_0	-4.04	4.32	0.355	0.78	7.30
		b_1	1.13	0.09	0.158		

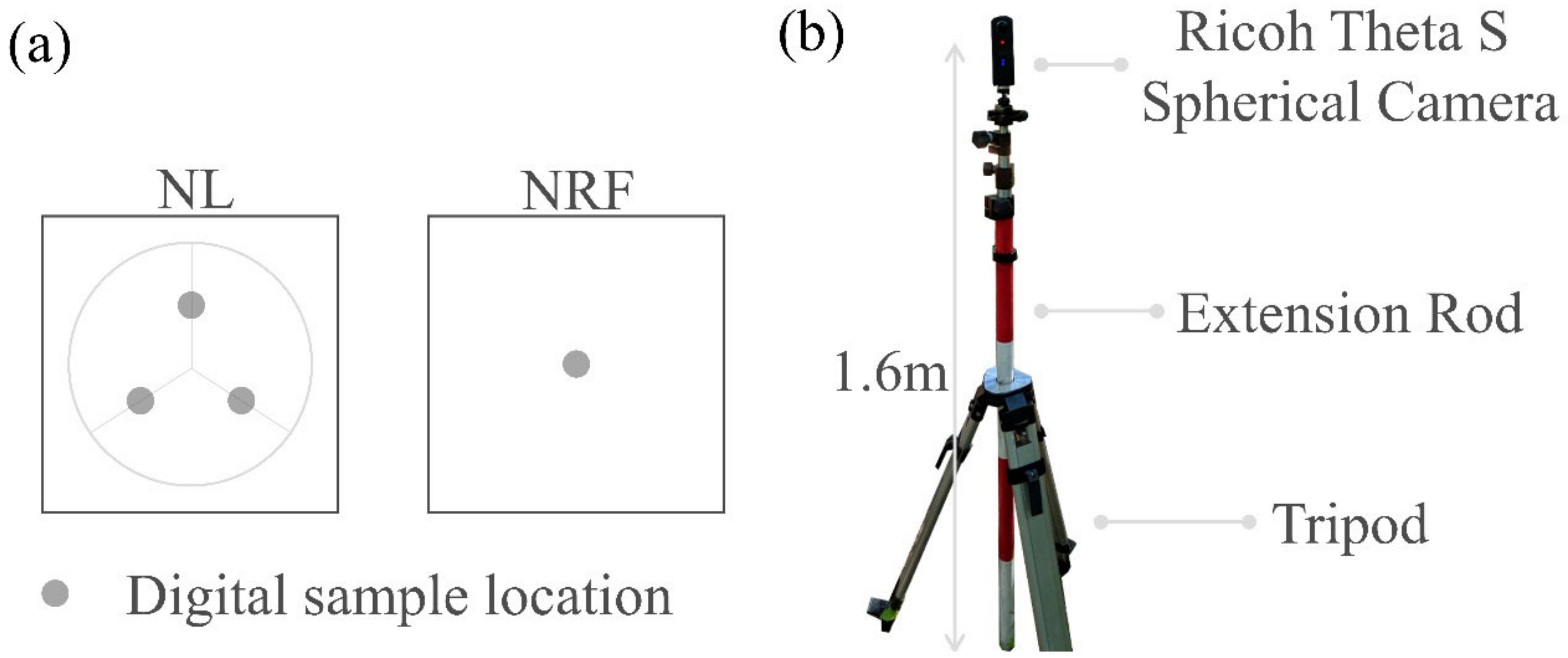

Fig. 2.1: Digital data collection methods: (a) Digital sample location design for Newfoundland (NL) and Noonan Research Forest (NRF) (Three locations were established at the midpoint of plot radius along azimuths of 120°, 240°, and 360° in each NL plot, while only one location was set in the center for each NRF plot); (b) tripod and camera set up for spherical image acquisition.

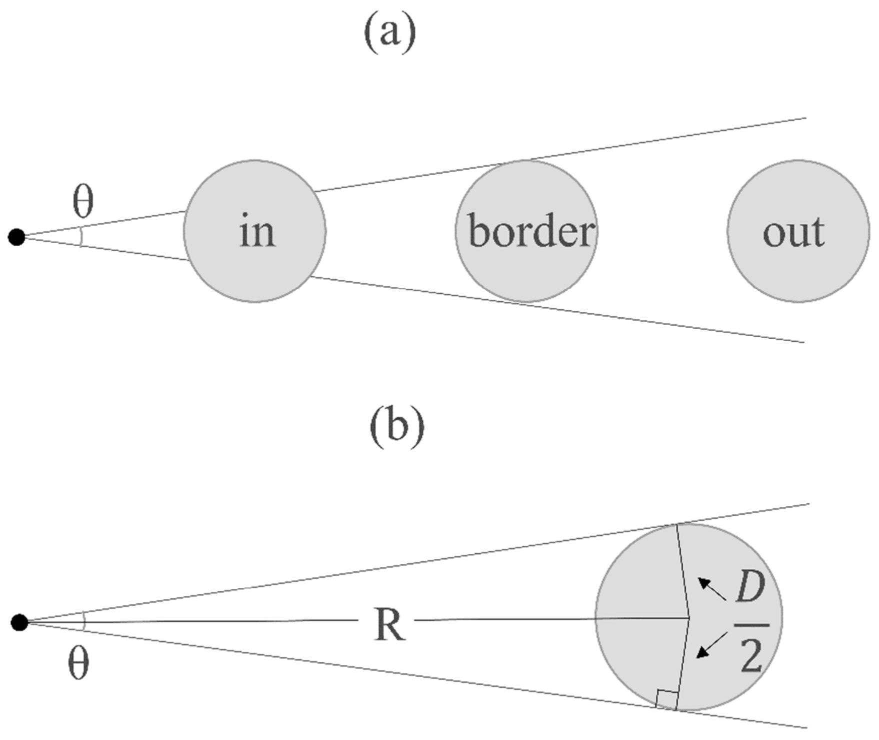

$$\frac{D/2}{R} = \sin(\frac{\theta}{2})$$

Fig. 2.2: Sample geometry. For angle count sampling: (a) overhead view showing “in”, “border” and “out” tree (gray circles represent tree trunks); (b) the relationship between horizontal angle (θ), tree diameter (D) and plot (inclusion zone) radius (R). The BAF determines the fixed horizontal angle θ which was used as the threshold to determine tree status on the spherical images.

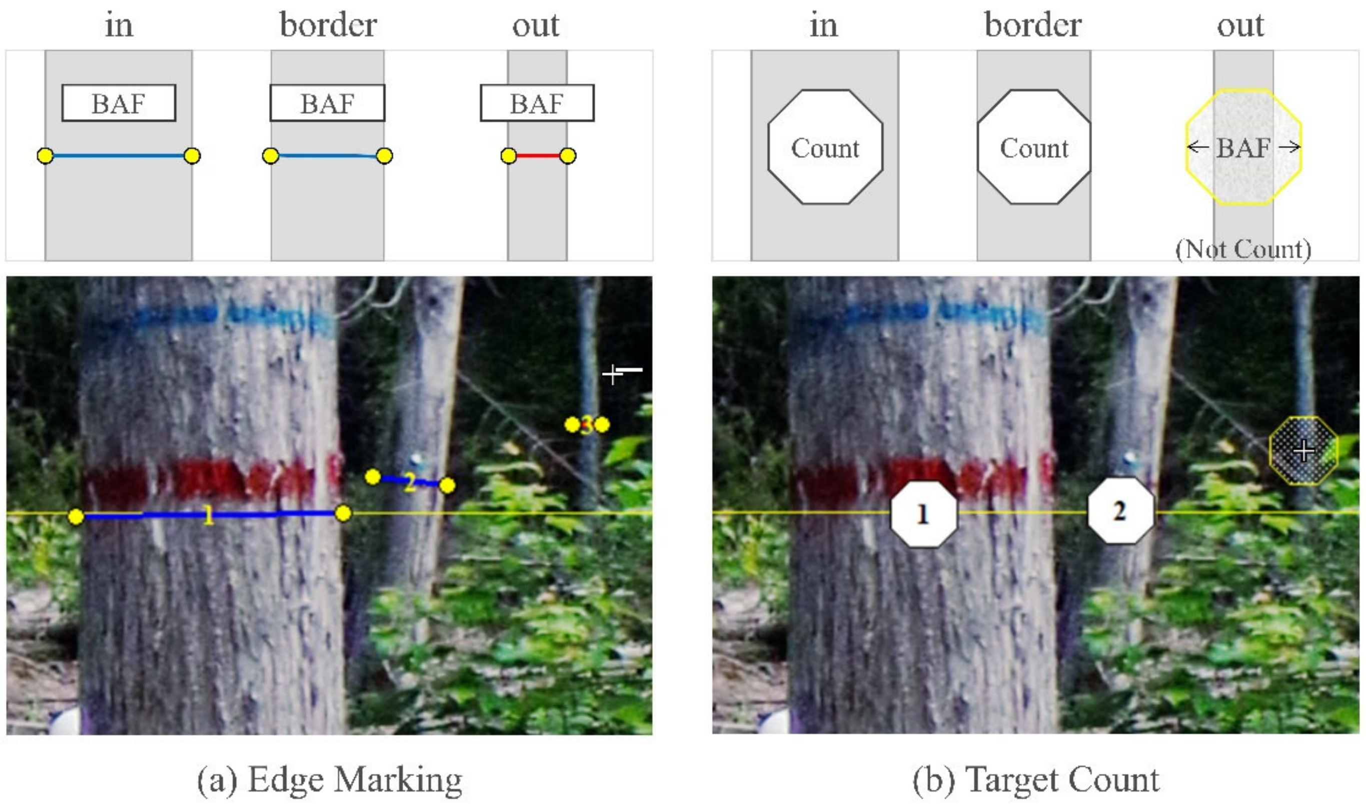

Fig. 2.3: Two image processing methods: (a) Edge marking method – users click on the edges of each tree. A reference bar (the length is based on BAF=1) is used to guide users so that every tree does not have to be marked; the line color indicates tree status based on desired BAF: black = "in", gray = "out"); (b) Target count method - a transparent reference octagon, scaled to the desired BAF is provided to mark "in" trees - "out" trees are those trees smaller than the octagon target and are not marked.

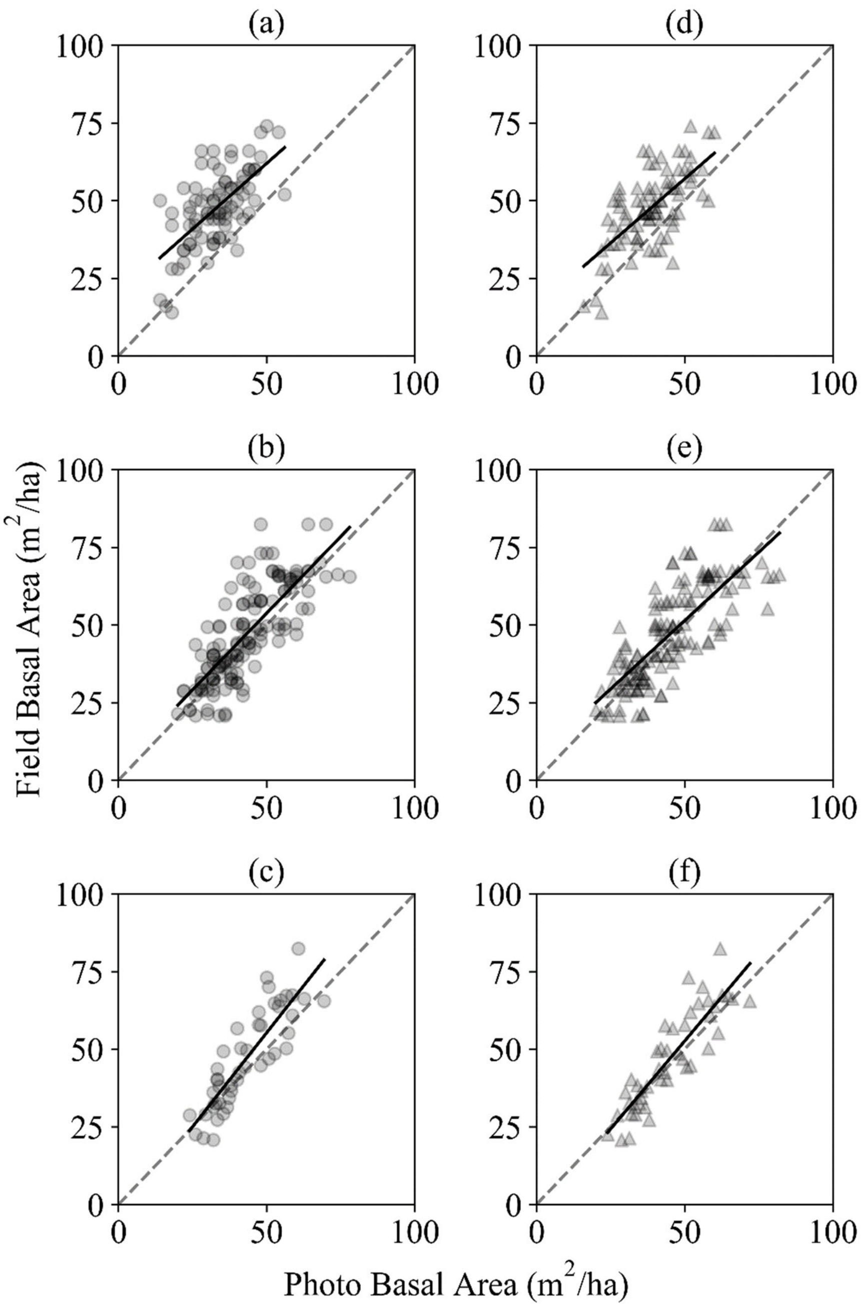

Fig. 2.4: Comparisons between photo estimated basal area (PBA) and field measured basal area (FBA) by digital sample location type (one center versus three individuals versus mean of three individuals) and two tree marking method (target counting (left panels) versus edge marking (right panels)). The one center estimates (a and d) were from the Noonan Research Forest (NRF) and the three estimates per plot (b and e) and mean of three estimates (c and f) were from the Newfoundland (NL) spacing trials.

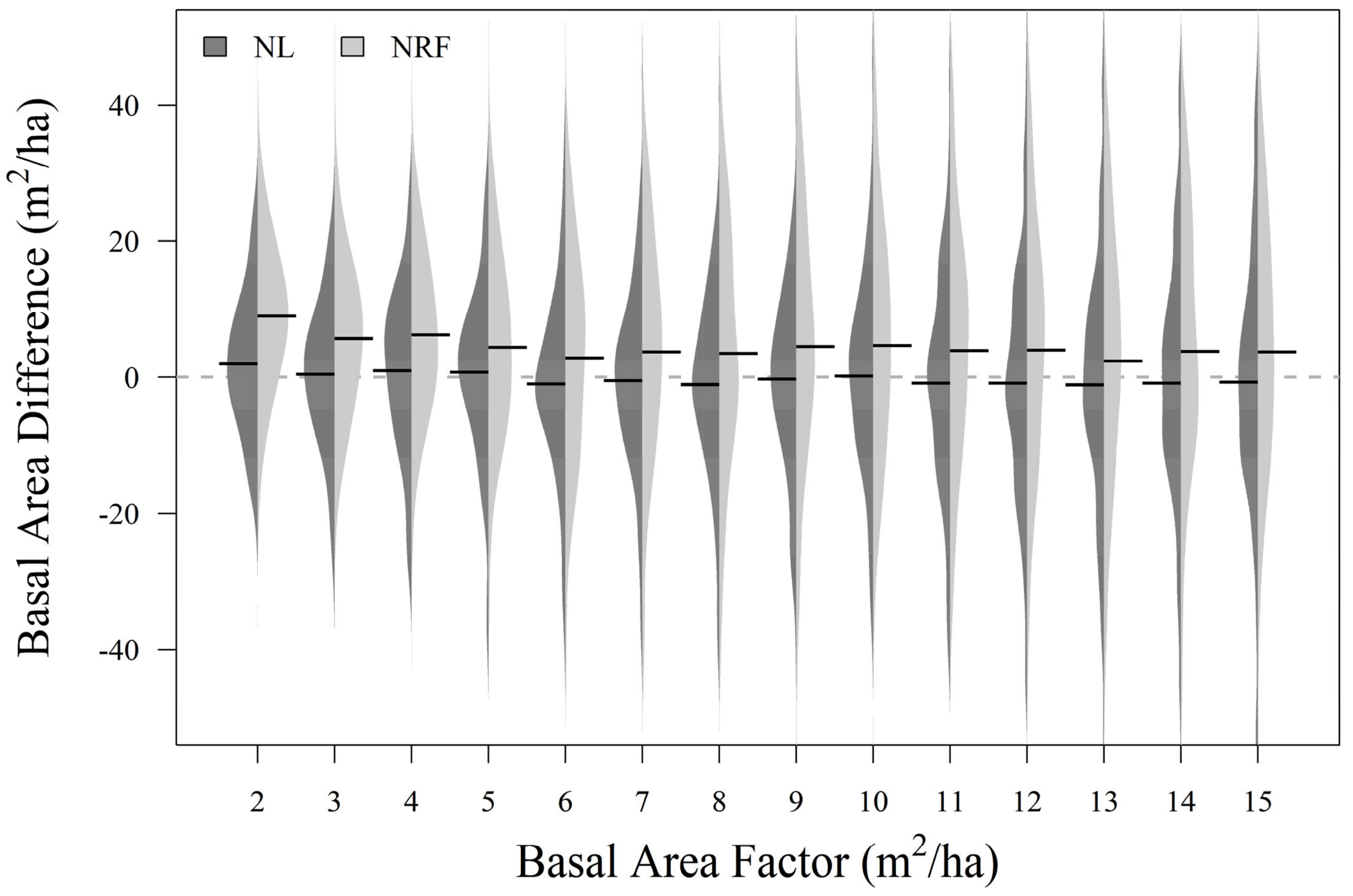

Fig. 2.5: The influence of photo basal area factor (BAF) choice on the basal area difference (field basal area – photo basal area, m^2/ha) for Newfoundland (NL) and Noonan Research Forest (NRF). The black solid line is the mean for each location and the gray dashed line indicates perfect fit

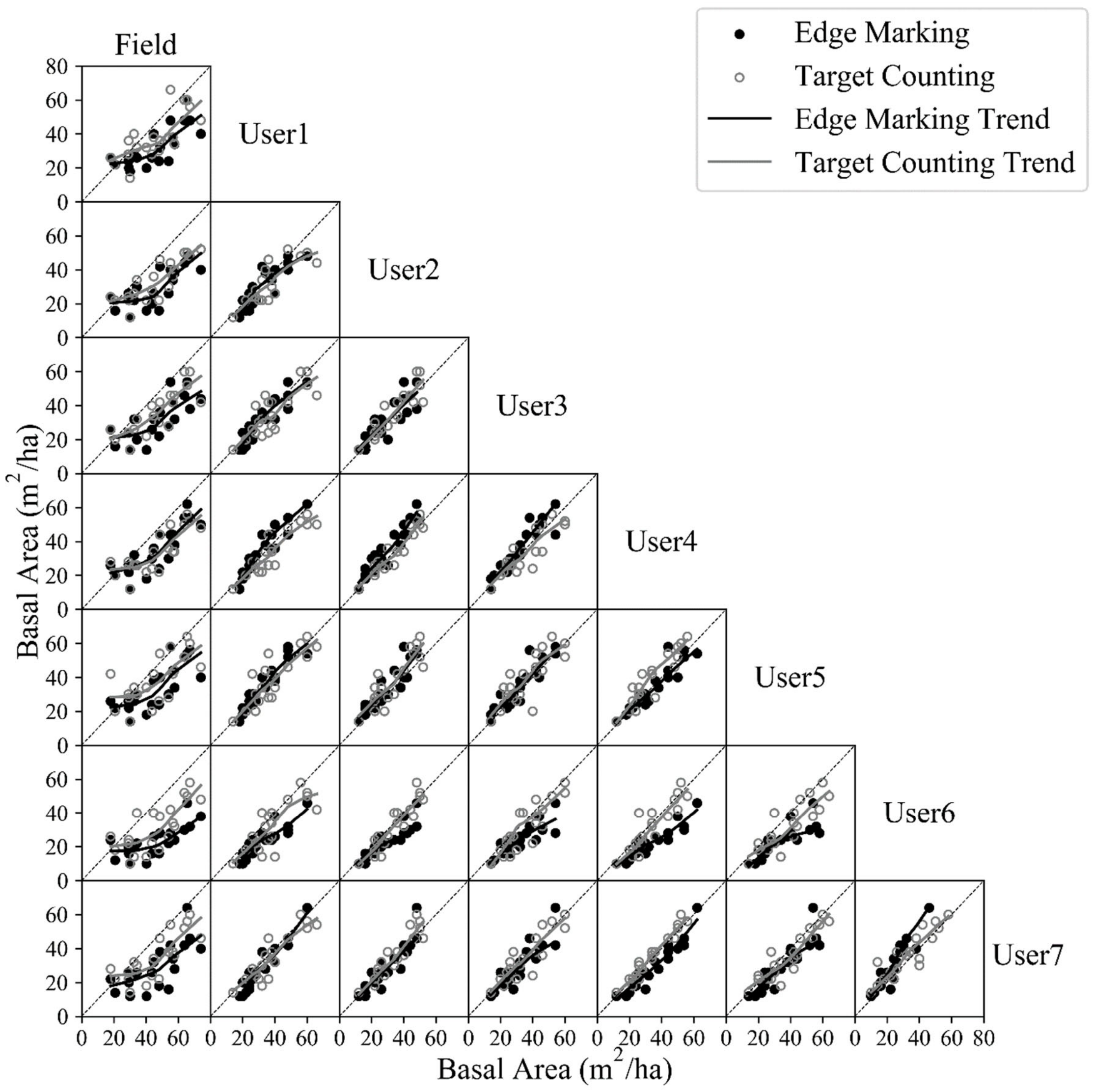

Fig. 2.6: Comparisons between field basal area and photo basal area by two marking methods (edge marking versus target counting) among seven different users. The locally weighted scatterplot smoothing (LOWESS) regression lines show the trends between field measure and photo.

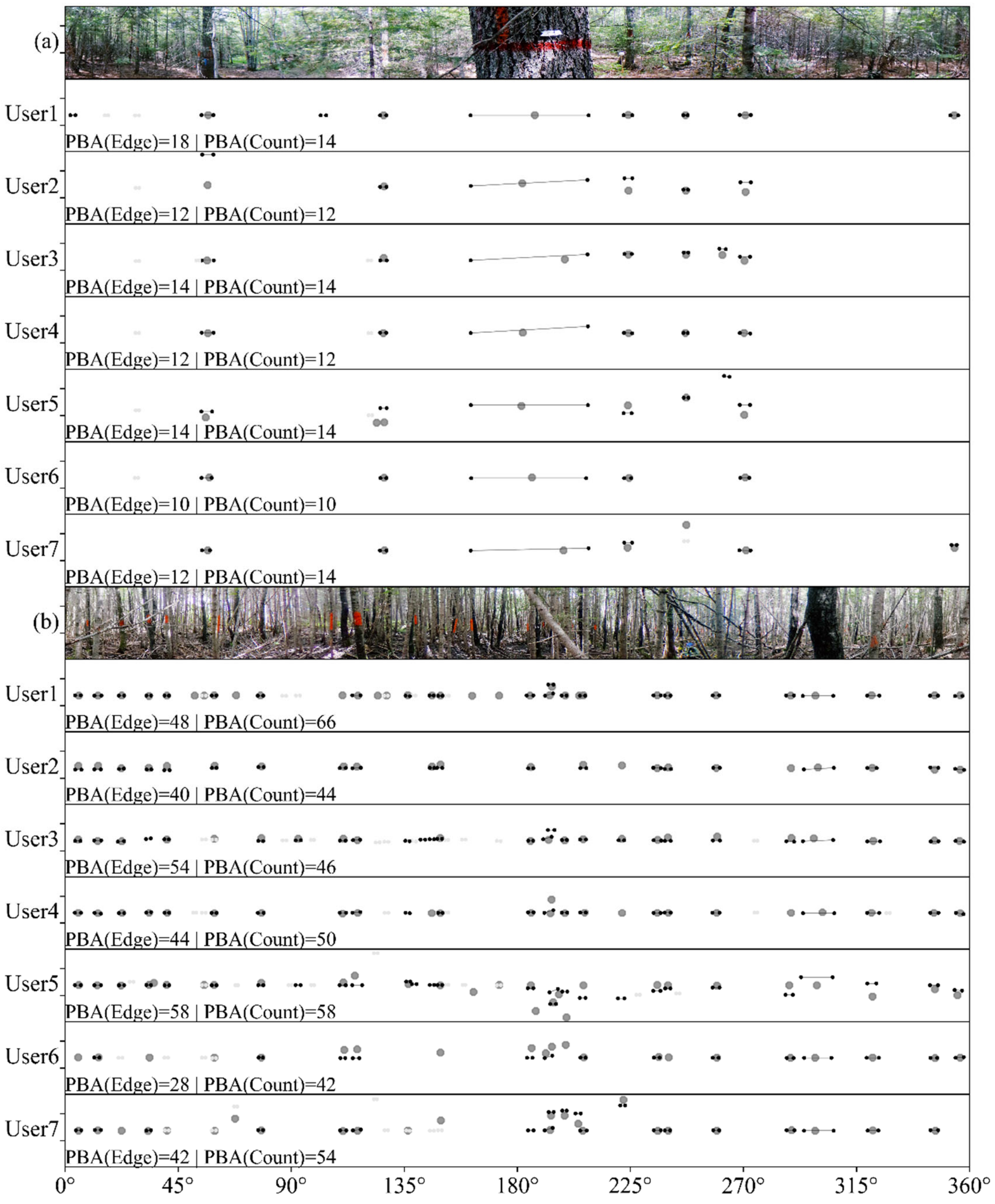

Fig. 2.7: Two plots with the smallest (a) and largest (b) variance among seven users by two tree marking methods (edge marking versus target counting). PBA means photo-based basal area and FBA means field-based basal area. The FBA of (a) is 30 m^2/ha, and FBA of (b) is 55.2 m^2/ha. The small dots are the tree edges that users marked. The black small dot with connected lines means this tree is counted as an “in” tree, while the light gray small dots means it is an “out” tree in edge marking mode. The dark gray octagon is the “in” tree marked in target counting mode.

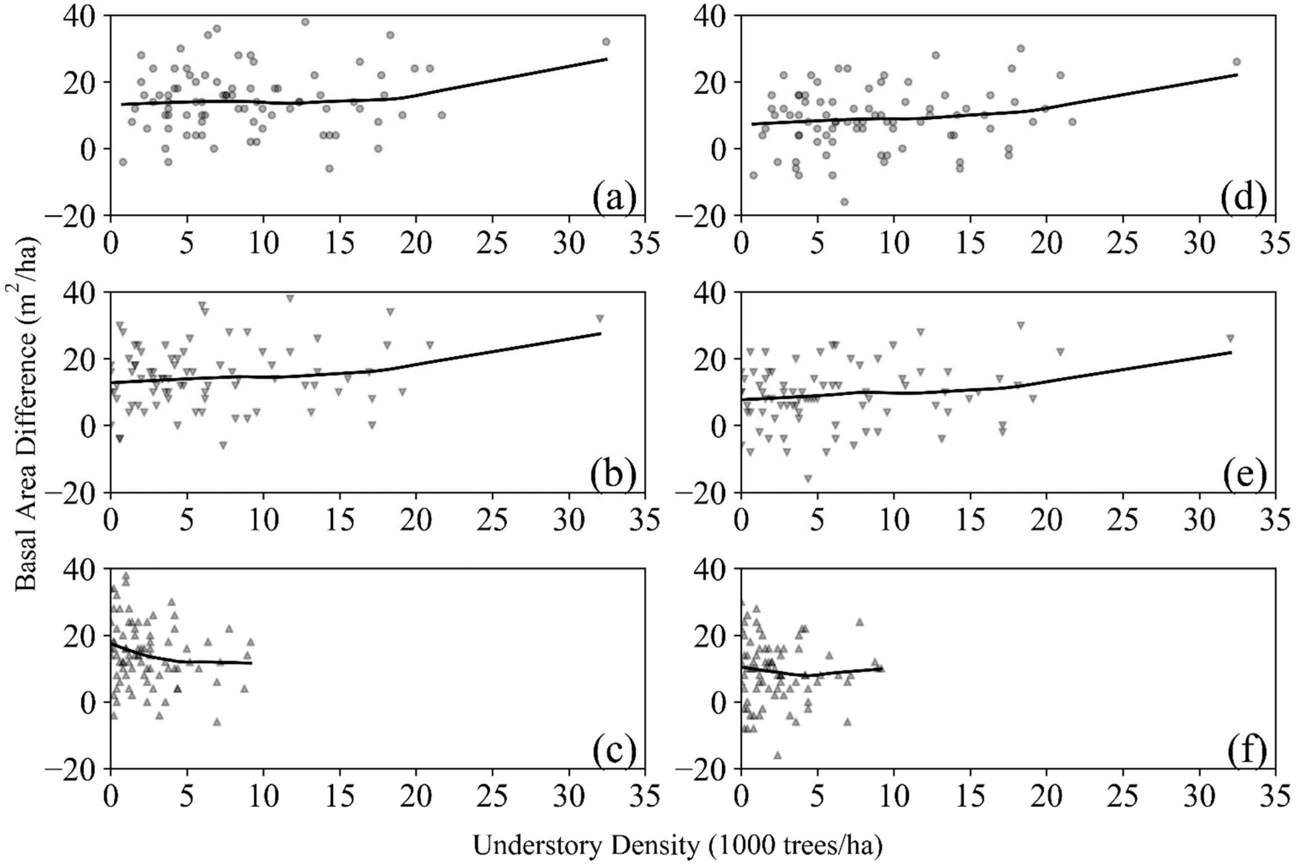

Fig. 2.8: Effects of understory density on the basal area difference (field basal area – photo basal area, m^2/ha) in the NRF plots by two marking methods (target counting (left panels) versus edge marking (right panels)). (a) and (d) are total understory trees, (b) and (e) are understory trees whose height smaller than 1.3 m, while (c) and (f) are those greater than 1.3 m.

Chapter 3: Plant Fraction Calculation from Spherical Images by HSV Color Space

3.1 Introduction

Applications of image analysis in forest inventory can be traced back to the middle of the 20th century. For example, Reineke (1940) used photos to establish a permanent plot record, Shelbourne and Namkoong (1966) developed a method for measuring trunk parameters based on image geometry. Upper canopy information and light conditions were first recorded using a hemispherical camera with a fisheye lens called the Robin Hill camera (Evans and Coombe 1959) which produced a single image by converting a full hemisphere to a circular plane with a polar projection (Coombe and Evans 1960, Rich et al. 1999). Forestry and ecological researchers developed methods to maximize the benefits of hemispherical images and improved and standardized the acquisition, analysis, and interpretation of images using hemispherical photos (Fournier and Hall 2017 p. 2).

Initially, analyses were based on manual processing of film images, and the information extracted from hemispherical photos was primarily used to calculate sunlight penetration and solar radiation through canopy openings (Fournier and Hall 2017 p. 3). Manual processing methods were slow and often subjective. With the advent of the digital camera and personal computer, the technology to process hemispherical photographs developed into a more automated, precise analysis based on the geometric distributions of plant structural elements (Rich 1990, Chen et al. 1991). Analyzing canopy gap information to derive canopy structure became a focus of research in forestry and ecology (van Gardingen et al. 1999, Leblanc et al. 2005, Cescatti 2007). The improvement in image resolution, dynamic range of sensors, and richness of image processing software greatly improved the procedures for hemispherical image acquisition and analysis compared to film-based photography (Chianucci and Cutini 2012, Fournier and Hall 2017 p. 117). Several studies have emphasized the effects of this revolution, especially in terms of image resolution and digitalization (Englund et al. 2000, Inoue et al. 2004).

Currently, image processing software can be separated into two types: commercial software and open source (free or low cost) software. Open source software includes: CAN-EYE (Baret and Weiss 2004), CIMES (Gonsamo et al. 2011), and GLA (Frazer et al. 1999). Commercial software includes: HemiView (Rich et al. 1999), and WinSCANOPY (Regent Instruments Inc. 2018). Several studies have compared different software (Bréda 2003, Jarčuška et al. 2010, Promis et al. 2011, Fournier and Hall 2017 chap. 7). Based on these studies, it is hard to draw conclusions about which is best; it depends on user preference, type of camera, and costs (free or commercial). Batch processing options are often very important (Fournier and Hall 2017 chap. 5). While well-integrated software is convenient to use, the flexibility to adjust to personal requirements and incorporation of new processing algorithms is often limited. As a result, several researchers chose to write their own programs to apply their novel ideas in image processing, including: DHPT (Loffredo et al. 2016), HSP (Lang et al. 2013), and the ImageJ Hemispherical_2.0 extension (Rasband 1997, Beckschäfer 2015).

As Chianucci and Cutini (2012) and Fournier and Hall (2017) summarized, the processing of forest hemispherical images has four main steps: 1) Image acquisition and quality control; 2) Image enhancement (optional); 3) Sky and canopy pixel classification (binarization); and 4) Extraction of attributes from classified binary images.

The first step is to obtain suitable images. Hemispherical images are normally taken in summer when canopies are fully developed. The ideal sunlight conditions are close to sunrise or sunset or when the sky is uniformly overcast (Leblanc et al. 2005). Uneven sky radiance and clouds complicate image analysis (Fournier and Hall 2017 p. 119). Zhang et al. (2005) pointed out that the exposure settings of cameras have great impacts on gaps and its fractional determination. Default auto-exposures often do not yield accurate and consistent gap fraction estimates (Chen et al. 1991, MacFarlane et al. 2000, Zhang et al. 2005). The best exposures for simple classification are set manually to ensure the sky is well diffused and appears almost white and the contrast between sky and plant is maximized (Chen et al. 1991). Generally, the most suitable manual setting is to overexpose images by 1 – 3 f-stops of shutter speed relative to the reference exposure measured in clear sky (Zhang et al. 2005).

The second (optional) step is image enhancement. A common enhancing filter is sharpening based on edge enhancement provided by almost all software packages. Edge enhancement is used to increase the contrast between small gaps and dense canopies. It is most useful for low resolution images containing a large proportion of mixed pixels, which means the pixel includes several different classes (Fournier and Hall 2017 p. 121). Gamma correction is another option. Although digital cameras respond linearly to light (Zhang et al. 2005), most camera software automatically applies a gamma logarithmic transformation to simulate the non-linear behavior of the human eye (Cescatti 2007). Commonly the gamma value of a camera ranges between 2.0 to 2.5 and darkens the midtones of an image. This often worsens the estimates of gaps within canopies (Cescatti 2007). MacFarlane et al. (2007a, 2007b) pointed out that restoring gamma values to 1.0 helps solve the large errors in those images. For cameras that record RAW image formats, the gamma function correction is unnecessary and can be easily transferred to binary images by linear transformation (Lang et al. 2010).

The third step is classification. Because of the importance of thresholding segmentation and pixel classification, this step has been thoroughly investigated over the past few decades, as Wagner and Hagemeier (2006) reviewed. Even though common digital images have three color channels (Red, Green, and Blue, RGB), most studies only use gray-scale values (0-255) from the blue channel for classification (Leblanc et al. 2005, Zhang et al. 2005, MacFarlane 2011). The blue portion of light is absorbed by plant pigments and darkens the foliage in hemispherical photos (Leblanc et al. 2005, Jonckheere et al. 2005). Using a single channel has the additional benefit of avoiding aberrations caused by lens imperfections (Frazer et al. 2001, Leblanc et al. 2002, Fournier and Hall 2017 chap. 5). Six binarization algorithms based on blue channel histograms were reviewed by Glatthorn and Beckschäfer (2014); however, all algorithms were sensitive to overexposure. Exposures need to be strictly controlled when taking images. Beckschäfer et al. (2013) suggested using the camera screen to check histograms in the field to determine whether exposures were suitable or not.

Even though images are well exposed and taken in deeply overcast conditions, luminance heterogeneity always exists (Wagner 1998, 2001, Schwalbe et al. 2006, Fournier and Hall 2017 p. 125). To minimize its effects, instead of using a global threshold in which a single threshold is applied to an entire image, different regional thresholds are applied to parts of images according to the zenith and horizon angles (Wagner 1998, Leblanc et al. 2005, Fournier and Hall 2017 p. 127). Appling different thresholds for different canopy densities has been explored as well (MacFarlane 2011). However, these optimization algorithms narrowed their attention to only blue channel information, rather than considering full color information and textural differences between sky and canopy.

With the development of computer vision algorithms, some novel algorithms such as edge detection (Nobis and Hunziker 2005, Glatthorn and Beckschäfer 2014) and integrated RGB channels with different weights based on brightness obtained by hue values (Loffredo et al. 2016) or external light sensors (Zhao and He 2016) have displayed better tolerance to overexposure. Converting RGB color space to HSV (hue, saturation, and value) color space (Riaz et al. 2008) is another option, For example, Chumuang et al. (2016) used hue ranges from 110 to 130 (255 maximum) to classify green leaves and white background while Yang et al. (2015) used an HSV decision tree to classify green vegetation from soil background. However, both HSV methods were applied to a common digital camera image. Based on our current literature search, this classification method has not been applied to hemispherical images.

The fourth step is extracting canopy attributes from classified binary images. This is a standard procedure for many hemispherical image analysis software packages. Attributes, such as canopy closure, gap fraction, canopy openness, and so on, are well defined by Gonsamo et al. (2013). However, for fisheye cameras, two things need consideration: projection distortion and lens vignetting (Fournier and Hall 2017 chap. 5). Projection distortion occurs when the fisheye lens does not conform, or strictly conform, to perfect polar or equidistant projection due to manufacture defects (Herbert 1987). In these cases, additional calibration is required (Frazer et al. 2001). Lens vignetting is due to the structure of the fisheye camera, the wide aperture always results in gradual light fall-off near the outer image edges. Although this can be improved by applying correction algorithms, the light conditions are difficult to correct to true values (Wagner 1998, 2001, Schwalbe et al. 2006).

The new 360-degree spherical cameras offer an inexpensive option for obtaining full spherical stand information with one exposure. The friendly price and compact size make it an easy-to-use tool in the forest and may be an acceptable alternative to traditional fisheye cameras. The purpose of this chapter is to explore whether spherical cameras can be used to extract canopy information and whether a novel HSV threshold can produce similar, or even enhanced, classification results compared to traditional blue channel-based classification algorithms. Specific objectives include: 1) propose a global HSV classification threshold to classify images into three classes: sky, foliage, and wood; 2) compare the new HSV threshold with a blue channel-based minimum threshold as implemented by ImageJ Hemispherical_2.0 extension (Beckschäfer 2015); 3) compare hemispherical and cylindrical projections of spherical images using the HSV threshold technique and analyze the consistency between projections.

3.2 Methods and Materials

3.2.1 Study sites

There were two different sites used in this study. The first site was three early spacing trails located in western Newfoundland (NL). These sites (Cormack, Pasadena, and Roddickton, Fig. 3.1) were dominated by balsam fir (Abies balsamea) with minor components of black spruce (Picea mariana) and other boreal species. The trials were established in the early 1980's. At each trial, there were three replicates of five spacing treatments: Control (no spacing), 1.2m, 1.8m, 2.4m, and 3.0m average spacing. Because of the early spacing treatments, the NL plots are even-aged, single stratum stands with relatively uniform stand structure.

The second site was the Femelschlag Research Study located on the Noonan Research Forest (NRF) in central New Brunswick, Canada (Fig. 3.1). The NRF plots were composed of a variety of stand types from pure coniferous stands to mixed hardwood-softwood stands. Because of the variety of stand types, the NRF plots were much more structurally diverse. A permanent 100m by 100m inventory sample grid was overlaid on the NRF in 1999. The 83 grid intersections within the Noonan Femelschlag Research Study were used in this study. Table 3.1 summarizes the species composition across the two study areas.

3.2.2 Digital data acquisition

A Ricoh Theta S (Ricoh Imaging Company, LTD. 2016) spherical camera was used to capture spherical images. Four single spherical images were captured at four different heights (1.6m, 2.6m, 3.6m, 4.6m) at each digital sampling point (Fig. 3.2.a) using a height pole (Fig. 3.2.b). On the NL sites, three digital sample points per replicate plot were used. Digital sample points were located at half the plot radius at azimuths of 360°, 120°, and 240°. Plot radii varied by spacing treatment: Control (5.2m);1.2m (7.2m); 1.8m

(10.4m); 2.4m (15.0m); 3.0m (18.0m). On the NRF plots a single digital sampling point was located at plot center (Fig. 3.2.a).

Although the spherical camera records a 3D image, the image is stored as a 2D digital image based on cylindrical equidistant projection using on-board camera software. The resolution of the projected 2D cylindrical images was 5367 pixels in width and 2688 pixels in height.

3.2.3 Image processing methods

Even though hemispherical cameras take full 360°/180° images, because of the projection distortion (Blennow 1995), resolution considerations (Leblanc et al. 2005), light degradation (Wilson 1963, Wagner 1998, Schwalbe et al. 2006), and biological considerations (lower parts of stems dominate more than canopy foliage) only the higher zenith angles of the hemispherical images were used. Based on these previous studies, *Plant fraction* (PF), in this study, was defined as the fraction of the image occupied by plant pixels within a 57.5° zenith angle after distortion calibration ($PF_{57.5}$) rather than using the full 90° hemispherical images. (Weiss et al. 2004, Jonckheere et al. 2005).

Two different approaches to calculate PF were developed in this study, the general workflow is shown in Fig. 3.4. One approach converted cylindrical images to hemispherical images first, then applied common fisheye processing methods (***hemispherical approach***), the other approach directly applied a weight function to classified cylindrical images (***cylindrical approach***). The hemispherical approach was good for comparing the new method with traditional image processing methods, while the cylindrical approach was more efficient for image processing.

3.2.3.1 Hemispherical Approach

There were three steps to estimate plant fraction from spherical images in this approach: 1) conversion from the stored cylindrical image to a hemispherical image; 2) distortion correction; and 3) threshold classification.

1) Image Transformation

The 3D spherical images were stored as 2D cylindrical images. To transform the cylindrical image to a hemispherical image, the spherical coordinates were required as an intermediate transformation. For a given point, C(x_i, y_i), in the x-y pixel coordinate system of the cylindrical image (Fig. 3.4.a), the related zenith angle (φ_i) and azimuth angle (λ_i) within the 3D spherical coordinate system (S, Fig. 3.4.b) was calculated using (Aghayari et al. 2017):

$$S(\lambda_i, \varphi_i) \Rightarrow \begin{cases} \lambda_i = (X - x_i) \times \dfrac{2\pi}{X} \\ \varphi_i = \left(y_i - \dfrac{Y}{2}\right) \times \dfrac{0.5\pi}{Y} \end{cases} \tag{3.1}$$

where X was the cylindrical image width in pixels (5367 pixels for the images used in this study) Y was the cylindrical image height in pixels (2688 pixels for the images used in this study); x_i is the horizontal pixel coordinate; and y_i is the vertical pixel coordinate (Fig. 3.4.d). The zenith angle (φ_i) ranged from -π/2 (-90°) to π/2 (90°) while the azimuth angle (λ_i) ranged from 0 (0°) to 2π (360°).

The points in spherical coordinates (S, Fig. 3.4.b) were then projected to hemispherical coordinates (H, Fig. 3.4.c) using:

$$H(m_i, n_i) \Rightarrow \begin{cases} m_i = \frac{Y}{2} + \sin(\lambda_i) \cdot r_i \\ n_i = \frac{Y}{2} + \cos(\lambda_i) \cdot r_i \end{cases} \tag{3.2}$$

where r_i is the radius from fisheye center to the projected point:

$$r_i = \frac{Y}{2} \cdot \frac{0.5\pi - \varphi_i}{0.5\pi} \tag{3.3}$$

Duplicate pixels in the converted hemisphere image (for example, all pixels in the first line of the original cylindrical image were converted to one center pixel in hemispherical image), were averaged as the final pixel value in the hemisphere image. For pixels in converted hemispherical images with no values (holes), the average value of the eight-neighbor pixels was used.

2) Distortion correction

As shown in Fig. 3.4.c, the projected hemispherical images had distortion (note how the edges of the ceiling light fixtures curve). To correct the distortion, an equisolid distortion correction method (Hughes et al. 2010) was applied:

$$r_i' = \frac{X}{2\sqrt{2}} \cdot tan\left[2 \cdot arctan\left(\frac{r_i}{\frac{\sqrt{2}X}{2}}\right)\right] \tag{3.4}$$

the distortion corrected point $\mathrm{H}'(m_i', n_i')$ in hemispherical coordinates (Fig. 3.4.d) was then equal to:

$$H'(m_i', n_i') \Rightarrow \begin{cases} m_i' = \frac{Y}{2} + \sin(\lambda_i) \cdot r_i' \\ n_i' = \frac{Y}{2} + \cos(\lambda_i) \cdot r_i' \end{cases} \tag{3.5}$$

The procedures for averaging duplicates and filling holes were the same as those in previous step.

3) Threshold classification

In this step, the HSV color space threshold is applied to classify the pixels into three classes (foliage-green; wood-red; and sky-blue; 3 color image) or two classes (plant-white; sky-black; binary image). Unlike RGB color space that uses the three primary colors (red, green, blue) to combine into a new color, the HSV color space uses attributes of hue, saturation, and brightness (value) to represent colors (Hanbury and Serra 2002).

The main benefit of using HSV color space was that it was easier to use simple linear boundaries (rectangles) to distinguish different classes such as sky pixels in different weather conditions and foliage pixels (Fig. 3.3). The thresholds applied in this study were Clear Sky (S1): ($0.5<h<0.68$, $0.45<s<1$, $0.75<v<1$), Diffused Sky (S2): ($0.48<h<0.61$, $0.15<s<0.45$, $0.85<v<1$), Cloudy Sky (S3): ($0<h<1$, $0<s<0.15$, $0.88<v<1$), and Foliage (F): ($0.17<h<0.48$, $0.15<s<0.45$, $0.2<v<1$). The remaining space was assumed to represent woody plant parts.

After pixel classification, hemispherical plant fraction (HPF), was calculated as the proportion of pixels covered by plants (foliage and wood):

$$HPF = \frac{count\ of\ plant\ pixels}{count\ of\ all\ pixels} \tag{3.6}$$

Similarly, hemispherical wood fraction (HWF) or hemispherical foliage fraction (HFF) was obtained by counting wood pixels or foliage pixels and dividing by total pixels.

3.2.3.2 Cylindrical Approach

The hemispherical approach was suitable for producing images to be used in traditional fisheye analysis software, however, it was possible to estimate PF directly from the cylindrical images without coordinate conversion. The procedure applied the

HSV classification algorithm directly to the cylindrical image and determined PF for each pixel line (CPF$_l$, cylindrical plant fraction of line l). Total CPF was then obtained by summing the CPF$_l$ multiplied by a weight that represented a functional transformation from row length to hemispherical annulus.

The classification procedure was the same as for the hemispherical approach described above, just applied directly to the cylindrical image. The weight of row l was calculated based on the relative area of the annulus of the circle at row l.

$$w_l = \frac{A(l) - A(l-1)}{A(859)} \cdot \tag{3.7}$$

where A(l) was the area of the hemispherical circle at row l, and $A(l) = \pi \cdot (r_l')^2$. In this equation, r_l' was the corrected hemispherical radius at row l $\left(l \xrightarrow{Eq.\ (3.1)} \varphi_l \xrightarrow{Eq.\ (3.3)} r_l \xrightarrow{Eq.\ (3.4)} r_l'\right)$. 859 is the row number of 57.5° zenith angle in this study ($\frac{Y}{2} \cdot \frac{57.5}{90} = \frac{2688}{2} \cdot \frac{57.5}{90} = 858.6$), so l_{859} is the circle boundary in hemispherical images and maximum row in cylindrical images.

The cylindrical plant fraction, CPF, was then calculated:

$$CPF = \sum_{l=1}^{859} CPF_l \cdot w_l \tag{3.8}$$

Similarly, cylindrical wood fraction (CWF) or cylindrical foliage fraction (CFF) can be obtained using the same process.

The hemispherical approaches and cylindrical approaches are quite different. The cylindrical approach is quite similar with the most common approaches applied by several fisheye analysis software: plant fraction is estimated by dividing the image into several zenith *annuli* and azimuthal *sectors* (Fournier and Hall 2017 p. 133). The PF in each sector is calculated and given a corresponding weight determined by a calibration algorithm. The total PF (within 57.5° zenith angle) is obtained by summing all of the sector PFs multiplied by their associated calibration weight. However, for the hemispherical approach, the calibration function is applied first, then the classification algorithm is used to create binary images. Which means, the hemispherical approach measures PF at the pixel-level, while the common methods and cylindrical approach applies calibration weight at the sector (or annulus) level.

3.2.4 Data analysis

We did not have access to a standard fisheye camera, so we are unable to compare 360° photos to standard hemispherical photos. Our analyses will instead focus on two aspects: 1) Comparison of the HSV classification method proposed here with the commonly used Blue-channel thresholding method; and 2) Comparison of PF estimated from cylindrical photos (CPF) to estimates from hemispherical photos (HPF).

3.2.4.1 Comparison of classification methods

We used two analyses to examine differences between the HSV classification method and the Blue-channel threshold method. For estimation of leaf area index, photography is generally restricted to a few hours in the morning and late afternoon or when sky conditions are uniform (Leblanc et al. 2005). This greatly limits the application of this technology in operational forest inventories. The HSV method should provide a greater range of conditions over which photography can be obtained and correctly classified.

The first analysis examined a series of photographs taken at the NL and NRF sites. The cylindrical photos were re-projected as hemispherical images (hemispherical approach) and the HSV classification method applied to estimate plant fraction (HPF), as described above. The re-projected hemispherical images also were used as input into the Hemispherical 2.0 ImageJ extension (Rasband 1997, Beckschäfer 2015), and a blue channel thresholding plant fraction estimate (BPF) obtained. The two PF estimates were compared using 1:1 scatterplots and locally weighted scatterplot smoothing (LOWESS) regressions. The photos were then visually classified by overall exposure level and presence of sunspots. Examples of extreme classification deviations were identified and performance of the two classification methods visually assessed using paired classification images.

The first analysis allows for a broad comparison of the classification methods but does not provide quantitative measures to judge which method performs better. In many remote sensing classification studies, the classifications resulting from algorithms are often compared to manual classification (Congalton 1991, Rau et al. 2011, Feng et al. 2015). However, manual classification is time consuming, since each pixel needs to be visually assessed and its class manually determined and marked on the images.

To reduce the time required to manually classify images, selected portions of photos were identified to represent contrasting classification challenges: 1) simple sky conditions (pure white clouds or pure blue sky) versus variable sky (blue sky and white clouds mixed); 2) ideal light conditions (diffuse light with uniform sky conditions) versus bright sunlight (overexposure); and 3) heterogeneity of light with some dark (underexposed) areas. Seven photo segments which were considered representative of different image features were selected and clipped from the hemispherical transformed images for classification. This merged image was then classified using the HSV method and the blue-channel (BC) method. The image also was manually classified using pixel by pixel assessment in GIMP (Gimp 2008). In the manual classification, each pixel was classified as either sky, foliage, or wood. The manual classification results were viewed as the "true" classification value.

Error matrices (Fig. 3.5.c) were created to summarize the number of pixels correctly classified between algorithm classified results and manual classified results. The producer's accuracy of each class (PA$_i$), average accuracy (AA), overall accuracy (OA), and Kappa coefficient were derived from the error matrices and used to evaluate classification accuracy (Congalton 1991).

The PA$_i$ attribute was the evaluator for accuracy of class *i*, it can be calculated by the following equation:

$$PA_i = \frac{n_{ii}}{n_{i\cdot}} \tag{3.9}$$

where n_{ij} is the number of pixels of class *i* in the manual classification classified as class j by the classification algorithm (thus n_{ii} is the number of correctly classified pixels in class i – the diagonal of the error matrix), and $n_{i\cdot} = \sum_{j=0}^{k} n_{ij}$ is the total number of class *i* pixels in manual classified image ($n_{1\cdot}$ is 15).

The other attributes (AA, OA, Kappa) can be used as the evaluator for whole images. **AA** is the average of individual class accuracies and was calculated using:

$$AA = \frac{\sum_{i=0}^{k} PA_i}{k} \tag{3.10}$$

where k is the number of classes, **OA** is the average of individual accuracies weighted by class sample size; it was defined as follows:

$$OA = \frac{\sum_{i=0}^{k} (PA_i \times n_{i\cdot})}{n_{\cdot\cdot}} = \frac{\sum_{i=0}^{k} n_{ii}}{n_{\cdot\cdot}} \tag{3.11}$$

where $n_{\cdot\cdot}$ is the number of all pixels ($n_{\cdot\cdot} = 36$ in this case).

By definition, the higher OA or AA is, the more pixels are correctly classified; however, misclassified pixels are not considered. The Kappa coefficient (K) is a measure of classification accuracy that accounts for all combinations of classifications (Congalton 1991). K was calculated using Bishop et al. (1975):

$$K = \frac{n_{\cdot\cdot} \cdot \sum_{i=1}^{k} n_{ii} - \sum_{i=1}^{k} (n_{i\cdot} \cdot n_{\cdot i})}{n_{\cdot\cdot}^2 - \sum_{i=1}^{k} (n_{i\cdot} \cdot n_{\cdot i})} \tag{3.12}$$

Higher K means higher similarity. While the seven photo segments were merged into a single image for classification, each segment was analyzed individually for classification accuracy. For comparing classification methods, a two-level classification (sky vs plant) was used.

3.2.4.2 Hemispherical versus cylindrical images

The PFs obtained from the field images using the hemispherical approach (HPF) and the cylindrical approach (CPF) were compared using a simple linear regression:

$$HPF = b_0 + b_1 \cdot CPF \tag{3.13}$$

If the cylindrical approach is the same as the hemispherical approach, then b_0=0 and b_1=1. The parameters were evaluated using Bonferroni-adjusted alpha levels (Zar 2009). Plant fraction (HPF vs. CPF), foliage fraction (HFF vs. CFF) and wood fractions (HWF vs. CWF) were evaluated.

3.3 Results

3.3.1 Classification algorithm comparison

There was a total of 957 images between the NL sites and the NRF site. Figure 3.6 shows the relationship between HPF and BPF. As can be seen in Fig. 3.6, the HSV classification (HPF) consistently produced higher estimates than the blue channel classification (BPF). In general, the NL values were closer than the NRF values. For both sites, as PF increased, the differences between HSV and blue-channel generally decreased (Fig. 3.6).

Sunflecks greatly affected the classification (Fig. 3.7), especially for the blue-channel method. The blue-channel method overclassified sky in high light conditions, and in one extreme case, the entire image was classified as sky.

For the seven image segments, the manual visual classification and the three autoclassification results are shown in Fig. 3.8. In general, the HSV 3 class method failed to classify most foliage correctly. Foliage seems to be better classified when the background sky is blue rather than white (compare the left-hand side of Figure 3.8 d-3 to the right hand-side). Overall, the HSV 2 class method appeared to works good in all but the lowest, most diffused light conditions (Fig. 3.8 g-4). The blue-channel method did not perform very well in bright light conditions (Fig. 3.8 c-5, e-5, and f-5) nor when woody plant parts were brightly lit (Fig. 3.8 b-5); however, in low, diffuse light conditions (Fig. 3.8 g-5) it performed much better than the HSV method.

The classification accuracy statistics confirm these results (Table 3.2). AA, OA, and K were all larger for HSV-2 than for BC-2 with the exception of image segment (g) – the low, diffuse light segment. The HSV-3 was not as accurate as the HSV-2 (Table 3.2), this was primarily due to the poor classification of foliage across all seven image segments (Table 3.3)

3.3.2 Cylindrical versus hemispherical image plant fraction estimates

Fig. 3.9 shows the relationship between PF from cylindrical images (CPF) versus PF from hemispherical images (HPF). Correspondence between all four fractional components was very high. The resulting regression fits and associated goodness-of-fit statistics are shown in Table 3.4. The high r^2 values (0.99) and low root mean square errors (rMSE) indicate strong linear relationships between the two image types. All b_0's were nearly equal to 0.0 and all b_1's were nearly equal to 1.0 (because of the large number of observations and strong linear trends, the standard errors of the parameter estimates were very small, thus making small differences statistically "significant", but of no importance to the assessment of equivalent estimates).

3.4 Discussion

The results here show the potential for using a 360° spherical camera to estimate PF as is currently done using more costly hemispherical cameras. The spherical images stored as cylindrical projections can be easily re-projected to hemispherical images using the coordinate transformations described in this study. These photos can then be processed using any package that processes hemispherical photos. We demonstrate this using Hemisphere 2.0 (Beckschäfer 2015) in ImageJ (Rasband 1997).

We did not compare our results with those obtained from a normal hemispherical camera; However, the results we obtained are comparable to those published by others.

For our NL plots which were boreal conifer stands, the mean PF is 68.93% ± 9.40% and with minimum 15.22% and maximum 86.61%. For related pure conifer studies, Smolander and Stenberg obtained mean plant fractions of 67% in one Scots pine (*Pinus sylvestris*) stand (2001). For *pinus tabulaeformis* and *Larix principis-rupprechtii* stand, the mean PF was 85.69% and 79.82% respectively (Sang et al. 2008). For a mixed conifer stand that included red fir (*Abies magnifica*), white fir (*Abies concolor*), Jeffrey pine (*Pinus jeffreyi*) and Lodgepole pine (*Pinus contorta*), the average PF was 65% and ranged from 43% to 78% (Musselman et al. 2012). Stenberg et al. also reported for a Norway spruce forest, the natural canopy density (similar definition of PF in this study, equals to 1 - openness) ranged from 10% to 77%, while the fertilized canopy ranged from 25% to 93% (1999). For our NRF plots which were mixed species forests, the mean PF value was 70.96% ± 9.94% and ranged from 11.60% to 85.61%. Souza et al. (2008) reported that PFs in mixed forests collected by 525 random points ranged from 83.7% to 95.8% with mean value of 89.2% ± 1.5%. Several studies report values that were not very close to our results because they used the full 90° zenith angle while our study using 57.5° zenith angle which is more effective for canopy estimation (Jonckheere et al. 2005, Pekin and MacFarlane 2009, Gonsamo et al. 2013). Future work should include a direct comparison with dedicated hemispherical cameras to clearly assess differences between spherical and hemispherical approaches.

In addition to the re-projected images being comparable, we show that nearly identical PF values can be obtained directly from the cylindrical projections provided the projection weights are applied to the latitudinal PFs (Fig. 3.9). The ability to obtained PFs from the cylindrical projections reduces the image processing time and preserves the full resolution of the 360° images (5367 by 2688 in the cylindrical space and 2688^2 in the hemispherical space). In addition, the cylindrical photos can be used to obtain other forest attributes useful for forest inventory such as basal area (Wang et al. Under review; Chapter 2, this thesis) and sum of height^2 (Hsu 2019). These parameters coupled with PF may be used to select forest inventory plots (Hsu 2019) or to estimate stand-level parameters such as volume or biomass.

The HSV thresholding method was able to obtain total PF estimates comparable with the commonly employed blue-channel thresholding method (Figs. 3.7 & 3.8). The PF values obtained using HSV thresholding were almost always larger than those obtained using the blue-channel thresholding (Fig. 3.7) especially on over-exposed images. The results obtained from the manual classified image segments suggest that the HSV method is more accurate than the blue-channel method except in low, diffused light conditions (Fig. 3.8, Table 3.3). Though ImageJ used the minimum threshold algorithm, which proved the most accurate in well exposed images, the sensitivity of single blue channel histogram to overexposure is unavoidable (Glatthorn and Beckschäfer 2014), because this minimum thresholding algorithm is based on the assumption of well diffused light conditions (one peak at the minimum, zero, gray value) and its histogram shape character. The overexposed images had blue channel histograms that were distorted to a distinct peak around the maximum value (Beckschäfer et al. 2013) and did not follow the ideal shape.

Initially, it was hypothesized that the HSV thresholding would be able to distinguish foliage from wood; however, these results were very poor (Fig. 3.8 and Table 3.4). One possible solution is setting different thresholds for different brightness (or canopy densities) in different horizon angle regions of individual images (Wagner 1998, Leblanc et al. 2005, MacFarlane 2011), or dynamically and automatically adjusting thresholds (Glatthorn and Beckschäfer 2014, Fournier and Hall 2017 p. 125). Almost all auto-thresholding algorithms are based on the histogram shape of the blue channel, which can be easily affected by overexposure that frequently occurs in auto-exposed photographs (Glatthorn and Beckschäfer 2014), the idea of auto-adjusting in these algorithms can be achieved by fitting general image brightness to suitable HSV thresholds. In addition to adjusting threshold values, edge detection algorithms, which are based on image texture (Nobis and Hunziker 2005); the gamma function correction, which shows more accurate than common histogram algorithm (MacFarlane et al. 2007b); and applying RGB channels by different weight (Loffredo et al. 2016, Zhao and He 2016) may address this issue as well.

The HSV thresholding method allows for greater range in exposure than the blue-channel method, thus extending the time of day for which quality photos can be obtained. However, even with the extended exposures, best results were obtained in uniform overcast sky, such as sunrise, sunset, or cloudy weather (Leblanc et al. 2005). We did not attempt to control the exposure of these images. Not only for higher efficiency and convenience in data collection, but also those well controlled image exposures are almost dark or binary, and have low compatibility with other attribute measurements such as wood and foliage fraction (this chapter), stand basal area (Chapter 2), and individual tree DBH, HT, and position mapping (Chapter 4). Also several, hemispherical studies use automatic exposure. As reviewed by Beckschäfer et al. (2013) in 61 publications using hemispherical images, there were 13 studies that clearly stated using auto-exposure, 20 studies did not state this but have high possibility of using default auto-exposure. Eleven studies used 2-3 EVs higher than reference open areas as suggested by Zhang et al. (2005), eight studies used other exposure settings compared with reference open areas, and five studies took several different exposures in the field and picked the best to analyze. Additional work examining exposure control may enhance the results obtained here.

For future work, several suggestions are recommended: 1) Taking brightness into consideration, the Z axis should be automatically adjusted by individual exposure to avoid misclassification in Fig. 3.8.g; 2) Update current Ricoh Theta S (Ricoh Imaging Company, LTD. 2016) to Ricoh Theta Z1 (Ricoh Imaging Company, LTD. 2019), which can provide finer resolution (6720 × 3360) and RAW image formats. Higher resolution can produce fewer mixed pixels and their effects (Blennow 1995, Glatthorn and Beckschäfer 2014). The RAW image format is not affected by gamma function and can be converted to images that are easier to classify (Lang et al. 2010).

3.5 Conclusion

In this study, a 360° spherical camera was applied to estimate plant fraction, an important canopy attribute. The resulting re-projected hemispherical photos could be used in existing hemispherical image processing software to estimate plant fraction and the values obtained were similar to those reported by others for similar forest types. A novel HSV color space thresholding method was developed to classify sky, wood and foliage pixels and compared with a traditional single blue channel based minimum thresholding classification algorithm implemented in ImageJ Hemispherical_2.0

extension. Based on manual classification, the HSV method performed better than the blue-channel method except in low diffused light conditions. Our results show the new HSV threshold can achieve better results in over-exposed conditions than Hemispherical 2.0. We also were able to estimate plant fraction directly from the cylindrical images without reprojection. Our results show that the spherical camera can be a powerful tool for canopy analysis with a much lower price tag. As this technology matures, finer resolution and the ability to obtain RAW image formats will improve the quality of canopy estimation obtainable with this technology.

3.6 References

Aghayari, S., M. Saadatseresht, M. Omidalizarandi, and I. Neumann. 2017. Geometric Calibration of Full Spherical Panoramic Ricoh-Theta Camera. ISPRS Annals of Photogrammetry, Remote Sensing and Spatial Information Sciences IV-1(W1):237–245.

Baret, F., and M. Weiss. 2004. Can-Eye: Processing digital photographs for canopy structure characterization. Tutorial. http://www. avignon. inra. fr/can_eye/page2.htm. Access Date: 28-06-2019

Beckschäfer, P. 2015. Hemispherical_2.0 – Batch processing hemispherical and canopy photographs with ImageJ – User Manual. https://www.doi.org/ 10.13140/rg.2.1.3059.4088. Access Date: 09-06-2019

Beckschäfer, P., D. Seidel, C. Kleinn, and J. Xu. 2013. On the exposure of hemispherical photographs in forests. iForest - Biogeosciences and Forestry 6(228).

Bishop, Y. M., S. E. Fienberg, and P. W. Holland. 1975. Discrete Multivariate Analysis: Theory and Practice. Cambridge, Massachusetts: Massachusetts Institute of Technology Press, New York.

Blennow, K. 1995. Sky View Factors from High-Resolution Scanned Fish-eye Lens Photographic Negatives. Journal of Atmospheric and Oceanic Technology 12:1357–1362.

Bréda, N. J. J. 2003. Ground-based measurements of leaf area index: a review of methods, instruments and current controversies. Journal of Experimental Botany 54:2403–2417.

Cescatti, A. 2007. Indirect estimates of canopy gap fraction based on the linear conversion of hemispherical photographs: Methodology and comparison with standard thresholding techniques. Agricultural and Forest Meteorology 143:1–12.

Chen, J. M., T. A. Black, and R. S. Adams. 1991. Evaluation of hemispherical photography for determining plant area index and geometry of a forest stand. Agricultural and Forest Meteorology 56:129–143.

Chianucci, F., and A. Cutini. 2012. Digital hemispherical photography for estimating forest canopy properties: current controversies and opportunities. iForest - Biogeosciences and Forestry 5(6):290-295.

Chumuang, N., S. Thaiparnit, and M. Ketcham. 2016. Algorithm Design in Leaf Surface Separation by Degree in HSV Color Model and Estimation of Leaf Area by Linear Regression. 2016 12th International Conference on Signal-Image Technology Internet-Based Systems (SITIS), pp. 628–631

Congalton, R. G. 1991. A review of assessing the accuracy of classifications of remotely sensed data. Remote Sensing of Environment 37:35–46.

Coombe, D. E., and G. C. Evans. 1960. Hemispherical photography in studies of plants. Medical and Biological Illustration 10:68–75.

DeCourt, N. 1956. Utilisation de la photographie pour mesurer les surfaces terrières (The use of photography for measuring basal area). Revue Forestière Française 8:505–507.

Englund, S. R., J. J. O'Brien, and D. B. Clark. 2000. Evaluation of digital and film hemispherical photography and spherical densiometry for measuring forest light environments. Canadian Journal of Forest Research 30:1999–2005.

Evans, G. C., and D. E. Coombe. 1959. Hemisperical and Woodland Canopy Photography and the Light Climate. Journal of Ecology 47:103–113.

Feng, Q., J. Liu, and J. Gong. 2015. UAV Remote Sensing for Urban Vegetation Mapping Using Random Forest and Texture Analysis. Remote Sensing 7:1074–1094.

Fournier, R. A., and R. J. Hall, editors. 2017. Hemispherical Photography in Forest Science: Theory, Methods, Applications. Springer Netherlands.

Frazer, G. W., C. Canham, and K. Lertzman. 1999. Gap Light Analyzer (GLA), Version 2.0: Imaging software to extract canopy structure and gap light transmission indices from true-colour fisheye photographs, users manual and program documentation. Simon Fraser University, Burnaby, British Columbia, and the Institude of Ecosystem Studies, Millbrook, New York.

Frazer, G. W., R. A. Fournier, J. A. Trofymow, and R. J. Hall. 2001. A comparison of digital and film fisheye photography for analysis of forest canopy structure and gap light transmission. Agricultural and Forest Meteorology 109:249–263.

van Gardingen, P. R., G. E. Jackson, S. Hernandez-Daumas, G. Russell, and L. Sharp. 1999. Leaf area index estimates obtained for clumped canopies using hemispherical photography. Agricultural and Forest Meteorology 94:243–257.

Gimp, G. 2008. Image manipulation program. User Manual, Edge-Detect Filters, Sobel, The GIMP Documentation Team 8:8–7.

Glatthorn, J., and P. Beckschäfer. 2014. Standardizing the Protocol for Hemispherical Photographs: Accuracy Assessment of Binarization Algorithms. PLoS ONE 9(11):e111924.

Gonsamo, A., P. D'odorico, and P. Pellikka. 2013. Measuring fractional forest canopy element cover and openness – definitions and methodologies revisited. Oikos 122:1283–1291.

Gonsamo, A., J.-M. N. Walter, and P. Pellikka. 2011. CIMES: A package of programs for determining canopy geometry and solar radiation regimes through hemispherical photographs. Computers and Electronics in Agriculture 79:207–215.

Hanbury, A., and J. Serra. 2002. A 3D-polar Coordinate Colour Representation Suitable for Image Analysis. Page Computer Vision and Image Understanding. Vienna University of Technology, Vienna, Austria.

Herbert, T. J. 1987. Area projections of fisheye photographic lenses. Agricultural and Forest Meteorology 39:215–223.

Hsu, Y.-H. 2019. Applications of variable probability sampling using remotely sensed covariates. MSc Forestry thesis, The University of New Brunswick.

Hughes, C., P. Denny, E. Jones, and M. Glavin. 2010. Accuracy of fish-eye lens models. Applied Optics 49:3338–3347.

Inoue, A., K. Yamamoto, N. Mizoue, and Y. Kawahara. 2004. Effects of image quality, size and camera type on forest light environment estimates using digital hemispherical photography. Agricultural and Forest Meteorology 126:89–97.

Jarčuška, B., S. Kucbel, and P. Jaloviar. 2010. Comparison of output results from two programmes for hemispherical image analysis: Gap Light Analyser and WinScanopy. Journal of Forest Science 56:147–153.

Jonckheere, I. G. C., B. Muys, and P. R. Coppin. 2005. Derivative analysis for in situ high dynamic range hemispherical photography and its application in forest stands. IEEE Geoscience and Remote Sensing Letters 2:296–300.

Lang, M., A. Kodar, and T. Arumäe. 2013. Restoration of above canopy reference hemispherical image from below canopy measurements for plant area index estimation in forests/ Metsa võrastiku läbipaistvuse mõõtmine digitaalsete poolsfäärikaamerate abil. Forestry Studies 59:13–27.

Lang, M., A. Kuusk, M. Mõttus, M. Rautiainen, and T. Nilson. 2010. Canopy gap fraction estimation from digital hemispherical images using sky radiance models and a linear conversion method. Agricultural and Forest Meteorology 150:20–29.

Leblanc, S. G., J. M. Chen, R. Fernandes, D. W. Deering, and A. Conley. 2005. Methodology comparison for canopy structure parameters extraction from digital hemispherical photography in boreal forests. Agricultural and Forest Meteorology 129:187–207.

Leblanc, S. G., R. Fernandes, and J. M. Chen. 2002. Recent advancements in optical field leaf area index, foliage heterogeneity, and foliage angular distribution measurements. IEEE International Geoscience and Remote Sensing Symposium.5:2902-2904

Loffredo, N., X. Sun, and Y. Onda. 2016. DHPT 1.0: New software for automatic analysis of canopy closure from under-exposed and over-exposed digital hemispherical photographs. Computers and Electronics in Agriculture 125:39–47.

MacFarlane, C. 2011. Classification method of mixed pixels does not affect canopy metrics from digital images of forest overstorey. Agricultural and Forest Meteorology 151:833–840.

MacFarlane, C., S. K. Arndt, S. J. Livesley, A. C. Edgar, D. A. White, M. A. Adams, and D. Eamus. 2007a. Estimation of leaf area index in eucalypt forest with vertical foliage, using cover and fullframe fisheye photography. Forest Ecology and Management 242:756–763.

MacFarlane, C., M. Coote, D. A. White, and M. A. Adams. 2000. Photographic exposure affects indirect estimation of leaf area in plantations of Eucalyptus globulus Labill. Agricultural and Forest Meteorology 100:155–168.

MacFarlane, C., A. Grigg, and C. Evangelista. 2007b. Estimating forest leaf area using cover and fullframe fisheye photography: Thinking inside the circle. Agricultural and Forest Meteorology 146:1–12.

Musselman, K. N., N. P. Molotch, S. A. Margulis, P. B. Kirchner, and R. C. Bales. 2012. Influence of canopy structure and direct beam solar irradiance on snowmelt rates in a mixed conifer forest. Agricultural and Forest Meteorology 161:46–56.

Nobis, M., and U. Hunziker. 2005. Automatic thresholding for hemispherical canopy-photographs based on edge detection. Agricultural and Forest Meteorology 128:243–250.

Pekin, B., and C. MacFarlane. 2009. Measurement of Crown Cover and Leaf Area Index Using Digital Cover Photography and Its Application to Remote Sensing. Remote Sensing 1:1298–1320.

Promis, A., S. Gärtner, D. Butler-Manning, C. Durán-Rangel, A. Reif, G. Cruz, and L. Hernández. 2011. Comparison of four different programs for the analysis of hemispherical photographs using parameters of canopy structure and solar radiation transmittance. Sierra Heft 11:19–33.

Rasband, W. 1997. ImageJ. US National Institutes of Health, Bethesda, MD, USA.

Rau, J. Y., J. P. Jhan, C. F. Lo, and Y. S. Lin. 2011. Landslide Mapping Using Imagery Acquired by a Fixed-Wing Uav. ISPRS - International Archives of the Photogrammetry, Remote Sensing and Spatial Information Sciences 3822:195–200.

Regent Instruments Inc. 2018. WinSCANOPY: Canopy Structure and Solar Radiation Analysis. https://www.regentinstruments.com/assets/winscanopy_about.html. Accessed Data: 28-06-2019

Reineke, L. H. 1940. Permanent sample plot photography. Journal of Forestry 38:813–815.

Riaz, M., G. Kang, Y. Kim, S. Pan, and J. Park. 2008. Efficient Image Retrieval Using Adaptive Segmentation of HSV Color Space. 2008 International Conference on Computational Sciences and Its Applications. pp. 491–496

Rich, P. M. 1990. Characterizing plant canopies with hemispherical photographs. Remote Sensing Reviews 5:13–29.

Rich, P. M., J. Wood, D. Vieglais, K. Burek, and N. Webb. 1999. HemiView user manual. Delta-T Devices, Ltd. https://www.delta-t.co.uk/download/2825/. Accessed Data: 13-06-2019.

Ricoh Imaging Company, LTD. 2016. Rioch Theta S 360 video camera. http://www.ricoh-imaging.co.jp/english/products/theta_s/. Accessed Date: 25-11-2019.

Ricoh Imaging Company, LTD. 2019. Richo Theta Z1 360 video camera. https://theta360.com/en/about/theta/z1.html. Accessed Date: 28-06-2019.

Sang, W., S. Chen, and G. Li. 2008. Dynamics of leaf area index and canopy openness of three forest types in a warm temperate zone. Frontiers of Forestry in China 3:416–421.

Schwalbe, E., H. Maas, M. Kenter, and S. Wagner. 2006. Profile Based Sub-Pixel-Classification of Hemispherical Images for Solar Radiation Analysis in Forest Ecosystems. Remote Sensing and Spatial Information Sciences 36(Part7):(on CD-ROM).

Shelbourne, C., and G. Namkoong. 1966. Photogrammetric technique for measuring bole straightness. Proceedings of the eight southern conference on forest tree improvement, June. pp. 16–17.

Smolander, S., and P. Stenberg. 2001. A method for estimating light interception by a conifer shoot. Tree Physiology 21:797–803.

Souza, A. F., C. Forgiarini, S. J. Longhi, and D. A. Brena. 2008. Regeneration patterns of a long-lived dominant conifer and the effects of logging in southern South America. Acta Oecologica 34:221–232.

Stenberg, P., T. Kangas, H. Smolander, and S. Linder. 1999. Shoot structure, canopy openness, and light interception in Norway spruce. Plant, Cell & Environment 22:1133–1142.

Wagner, S. 1998. Calibration of grey values of hemispherical photographs for image analysis. Agricultural and Forest Meteorology 90:103–117.

Wagner, S. 2001. Relative radiance measurements and zenith angle dependent segmentation in hemispherical photography. Agricultural and Forest Meteorology 107:103–115.

Wagner, S., and M. Hagemeier. 2006. Method of segmentation affects leaf inclination angle estimation in hemispherical photography. Agricultural and Forest Meteorology 139:12–24.

Wang, H., J. A. Kershaw, T.-R. Yang, Y.-H. Hsu, X. Ma, and Y. Chen. Under review. An Integrated System for Estimating Forest Basal Area from Spherical Images. Mathematical and Computational Forestry & Natural-Resource Sciences.

Weiss, M., F. Baret, G. J. Smith, I. Jonckheere, and P. Coppin. 2004. Review of methods for in situ leaf area index (LAI) determination: Part II. Estimation of LAI, errors and sampling. Agricultural and Forest Meteorology 121:37–53.

Wilson, J. W. 1963. Estimation of foliage denseness and foliage angle by inclined point quadrats. Australian Journal of Botany 11:95–105.

Yang, W., S. Wang, X. Zhao, J. Zhang, and J. Feng. 2015. Greenness identification based on HSV decision tree. Information Processing in Agriculture 2:149–160.

Zar, J. H. 2009. Biostatistical analysis. 5th edition. Pearson, New York.

Zhang, Y., J. M. Chen, and J. R. Miller. 2005. Determining digital hemispherical photograph exposure for leaf area index estimation. Agricultural and Forest Meteorology 133:166–181.

Zhao, K., and F. He. 2016. Estimating light environment in forests with a new thresholding method for hemispherical photography. Canadian Journal of Forest Research 46:1103–1110.

Table 3.1: Percent species composition (by basal area) across the two study sites used in this study

Species Name		Percent Species Composition[1]			
Common Name	Scientific Name	Cor	Pas	Rod	NRF
Balsam Fir	*Abies balsamea*	72.39	97.94	97.51	12.55
Larch/Tamarack	*Larix laricina*	-	-	-	2.79
White Spruce	*Picea glauca*	12.21	1.14	1.86	-
Black Spruce	*Picea mariana*	3.40	-	0.42	13.16
Red Spruce	*Picea rubens*	-	-	-	21.02
Eastern White Pine	*Pinus strobus*	-	-	-	2.98
Eastern Hemlock	*Tsuga canadensis*	-	-	-	1.47
Manitoba Maple	*Acer negundo*	-	-	-	0.50
Red Maple	*Acer rubrum*	-	-	-	22.71
Sugar Maple	*Acer saccharum*	-	-	-	0.46
Yellow Birch	*Betula alleghaniensis*	0.05	-	-	0.87
Paper Birch	*Betula papyrifera*	1.85	0.92	0.21	16.64
White Ash	*Fraxinus americana*	-	-	-	1.75
Black Ash	*Fraxinus nigra*	-	-	-	0.03
Tupelo Spp.	*Nyssa sylvatica*	-	-	-	0.22
Eastern Cottonwood	*Populus deltoides*	-	-	-	2.02
Largetooth Aspen	*Populus grandidentata*	-	-	-	0.83
Trembling Aspen	*Populus tremuloides*	10.09	-	-	-
Other Hardwood		1.20	-	-	0.12

[1]Newfoundland Early Spacing Trials: Cor = Cormack; Pas = Pasadena; Rod = Roddickton. NRF = Noonan Femelschlag Research Area

Table 3.2: Classification accuracy assessment results. (BC-2 = blue-channel classification with 2 classes (sky – plant), by ImageJ, HSV-2 = HSV thresholding with two classes, and HSV-3 = HSV thresholding with three classes (sky – wood – foliage))

Image	Average Accuracy (AA)			Overall Accuracy (OA)			Kappa (K)		
Segment	BC-2	HSV-2	HSV-3	BC-2	HSV-2	HSV-3	BC-2	HSV-2	HSV-3
(a)	0.780	0.926	0.679	0.800	0.930	0.846	0.581	0.858	0.718
(b)	0.619	0.936	0.641	0.594	0.933	0.891	0.227	0.867	0.792
(c)	0.734	0.843	0.630	0.778	0.866	0.761	0.506	0.713	0.551
(d)	0.906	0.945	0.739	0.964	0.977	0.867	0.868	0.917	0.565
(e)	0.627	0.699	0.510	0.689	0.748	0.726	0.284	0.434	0.413
(f)	0.500	0.753	0.528	0.450	0.729	0.710	0.000	0.481	0.474
(g)	0.875	0.590	0.428	0.940	0.867	0.545	0.770	0.265	0.150
Average	0.720	0.813	0.593	0.745	0.864	0.764	0.462	0.648	0.523

Table 3.3: Classification accuracy assessment for HSV 3 classes

Image	Producer's Accuracy		
Segment	Sky	Wood	Foliage
(a)	0.963	0.874	0.226
(b)	0.984	0.881	0.058
(c)	0.979	0.472	0.440
(d)	0.994	0.949	0.274
(e)	0.995	0.452	0.083
(f)	0.989	0.594	0.002
(g)	0.182	0.988	0.115
Average	0.869	0.744	0.171

Table 3.4: Simple linear regression results for hemispherical approach versus cylindrical approach. The linear model is $PF^c = b0 + b1*PF^d$, if PF^d is the same as PF^c, then b0=0 and b1=1

Elements	**Parameters**	**Estimate**	**Std. Err.**	**r^2**	**rMSE**
(a) Plant Fraction	b0	0.029	0.0010	0.99	0.004
	b1	0.977	0.0014		
(b) Sky Fraction	b0	-0.006	0.0004	0.99	0.004
	b1	0.977	0.0014		
(c) Foliage Fraction	b0	0.002	0.0003	0.99	0.004
	b1	1.008	0.0013		
(d) Wood Fraction	b0	0.009	0.0006	0.99	0.004
	b1	0.998	0.0011		

Param. = Parameter; Est. = Estimate; Std. Err. = Standard Error; rMSE = root Mean Square Error.

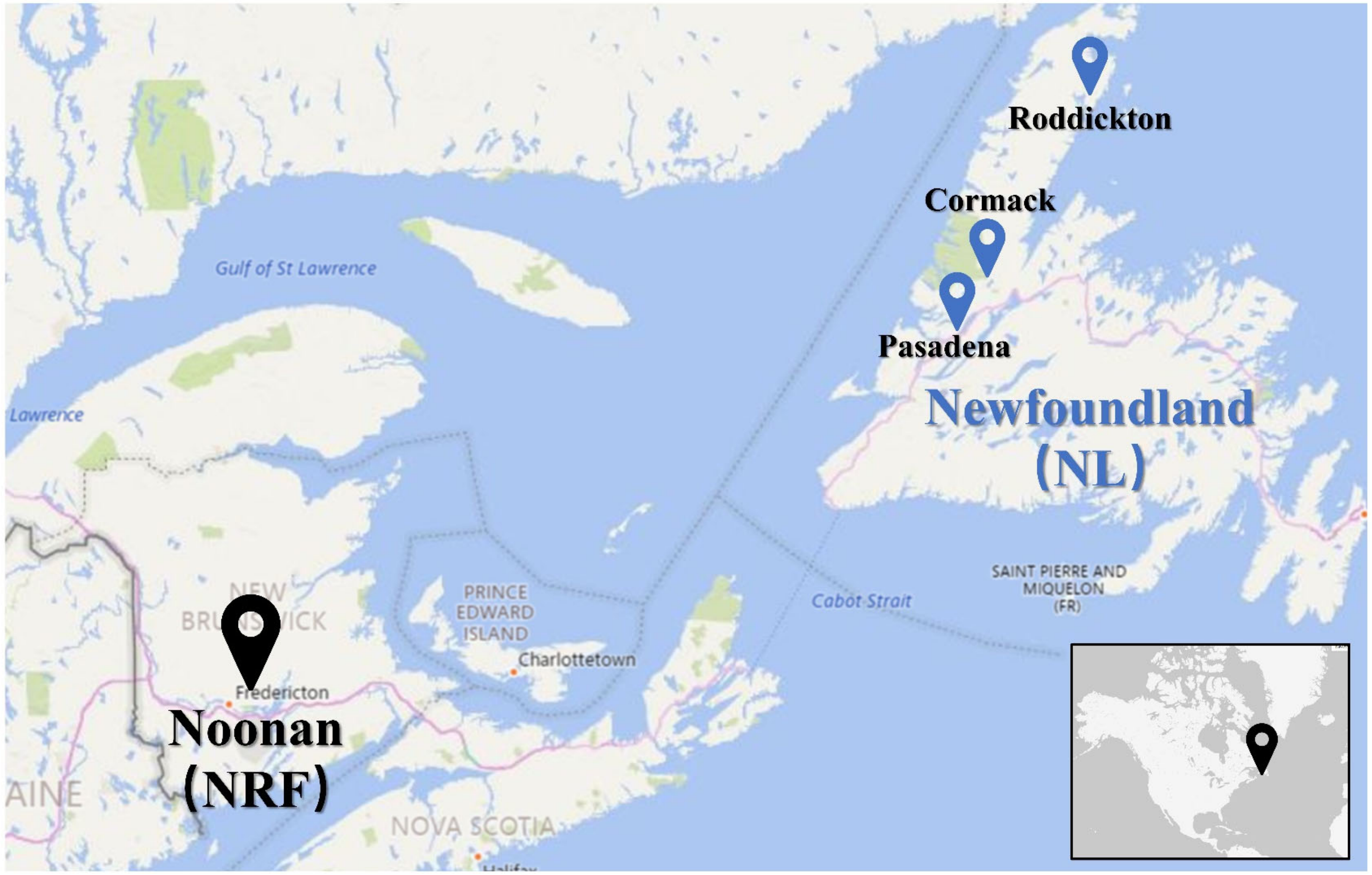

Fig. 3.1: The location of sites used in this study. The first site was three early spacing trails located in western Newfoundland (NL), Canada, the second site was the Femelschlag Research Study located on the Noonan Research Forest (NRF) in central New Brunswick, Canada.

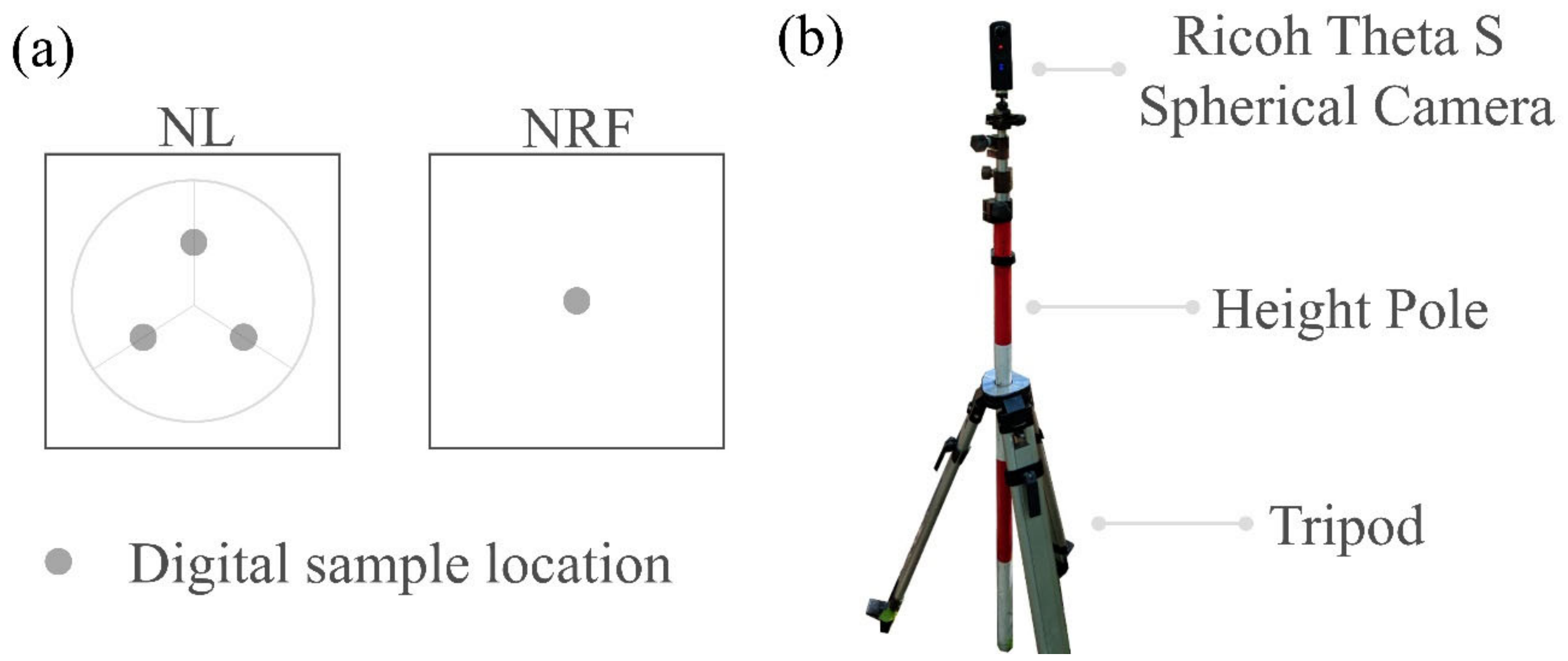

Fig. 3.2: Digital data collection methods. (a) Digital sample location design for three sites in Newfoundland (NL) and Noonan Research Forest (NRF) Study. For NL sites, three locations were established at the midpoint of plot radius along azimuths of 360°, 120°, and 240°. For NRF, only one location center was set. (b) tripod and spherical camera set up for spherical image acquisition at different heights (1.6m, 2.6m, 3.6m, 4.6m).

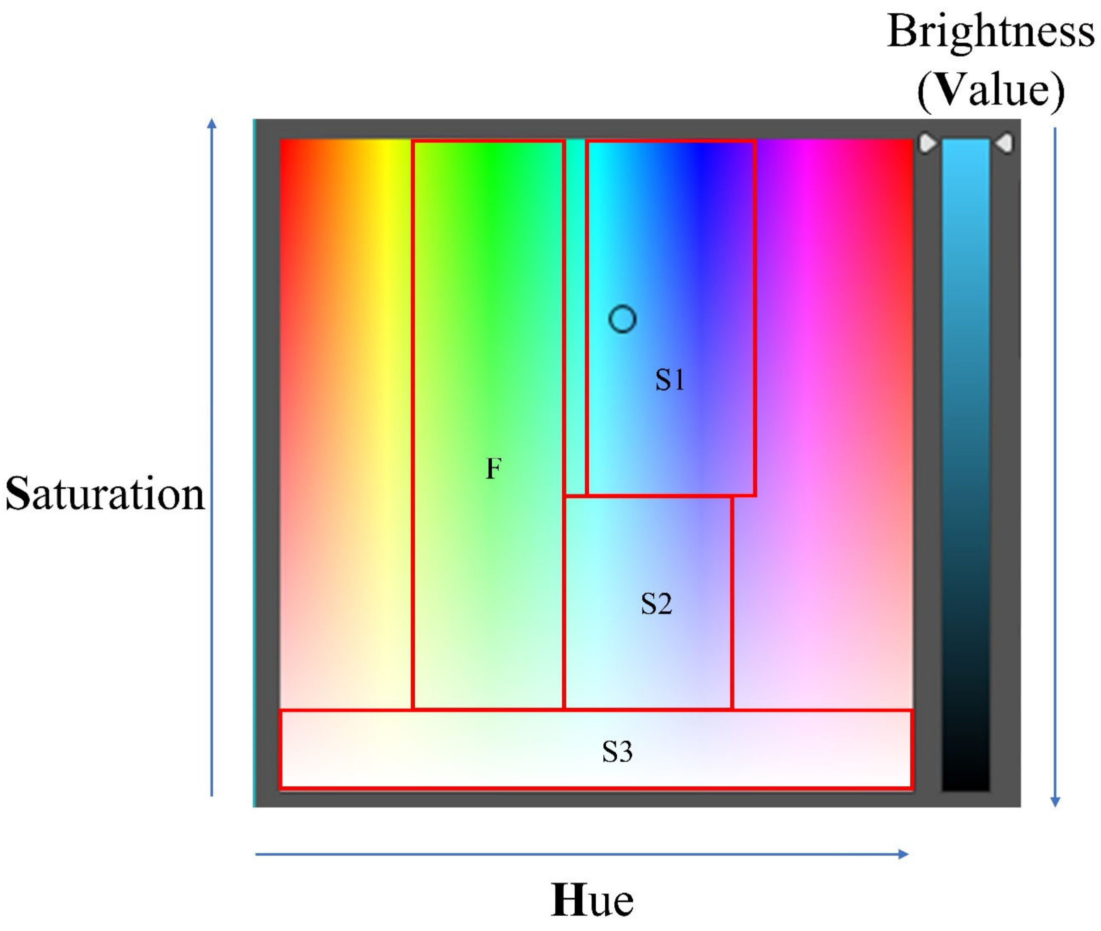

Fig. 3.3: The HSV thresholds for different classes. S1 is clear sky, S2 is diffused sky, S3 is cloudy sky, while F is foliage. (the remaining space is assumed to be woody stems and branches)

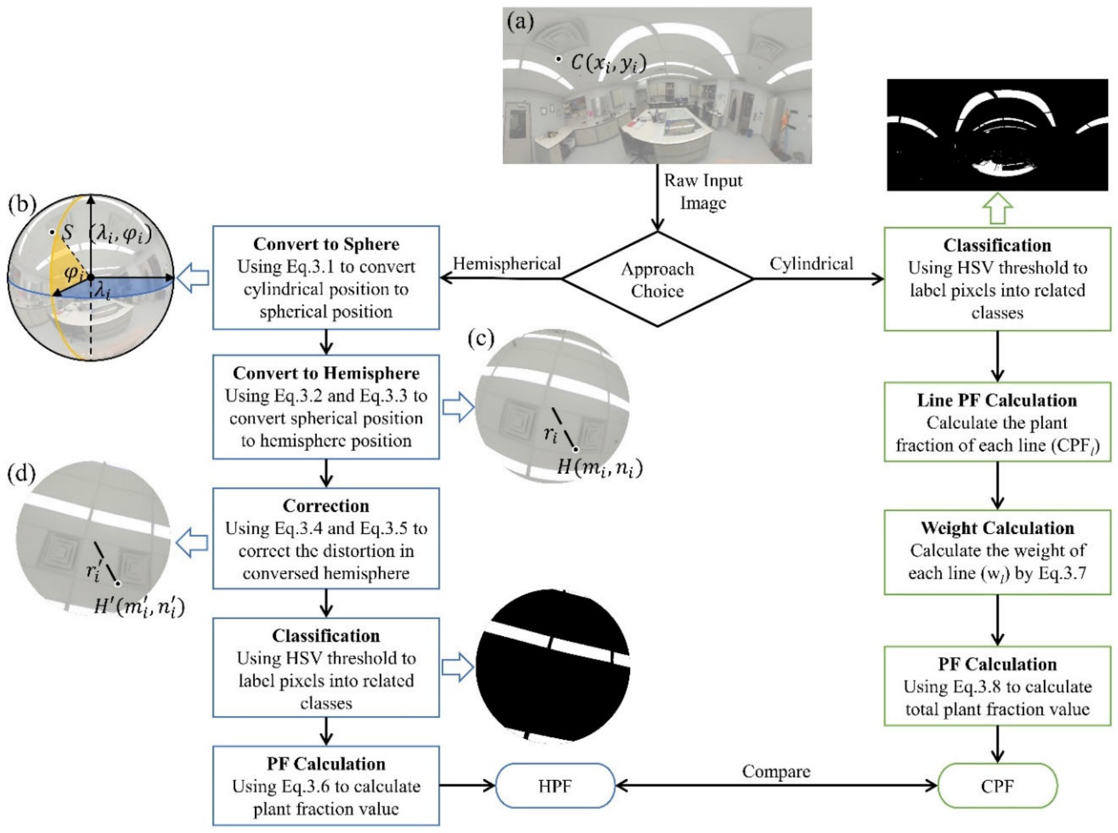

(a)
$C(x_i, y_i)$
Raw Input Image
Approach Choice
Hemispherical
Cylindrical
(b)
S (λ_i, φ_i)
φ_i
λ_i
Convert to Sphere
Using Eq.3.1 to convert cylindrical position to spherical position
Convert to Hemisphere
Using Eq.3.2 and Eq.3.3 to convert spherical position to hemisphere position
(c)
r_i
$H(m_i, n_i)$
(d)
r_i'
$H'(m_i', n_i')$
Correction
Using Eq.3.4 and Eq.3.5 to correct the distortion in conversed hemisphere
Classification
Using HSV threshold to label pixels into related classes
PF Calculation
Using Eq.3.6 to calculate plant fraction value
HPF
Compare
CPF
Classification
Using HSV threshold to label pixels into related classes
Line PF Calculation
Calculate the plant fraction of each line (CPF_l)
Weight Calculation
Calculate the weight of each line (w_l) by Eq.3.7
PF Calculation
Using Eq.3.8 to calculate total plant fraction value

Fig. 3.4: The workflow of two approaches to estimate plant fraction (PF) from spherical photos. The left blue workflow is the hemispherical approach (HPF) which converts original cylindrical images to hemispherical images first then apply algorithms commonly used in hemispherical images. The right green one is the cylindrical approach (CPF) which directly calculate the PF value on original cylindrical images without image converting.

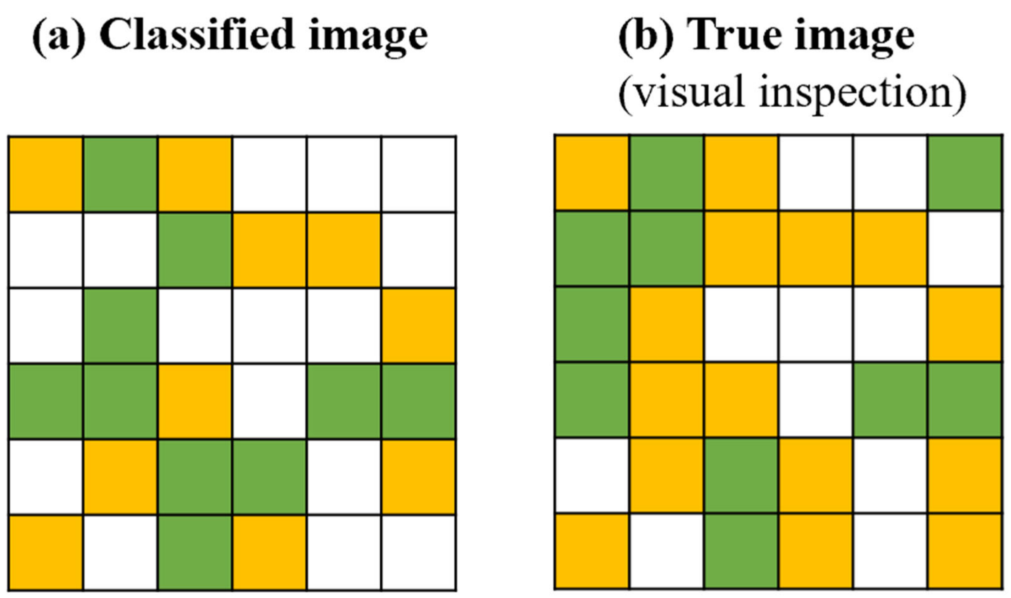

Class: sky = □ stem = 🟨 foliage = 🟩

(c) Error matrix

	Class	True (visual inspection)			Total
		0	1	2	
Classified	0	11	1	4	16
	1	0	10	0	10
	2	0	4	6	10
Total		11	15	10	36

Fig. 3.5: Classification accuracy assessment by error matrix. (a) is the result produced by image classification algorithm, (b) is the result by visual inspection as true value, (c) is a comparison error matrix generated by classified and true images.

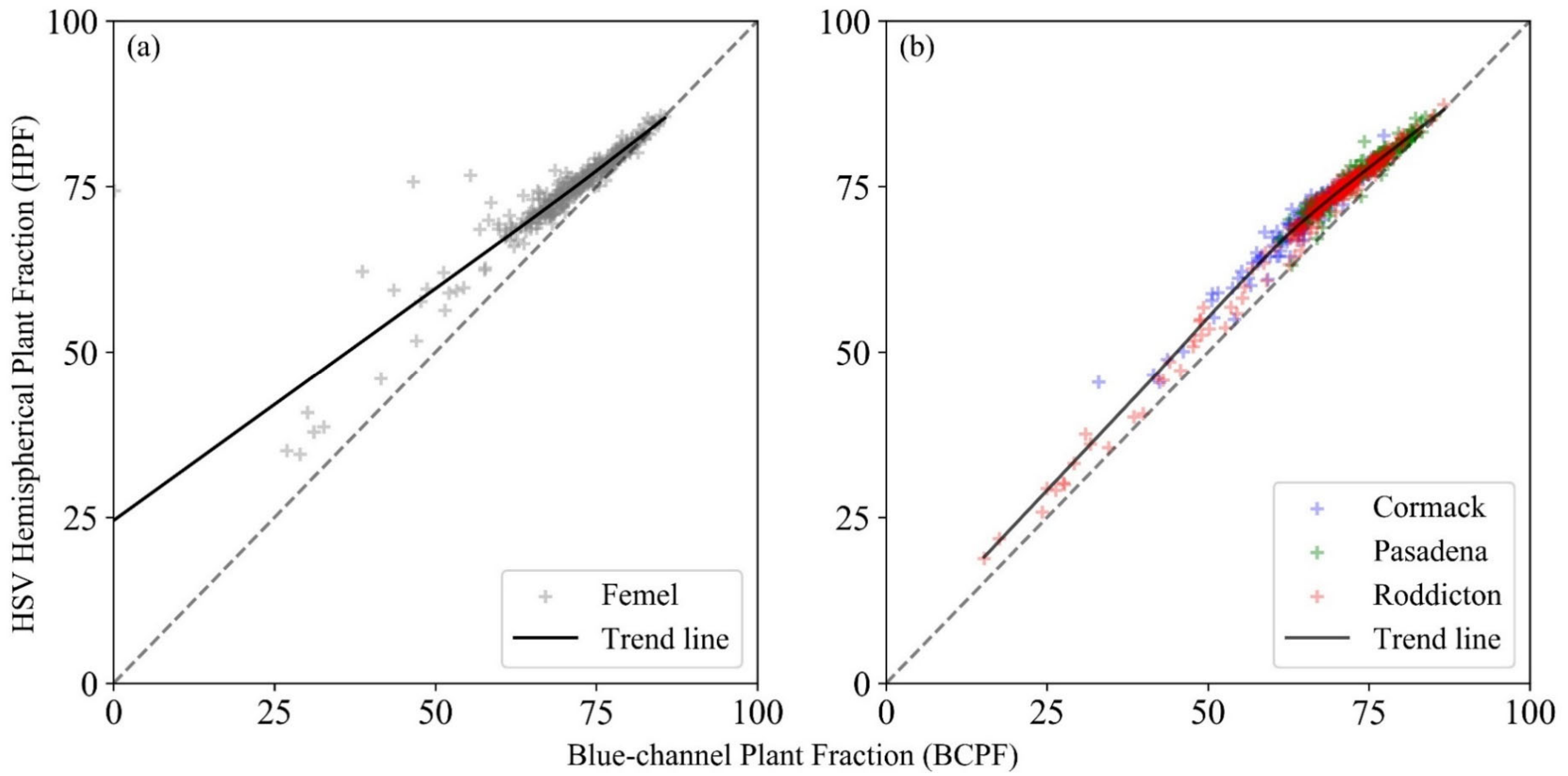

Fig. 3.6: Classification results comparison between HSV threshold in hemispherical approach (HPF) and ImageJ blue channel threshold (BPF). (a) is NRF site and (b) is NL sites

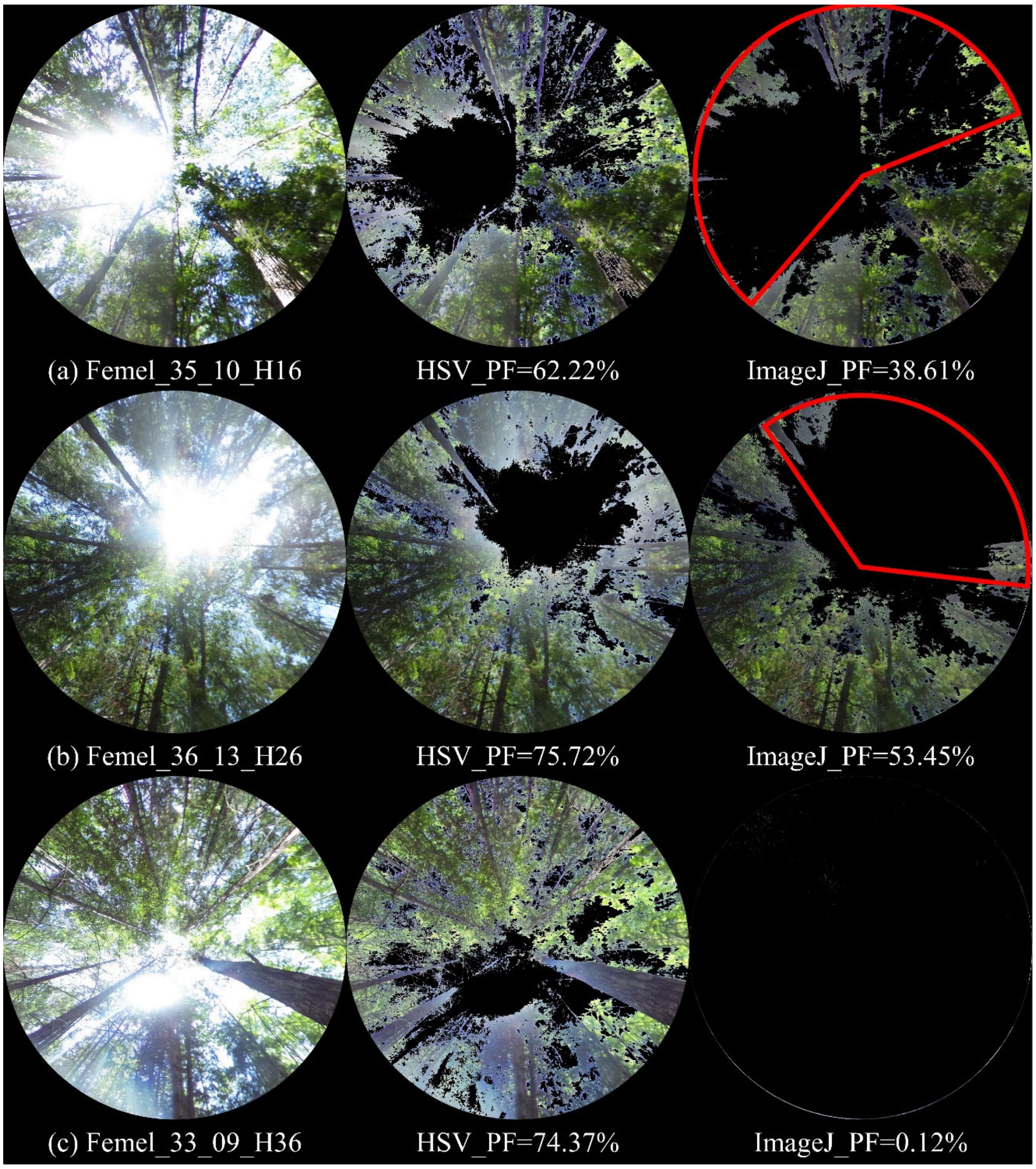

Fig. 3.7: Several extreme plant fraction values differences caused by overexposure and flashed out.

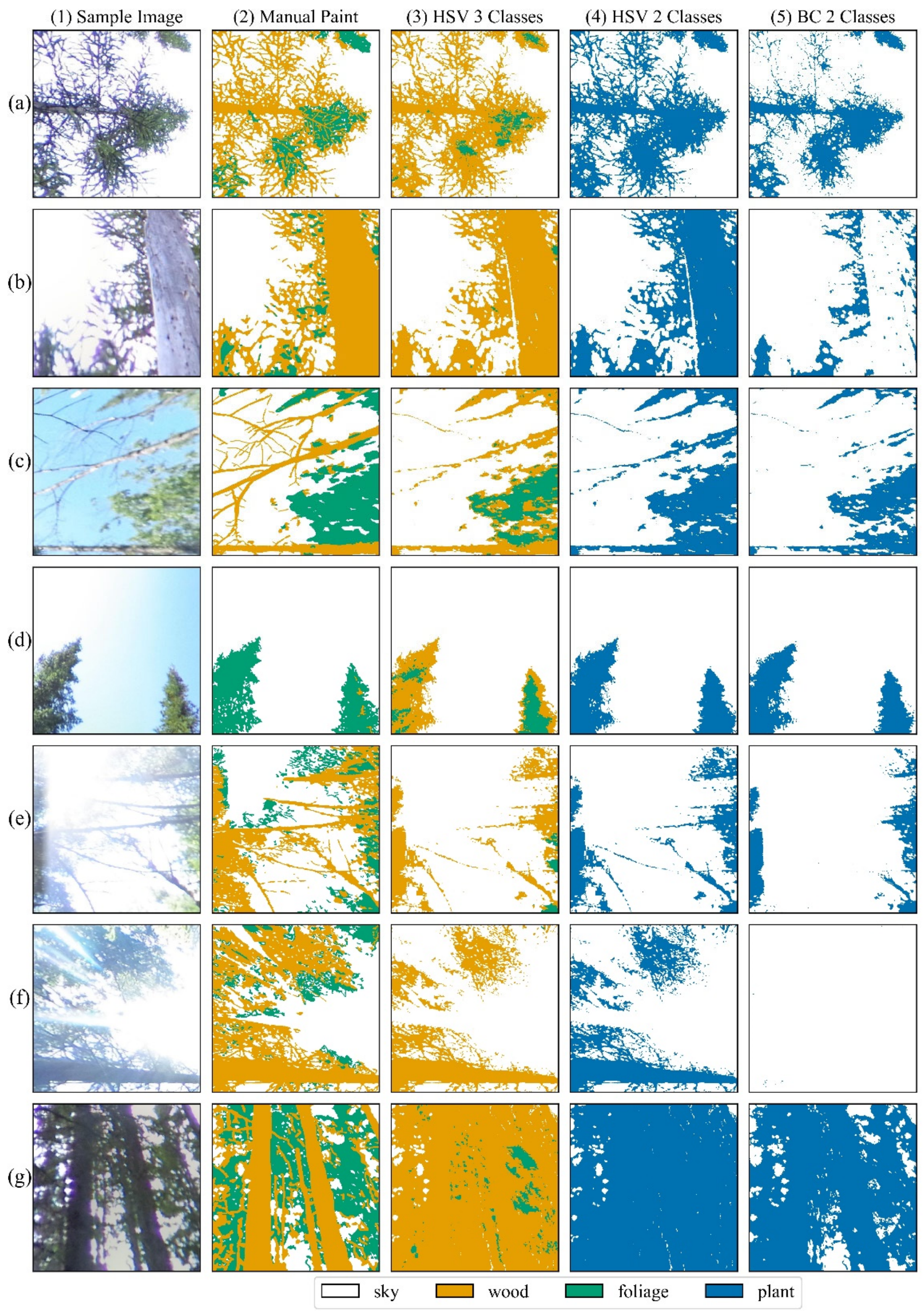

Fig. 3.8: Classification results for two algorithms (HSV threshold and Blue-Channel threshold) by 7 representative image segments. (a) (b) white pure sky from COR_R3_S18_1; (c) pure blue sky from Femel_33_11; (d) gradual change sky from ROD_R2_S18_1; (e) (f) over exposure from Femel_29_16 and Femel_33_13 respectively; (g) underexposure from Femel_31_13.

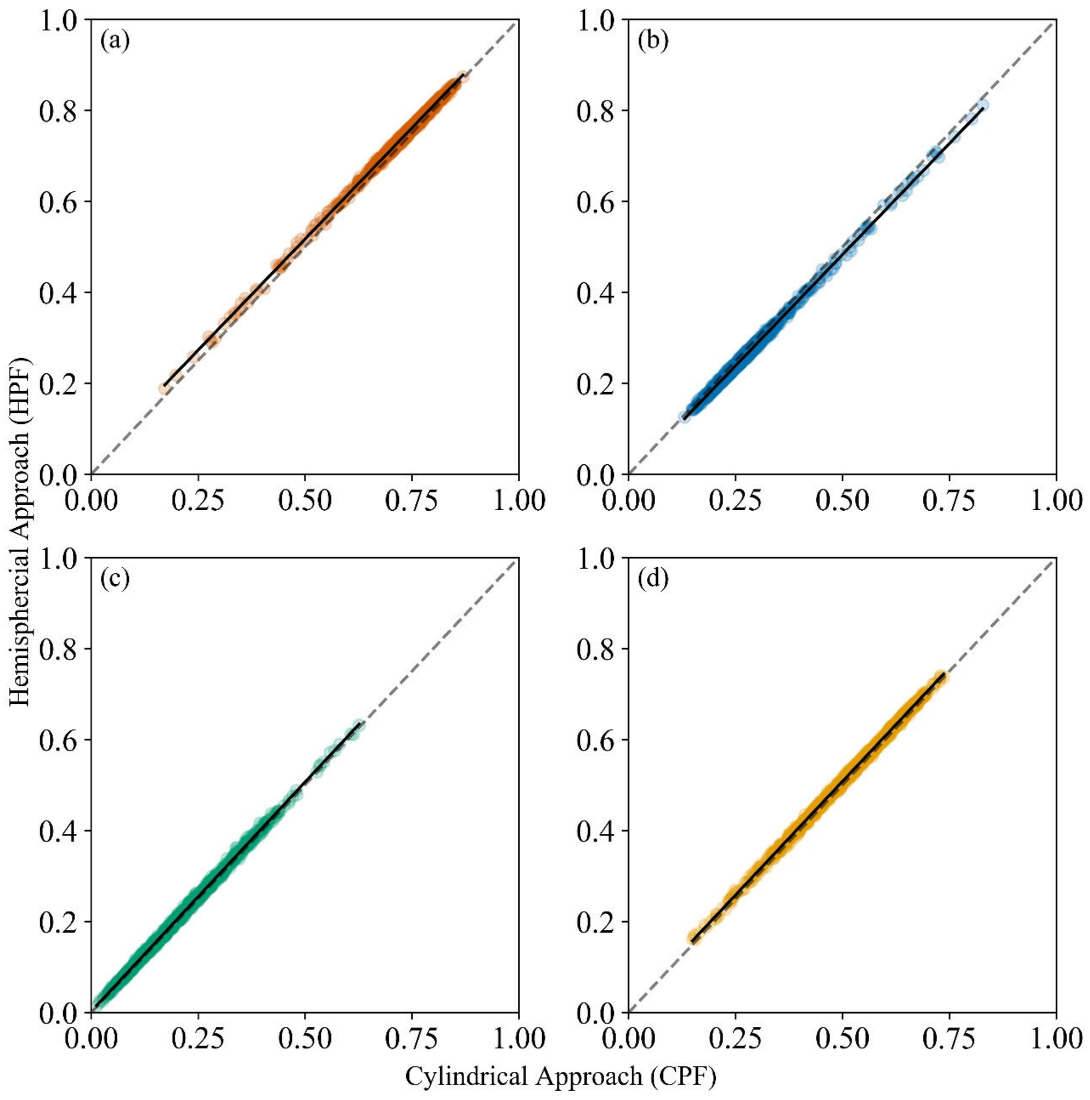

Fig. 3.9: Classification results comparison by two approaches. The spherical images were classified into 3 classes: sky (b), foliage (c), wood (d). The plant class (a) is the sum of foliage and wood.

Chapter 4: Estimating Individual Tree Heights and DBHs from Spherical Images

4.1 Introduction

Forests are the dominant terrestrial ecosystems which account for over three quarters of gross primary productivity and plant biomass on the Earth (Pan et al. 2013). They can provide many ecosystem services including watershed protection, soil structure maintenance, and global carbon storage (Chazdon 2008). To better manage these forest areas, detailed and accurate forest inventories at different levels should be conducted to obtain required information about forest conditions and resources (Kershaw et al. 2016).

Individual tree stem attributes, such as diameters, heights and spatial locations, are critical measurements in most forest inventories (Kershaw et al. 2016, Lam et al. 2017, Mulverhill et al. 2019). Diameter at breast height and total tree height are the fundamental parameters used in allometric equations to estimate biomass, volume, and carbon (Smith and Brand 1983, Blake et al. 1991, Lambert et al. 2005, Xing et al. 2005, Zianis et al. 2005). How to measure these parameters across large scale forests with high efficiency and low costs is a continuing challenge for all forest inventory specialists.

Compared to field data collection, remote sensing is a more time and labor-saving method for large-scale landscape inventories. Although total height can be estimated from 3D point clouds generated from airborne LiDAR (Hilker et al. 2010, Giannetti et al. 2018), and some algorithms have shown success in estimating DBH from canopy data based on individual tree segmentation (Li et al. 2012, Kaartinen et al. 2012, Strîmbu and Strîmbu 2015), individual tree attributes are still difficult to estimate accurately and precisely due to canopy cover (Strimbu et al. 2019) and low point cloud densities below the canopy. Under canopy measurements are still required due to the limitations of the above canopy methods (Wells 2018, Strimbu et al. 2019).

For under canopy measurements, traditional tools such as diameter tapes and clinometers are widely used. These basic tools have been modified and digitized to make field data collection more efficient. Field measurement tools can be lumped into 2 broad classes: contact and optical (Clark et al. 2000a). Contact tools are often used for diameter measurements. The Biltmore stick (Jackson 1911), calipers, diameter tape, and sector fork (Bitterlich 1959, Clark et al. 2000a) are contact tools for measuring diameters. All of these tools have been refined and improved over time including several digital versions (Clark et al. 2000a). Most non-contact tools focus on optical methods. Optical calipers, rangefinder dendrometers, and optical forks for measuring diameters are a few examples (Clark et al. 2000a), and even some smartphone applications (Anton 2019).

Although several of these instruments have high accuracy and precision, the higher costs and the continued focus on individual trees limit wide-spread use, and many instruments have disappeared from the market (Clark et al. 2000a, Shimizu et al. 2014, Perng et al. 2018). Laser and sonic instruments for measuring tree heights have had greater success than digital instruments for diameter measurement (Clark et al. 2000a). The success of these instruments over similar ones for DBH measurement is probably due to the difficulty and time-consuming nature of height measurement using traditional tools. More repeatable measurements and reduced field time has contributed to these instruments being widely adopted in forest inventory operations.

Photogrammetry has had a long history of use in forestry. Reineke (1940) was among the first to develop the idea of using terrestrial images in forestry. Field measured distances were commonly used in early studies (Reineke 1940, Clark et al. 2000b). In addition to using distance to establish scale, reference targets with known length or size (poles, tags, or laser facula) was another popular method to establish scale and has been widely applied in photogrammetry studies (Dean 2003, Varjo et al. 2006, Pengle et al. 2013, Shimizu et al. 2014, Celes et al. 2019). Multiple images with known shifts in position can also be used to establish scale (Clark et al. 1998).

Many studies focus only on single tree images and individual tree measurements. However, for inventory efficiency, methods to extract estimates for multiple trees without the need to shift the camera for each tree of interest are required (Stewart 2004, Perng et al. 2018). DeCourt (1956) demonstrated how images could be used to estimate basal area per ha using angle count sampling methods (Bitterlich 1984). However, the cost of print images and manual processing limited the use of this method, especially since field implementation of angle count sampling was already a very efficient forest inventory technique. With the advent of affordable digital cameras, Stewart (2004) revived this idea and took a series of 8 photographs at 45° intervals to estimate stand basal area. Fastie (2010) took images at 8.5° intervals (504 images in 12 rows by 42 columns) to stitch ultra-high resolution panoramas to estimate stand basal area. Dick et al. (2010) used a single row of 24 horizontal images to map tree locations from stitched panoramas. Lu et al. (2019) recently expanded this idea to measure tree diameters at different heights. However, for parameters other than stand basal area based on angle count sampling, all of these studies required scale tags (Dick et al. 2010, Lu et al. 2019) on each tree or measured field distances and slopes (Lu et al. 2019). Measuring or tagging individual trees is time consuming and costly, and, other than providing a permanent record of field conditions, the images have no benefit for improving inventory field efficiency. In addition, errors resulting from the stitching of several digital image cannot be avoided (Fastie 2010, Dick et al. 2010, Perng et al. 2018, Lu et al. 2019).

Structure from motion (SfM) technology enables 3D reconstruction from image series without actual measurements (Snavely et al. 2008). Several studies have shown its potential to solve the need for field targets and/or measuring dependencies. This technique has been applied to 3D reconstruction of individual stems (Larsen 2006a, 2006b, Miller et al. 2015, Surový et al. 2016, Mokroš et al. 2018), and to stand level forest point cloud development (Liang et al. 2014, 2015, Forsman et al. 2016, Liu et al. 2018). The mapping accuracy from SfM is similar to TLS (Liang et al. 2014). However, the inconveniences of this technology include: 1) requiring walking through sample plots and obtaining a large number of images (Berveglieri et al. 2017, Liu et al. 2018); 2) although point clouds can be generated automatically by commercial software, the quality control (always a factor when stitching images) and point cloud generation and analyzes requires a high performance computer and complex algorithms (Belton et al. 2013, Liang et al. 2015, Mulverhill et al. 2019); and 3) measurements still need to be extracted from the point clouds.

Using wide-angle hemispherical lenses has potential to eliminate errors caused by stitching images and could potentially simplify calculations. Paired fisheye cameras have been used to obtain stem diameter, basal area, mapping and volume without dependence on field measurements (Rodríguez-García et al. 2014, Sánchez-González et al. 2016). Berveglieri et al. (2017) developed an automated algorithm by matching hemispherical images at different heights to estimate stem diameters. More recently, the development of affordable 360° spherical cameras offer new opportunities for obtaining optical tree measurements (Perng et al. 2018). Spherical cameras, like the Ricoh Theta S (Ricoh Imaging Company, LTD. 2016), offer an inexpensive option for obtaining spherical inventory images directly. The compact size of a spherical camera makes it an easy-to-use tool in the forest and can be moved through the canopy using a height pole to obtain structural estimates more easily than traditional fisheye cameras and other digital cameras. For example, Mulverhill et al. (2019) used this new technology to generate 3D plot point clouds and significantly decreased the number of images required for accurate point cloud rendering. The results showed high correspondence with field measured data (Mulverhill et al. 2019). Although the procedures are mostly automatic, the other inconveniences of using SfM technology mentioned above remain.

Furthermore, it might be questioned as to the need to generate a 3D point cloud and then do measurements, when those basic measurements can often be done directly on the images. What is really required is a simplified system for obtaining spherical images in stereo. The goal of this study was to develop an approach to obtain such spherical image pairs and apply stereoscopic geometry to estimate diameter, height, and location (mapping) of individual trees directly without any field measurement dependency. The specific objectives were: 1) derive the geometry for two vertically displaced spherical image pairs to estimate desired tree attributes; 2) test the technique in an open urban setting; and 3) assess accuracy and precision in a real forest situation.

4.2 Methods and materials

4.2.1 Study sites

Urban Site – The University of New Brunswick campus located in Fredericton, New Brunswick, Canada (Fig. 4.1) was used for validating the approach in an open situation where visibility was not an issue. Two plots were selected for this phase of the study. The criteria for sample point selection included: 1) Open forest conditions with a moderate number of trees (7-12 trees) with each tree's tip and base clearly visible; 2) Trees have different distances to the sampling point; and 3) Variable diameters and heights of the individual trees.

Forest Site – One replicate from an early spacing trail located on western Newfoundland Island, near Roddickton, Newfoundland, Canada (Fig. 4.1) was used for testing the approach in a real forest condition. The spacing trials, with different densities and resulting tree sizes was an ideal field setting for this test. The site was dominated by balsam fir (*Abies balsamea*) with minor components of black spruce (*Picea mariana*) and other boreal species. The trials were established in the early 1980's. Five spacing treatments were applied: Control (no spacing), 1.2m, 1.8m, 2.4m, and 3.0m average spacing. Because of the early spacing treatments, the NL plots were even-aged, single stratum stands with relatively uniform stand structures within spacing treatments.

4.2.2 Data collection

The method developed here uses stereo pairs of spherical images and spherical geometry to estimate diameter at breast height (DBH, cm) and total height (HT, m). Images are acquired at 1.6m and 2.6m above ground. The geometric derivations are given and the method is validated in an urban forest situation and then tested in a real forest situation.

4.2.2.1 Digital Image Pairs

A Ricoh Theta S (Ricoh Imaging Company, LTD. 2016) spherical camera was used to capture spherical images. Two single spherical images were captured at 1.6m and 2.6m above ground at each digital sampling point at both study sites. The spherical camera was mounted on a height plot that was stabilized using a tripod (Fig. 4.2.a) and raised to the desired digital sample heights. On the Urban Site, a single digital sampling point was located strategically among the trees of interest (Fig. 4.2.b) to ensure visibility and a variety of camera to tree distances.

On the Forest Site, three digital sample points per replicate plot were used (Fig. 4.2.b). Multiple digital sample points were used to minimize tree occlusion and facilitate measurement of as many plot trees as possible. Digital sample points were located at half the plot radii at azimuths of 0°, 120°, and 240°. Plot radii varied by spacing treatment (Control (5.2m);1.2m (7.2m); 1.8m (10.4m); 2.4m (15.0m); 3.0m (18.0m)) with the aim of having about 100 trees per plot at the time of treatment establishment (1982). For each digital sampling point the GPS coordinates were obtained using multiple sampling over a 10 – 15 minutes period using a Garmin Map76CS GPS.

Although the spherical camera recorded 360° spherical images, the images were stored using cylindrical equidistant projections. The resolution of the projected cylindrical images was 5367 pixels in width and 2688 pixels in height.

4.2.2.2 Urban Site Data

The Urban Site was used to test the feasibility and check the algorithm logic. Using the criteria described above, the sampling points were located and all trees who's base and top were clearly visible from the sampling point were identified. For each selected tree, flagging tape was wrapped around the tree circumference at breast height (1.3m) to facilitate visibility and a numbered target placed on each tree to facilitate matching field and image measurements.

The DBH of each tree was measured using calipers and diameter tape. Diameter tapes are often used in operational forest inventories. The DBH estimates using the diameter tape was used as the "field value" (FieldDBH). Because cross-sections of tree trunks are not, generally, perfect circles and often elliptical, at best, and normally irregular, the diameter projected onto an image may vary substantially depending on projection azimuth. The projected DBH was measured using calipers and was measured along the tree axis perpendicular to the projection azimuth (ProjectedDBH).

The algorithms used to estimate DBH and HT were derived using projection geometry (Section 4.2.3). HT was measured in the field from 2 different perspectives: 1) the mean height (ProjectedHT) measured at the digital sampling point; and 2) from a convenient and reasonable location to clearly see the tree tip and base (FieldHT).

To be able to separate logic errors from image measure errors, the required projection angles from the two digital sample heights to the tree tips and bases were measured in the field using a TruPulse laser hypsometer (Laser Tech, Denver, CO) and recorded to the nearest degree (Y°). The four field measured projection angles were labeled as: $FieldU_{1.6}$, $FieldB_{1.6}$, $FieldU_{2.6}$, and $FieldB_{2.6}$ corresponding to the upper projections angles (FieldU) and base projection angles (FieldB) and the subscripts denoting digital sample height. The field projected angles were measured at the digital sample heights using a ladder. Finally, the horizontal distance (FieldR) from camera to each tree was measured using a TruPulse laser hypsometer.

4.2.2.3 Forest Site Data

As with the Urban Site Data, DBH (nearest 0.1cm) and HT (nearest 0.1m) of each individual tree in one replicate from the spacing trial were measured using a diameter tape and laser hypsometer. However, because the spherical images were acquired for a different purpose than individual tree measurement, trees were not individually identified and tagged in the field so that they could be aligned on the spherical image. Therefore, comparisons between field measurements and spherical measurements were limited to plot level rather than individual tree level.

4.2.3 **Image processing algorithms**

The general workflow includes: 1) marking the key points (base and tip) of each individual tree on the cylindrical image; 2) determining the pixel coordinates of the key points in the cylindrical images and conversion to latitude and longitude in spherical coordinates; 3) applying spherical geometry to the spherical coordinates to estimate distance, slope deviation and tree height parameters; and 4) determining the vertical pixel coordinate (y) for breast height (1.3m) in the cylindrical images, marking the left and right tree trunk edges (horizontal angles) at 1.3m, determining the intersection angles to camera center, and estimating DBH by spherical geometry.

The goal of this study was to estimate individual tree DBH and HT using two stereographic spherical images. The images were obtained at 1.6m and 2.6m above ground at the digital sampling point as described above. In preliminary analyses, other digital sample heights were examined (3.6m and 4.6m) and, while tree tip visibility improved, these heights resulted in increased difficulties observing tree bases, so 1.6m and 2.6m were selected for ease of implementation.

We used a spherical geometric approach to estimate tree distance from camera (R), slope elevation change (Δh), HT, and DBH (Fig. 4.3 & Fig. 4.4). The digital sample height, P_1 and P_2 were located at (0, Z_1) and (0, Z_2) respectively (Z_1 = 1.6m and Z_2 = 2.6m in this study, Fig. 4.3.a). R was defined as the radial distance (m) of the tree from the digital sample point (R was always considered positive in our derivations). Δh (m) was defined as the slope elevation change from ground level at the digital sampling point to ground level at the base of the tree.

Tree base and tree tip were the key points (Fig. 4.3) needing to be marked in the cylindrical images which are stored as a simple x-y matrix images using a cylindrical projection. All key points extracted from the cylindrical images were in pixel coordinates. To implement spherical geometry, these pixel coordinates (x_i, y_i) needed to be transformed into spherical angles (lon_i, lat_i) using the methods of Aghayari et al. (2017):

$$\begin{Bmatrix} lon_i = (X - x_i) \times \dfrac{2\pi}{X} \\ lat_i = (y_i - \dfrac{Y}{2}) \times \dfrac{0.5\pi}{Y} \end{Bmatrix} \tag{4.1}$$

where X was the cylindrical image width in pixels (5367 pixels for the images used in this study); Y was the cylindrical image height in pixels (2688 pixels for the images used in this study); x_i was the horizontal pixel coordinate; and y_i was the vertical pixel coordinate. The zenith angle (latitude, lat_i) ranged from -π/2 (-90°) to π/2 (90°) while the azimuth angle (longitude, lon_i) ranged from 0 (0°) to 2π (360°).

There were four key heights for each tree: T_0, T_1, T_2, and T_3 (Fig. 4.3.b). Determination of R and Δh required the angles from the digital sample heights to the tree base (β_1 and β_2, derived from lat_i):

$$\begin{bmatrix} \tan(\beta_1) = (Z_1 - \Delta h)/R \\ \tan(\beta_2) = (Z_2 - \Delta h)/R \end{bmatrix} \tag{4.2}$$

Solving the system of equations in (4.2) for Δh leads to:

$$\Delta h = \frac{Z_2 \tan(\beta_1) - Z_1 \tan(\beta_2)}{\tan(\beta_1) - \tan(\beta_2)} \tag{4.3}$$

and R is then obtained using:

$$R_1 = \frac{Z_1 - \Delta h}{\tan(\beta_1)} \quad \text{or} \quad R_2 = \frac{Z_2 - \Delta h}{\tan(\beta_2)} \tag{4.4}$$

The point T_0 was then defined as, relative to the ground level of the digital sample point (0,0), as (R, Δh). The points T_1 and T_2 were then defined as (R, Z_1) and (R, Z_2) respectively and the heights are: $H_1 = Z_1 - \Delta h$ and $H_2 = Z_2 - \Delta h$ (if $\Delta h < 0$, $H_i > Z_i$). Point T_3 was then (R, $Z_1+R*\tan(\tau_1)$) or (R, $Z_2+R*\tan(\tau_2)$). H_3 is then $H_1+R*\tan(\tau_1)$ or $H_2+R*\tan(\tau_2)$ and is the total height (HT) that we desired. Because our spherical geometric definitions assume that both the camera and the tree are perfectly vertical, any lean in either will produce errors. To account for some of this error, we expressed HT as the average of H_3 derived using P_1 and H_3 derived using P_2. The effect of camera lean was further explored below, effect of tree lean was not considered further.

Tree diameter (DBH) is typical measured at 1.3m (breast height). To estimate DBH from the images, it was first necessary to locate 1.3m on each image. The angle from horizontal to 1.3m was estimated for each image (Fig. 4.4.a) using:

$$\begin{Bmatrix} \gamma_1 = \tan^{-1}\left(\dfrac{1.3-(Z_1-\Delta h)}{R}\right) \\ \gamma_2 = \tan^{-1}\left(\dfrac{1.3-(Z_2-\Delta h)}{R}\right) \end{Bmatrix} \tag{4.5}$$

Because the cylindrical projection places the horizon at the center of the image, the vertical pixel coordinate for 1.3m on both cylindrical images was calculated using the two horizontal angles:

$$\begin{Bmatrix} y_1 = \left(\dfrac{Y}{2}\right) - \dfrac{\gamma_1}{180^\circ} \times Y \\ y_2 = \left(\dfrac{Y}{2}\right) - \dfrac{\gamma_2}{180^\circ} \times Y \end{Bmatrix} \tag{4.6}$$

where y_i = the pixel number of the row, Y = the total number of vertical pixels, and γ_i are the horizontal angles calculated in (4.5).

DBH was then estimated from the tree projection angle on each image (Fig. 4.4.b). Tree projection angle (ω) was estimated by marking the left (B_l) and right (B_r) tree boundaries:

$$\begin{Bmatrix} \omega_1 = 360\left(\dfrac{x_{r,1}-x_{l,1}}{X}\right) \\ \omega_2 = 360\left(\dfrac{x_{r,2}-x_{l,2}}{X}\right) \end{Bmatrix} \tag{4.7}$$

where x_l and x_r were the horizontal pixel coordinates of the left and right side of the tree at 1.3m in cylindrical images (projected B_l and B_r points in stereo coordinates), X = the pixel width of the image. The distance from the camera to the tree center, as shown in Fig. 4.4.c, was the slope distance (L) shown by the blue line in Fig. 4.4.b:

$$\begin{Bmatrix} L_1 = \dfrac{R + DBH/2}{\cos(\gamma_1)} \\ L_2 = \dfrac{R + DBH/2}{\cos(\gamma_2)} \end{Bmatrix} \tag{4.8}$$

DBH (cm) was then estimated using (Fig. 4.4.c):

$$\begin{Bmatrix} DBH_1 = 200L_1 \sin(\omega_1) \\ DBH_2 = 200L_2 \sin(\omega_2) \end{Bmatrix} \tag{4.9}$$

Because L_i depends on DBHi, eq. (4.9), must be solved for DBH yielding:

$$\begin{Bmatrix} DBH_1 = \dfrac{200\sin\left(\dfrac{\omega_1}{2}\right)R}{\left[\cos(\gamma_1) - \sin\left(\dfrac{\omega_1}{2}\right)\right]} \\ DBH_2 = \dfrac{200\sin\left(\dfrac{\omega_2}{2}\right)R}{\left[\cos(\gamma_2) - \sin\left(\dfrac{\omega_2}{2}\right)\right]} \end{Bmatrix} \tag{4.10}$$

As with R and HT, DBH was estimated as the average from the two images: $DBH = (DBH_1 + DBH_2)/2$. To facilitate extraction of the required image measurements, a graphical interface was developed in Python3.6 (Fig. 4.5).

4.2.4 Data analysis

4.2.4.1 Urban Data Analyses

The primary purpose of the Urban study was to collect data in an idea situation and then identify which components of the process were most difficult to extract from the images. In the field we collected all distances (FieldR) and view angles (FieldB and FieldU) as if they were extracted from the images (ImageR, ImageB, and ImageU). These values were then compared to the values obtained from the images using linear regression to check whether logic errors exist in geometry when deriving key points marked in pixel coordinates to projection angles. If the image and field values were the same, then the intercept for the regression should be 0 and the slope 1. To check whether logic errors exist in geometry of tree traits calculation, these field view angles (FieldB and FieldU) were used to calculate the distance (FieldRDerived) and tree heights (FieldHTDerived) by image geometries and compared with those actually measured in field (FieldR, ProjectedHT, and FieldHT) by linear regression mentioned above. Then all the image derived traits (ImageR, ImageDBH, and ImageHT) were compared with field measured (FieldR, ProjectedDBH, FieldDBH, ProjectedHT, FieldHT) by linear regressions. Finally, an analysis about what factors contribute to potential errors was conducted, the distance from tree to camera (R), the horizontal view angle of tree trunk edges (ω), the mean projection angle of tree tip from two digital sample heights (τ), and mean vertical view angle from tree bases to tree tips ($\tau+\beta$) were taken into consideration, the trend of error changes with increasing of these factors is shown by LOWESS regression.

4.2.4.2 Forest Data Analyses

As noted above, the images from the Roddickton spacing trials were originally taken for area-based estimation, not individual tree measurement. As a result, there was no attempt to match individual trees within the images, so the trees were not tagged. This made it very difficult, if not impossible, to match individual field measurements with image measurements for conducting pairwise statistical tests. Instead, we focused on distributional statistics at the plot level to compare DBH and HT estimates. The two-sample Kolmogorov-Smirnov test (Hodges 1958) which tests whether two samples were drawn from the same continuous distribution, was used here. Our null hypothesis was that the field measured samples and image measured samples were distributed the same. The alternative hypothesis was that they were not distributed the same. We assume that equal distributions convey a level of confidence that our technique was measuring DBH and HT correctly. This assumption ignores potential bias in trees visible in the images.

4.3 Results

4.3.1 Urban forest validation

Fig. 4.6 shows the relationship between image measured angles for individual tree key points versus field measured angles for the key points at the two digital sample heights. The key points of tree tip and tree base in images from the two digital sample heights were fundamental for estimating HT and DBH. The correspondence between all image measured angles (ImageB and ImageU) and field measured angles (FieldB and FieldU) was generally very high (Fig. 4.6). There was more deviation in tree tip angles than in tree base angles (Fig. 4.6). The associated goodness-of-fit statistics are shown in Table 4.1. All b_1s were nearly equal to 1. Only b_1 for the 2.6m tip angle was significantly different ($p<0.05$) from 1. The b_0s were more variable; however, none were significantly different ($p<0.05$) from 0 (though b_0 for the 2.6m tip angle was close to $p = 0.05$). The high r^2 values and low rMSE further confirm strong linear relationships between field and image angle measures, which indicates that the key points for the individual trees were marked correctly on the images and demonstrates that there are not logic errors in angle calculation using the spherical projections.

Fig. 4.7 shows comparisons between tree measures derived from field measured angles to those values measured in field (only vertical angles were measured in the field - horizontal angles were too small to reliably measure using hand tools). The radial distance, R (Fig. 4.7.a), which was only a function of base angles was very accurately estimated from the images. Similarly, ProjectedHT, the tree height as viewed from the digital sample point, was also very accurately estimated using image measurements (Fig. 4.7.b). FieldHT, the actual tree height as measured from an appropriate view angle, however, was not very accurately estimated, especially in the upper range (Fig. 4.7.c).

Table 4.2 shows the goodness-of-fit statistics for the simple linear regressions of field measured values versus field derived values. For ProjectedHT, b_0 was close to 0 and b_1 to 1 with high r^2 and low rMSE. However, the DerivedHTs were significantly different ($p<0.05$) from the FieldHTs (Table 4.2). The r^2 was lower and the rMSE was much higher for FieldHT versus DerivedHT. While DerivedHT was significantly different ($p<0.05$) than FieldHT, similar results were obtained if we fit FieldHT versus ProjectedHT with $r^2=0.88$ and rMSE=1.16, demonstrating the importance of measuring tree heights at an appropriate location.

Fig. 4.8 shows the relationships between field measured distance (FieldR) and image estimated distance (ImageR). While the ImageR was slightly underestimated compared to FieldR, the simple linear regression (Table 4.3) showed no significant differences ($p>0.05$) with a high r^2 and low rMSE.

As with DerivedHT, ImageHT was not significantly different ($p > 0.05$) from ProjectedHT (Fig. 4.9); however, ImageHT was significantly different ($p < 0.05$) from FieldHT. As FieldHT increased, there was a trend of increasing overestimation (Fig. 4.9b) similar to what was observed for DerivedHT (Fig. 4.7c). The significance of these trends was confirmed by the linear regressions (Table 4.3).

For DBH estimation (Fig. 4.10), all b_0s and b_1s were not significantly different from 0 and 1, respectively, ($p > 0.05$) for both ProjectedDBH and FieldDBH. The high r^2s (0.96) and low rMSEs (around 2.4) confirmed strong linear relationships between image measured DBHs and field measured DBHs.

4.3.2 Field forest test

The distributional comparisons between field measured attributes and image estimated attributes for the NL spacing study are shown in Fig. 4.11 and the KS test results are given in Table 4.4. With the exception of the 1.2m spacing treatment, the number of measurable trees on the images were lower than the number of trees measured on the actual field plots (Table 4.4), despite having 3 digital sample points per plot. A previous study using the NL spacing trials and spherical images to estimate basal area via modified angle count sampling (Wang et al. In Review, chapter 2, this thesis) showed no visibility bias for angle count sampling; however, this does not appear to be the case for numbers of trees on fixed area plots.

For DBH and HT measurements of individual trees, the results obtained in the forest situation are very different from what were observed in the urban setting. With the exception of the Control spacing (S00), all image HT distributions were not significantly different (p>0.05) from field distributions (Fig. 4.11 and Table 4.4). On the other hand, only the 3.0m spacing (S30) produced DBH distributions that were not significantly different from field distributions (Fig. 4.11 and Table 4.4). These results are the opposite of what was observed in the Urban situation where DBH was estimated consistently more accurately than HT.

4.3.3 Factors contributing to potential errors

To understand how different attributes contribute to the errors in tree measurement obtained from the images, we focus assessment on the urban trees because there were more controls on the field measurements and we could align individual trees between field and image measures. The effects of distance (R), HT, and DBH on the errors between field and image measurements (Error = Image – Field) are shown in Fig. 4.12, Fig. 4.13, and Fig. 4.14, respectively.

The overall trend for errors associated with R was an increasing negative error with increasing distance (increasing underestimation of ImageR with increasing FieldR); however, this trend was largely driven by a single tree located far from the digital sampling point. FieldR errors ranged from about -5.0m to about 1.0m, again with the largest absolute error associated with the farthest tree from the digital sampling point. The more general trend was an increasing variability in error with increasing FieldR. Within the range of most field plot radii (11.28m is widely used in eastern North America), the results are very good with almost no trends in errors (Fig. 4.12.a). The trends of increasing negative errors with increasing tree size was primarily due to extreme trees in the urban setting – extremely far away, extremely tall, or extremely large diameter. Excluding these trees results in much less obvious effects of tree size on distance errors, as would be expected, since distance does not depend on tree size (other than large trees are easier seen on the images).

For FieldHT, with the exception of one tree, all errors were within about ± 2.5m (Fig. 4.13). Surprisingly there was no consistent, obvious trend with increasing FieldR (Fig. 4.13.a); however, while there was no obvious bias, there was decreasing variation in error with increasing FieldR. Similarly, field measured tree size had very little influence on error (Fig. 4.13.b&c). The lack of bias with increasing FieldHT was offset by an increasing trend in variance: as FieldHT increased, the range of errors tended to increase (Fig. 4.13.b). Similar trends were observed for FieldDBH (Fig. 4.13.c). The trends in errors associated with FieldDBH are the result of high correlation between FieldDBH and FieldHT rather than a cause and effect relationship between error and FieldDBH.

Errors for DBH are shown in Figure 4.14. DBH errors ranged from about -5.0 cm to 5.0 cm. Variation in error decreased with increasing FieldR; however, there was no noticeable trends (bias) in error with increasing FieldR (Fig. 4.14.a). Initially, it looks like there was a very strong increasingly negative trend with increasing tree size (especially for FieldHT; Fig. 4.14.b); however, both the FieldHT trend (Fig. 4.14.b) and FieldDBH trend (Fig. 4.14.c) were driven by a single tree that was both the tallest and largest diameter tree in the data set. If this tree was excluded, there were no trends associated with FieldHT and a slightly increasing variability with increasing FieldDBH, especially above 30cm DBH (Fig. 4.14. c).

4.4 Discussion

The goal of this study was to examine the potential of using spherical images to estimate individual tree diameter and height. This method was applied in an open urban setting and in a real forest situation. Our results observed a good correspondence with field measured data in the urban area, while the real forest results were more mixed.

Our urban area validation showed that correspondence between image measured and field measured DBHs was high for both ProjectedDBH (measured by caliper at image view angle) and for FieldDBH (measured with diameter tape) (Fig. 4.8). However, for the real forest test, the results were not as good, distributions of image derived DBHs were consistently larger than distributions of field measured DBHs (Fig. 4.11). For height estimation, the urban forest study showed a high correspondence with ProjectedHT measured in field, however, it did not perform as well with height measured from proper place where the tree tip can be seen clearly (FieldHT). However, surprisingly, in the forest situation, the image measured height (ImageHT) was distributed similarly to field measured height (FieldHT) for all spacings except the control.

There are several possible explanations for the reversed results in the two study areas. First, the urban trees were substantially larger (bigger DBH and higher height) than the forest trees. The urban tree height ranged from 10 m to 25 m (Fig. 4.9), and the urban DBH ranged from 15 cm to 70 cm (Fig. 4.10), while, the forest trees had a DBH range from 5 cm to 25 cm with large variation within and between the different spacing treatments (Fig. 4.11.a-e). Only the 3.0m spacing treatment had low variability within the treatment, and this was the treatment that was not significantly different for DBH. In contrast, the forest trees had HTs lower than about 15m with very narrow variability within and between the spacing treatments (Fig. 4.11.f-j).

Density probably played an important role as well. In the urban setting, the trees were well spaced and the boles clearly distinguishable against a background of grass. In the forested situation, especially at the narrower spacings, the tree trunks often overlapped in the background making it very difficult to clearly distinguish the tree edges. The smaller trees were most likely easier be missed when marking trees for measurement. If the trunk edge was not clearly distinguishable, those trees were not marked on the images. Given that we had three digital sampling points per forest plot, the larger trees were probably more visible across multiple images as well, further contributing to the bias toward larger trees. For example, consider the control plot (S00) and 1.2m spacing plot (S12) field distribution which showed an abundance of very small trees (Fig. 4.11.a&b) - these two plots had the worst performance for DBH estimation. Because we did not attempt to eliminate the repeated measures of trees across images, this probably contributed significantly to the overestimation problem observed in this study. Furthermore, the problem with hidden trees, which exists in all panoramic images (Dick et al. 2010), was an additional source of bias in this study.

The uniformity in the field height distributions (Fig. 4.11) negated any visibility bias for the image height distributions. In addition, the shorter conifer trees in the forested situation, with their cone-shaped crowns, made it easier to identify the real tree tip. As Kershaw et al. (2016 p. 117) pointed out, there is a tendency to overestimate the height of large, flat-crowned trees using the tangent method. Our results in Fig. 4.13 also show

how even isolated trees can be overestimated (in this case, greater than 7 m) due to close proximity to measurement location.

Unlike other under canopy remote sensing techniques, irregularity in tree cross-sectional shape did not appear to be a problem in this study, at least in the Urban setting (Fig. 4.10). Stem irregularities can cause errors in image derived DBH estimates (Perng et al. 2018). Several studies have addressed this issue by either taking images at different azimuths around the stem, or constructing 3D models (Larsen 2006a) or even generating 3D point clouds to assess stem geometric structure (Ringdahl et al. 2013, Liang et al. 2014, Surový et al. 2016, Mokroš et al. 2018). Though these methods produce small errors (<12%; (Ringdahl et al. 2013) and low rMSEs: 1.27cm – 2.39cm (Liang et al. 2014, Surový et al. 2016, Mokroš et al. 2018)), however, the computation requirements limit their wide-scale application in forest inventories. Our results show, if accounting for the optical fork effects (Grosenbaugh 1963), the error can be decreased to an acceptable level. In our case, errors were 2.4 ± 1.6 cm. Similarly, Celes et al. (2019) reported an uncertainty of approximately ±1 cm and Lu et al. (2019) had errors within ±6 cm with the assistance of field reference targets.

One of the biggest limitations for applying spherical images to whole plot measurement is tree visibility, not only for small trees far away from plot center with very narrow view angles, but also for trees occluded by larger trees near plot center. Instead of using fixed area sampling with spherical images, angle count sampling (as shown in Chapter 2) is a powerful sampling technique that could eliminate or minimize this limitation. By controlling the basal area factor, the visibility issue can be controlled (Wang et al. In Press (chapter 2, this thesis); Dick 2012). As shown by Wang et al. (In

Press; this thesis Chapter 2), hidden tree effects can be further minimized using three digital sampling points.

The measurement methods developed here could be integrated into a Big BAF sampling scheme as well (Bell et al. 1983, Iles 2003, Marshall et al. 2004). The Big BAF system uses a small BAF to estimate basal area, and larger BAF to select trees to measure HT and DBH. If designed carefully, less than one tree per plot, on average, needs measured (Bell et al. 1983, Marshall et al. 2004, Yang et al. 2017), thus eliminating the potential for bias due to visibility, as observed here.

One of the key next steps is to replicate the measurement protocols used in the urban setting in a forested situation where field and image measurements could be matched. This will help eliminate some of the uncertainty we obtained in our forested test. There are several additional improvements that could greatly improve the efficiency and accuracy of this technique. Development of an automatic key point matching algorithm between the two spherical images using pattern matching algorithms would decrease the image processing workload and eliminate some user error associated with manual marking. Time-motion studies comparing in field measurement times with image measurement times would also provide additional insight into gains in measurement efficiency associated with this technique.

4.5 Conclusion

Though the use of images in forest inventory has a long history with numerous methods to estimate desired forest attributes, the use of vertical paired spherical images has not been explored prior to this study. Our results show this novel technology can achieve good correspondence with field measures; however, issues of visibility need to be considered when applying the technique operationally. Appropriate sampling units, such as angle count sampling, may minimize some of these issues.

4.6 References

Aghayari, S., M. Saadatseresht, M. Omidalizarandi, and I. Neumann. 2017. Geometric Calibration of Full Spherical Panoramic Ricoh-Theta Camera. ISPRS Annals of Photogrammetry, Remote Sensing and Spatial Information Sciences IV-1(W1):237–245.

Anton, H. 2019, Forest measurement by smartphone | LinkedIn. https://www.linkedin.com/pulse/forest-measurement-smartphone-anton-holmstr%C3%B6m/. Accessed Date: 28-07-2019.

Bell, J. F., K. Iles, and D. Marshall. 1983. Balancing the ratio of tree count-only sample points and VBAR measurements in variable plot sampling.Bell J.F. and Atterbury, T. (eds.). Proceedings: Renewable Resource Inventories for Monitoring Changes and Trends. College of Forestry, Oregon State University, Corvallis, OR. pp. 699–702.

Belton, D., S. Moncrieff, and J. Chapman. 2013. Processing tree point clouds using Gaussian Mixture Models. ISPRS Annals of Photogrammetry, Remote Sensing and Spatial Information Sciences. Copernicus GmbH, Antalya, Turkey. pp. 43–48.

Berveglieri, A., A. Tommaselli, X. Liang, and E. Honkavaara. 2017. Photogrammetric measurement of tree stems from vertical fisheye images. Scandinavian Journal of Forest Research 32:737–747.

Bitterlich, W. 1959. Sektorkluppern aus Leichmetall. (Calipering forks made of light alloys). Holzkurier 14:15–17.

Bitterlich, W. 1984. The relascope idea: Relative measurements in forestry. First. CAB International, Slough, England.

Blake, J., G. Somers, and G. Ruark. 1991. Estimating limiting foliar biomass in conifer plantations from allometric relationships and self-thinning behavior. Forest Science 37:296–307.

Celes, C. H. S., R. F. de Araujo, F. Emmert, A. J. N. Lima, and M. A. A. Campos. 2019. Digital Approach for Measuring Tree Diameters in the Amazon Forest. Floresta e Ambiente 26.

Chazdon, R. L. 2008. Beyond Deforestation: Restoring Forests and Ecosystem Services on Degraded Lands. Science 320:1458–1460.

Clark, N. A., R. H. Wynne, and D. L. Schmoldt. 2000a. A review of past research on dendrometers. Forest Science 46:570–576.

Clark, N. A., R. H. Wynne, D. L. Schmoldt, and M. Winn. 2000b. An assessment of the utility of a non-metric digital camera for measuring standing trees. Computers and Electronics in Agriculture 28:151–169.

Clark, N., R. H. Wynne, D. L. Schmoldt, P. A. Araman, and M. F. Winn. 1998. Use of a non-metric digital camera for tree stem evaluation. Page Proceedings, 1998 ASPRS/RT Annual Convention.(pre-published version).

Dean, C. 2003. Calculation of wood volume and stem taper using terrestrial single-image close-range photogrammetry and contemporary software tools. Silva Fennica 37:359–380.

DeCourt, N. 1956. Utilisation de la photographie pour mesurer les surfaces terrières (The use of photography for measuring basal area). Revue Forestière Française 8:505–507.

Dick, A. R., J. A. Kershaw, and D. A. MacLean. 2010. Spatial Tree Mapping Using Photography. Northern Journal of Applied Forestry 27:68–74.

Fastie, C. L. 2010. Estimating stand basal area from forest panoramas. Page 8 Proceedings of the Fine International Conference on Gigapixel Imaging for Science. Carnegie Mellon University, Pittsburg, PA.

Forsman, M., N. Börlin, and J. Holmgren. 2016. Estimation of Tree Stem Attributes Using Terrestrial Photogrammetry with a Camera Rig. Forests 7(61).

Giannetti, F., N. Puletti, V. Quatrini, D. Travaglini, F. Bottalico, P. Corona, and G. Chirici. 2018. Integrating terrestrial and airborne laser scanning for the assessment of single-tree attributes in Mediterranean forest stands. European Journal of Remote Sensing 51:795–807.

Grosenbaugh, L. R. 1963. Optical dendrometers for out-of-reach diameters: A conspectus and some new theory. Forest Science Monographs 4(48).

Hilker, T., M. van Leeuwen, N. C. Coops, M. A. Wulder, G. Newnham, D. L. B. Jupp, and D. S. Culvenor. 2010. Comparing canopy metrics derived from terrestrial and airborne laser scanning in a Douglas-fir dominated forest stand. Trees, Structure and Function 24:819–832.

Hodges, J. L. 1958. The significance probability of the smirnov two-sample test. Arkiv för Matematik 3:469–486.

Iles, K. 2003. A sampler of inventory topics. 2nd edition. Kim Iles and Associates, Nanaimo, BC.

Jackson, A. 1911. The Biltmore stick and its use on national forests. Journal of Forestry 9:406–411.

Kaartinen, H., J. Hyyppä, X. Yu, M. Vastaranta, H. Hyyppä, A. Kukko, M. Holopainen, C. Heipke, M. Hirschmugl, F. Morsdorf, E. Næsset, J. Pitkänen, S. Popescu, S. Solberg, B. M. Wolf, and J.-C. Wu. 2012. An International Comparison of Individual Tree Detection and Extraction Using Airborne Laser Scanning. Remote Sensing 4:950–974.

Kershaw, J. A., Jr., M. J. Ducey, T. W. Beers, and B. Husch. 2016. Forest Mensuration. 5th edition. Wiley/Blackwell, Hobokin, NJ.

Lam, T. Y., J. A. Kershaw, Z. S. N. Hajar, K. A. Rahman, A. R. Weiskittel, and M. D. Potts. 2017. Evaluating and modelling genus and species variation in height-to-diameter relationships for Tropical Hill Forests in Peninsular Malaysia. Forestry: An International Journal of Forest Research 90:268–278.

Lambert, M.-C., C.-H. Ung, and F. Raulier. 2005. Canadian national tree aboveground biomass equations. Canadian Journal of Forest Research 35:1996–2018.

Larsen, D. R. 2006a. Use of very high resolution digital oblique photography in the development of 3-dimensional models for tree measurements: Examples from ground based and aerial based platforms. American Society of Photogrammetry and Remote Sensing (published by ASPRS on CD).

Larsen, D. R. 2006b. Development of a photogrammetric method of measuring tree taper outside bark. Gen. Tech. Rep. SRS-92. Asheville, NC: U.S. Department of Agriculture, Forest Service, Southern Research Station. pp. 347-350.

Li, W., Q. Guo, M. Jakubowski, and M. Kelly. 2012. A new method for segmenting individual trees from the lidar point cloud. Photogrammetric Engineering and Remote Sensing 78:75–84.

Liang, X., A. Jaakkola, Y. Wang, J. Hyyppä, E. Honkavaara, J. Liu, and H. Kaartinen. 2014. The Use of a Hand-Held Camera for Individual Tree 3D Mapping in Forest Sample Plots. Remote Sensing 6:6587–6603.

Liang, X., Y. Wang, A. Jaakkola, A. Kukko, H. Kaartinen, J. Hyyppä, E. Honkavaara, and J. Liu. 2015. Forest Data Collection Using Terrestrial Image-Based Point Clouds From a Handheld Camera Compared to Terrestrial and Personal Laser Scanning. IEEE Transactions on Geoscience and Remote Sensing 53:5117–5132.

Liu, J., Z. Feng, L. Yang, A. Mannan, T. U. Khan, Z. Zhao, and Z. Cheng. 2018. Extraction of Sample Plot Parameters from 3D Point Cloud Reconstruction Based on Combined RTK and CCD Continuous Photography. Remote Sensing 10(1299).

Lu, M.-K., T. Y. Lam, B.-H. Perng, and H.-T. Lin. 2019. Close-range photogrammetry with spherical panoramas for mapping spatial location and measuring diameters of trees under forest canopies. Canadian Journal of Forest Research 49:865–874.

Marshall, D. D., K. Iles, and J. F. Bell. 2004. Using a large-angle gauge to select trees for measurement in variable plot sampling. Canadian Journal of Forest Research 34:840–845.

Miller, J., J. Morgenroth, and C. Gomez. 2015. 3D modelling of individual trees using a handheld camera: Accuracy of height, diameter and volume estimates. Urban Forestry & Urban Greening 14:932–940.

Mokroš, M., J. Výbošťok, J. Tomaštík, A. Grznárová, P. Valent, M. Slavík, and J. Merganič. 2018. High Precision Individual Tree Diameter and Perimeter Estimation from Close-Range Photogrammetry. Forests 9(696).

Mulverhill, C., N. C. Coops, P. Tompalski, C. W. Bater, and A. R. Dick. 2019. The utility of terrestrial photogrammetry for assessment of tree volume and taper in boreal mixedwood forests. Annals of Forest Science 76(83).

Pan, Y., R. A. Birdsey, O. L. Phillips, and R. B. Jackson. 2013. The Structure, Distribution, and Biomass of the World's Forests. Annual Review of Ecology, Evolution, and Systematics 44:593–622.

Pengle, C., L. Jinhao, and W. Dian. 2013. Measuring diameters at breast height using combination method of laser and machine vision (In Chinese). Transactions of the Chinese Society for Agricultural Machinery 44:271–275.

Perng, B.-H., T. Y. Lam, and M.-K. Lu. 2018. Stereoscopic imaging with spherical panoramas for measuring tree distance and diameter under forest canopies. Forestry: An International Journal of Forest Research 91:662–673.

Reineke, L. H. 1940. Permanent sample plot photography. Journal of Forestry 38:813–815.

Ricoh Imaging Company, LTD. 2016. Rioch Theta S 360 video camera. http://www.ricoh-imaging.co.jp/english/products/theta_s/. Last Accessed 26-08-2016.

Ringdahl, O., P. Hohnloser, T. Hellström, J. Holmgren, and O. Lindroos. 2013. Enhanced Algorithms for Estimating Tree Trunk Diameter Using 2D Laser Scanner. Remote Sensing 5:4839–4856.

Rodríguez-García, C., F. Montes, F. Ruiz, I. Cañellas, and P. Pita. 2014. Stem mapping and estimating standing volume from stereoscopic hemispherical images. European Journal of Forest Research 133:895–904.

Sánchez-González, M., M. Cabrera, P. J. Herrera, R. Vallejo, I. Cañellas, and F. Montes. 2016. Basal Area and Diameter Distribution Estimation Using Stereoscopic Hemispherical Images. Photogrammetric Engineering & Remote Sensing 82:605–616.

Shimizu, A., S. Yamada, and Y. Arita. 2014. Diameter Measurements of the Upper Parts of Trees Using an Ultra-Telephoto Digital Photography System. Open Journal of Forestry 4:316–326.

Smith, W. B., and G. J. Brand. 1983. Allometric biomass equations for 98 species of herbs, shrubs, and small trees. Page 8. Research Note, USDA, Forest Service, North Central Forest Experiment Station.

Snavely, N., S. M. Seitz, and R. Szeliski. 2008. Modeling the World from Internet Photo Collections. International Journal of Computer Vision 80:189–210.

Stewart, B. 2004, August. Using a camera as an angle gauge in angle-count sampling. MF Thesis, The University of Georgia.

Strimbu, B. M., C. Qi, and J. Sessions. 2019. Accurate Geo-Referencing of Trees with No or Inaccurate Terrestrial Location Devices. Remote Sensing 11(16).

Strîmbu, V. F., and B. M. Strîmbu. 2015. A graph-based segmentation algorithm for tree crown extraction using airborne LiDAR data. ISPRS Journal of Photogrammetry and Remote Sensing 104:30–43.

Surový, P., A. Yoshimoto, and D. Panagiotidis. 2016. Accuracy of Reconstruction of the Tree Stem Surface Using Terrestrial Close-Range Photogrammetry. Remote Sensing 8:123.

Varjo, J., H. Henttonen, J. Lappi, J. Heikkonen, and J. Juujärvi. 2006. Digital horizontal tree measurements for forest inventory. Working papers of the Finnish Forest Research Institute 40(23).

Wells, L. A. 2018. A Vision System for Automatic Dendrometry and Forest Mapping. Ph.D. Thesis, Oregon State University, Corvallis, Oregon.

Xing, Z., C. P.-A. Bourque, D. E. Swift, C. W. Clowater, M. Krasowski, and F.-R. Meng. 2005. Carbon and biomass partitioning in balsam fir (Abies balsamea). Tree Physiology 25:1207–1217.

Yang, T.-R., Y.-H. Hsu, J. A. Kershaw, E. McGarrigle, and D. Kilham. 2017. Big BAF sampling in mixed species forest structures of northeastern North America: influence of count and measure BAF under cost constraints. Forestry: An International Journal of Forest Research 90:649–660.

Zianis, D., P. Muukkonen, R. Mäkipää, and M. Mencuccini. 2005. Biomass and stem volume equations for tree species in Europe. Silva Fennica Monographs 4(63).

Table 4.1: Simple linear regression results for angle measured from image and field. The linear model is Y=b0+b1*X, if Image (X) is the same as Field (Y), then b0=0 and b1=1

X	Y	Param.	Estimate	Std. Err.	p-value	r^2	rMSE
ImageB_{16}	FieldB_{16}	b_0	0.093	0.258	0.722	0.991	0.809
		b_1	1.028	0.022	0.209		
ImageU_{16}	FieldU_{16}	b_0	1.247	1.064	0.255	0.989	1.557
		b_1	0.963	0.224	0.116		
ImageB_{26}	FieldB_{26}	b_0	-0.039	0.357	0.914	0.991	0.964
		b_1	0.994	0.022	0.800		
ImageU_{26}	FieldU_{26}	b_0	1.941	1.008	0.069	0.989	1.563
		b_1	0.951	0.022	0.040		

Param. = Parameter; Std. Err. = Standard Error; rMSE = root Mean Square Error.

Table 4.2: Simple linear regression results for factors measured from field and field angle derived. The linear model is Y=b0+b1X, if field angle derived (X) is the same as Field measured (Y), then b0=0 and b1=1

X	Y	Param.	Est.	Std. Err.	p-value	r^2	rMSE
DerivedR	FieldR	b_0	-0.180	0.542	0.743	0.974	0.952
		b_1	1.058	0.039	0.153		
DerivedHT	ProjectedHT	b_0	0.653	0.743	0.390	0.949	0.971
		b_1	0.990	0.052	0.851		
DerivedHT	FieldHT	b_0	3.954	1.245	0.005	0.761	1.627
		b_1	0.692	0.087	0.002		
ProjectedHT	FieldHT	b_0	3.032	0.900	0.003	0.880	1.155
		b_1	0.731	0.060	<0.001		

Param. = Parameter; Est.=Estimate; Std. Err. = Standard Error; rMSE = root Mean Square Error.

Table 4.3: Simple linear regression results between image estimates and field measures. The linear model is Y=b0+b1*X, if Image measured (X) is the same as Field measured (Y), then b0=0 and b1=1

X	Y	Param.	Est.	Std. Err.	p-value	r^2	rMSE
ImageR	FieldR	b_0	-0.180	0.542	0.743	0.974	0.153
		b_1	1.058	0.039	0.153		
ImageHT	ProjectedHT	b_0	0.653	0.743	0.390	0.949	0.971
		b_1	0.990	0.052	0.851		
ImageHT	FieldHT	b_0	3.954	1.245	0.005	0.762	1.627
		b_1	0.692	0.087	0.002		
ImageDBH	ProjectedDBH	b_0	-1.246	1.546	0.430	0.966	2.398
		b_1	1.039	0.044	0.378		
ImageDBH	FieldDBH	b_0	0.116	1.578	0.942	0.962	2.448
		b_1	0.999	0.044	0.963		

Param. = Parameter; Est. = Estimate; Std. Err. = Standard Error; rMSE = root Mean Square Error.

Table 4.4: Summary of KS-Tests for real forest validation. Plot radii varied by spacing treatment (Control (S00, 5.2m);1.2m (S12, 7.2m); 1.8m (S18, 10.4m); 2.4m (S24, 15.0m); 3.0m (S30, 18.0m))

Plot	**Field Tree #**	**Image Tree #**	**Factor**	**KS Value**	**p-value**
S00	94	63	DBH	0.4262	<0.001
			HT	0.2518	0.013
S12	56	92	DBH	0.3602	<0.001
			HT	0.2096	0.079
S18	103	60	DBH	0.2589	<0.001
			HT	0.1126	0.6697
S24	137	96	DBH	0.2600	<0.001
			HT	0.1393	0.198
S30	122	59	DBH	0.1555	0.257
			HT	0.1188	0.577

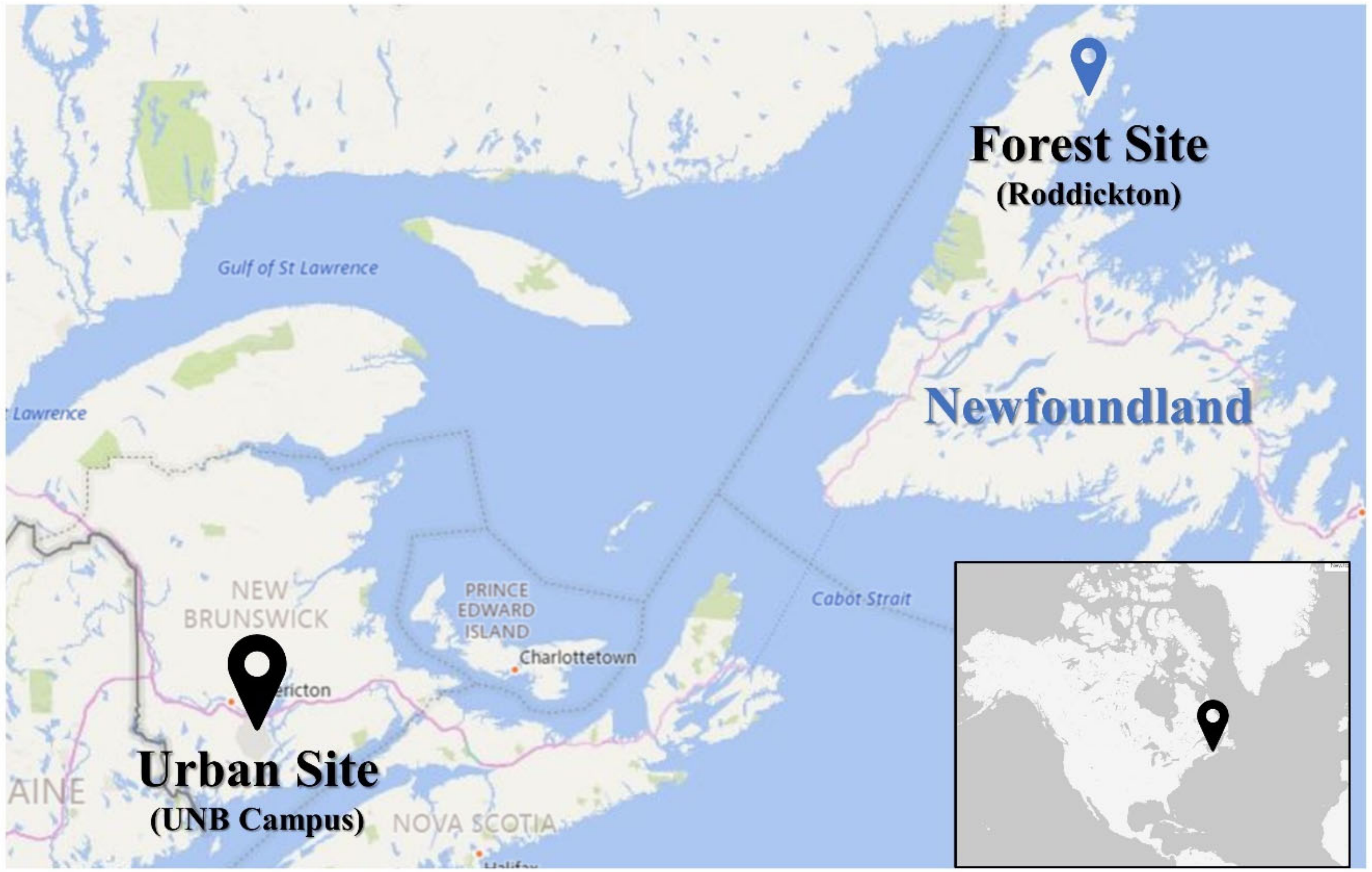

Fig. 4.1: Two study sites locations in this study.

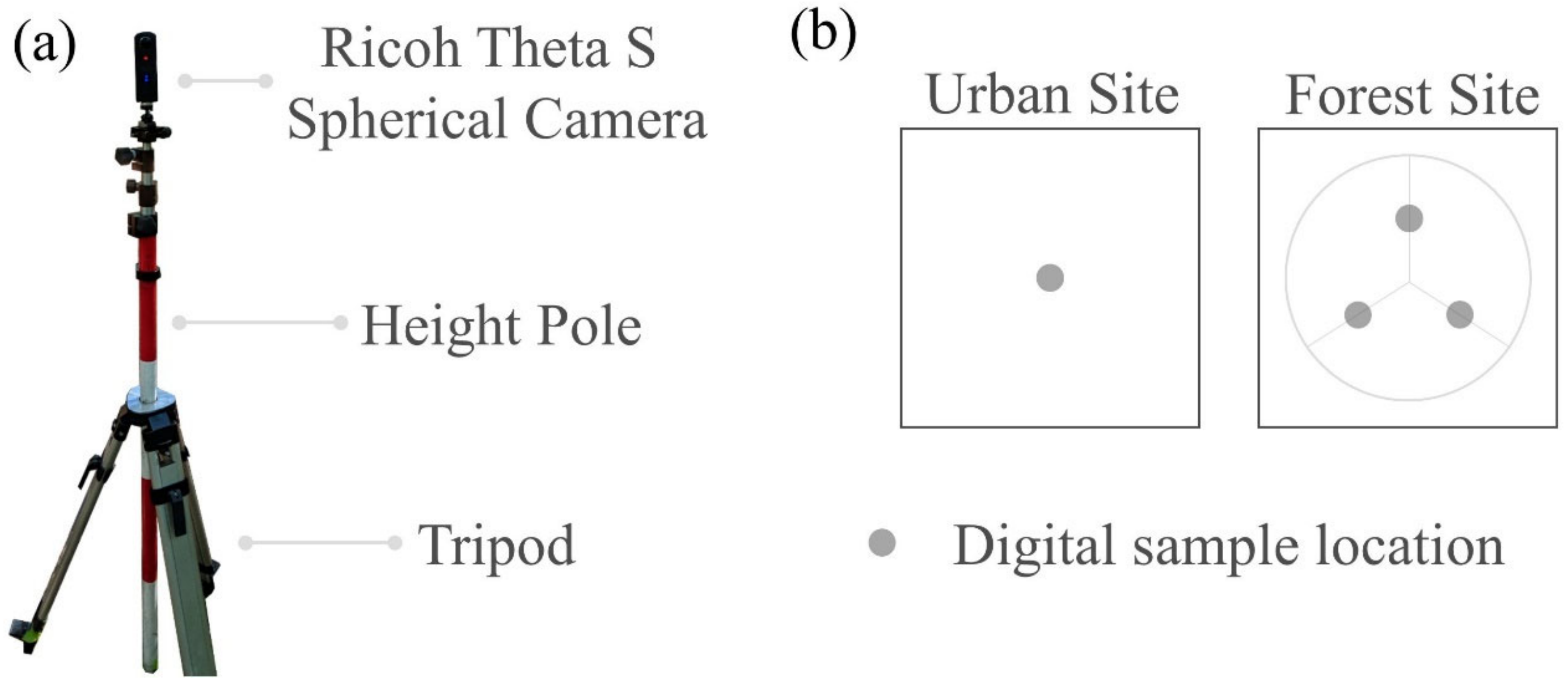

Fig. 4.2: Digital data collection methods. (a) tripod and spherical camera set up for spherical image acquisition at two different heights (1.6m and 2.6m). (b) Digital sample location design for urban area feasibility validation and real forest application. For Urban Site, only one location center was set. For Forest Site, three locations were established at the midpoint of plot radius along azimuths of 0°, 120°, and 240°.

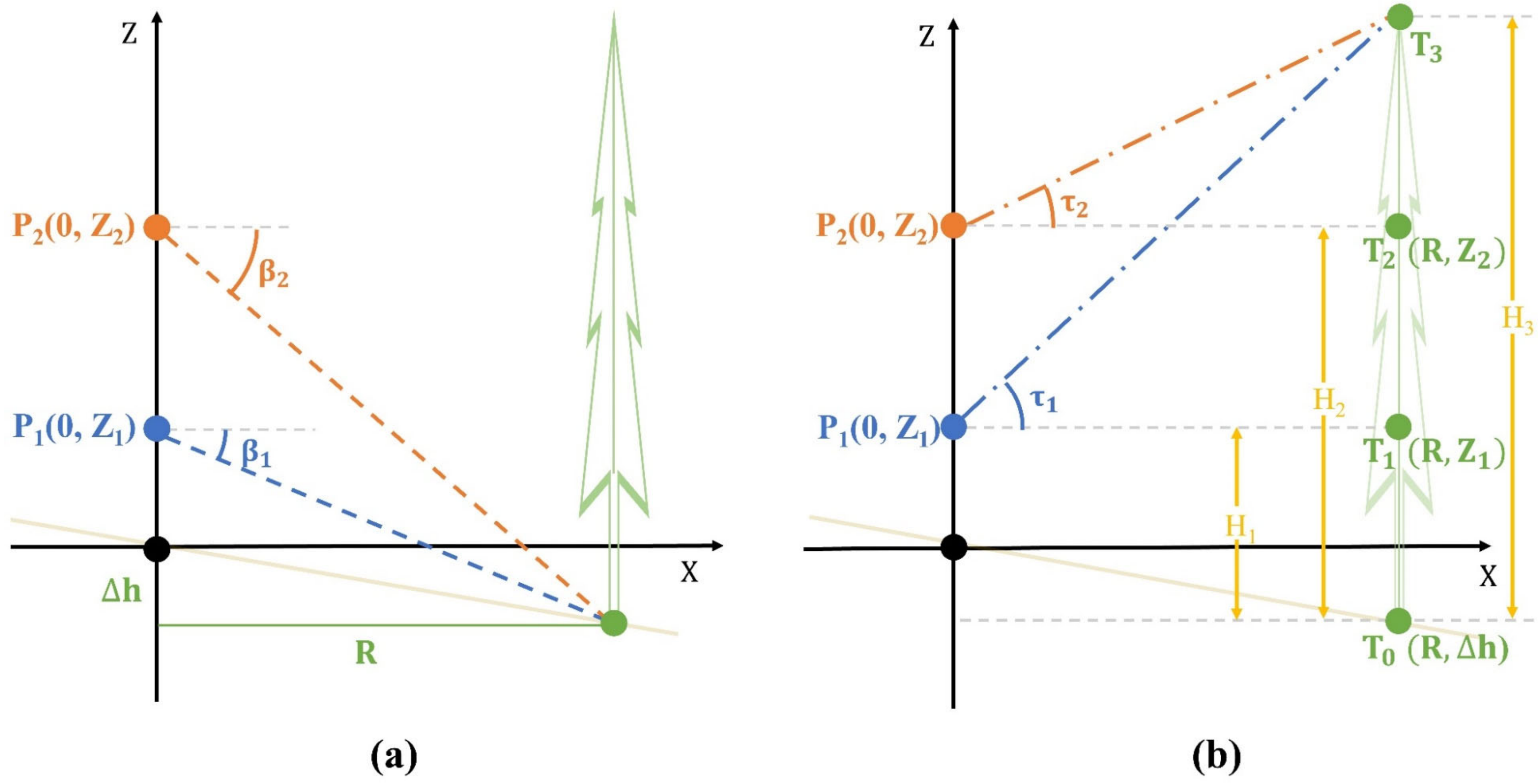

Fig. 4.3: The distance, slope deviation, and tree height calculation from the side view of spherical geometry. (a) derived the distance (R) and slope deviation (△h) caused by terrain by key points of tree bases. (b) is the height calculation by key points of tree tips.

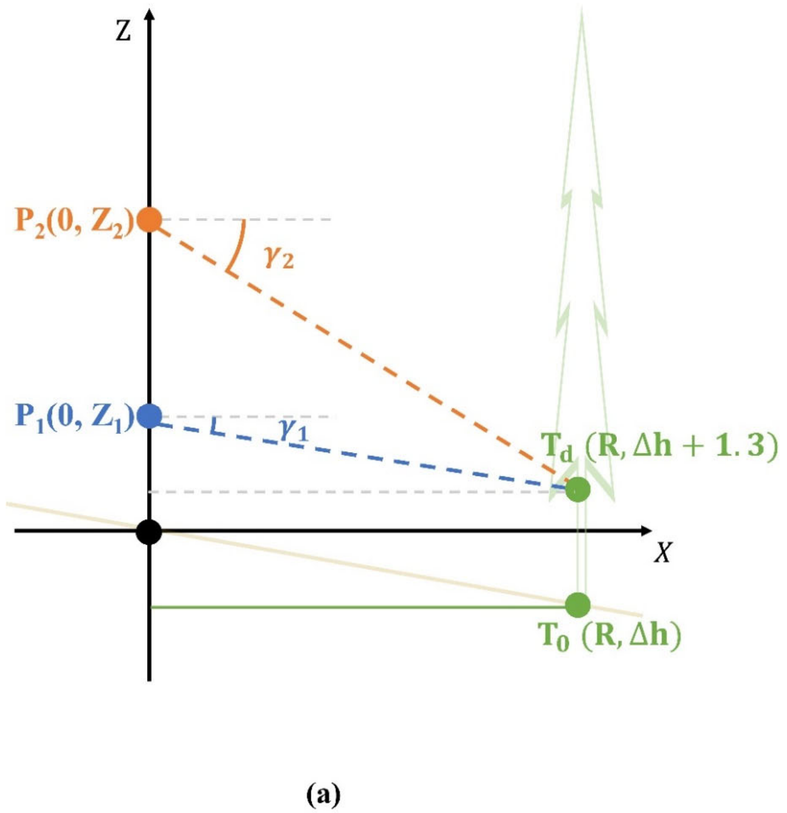

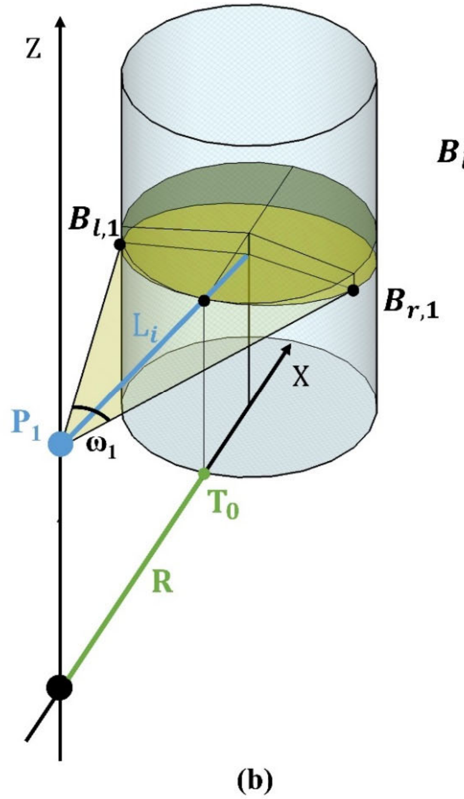

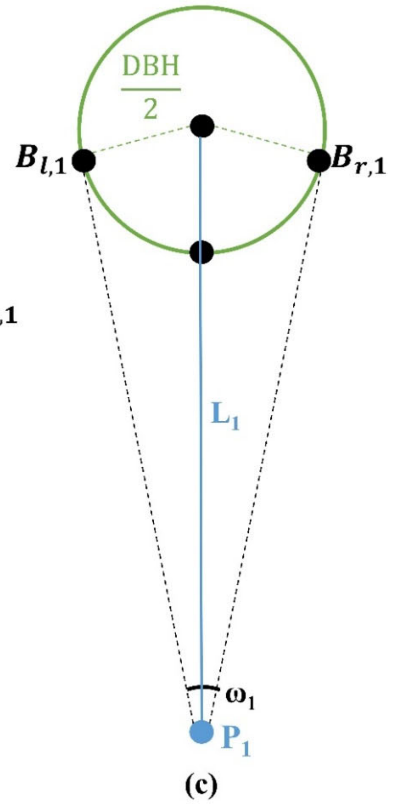

Fig. 4.4: The DBH calculation in spherical geometry. (a) is the calculation for 1.3m height in image. (b) is the hint about DBH boundary marking and distance to tree center in stereo coordinates (using 1.6m digital sample height for example); (c) is the geometry calculation for DBH.

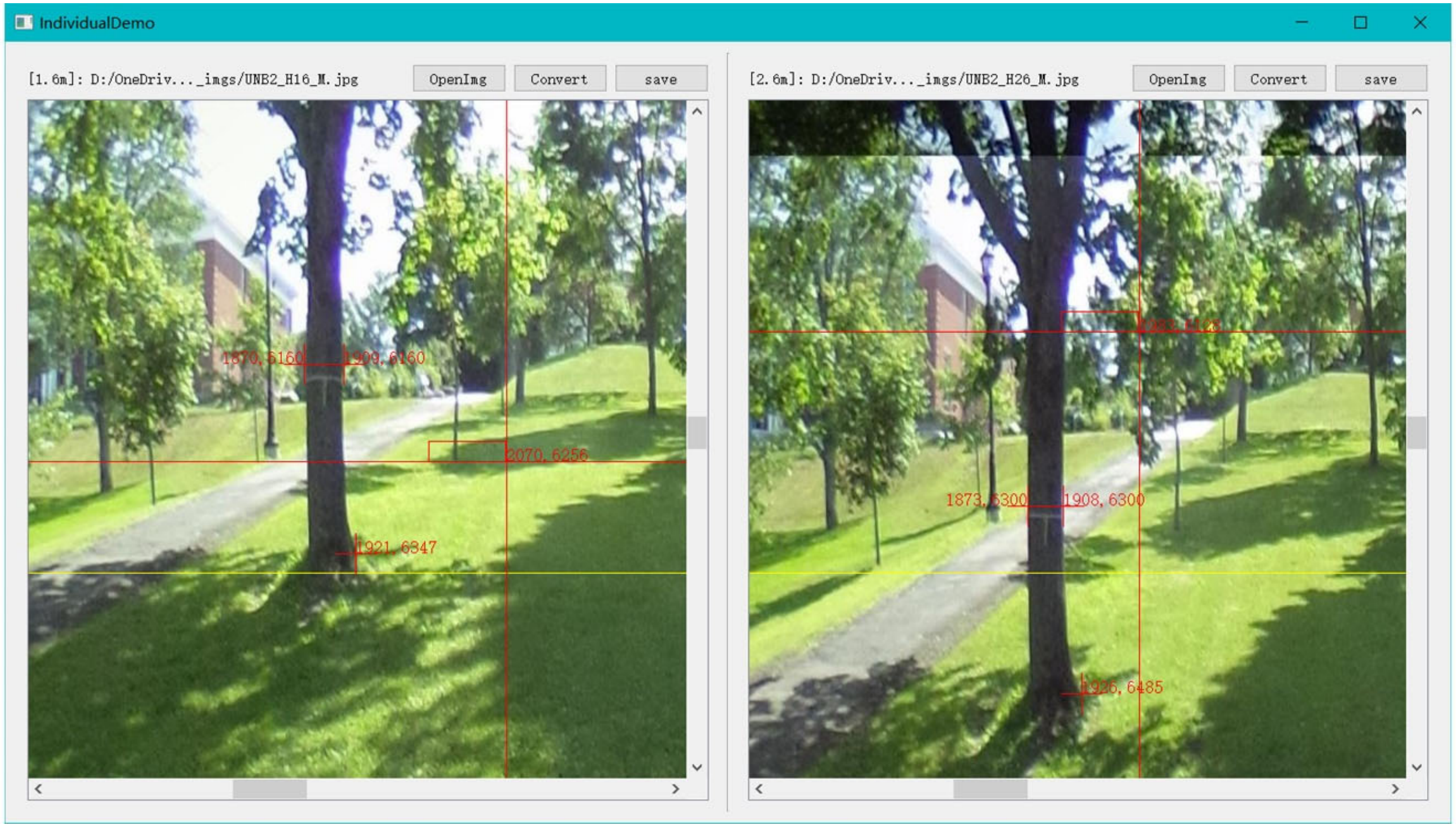

Fig. 4.5: The graphical user interface that used to extract the key points coordinates of individual trees for parameter calculation. The images show in this figure are plot B with steep slope. And the yellow line shows the horizontal line (the equator) of spherical images.

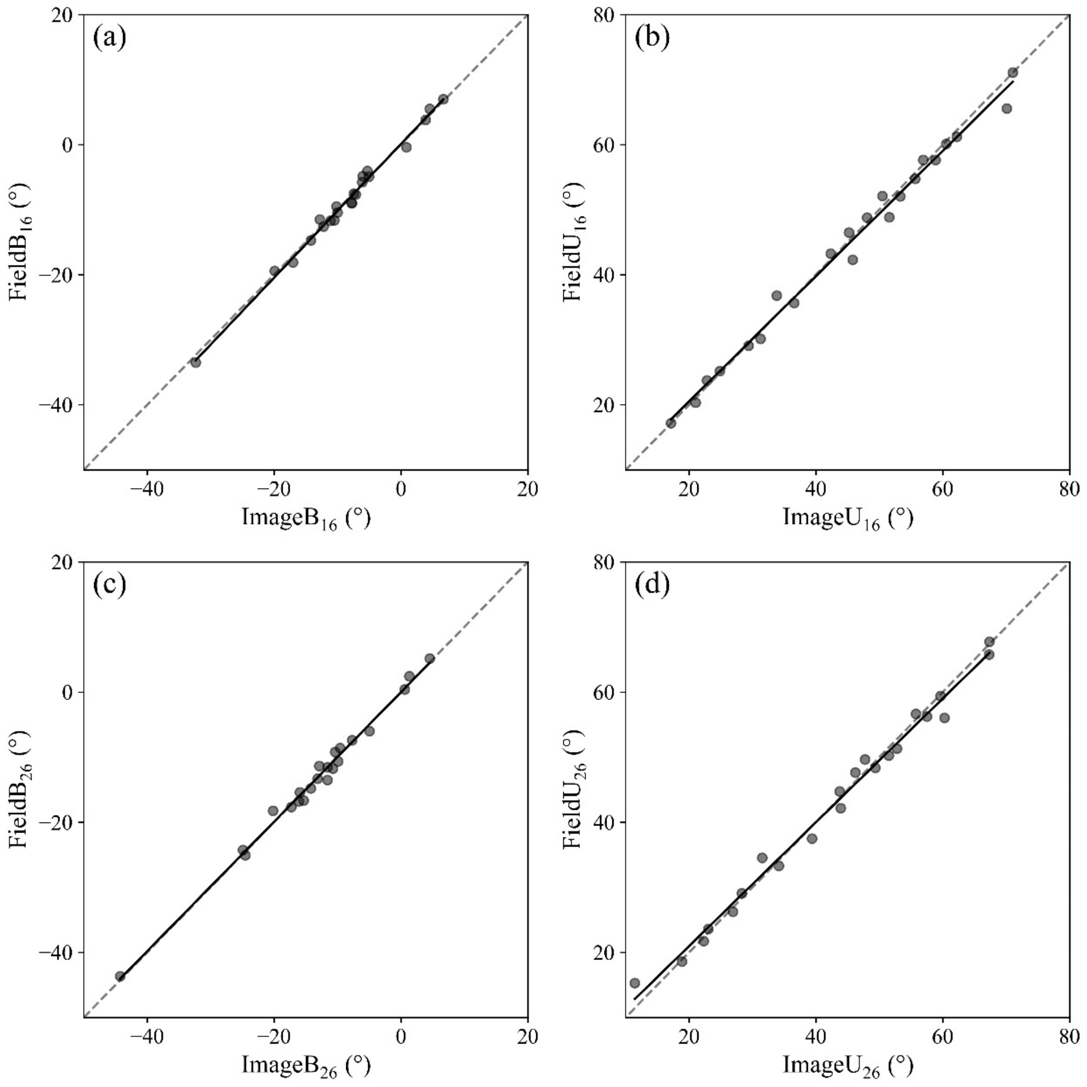

Fig. 4.6: The angle comparison between image measured and field measured.

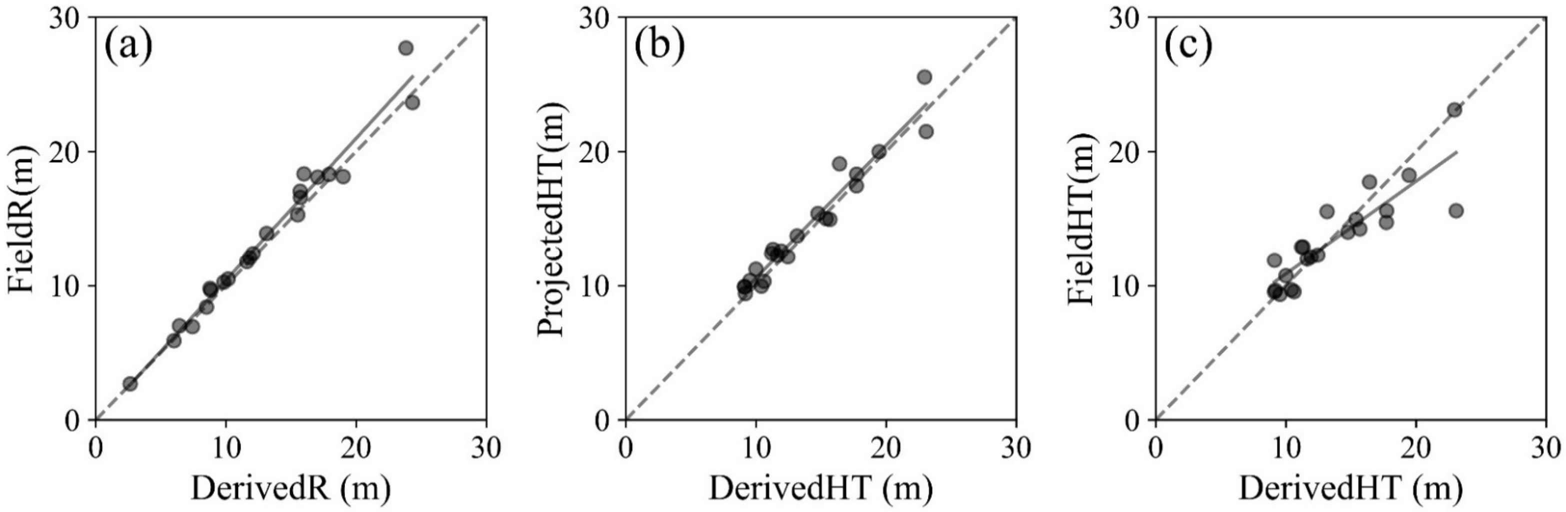

Fig. 4.7: Comparisons between field measures and those derived from field measured angles using spherical geometry: (a) comparison between radial distance (R) derived from field angles (DerivedR) and R as measured in the field (FieldR); (b) comparison between height derived from field angles (DerivedHT) and HT as measured at digital sampling point (ProjectedHT); (c) comparison between height derived from field angles (DerivedHT and HT as measured in the field at proper place where tree tip and base were clearly visible (FieldHT).

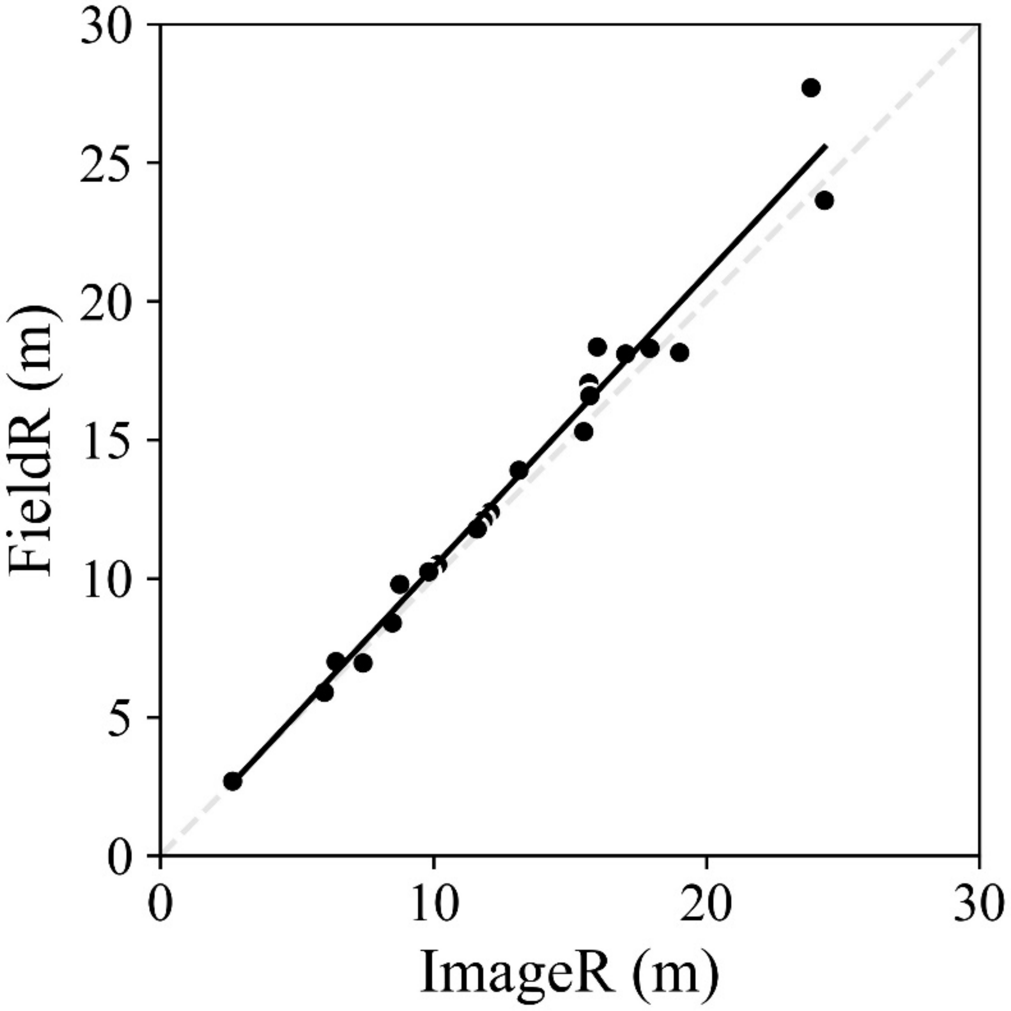

Fig. 4.8: Radial distance comparisons between field measured and image estimates.

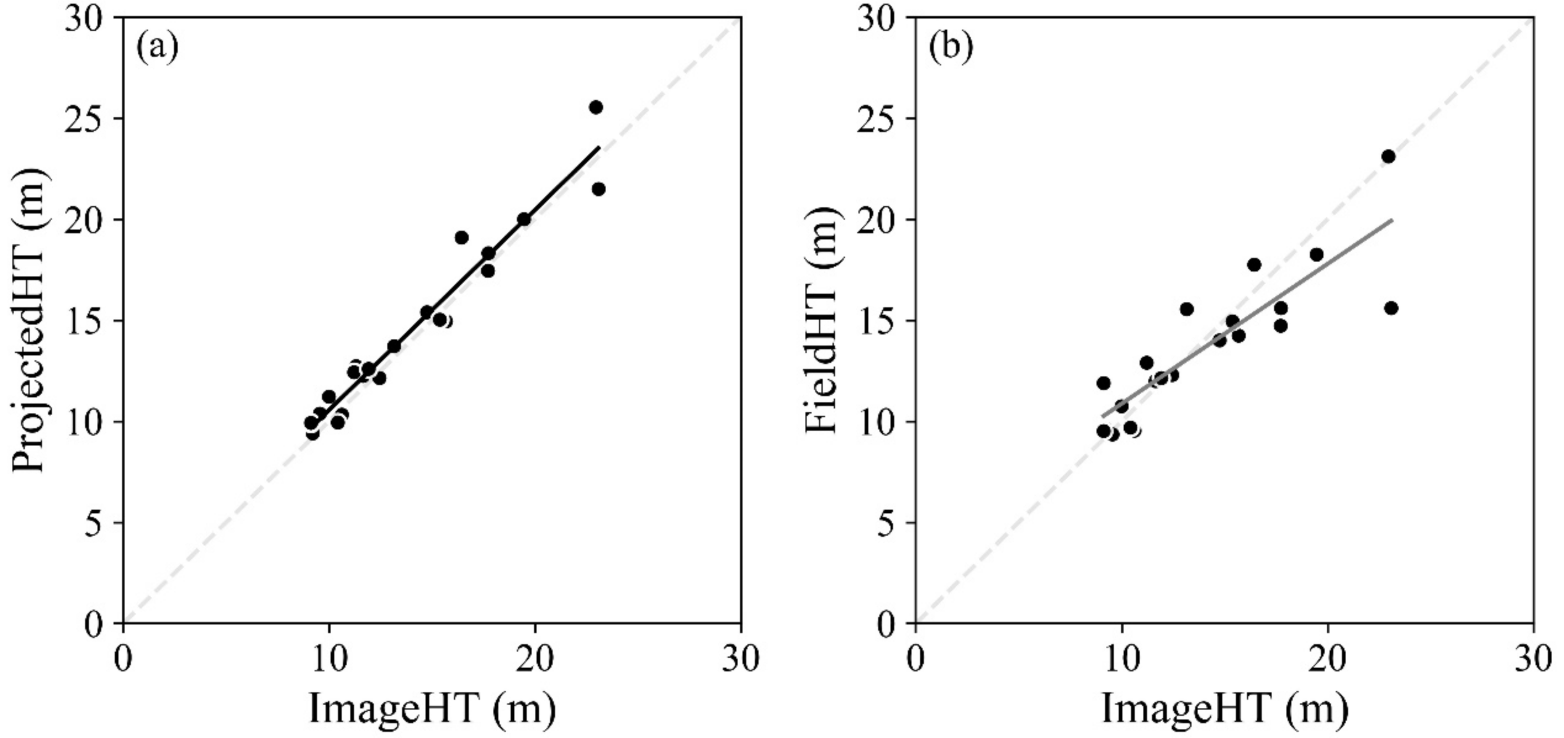

Fig. 4.9: Individual height (HT) comparisons between field measured and image estimates. (a) is compared with field height measured at the digital sampling points, (b) is compared with field height measured at proper place that can see the tree tip clearly.

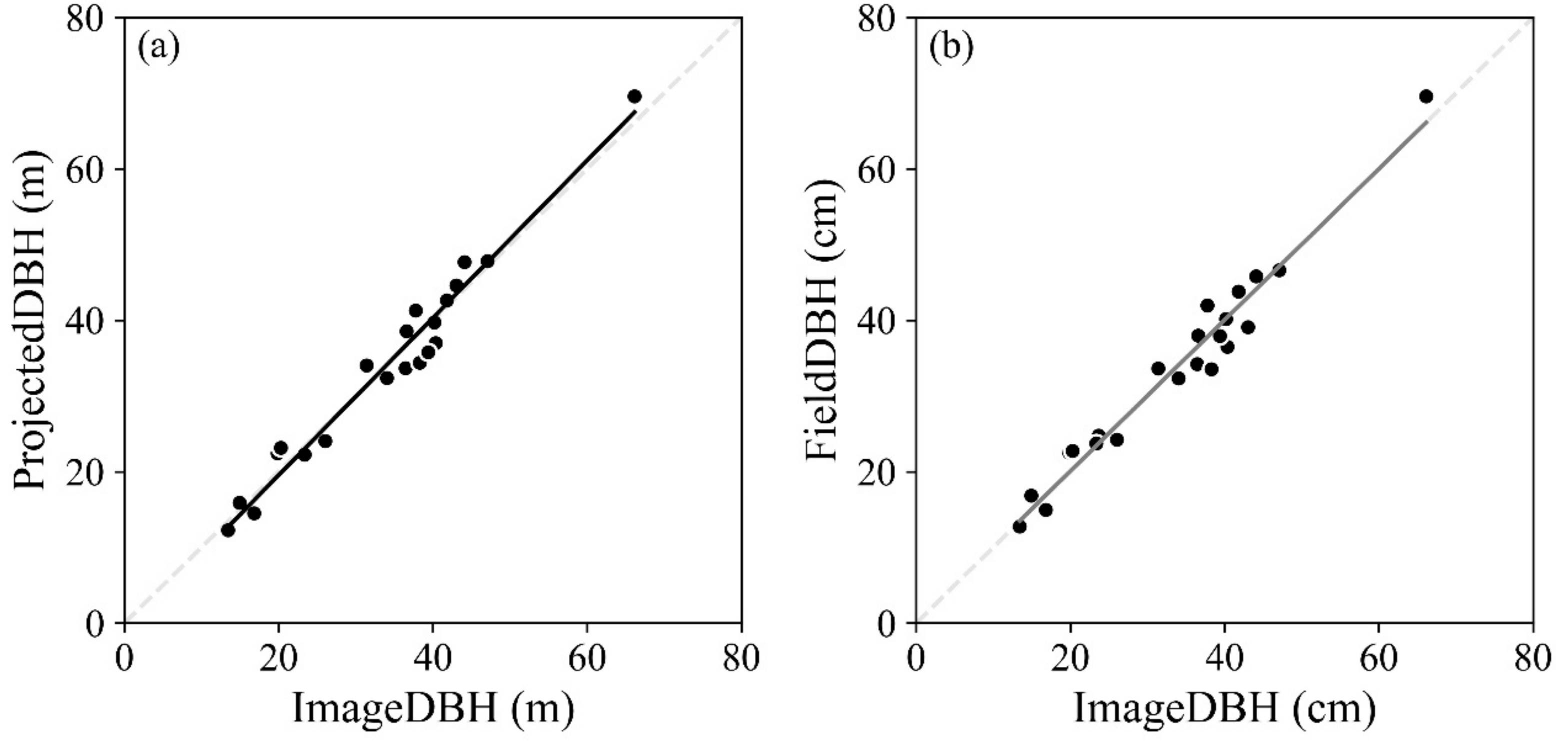

Fig. 4.10: DBH comparisons between field measured and image estimates (a) is compared with projected DBH measured by caliper, (b) is compared with DBH measured by dimeter tape.

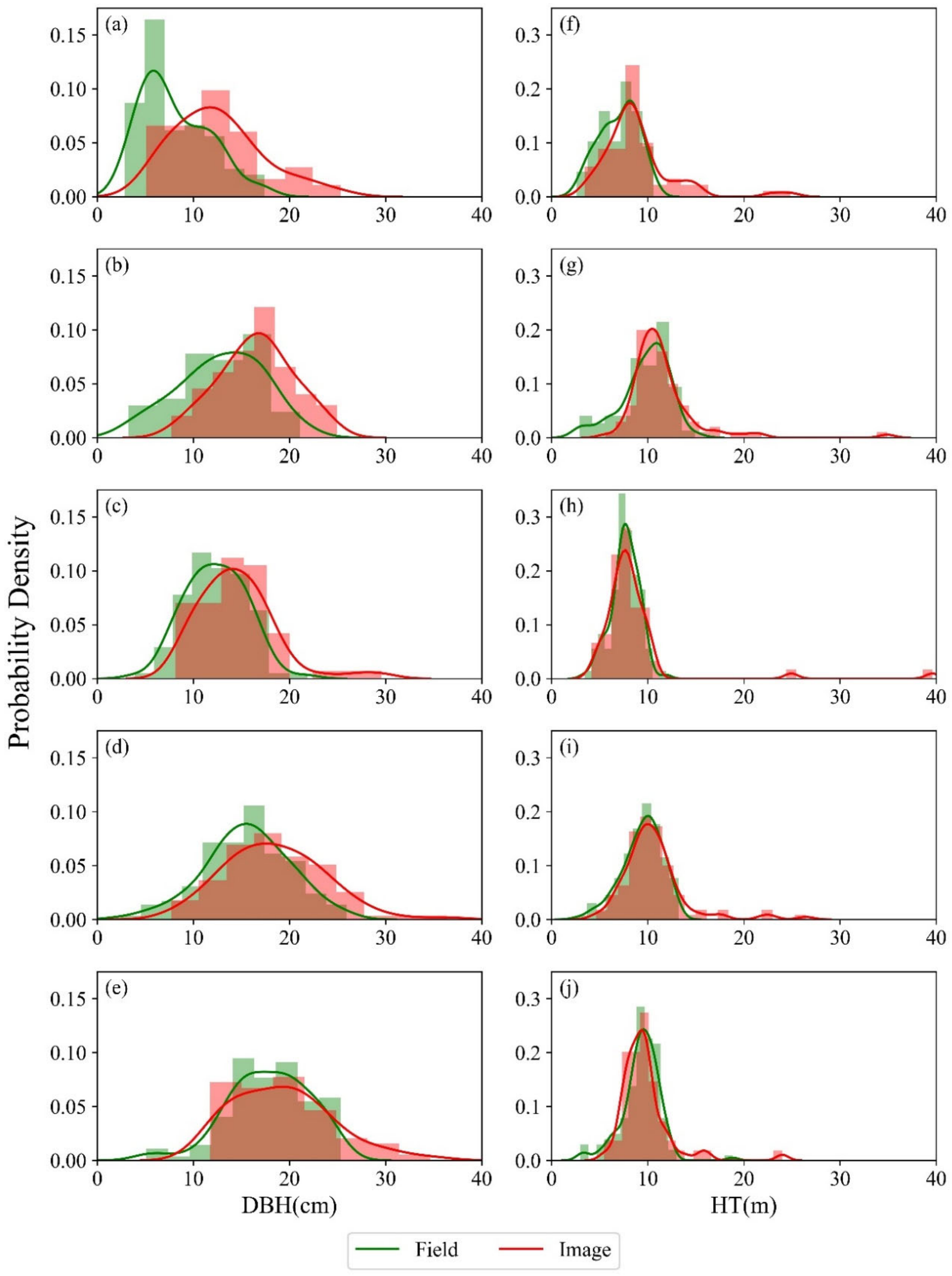

Fig. 4.11: Field measured (green) distributions versus image estimated (red) distributions for DBH and HT by spacing treatment: (a) and (f) Control; (b) and (g) 1.2m Spacing; (c) and (h) 1.8m Spacing; (d) and (i) 2.4m spacing; and (e) and (j) 3.0m Spacing.

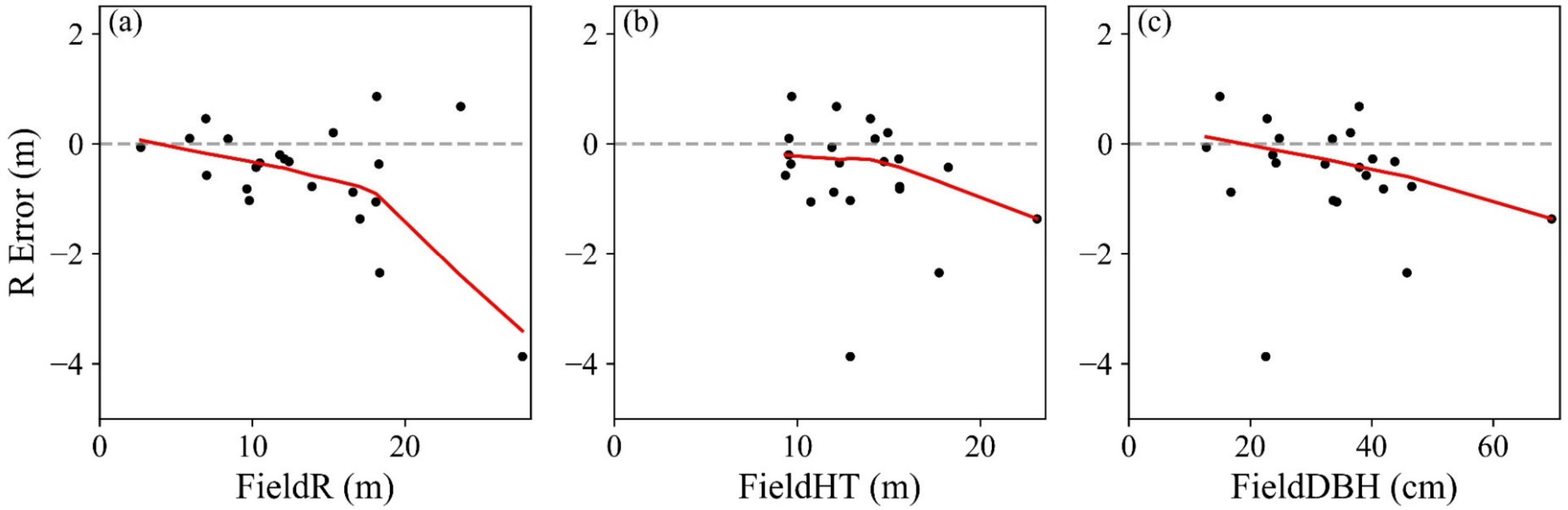

Fig. 4.12: The residual error between field measured and image measured distances (imageR - fieldR) under different factors (radial distance, R; tree height, HT; diameter at breast height, DBH). The red line is the LOWESS regression and shows the trend of errors with the factor changes.

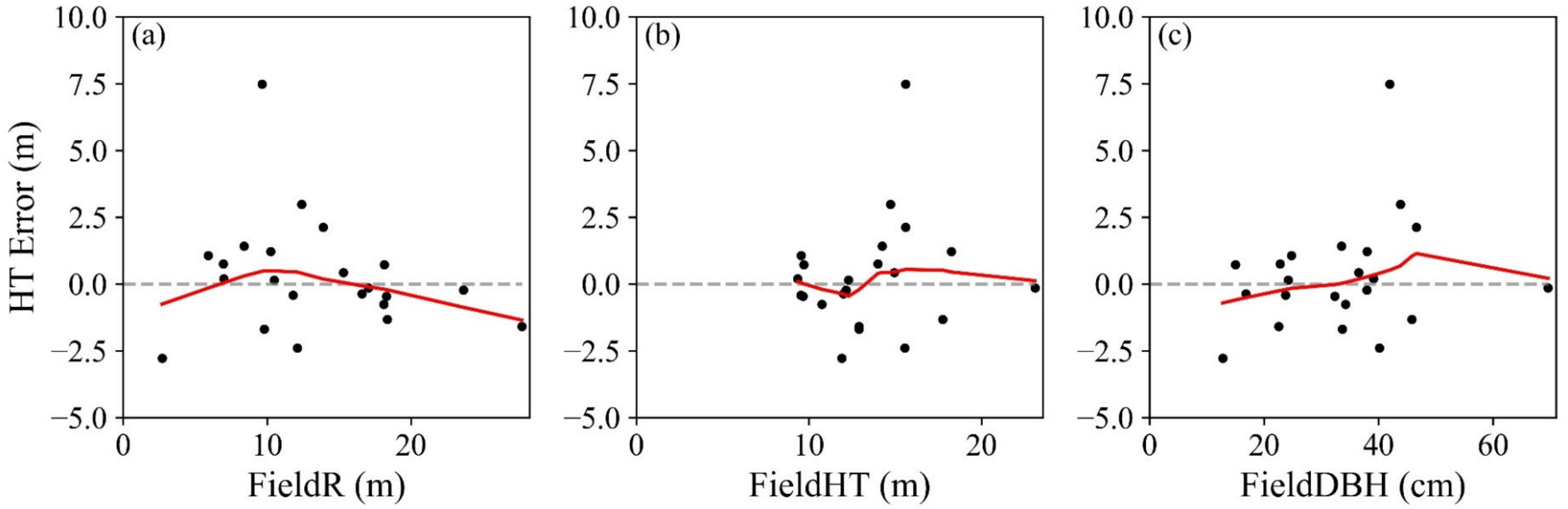

Fig. 4.13: The residual error between field measured and image measured heights (imageHT - fieldHT) under different factors (radial distance, R; tree height, HT; diameter at breast height, DBH). The red line is the LOWESS regression and shows the trend of errors with the factor changes.

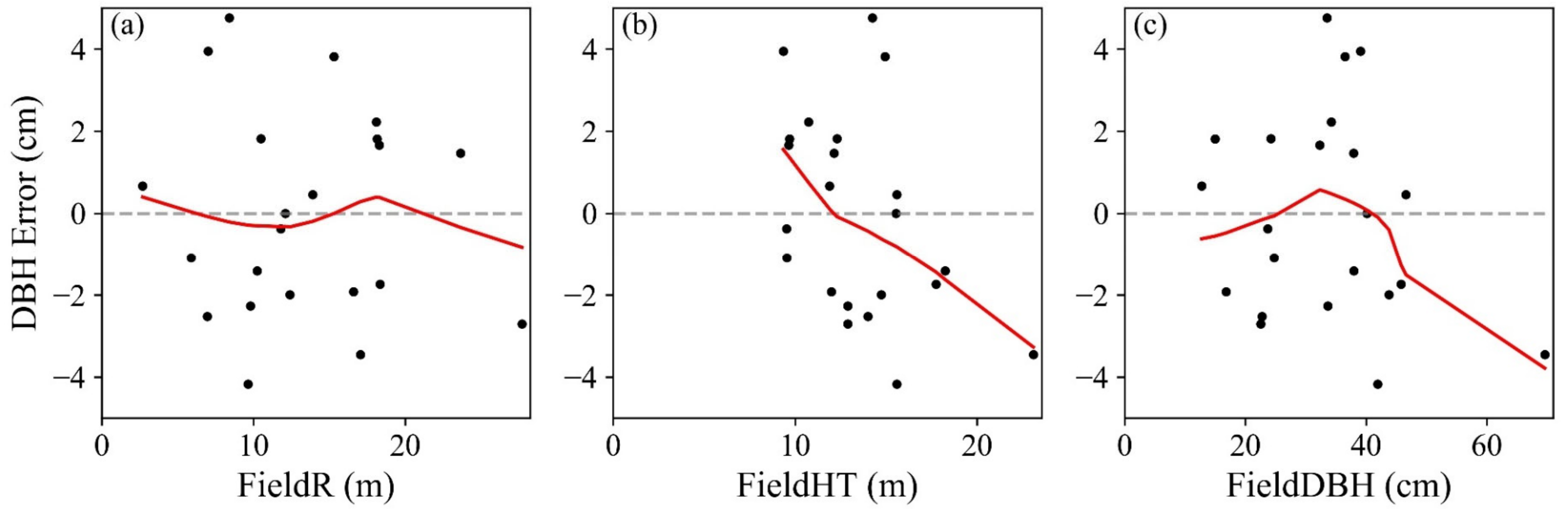

Fig. 4.14: The residual error between field measured and image measured DBHs (imageDBH - fieldDBH) under different factors (radial distance, R; tree height, HT; diameter at breast height, DBH). The red line is the LOWESS regression and shows the trend of errors with the factor changes.

Chapter 5: General Conclusion

A new 360° spherical camera was used to obtain several tree and forest attributes in this pilot study. It offers an inexpensive option for not only recording current forest conditions, but also for obtaining similar stand and tree measurements as commonly obtained with traditional inventory tools. The compact size of a spherical camera enables it to be easily used in the forest and lifted through the canopy to get canopy structural information. It is much more compact and affordable than traditional digital or hemispherical cameras. This study showed the potential for spherical camera applications by: 1) extracting stand basal area using angle gauge sampling concepts; 2) estimating plant fraction using an automated classification based on a new HSV thresholding algorithm that can classify sky, foliage, and woody components of the image; and 3) applying spherical geometry to estimate DBH, and height of individual trees based on stereoscopic spherical photos.

Stand basal area was extracted from spherical images using modified angle-count sampling methods. An open source software called "Panorama2BasalArea" (https://github.com/HowcanoeWang/Panorama2BasalArea) was developed in Python3.6 to estimate basal area from spherical photos. Two modes for identifying "in" trees were developed. The first mode, referred to as edge marking, required edges of each tree on an image to be carefully marked. From the edge boundaries, the projection angle was calculated, and the projection angle compared with the desired horizontal angle to determine whether the tree is counted or not. The second mode, referred to as target counting, used a reference octagon target to compare tree projection angle to desired horizontal angle. Trees larger than the target are counted as "in" trees. The first mode has the advantage that, once trees are marked, any basal area factor (BAF) can be applied. Using appropriate basal area factors can reduce the number of hidden trees (Bitterlich 1984, Iles 2003, Yang et al. 2017), eliminates the need to mark very small trees, and can be incorporated into more sophisticated sampling schemes such as big BAF sampling (Iles 2012, Yang et al. 2017), On-the-other-hand, target marking is simpler, more similar to field applications of angle count sampling, and results in higher consistency between different users, but requires repeated marking for different BAFs. Careful selection of BAFs can reduce visibility bias without increasing variation substantially. Multiple digital sampling locations within a sample point can also decrease effects of visibility bias.

Hemispherical estimates of plant fraction and/or gap fraction have been widely used in forestry and ecological studies (Cescatti 2007, Lang et al. 2010, Fournier and Hall 2017). Traditionally, hemispherical cameras have been used to estimate canopy structure. In this study, we show how the upper part of the spherical image can produce similar images through projection transformation and similar estimates of canopy structure. We also develop the geometry to produce plant fraction estimates directly from the cylindrical projections of spherical images (the native format that spherical images are stored). Our results showed that the two approaches can achieve almost identical estimates. The cylindrical approach is more efficient since it does not require reprojection. A major advantage of the spherical camera is its cost compared to hemispherical cameras with the spherical camera costing less than 5% of most commercial hemispherical cameras and often producing higher resolution images.

In addition to simply extracting plant fraction from spherical images, we also explore new ways for pixel classification. The most basic image processing step is pixel classification, which separates the sky from the plant portions of the image. Traditional classification algorithms are often based on blue channel histogram thresholding which has narrow requirements for photo brightness and exposure quality control. Obtaining suitable photos for blue channel thresholding limits the time of day and weather conditions under which photos can be obtained. The ideal photos for blue channel thresholding are almost black and white and are not suitable for any other analyses. We developed a novel classification algorithm based on HSV color space. In addition to simply classifying sky versus plant, this classification scheme can also specify foliage and wood classes.

Several manually classified representative samples were used as true values, and the HSV versus blue channel thresholding were compared. Based on the kappa coefficient, the new HSV algorithm was more tolerant to overexposed images than the traditional blue channel classification algorithm. However, underexposed images did not result in good classification results based on current thresholds for overexposed images. The spherical camera will be more powerful as finer resolution, RAW image formats, and automatic brightness adjustment become available in newer camera models. The availability of user software development kits (SDKs) have to the potential to make these cameras extremely powerful canopy analyzers in the near future.

Finally, we applied spherical geometry to stereo spherical images to obtain estimates of tree diameters and heights. Using trees from an open urban setting demonstrated that tip and base angles can be accurately obtained from cylindrical projections of spherical images to obtain tree height estimates and that tree horizontal projection angles can be accurately measured to obtain diameter estimates. While projection angles can be accurately measured, the resulting tree heights were not comparable to properly measured tree heights primarily because of the inability to clearly see tree tips in many of the images. Diameters, on the other hand, were accurately measured both in terms of projected diameter and diameter based on diameter tape measures.

When applied in a forest setting, heights were more accurately measured than diameters – the opposite of what was obtained in the urban setting. This was primarily a function of differences in tree size. The spacing trial used in this study produced a broad range of tree diameters. As spacing increased, tree diameter increased, and so did the accuracy of diameter estimation from photos (Fig 4.9). Small trees produce very small horizontal angles, and small errors in edge pixel identification can result in large errors in diameter estimation. Another limitation of the field test was that we did not identify individual trees so that measurements could be aligned. The multiple digital photo points probably resulted in multiple measurements of the larger trees and more chances of missing the smaller trees. The wider spacing produced bigger trees that were farther apart, thus making it easier to identify tree edges. Accuracy of height estimates, on the other hand, were not affected by the differences in spacing trials. Height is generally insensitive to spacing (Lanner 1985). The Newfoundland trees were also quite short (generally less than 20m) making it easier to see tree tips and minimizing errors associated with identifying tree tips.

This work demonstrated the potential of spherical cameras for obtaining basic forest inventory estimates and individual tree estimates. While there are some limitations to these values, there are many benefits to them that merit additional investigation. First, the spherical images provide quick estimates of important forest attributes that can be subsequently used in hierarchical sampling schemes to improve field efficiency (Hsu 2019). Implementation of onboard camera processing may also improve the efficiency of spherical images for forest inventory applications. Image segmentation or machine learning classification may produce more automated identification and marking of individual trees further reducing individual observer variation. The spherical camera represents a low-cost option to terrestrial laser scanning and may be able to produce more accurate forest-level estimates in a quicker time frame than what is currently possible with TLS technology.

5.1 References

Bitterlich, W. 1984. The relascope idea: Relative measurements in forestry. First. CAB International, Slough, England.

Cescatti, A. 2007. Indirect estimates of canopy gap fraction based on the linear conversion of hemispherical photographs: Methodology and comparison with standard thresholding techniques. Agricultural and Forest Meteorology 143:1–12.

Fournier, R. A., and R. J. Hall, editors. 2017. Hemispherical Photography in Forest Science: Theory, Methods, Applications. Springer Netherlands.

Hsu, Y.-H. 2019. Applications of variable probability sampling using remotely sensed covariates. MSc Forestry thesis, The University of New Brunswick.

Iles, K. 2003. A sampler of inventory topics. 2nd edition. Kim Iles and Associates, Nanaimo, BC.

Iles, K. 2012. Some Current Subsampling Techniques in Forestry. Mathematical & Computational Forestry & Natural Resource Sciences 4(2).

Lang, M., A. Kuusk, M. Mõttus, M. Rautiainen, and T. Nilson. 2010. Canopy gap fraction estimation from digital hemispherical images using sky radiance models and a linear conversion method. Agricultural and Forest Meteorology 150:20–29.

Lanner, R. M. 1985. On the insensitivity of height growth to spacing. Forest Ecology and Management 13:143–148.

Yang, T.-R., Y.-H. Hsu, J. A. Kershaw, E. McGarrigle, and D. Kilham. 2017. Big BAF sampling in mixed species forest structures of northeastern North America: influence of count and measure BAF under cost constraints. Forestry: An International Journal of Forest Research 90:649–660.

Appendix A: Panorama2BA Software Code

All the following codes in this appendix can be download from: https://github.com/HowcanoeWang/Panorama2BasalArea/tree/master/app

gui.py

```python
# -*- coding:utf-8 -*-
"""
################################################################################
Panorama2BasalArea Beta 0.1: Calculate forest BA values from spherical
(panorama) images by manual tree selection.

Author: Howcanoe WANG

GUI class structure:
-- Pano2BA()
 |-- class MenuBar(pack='top')
 |-- self.progressbar(pack='bottom')
 |-- self.left_frame(pack='left')
 | |-- self.img_table(pack='top')
 | |-- self. btn_frame(pack='bottom')
 |   |-- self.add_img_btn(pack='left')
 |   |-- self.del_img_btn(pack='right')
 |-- self.right_frame(pack='right')
 | |-- self.tree_table(pack='right')
 |-- class ScrolledCanvas(pack='top')

################################################################################
"""
import os
import sys
import xlwt
import traceback
from tkinter import Tk, Button, Menubutton, Menu, Canvas, Scrollbar, Label, Frame, TclError, IntVar, Radiobutton
from tkinter.simpledialog import askstring, askfloat
from tkinter.filedialog import asksaveasfilename, askopenfilename, askdirectory
from tkinter.messagebox import askokcancel, showwarning, showinfo, showerror, askyesno, askyesnocancel
from tkinter.ttk import Treeview, Progressbar
from PIL import Image, ImageDraw
from PIL.ImageTk import PhotoImage
from PIL.ImageOps import equalize
from db import DataBase
from numpy import ones, arange, sqrt, sin, cos, pi
from ba import plot_ba_calculator, max_baf, in_tree_pixel


class Pano2BA(Tk):

    saved = True
    title_name = 'Panorama2BA'
    img_info = {'img_id': [], 'img_dir': [], 'img_name': [],
                'width': [], 'height': [], 'baf': [], 'in_num': [], 'ba': []}
    # edge mode
    tree_info = {'tree_id': [], 'left': [], 'right': [], 'width': [], 'state': []}
    # click mode
    # tree_info = {'click_id': [], 'x':[], 'y':[], 'width':[], 'state':[]}

    def __init__(self):
        Tk.__init__(self)

        self.config(bg='white')
        self.protocol("WM_DELETE_WINDOW", self.quit_save_confirm)
        self.wm_state('zoomed')  # maximize windows

        self.w = self.winfo_width()
        self.h = self.winfo_height()

        self.mode = IntVar()  # 0 for edge mode, 1 for bar mode
        self.mode.set(0)  # default edge mode

        # ====================
        #  creating components
        # ====================
        self.MenuBar = MenuBar(self)

        self.progressbar = Progressbar(self, orient='horizontal', length=100, mode='determinate')

        self.left_frame = Frame(self)
        self.img_label = Label(self.left_frame, text="Image Management Panel")
        self.img_table = Treeview(self.left_frame, show="headings", columns=('Image Name', 'BAF', 'In', 'BA'))
        self.img_table_bar = Scrollbar(self.left_frame)

        self.btn_frame = Frame(self.left_frame)
        self.add_img_btn = Button(self.btn_frame, text="Add img(s)", state='disabled', command=self.add_img)
        self.del_img_btn = Button(self.btn_frame, text="Del img(s)", state='disabled', command=self.del_img)

        self.right_frame = Frame(self)
        self.tree_label = Label(self.right_frame, text="Tree Management Panel")
        self.mode_frame = Frame(self.right_frame)
        self.edge_mode = Radiobutton(self.mode_frame, text="Edge Selection", command=self.change_selection_mode,
                                     variable=self.mode, value=0)
        self.ball_mode = Radiobutton(self.mode_frame, text="Ref.Ball Clicking", command=self.change_selection_mode,
                                    variable=self.mode, value=1)
        self.tree_table = Treeview(self.right_frame, show="headings", columns=('No.', 'Width', 'State'))
        self.tree_table_bar = Scrollbar(self.right_frame)
        self.del_tree_btn = Button(self.right_frame, text="Del selection(s)", state='disabled', command=self.del_tree)

        self.ScrolledCanvas = ScrolledCanvas(self)

        # ====================
        #  Components configs
        # ====================
        self.add_img_btn.config(bg='white')
        self.del_img_btn.config(bg='white')
        self.del_tree_btn.config(bg='white')

        self.img_table.column('Image Name', width=130, anchor='center')
        self.img_table.column('BAF', width=40, anchor='center')
        self.img_table.column('In', width=40, anchor='center')
        self.img_table.column('BA', width=40, anchor='center')
        self.img_table.heading('Image Name', text='Image Name')
        self.img_table.heading('BAF', text='BAF')
        self.img_table.heading('In', text='In')
        self.img_table.heading('BA', text='BA')

        self.img_table_bar.config(command=self.img_table.yview, bg='white')
        self.img_table.config(yscrollcommand=self.img_table_bar.set)

        self.tree_table.column('No.', width=40, anchor='center')
        self.tree_table.column('Width', width=50, anchor='center')
        self.tree_table.column('State', width=45, anchor='center')
        self.tree_table.heading('No.', text='No.')
        self.tree_table.heading('Width', text='Width')
        self.tree_table.heading('State', text='State')

        self.tree_table_bar.config(command=self.tree_table.yview, bg='white')
        self.tree_table.config(yscrollcommand=self.tree_table_bar.set)

        self.bind('<Control-n>', self.MenuBar.new_project)
        self.bind('<Control-o>', self.MenuBar.open_project)
        self.bind('<Control-s>', self.MenuBar.save_project)
        self.bind('<Lock-KeyPress>', self.show_capslock_warning)

        # connect to the control of Scrolled Canvas
        self.bind('<space>', self.ScrolledCanvas.open_create_tree_mode)
        self.bind('<KeyPress-Shift_L>', self.ScrolledCanvas.press_shift)
        self.bind('<KeyRelease-Shift_L>', self.ScrolledCanvas.release_shift)
        self.bind('<KeyRelease-Control_L>', self.ScrolledCanvas.refresh_zoomed_image)
        self.bind('<KeyPress-r>', self.ScrolledCanvas.press_r)

        self.img_table.bind('<ButtonRelease-1>', self.open_img_project)
        self.img_table.bind('<Button-3>', self.change_baf)
        self.img_table.bind('<Button-2>', self.change_baf_all)

        self.tree_table.bind('<ButtonRelease-1>', self.center_tree)
        self.tree_table.bind('<KeyPress-Delete>', self.del_tree)

        # ====================
        #  packing components
        # ====================
        self.MenuBar.pack(side='top', fill='x')

        self.progressbar.pack(side='bottom', fill='x')

        self.left_frame.pack(side='left', fill='y')
```

```
        self.img_label.pack(side='top', fill='x')
        self.btn_frame.pack(side='bottom', fill='x')
        self.add_img_btn.pack(side='left', fill='x', expand='yes')
        self.del_img_btn.pack(side='right', fill='x', expand='yes')
        self.img_table_bar.pack(side='right', fill='y')
        self.img_table.pack(side='top', fill='y', expand='yes')

        self.right_frame.pack(side='right', fill='y')
        self.tree_label.pack(side='top', fill='both')
        self.mode_frame.pack(side="top", fill='both')
        self.edge_mode.pack(side="left", fill='both')
        self.ball_mode.pack(side="right", fill='both')
        self.del_tree_btn.pack(side='bottom', fill='x')
        self.tree_table_bar.pack(side='right', fill='y')
        self.tree_table.pack(side='top', fill='both', expand='yes')


        self.ScrolledCanvas.pack(side='top', fill='both', expand='yes')

        self.update_title()

    def make_unsaved(self):
        self.saved = False
        self.update_title()

    def update_title(self):
        if self.saved:
            title_suffix = ''
        else:
            title_suffix = '* (Not saved)'
        if self.ScrolledCanvas.zoom_ratio != 1:
            title_zoom = ' [' + str(self.ScrolledCanvas.zoom_ratio * 100)[:3] + '%]'
        else:
            title_zoom = ''

        full_title = self.title_name + title_suffix + title_zoom
        self.title(full_title)

    def quit_save_confirm(self):

        def _do_quit():
            self.quit()
            if os.path.exists('~$default.sqlite'):
                db.conn.close()
                os.remove('~$default.sqlite')

        if not self.saved:
            ans = askokcancel('Warning', "Changes not saved, continue quit and drop all changes?")
            if ans:
                _do_quit()
        else:
            _do_quit()

    def update_progress(self, value):
        # value is between 0 and 100
        self.progressbar['value'] = value
        self.progressbar.update()

    def add_img(self):
        mode = askyesnocancel('Add mode selection', 'Add images from folder? (Choose no to just add a single image)')
        if mode is not None:
            if mode:  # add by folder
                folder_name = askdirectory(title='Choose an image folder')
                if folder_name != '':  # select a folder
                    ask_keyword = True
                    while ask_keyword:
                        keyword_string = askstring(title='Input include keywords',
                                                   prompt="support image type:(*.jpg, *.jpeg, *.png)\n"
                                                          "leave empty or type '*' to add all images,\n"
                                                          "keywords should split by ';' or space ' ',"
                                                          "'-' before a word to exclude this word\n===============\n"
                                                          "e.g. 'cor; rua -19' means "
                                                          "add images have 'cor' OR 'rua' but do not contain '19'")
                        if keyword_string is not None:  # input a string
                            keyword_string = keyword_string.replace('; ', ';')
                            keyword_string = keyword_string.replace(' ', ';')
                            if keyword_string == '' or keyword_string == '*':  # input all images
                                img_dir_list, img_name_list = self._get_all_image_dirs(folder_name, '*')
                            else:
                                keywords = keyword_string.split(';')
                                img_dir_list, img_name_list = self._get_all_image_dirs(folder_name, keywords)
                            satisfy = askyesnocancel('Import confirm', 'Import all the following images? '
                                                                       '[Yes] to add, [No] to re-input keywords, '
                                                                       '[Cancel] to stop adding\n'+str(img_name_list))
                            if satisfy is None:  # stop adding
                                ask_keyword = False
                            else:
                                if satisfy:  # confirm to add
                                    img_mode_choice = askyesnocancel('Default mode Selection',
                                                                     'The default tree marking mode is '
                                                                     'Edge Marking[Yes] or Clicking[No] '
                                                                     'or ignore[Cancel]?')
                                    if img_mode_choice:
                                        img_mode = 0
                                    else:
                                        img_mode = 1

                                    ask_keyword = False
                                    length = len(img_dir_list)
                                    for i, img_dir in enumerate(img_dir_list):
                                        # -----for Lab use only------
                                        if img_mode_choice is None:
                                            if '_r' in os.path.basename(img_dir):
                                                img_mode = 1
                                            else:
                                                img_mode = 0
                                        # ------for Lab use only------
                                        db.add_img(img_dir, img_mode)
                                        self.update_progress(int(100 * i / length))
                                    self.refresh_img_table()
                                    self.open_img_project()
                                    self.make_unsaved()
                                    self.update_progress(100)
                        else:  # cancel adding
                            ask_keyword = False
            else:  # add single img
                img_dir = askopenfilename(title='Choose an image',
                                          filetypes=[('JPEG', '.jpeg, .jpg'), ('PNG', '.png')])
                if img_dir != '':
                    img_mode_choice = askyesnocancel('Default mode Selection',
                                                     'The default tree marking mode is Edge Marking[Yes]'
                                                     ' or Clicking[No] or ignore[Cancel]?')
                    if img_mode_choice is None:  # Cancel
                        # for Lab use only
                        if '_r' in os.path.basename(img_dir):
                            img_mode = 1
                        else:
                            img_mode = 0
                    elif img_mode_choice == True:
                        img_mode = 0
                    else:
                        img_mode = 1
                    db.add_img(img_dir, img_mode)
                    self.update_progress(50)
                    self.refresh_img_table()
                    self.open_img_project()
                    self.update_progress(100)
                    self.make_unsaved()

    @staticmethod
    def _get_all_image_dirs(folder_name, keywords='*'):
        img_dir_list = []
        img_name_list = []
        g = os.walk(folder_name)
        for path, dir_list, file_list in g:
            for file_name in file_list:
                # check whether it is a image file
                pick = False
                for suffix in ['.jpg', '.jpeg', '.JPG', '.JPEG', '.png']:
                    if suffix in file_name:
                        pick = True
                if not pick:
                    continue

                if keywords == '*':  # add all images
                    img_dir = os.path.join(path, file_name)
                    img_dir_list.append(img_dir)
                    img_name_list.append(file_name)
                else:
                    include = False
                    exclude = False
                    for key in keywords:
                        if '-' in key:  # exclude keywords
```

```
                        ex_key = key[1:]
                        if ex_key in file_name:
                            exclude = True
                    else:  # include keyword
                        if key in file_name:
                            include = True
                if include and not exclude:
                    img_dir = os.path.join(path, file_name)
                    img_dir_list.append(img_dir)
                    img_name_list.append(file_name)

        return img_dir_list, img_name_list

    def del_img(self):
        selections = self.img_table.selection()
        length = len(selections)

        rm_img_id_list = []
        rm_img_name_list = []
        for iid in selections:
            img_id = int(iid)
            img_table_row = self.img_info['img_id'].index(img_id)
            img_name = self.img_info['img_name'][img_table_row]
            rm_img_id_list.append(img_id)
            rm_img_name_list.append(img_name)

        self.update_progress(20)
        confirm = askyesno('warning', 'Are you sure to remove the following images?\n' +
                           str(rm_img_name_list) + '\nall tree data in these image will also get lost')
        if confirm:
            for i, img_id in enumerate(rm_img_id_list):
                db.rm_img(img_id)
                steps = int(70 * i / length)
                self.update_progress(20 + steps)
            self.refresh_img_table()
            self.update_progress(95)
            self.open_img_project()
            self.make_unsaved()
            self.update_progress(100)
        else:  # cancel remove
            self.update_progress(100)

    def change_baf(self, event=None):
        if self.del_img_btn['state'] == 'normal':  # have data in img_table
            baf = askfloat('Change BAF', 'Input the BAF value (float, e.g. 2.0) changing to:')
            if baf is not None:
                self.update_progress(10)
                db.edit_img_baf(self.ScrolledCanvas.img_id, baf)
                self.ScrolledCanvas.baf = baf
                self.refresh_tree_table()
                self.update_progress(40)
                self.local_refresh_img_table(baf)
                self.update_progress(70)
                self.ScrolledCanvas.open_img(reload=False, recenter=False)
                self.update_progress(100)
                self.make_unsaved()

    def change_baf_all(self, event=None):
        if self.del_img_btn['state'] == 'normal':  # have data in img_table
            if not self.saved:
                asksave = askyesnocancel("Warning", "You changes have not been saved, save it? \n"
                                                    "[Cancel] to cancel changing all BAFs, \n"
                                                    "[No] to changing all BAFs without saving current changes")
                if asksave is None:
                    return
                if asksave:  # == True
                    self.MenuBar.save_project()

            baf = askfloat('Change all BAFs', 'Input the BAF value (float, e.g. 2.0) changing all the images to:')
            if baf is not None:
                confirm2 = askyesno("Warning", "Confirm changing all BAF to value " +
                                    str(baf) + '?\nThis operation can not undo.')
                if confirm2:
                    db.edit_img_baf_all(baf)
                    self.refresh_img_table()
                    self.refresh_tree_table()
                    self.ScrolledCanvas.open_img(reload=False, recenter=False)
                    self.make_unsaved()

    def del_tree(self, event=None):
        confirm = askyesno('warning', 'Are you sure to remove selected records?')
        if confirm:
            selections = self.tree_table.selection()
            length = len(selections)
            for i, iid in enumerate(selections):
                tree_id = int(iid)
                if self.mode.get() == 0:  # edge mode
                    db.rm_tree(tree_id)
                else:   # click mode
                    db.rm_click(tree_id)
                steps = int(90 * i / length)
                self.update_progress(steps)
            self.refresh_tree_table()
            self.local_refresh_img_table(baf=self.ScrolledCanvas.baf)
            self.update_progress(95)
            self.ScrolledCanvas.open_img(reload=False, recenter=False)
            self.update_progress(100)
            self.make_unsaved()
        else:  # cancel remove
            self.update_progress(100)

    def center_tree(self, event=None):
        selections = self.tree_table.selection()
        if len(selections) == 1:  # select one tree.
            tree_id = int(selections[0])
            if self.mode.get() == 0:
                tree_row = self.tree_info['tree_id'].index(tree_id)
                x1, y1 = self.tree_info['left'][tree_row]
                x2, y2 = self.tree_info['right'][tree_row]
                center_x = (x1 + x2) / 2 * self.ScrolledCanvas.zoom_ratio
                center_y = (y1 + y2) / 2 * self.ScrolledCanvas.zoom_ratio
            else:
                tree_row = self.tree_info['click_id'].index(tree_id)
                center_x = self.tree_info['x'][tree_row] * self.ScrolledCanvas.zoom_ratio
                center_y = self.tree_info['y'][tree_row] * self.ScrolledCanvas.zoom_ratio

            self.ScrolledCanvas.change_canvas_position(center_x, center_y)

    def local_refresh_img_table(self, baf):
        # update img_table information
        selections = self.img_table.selection()
        if len(selections) == 1:  # not multiple selection
            img_id = int(selections[0])
            img_table_row = self.img_info['img_id'].index(img_id)
            in_tree_num = self.tree_info['state'].count('in')
            ba = plot_ba_calculator(baf, in_tree_num)
            self.img_info['baf'][img_table_row] = baf
            self.img_info['in_num'][img_table_row] = in_tree_num
            self.img_info['ba'][img_table_row] = ba

            # update img_table
            values = [self.img_info['img_name'][img_table_row],
                      self.img_info['baf'][img_table_row],
                      self.img_info['in_num'][img_table_row],
                      self.img_info['ba'][img_table_row]]
            self.img_table.item(img_id, values=values)

    def refresh_img_table(self):
        # clear table info
        self.img_table.delete(*self.img_table.get_children())
        # get image info
        self.img_info = db.get_img_info()
        length = len(self.img_info['img_id'])
        if length > 0:  # have img data
            self.del_img_btn.config(state='normal')
            for i in range(length):
                img_values = [self.img_info['img_name'][i], self.img_info['baf'][i],
                              self.img_info['in_num'][i], self.img_info['ba'][i]]
                self.img_table.insert('', 'end', iid=str(self.img_info['img_id'][i]), values=img_values)
            self.img_table.selection_set(str(self.img_info['img_id'][0]))
        else:  # no img data, empty project
            self.del_img_btn.config(state='disabled')
            self.refresh_tree_table()
            self.ScrolledCanvas.initialize(clean_canvas=True)

    def refresh_tree_table(self):
        # clear table info
        self.tree_table.delete(*app.tree_table.get_children())
        # get new tree info
        if self.mode.get() == 0:
            self.tree_info = db.get_tree_info(self.ScrolledCanvas.img_id)
        else:
            self.tree_info = db.get_click_info(self.ScrolledCanvas.img_id)
        length = len(self.tree_info['state'])

        if length > 0:  # tree exist
            self.del_tree_btn.config(state='normal')
            for i in range(length):
                # here start counting tree number (display in tree_table) from 1
                tree_values = [i+1, self.tree_info['width'][i], self.tree_info['state'][i]]
                # but the actual tree index start from 0 in software
                if self.mode.get() == 0:
                    self.tree_table.insert('', 'end', iid=str(self.tree_info['tree_id'][i]), values=tree_values)
                else:
                    self.tree_table.insert('', 'end', iid=str(self.tree_info['click_id'][i]), values=tree_values)
        else:
            self.del_tree_btn.config(state='disabled')

    def open_img_project(self, event=None, force_fresh=False):
        if self.del_img_btn['state'] == 'normal':  # ensure it is not an empty list
            selections = self.img_table.selection()
            if len(selections) == 1:  # not multiple selection
                img_id = int(selections[0])
                img_table_row = self.img_info['img_id'].index(img_id)
                # check if click on the older one
                new_img_id = self.img_info['img_id'][img_table_row]
                if new_img_id != self.ScrolledCanvas.img_id or force_fresh:  # click not the same
                    self.ScrolledCanvas.img_id = self.img_info['img_id'][img_table_row]
                    self.ScrolledCanvas.img_dir = self.img_info['img_dir'][img_table_row]
                    self.ScrolledCanvas.baf = self.img_info['baf'][img_table_row]
                    self.ScrolledCanvas.img_width = self.img_info['width'][img_table_row]
                    self.ScrolledCanvas.img_height = self.img_info['height'][img_table_row]
                    if self.img_info['mode'][img_table_row] == 0:
                        self.mode.set(0)
                    else:
                        self.mode.set(1)
                    self.refresh_tree_table()
                    self.update_progress(30)
                    self.ScrolledCanvas.zoom_ratio = 1.0
                    self.ScrolledCanvas.open_img(reload=True)
                    self.update_progress(100)
                    self.update_title()

    def show_capslock_warning(self, event=None):
        if event.keysym != "Caps_Lock":
            showwarning('Caution', 'You activate CapsLock, it may effects some operation, please turn it off')

    def change_selection_mode(self):
        if self.del_img_btn['state'] == 'normal':  # ensure it is not an empty list
            img_table_row = self.img_info['img_id'].index(self.ScrolledCanvas.img_id)
            if self.mode.get() == 0:
                db.edit_img_mode(self.ScrolledCanvas.img_id, 0)
                self.img_info['mode'][img_table_row] = 0
                self.tree_info = db.get_tree_info(self.ScrolledCanvas.img_id)
            else:
                db.edit_img_mode(self.ScrolledCanvas.img_id, 1)
                self.img_info['mode'][img_table_row] = 1
                self.tree_info = db.get_click_info(self.ScrolledCanvas.img_id)

            # clear canvas and draw images
            self.refresh_tree_table()
            self.local_refresh_img_table(baf=self.ScrolledCanvas.baf)
            self.ScrolledCanvas.initialize()
            self.ScrolledCanvas.open_img(reload=False)
            self.make_unsaved()
            self.update_progress(100)


class MenuBar(Frame):
    def __init__(self, parent=None):
        Frame.__init__(self, parent)
        self.pack()
        self.menubar = Frame(self)
        self.menubar.config(bg='white')
        self.menubar.pack(side='top', fill='x')

        self.fbutton = Menubutton(self.menubar, text='File', underline=0)
        self.fbutton.pack(side='left')
        self.file = Menu(self.fbutton, tearoff=False)
        self.file.add_command(label='New', command=self.new_project, underline=0)
        self.file.add_command(label='Open', command=self.open_project, underline=1)
        self.file.add_command(label='Save', command=self.save_project, underline=1, state='disabled')
        self.fbutton.config(menu=self.file, bg='white')

        self.ebutton = Menubutton(self.menubar, text='Export', underline=0, state='disabled')
        self.ebutton.pack(side='left')
        self.export = Menu(self.ebutton, tearoff=False)
        self.export.add_command(label='Default BAF', command=self.default_baf_export, underline=0)
        self.export.add_command(label='BAF sequence', command=self.sequence_baf_export, underline=0)
        self.ebutton.config(menu=self.export, bg='white')

    def new_project(self, event=None):
        ans = True
        if not app.saved:
            ans = askyesnocancel('Warning',
                                 'Changes not saved, save current changes[Y], discard changes[N], or cancel?')

        if ans is None:  # cancel
            return
        elif ans:  # save changes
            self.save_project()

        project_dir = asksaveasfilename(title='New project', defaultextension=".sqlite", initialdir='.',
                                        filetypes=[('Pano2ba project', '.sqlite')])
        if project_dir != '':
            if project_dir[-7:] == '.sqlite':
                app.add_img_btn.config(state='normal')
                app.del_img_btn.config(state='disabled')
                app.title_name = project_dir[:20] + '...' + project_dir[-30:]
                app.update_title()
                app.update_progress(20)

                if os.path.exists(project_dir):
                    os.remove(project_dir)
                app.update_progress(50)

                db.create_db(project_dir)
                if os.path.exists('~$default.sqlite'):
                    os.remove('~$default.sqlite')
                app.update_progress(70)

                app.img_table.delete(*app.img_table.get_children())
                app.tree_table.delete(*app.tree_table.get_children())
                app.ScrolledCanvas.initialize(clean_canvas=True)

                self.file.entryconfigure('Save', state="normal")
                self.ebutton.config(state='normal')
                app.update_progress(100)

    def open_project(self, event=None):
        ans = True
        if not app.saved:
            ans = askyesnocancel('Warning',
                                 'Changes not saved, save current changes[Y], discard changes[N], or cancel?')

        if ans is None:  # cancel
            return
        elif ans:  # save changes
            self.save_project()

        project_dir = askopenfilename(title='Open project', initialdir='.',
                                      filetypes=[('Pano2ba project', '.sqlite')])
        if project_dir != '':
            former_db_path = db.db_path
            db.change_db(project_dir)
            # check if is the pano2ba project db
            db.curs.execute("SELECT name FROM sqlite_master WHERE type='table';")
            table_columns = db.curs.fetchall()
            app.update_progress(5)
            if table_columns == [('ImageInfo',), ('TreeInfo',)]:
                db.update_db()
                showinfo('Update', 'Detect older version database, updated successfully')
                db.curs.execute("SELECT name FROM sqlite_master WHERE type='table';")
                table_columns = db.curs.fetchall()

            if table_columns == [('ImageInfo',), ('TreeInfo',), ('ClickInfo',)]:
                app.add_img_btn.config(state='normal')
                self.file.entryconfigure('Save', state="normal")
                self.ebutton.config(state='normal')
                app.title_name = project_dir[:20] + '...' + project_dir[-30:]
                app.update_title()
                app.update_progress(10)

                if os.path.exists('~$default.sqlite'):
                    os.remove('~$default.sqlite')
                app.update_progress(15)
                # loading img_info
                app.refresh_img_table()
                app.update_progress(20)

                app.open_img_project(force_fresh=True)
                app.update_progress(100)
            else:
                db.change_db(former_db_path)
                app.update_progress(100)
                showwarning('Open Errors', 'This sqlite file is not pano2BA project database')

    def save_project(self, event=None):
        if app.title_name != 'Panorama2BA':
            app.update_progress(20)
            db.commit()
            app.update_progress(70)
            app.saved = True
            app.update_title()
            app.update_progress(100)

    @staticmethod
    def default_baf_export():
        save_path = asksaveasfilename(title='export data', defaultextension=".xls",
                                      filetypes=[('2003 excelfile', '.xls')])
        if save_path != '':
            app.update_progress(10)
            wb = xlwt.Workbook(encoding='uft-8')
            plot_info = wb.add_sheet(sheetname='Plot Info')
            tree_info = wb.add_sheet(sheetname='Tree Info')
            click_info = wb.add_sheet(sheetname='Click Info')

            # plot info
            img_data = app.img_info
            img_length = len(img_data['img_id'])
            img_title = ['Image ID', 'Image Name', 'BAF', 'In Tree Number', 'BA']
            for i, name in enumerate(img_title):
                plot_info.write(0, i, label=name)
            for i in range(img_length):
                plot_info.write(i + 1, 0, img_data['img_id'][i])
                plot_info.write(i + 1, 1, img_data['img_name'][i])
                plot_info.write(i + 1, 2, img_data['baf'][i])
                plot_info.write(i + 1, 3, img_data['in_num'][i])
                plot_info.write(i + 1, 4, img_data['ba'][i])
                app.update_progress(10 + 30 * i / img_length)

            # tree_info
            tree_data = db.get_tree_info_all()
            tree_length = len(tree_data['tree_id'])
            tree_title = ['Tree ID', 'Image ID', 'Tree Width Pixel', 'Max BAF']
            for i, name in enumerate(tree_title):
                tree_info.write(0, i, label=name)
            for i in range(tree_length):
                tree_info.write(i + 1, 0, tree_data['tree_id'][i])
                tree_info.write(i + 1, 1, tree_data['img_id'][i])
                tree_info.write(i + 1, 2, tree_data['width'][i])
                tree_info.write(i + 1, 3, tree_data['max_baf'][i])
                app.update_progress(40 + 30 * i / tree_length)

            # click_info
            click_data = db.get_click_info_all()
            click_length = len(click_data['click_id'])
            click_title = ['img_id','click_id','x','y','BAF']
            for i, name in enumerate(click_title):
                click_info.write(0, i, label=name)
            for i in range(click_length):
                click_info.write(i + 1, 0, click_data['click_id'][i])
                click_info.write(i + 1, 1, click_data['img_id'][i])
                click_info.write(i + 1, 2, click_data['x'][i])
                click_info.write(i + 1, 3, click_data['y'][i])
                click_info.write(i + 1, 4, click_data['baf'][i])
                app.update_progress(70 + 25 * i / click_length)

            wb.save(save_path)
            app.update_progress(100)
            showinfo('Success', 'Successfully export result into ' + save_path)

    @staticmethod
    def sequence_baf_export():
        showinfo('Notice', 'Please aware that this only applicable for images have "edge selection" records.')
        save_path = asksaveasfilename(title='export data', defaultextension=".xls",
                                      filetypes=[('2003 excelfile', '.xls')])
        if save_path != '':
            baf_list = [2]
            ask_loop = True
            while ask_loop:
                st = askfloat('start', 'please type the start baf value (>= 1)', minvalue=1, maxvalue=50)
                ed = askfloat('end', 'Please type the end baf value (<=50)', minvalue=st, maxvalue=50)
                step = askfloat('step', 'Please type the step of interval', minvalue=0.05, maxvalue=ed - st)
                try:
                    baf_list = list(arange(st, ed + step, step))
                except TypeError:
                    return

                confirm = askyesnocancel('Confirm', 'Are you sure to export results related to the following BAFs? \n'
                                                    + str(baf_list) + '\n[Yes] to continue, [No] to reinput BAFs, '
                                                                      '[Cancel] to cancel export')
                if confirm is None:
                    return
                elif not confirm:  # false, re input
                    pass
                else:  # true ,start export
                    ask_loop = False

            app.update_progress(10)
            # export excels
            wb = xlwt.Workbook(encoding='uft-8')
            plot_info = wb.add_sheet(sheetname='Plot Info')
            tree_info = wb.add_sheet(sheetname='Tree Info')
            click_info = wb.add_sheet(sheetname='Click Info')

            # plot info
            img_data = db.get_img_info_baf_range(baf_list)
            img_length = len(img_data['img_id'])
            plot_info.write(0, 0, label='Image ID')
            plot_info.write(0, 1, label='Image Name')
            col = 2
            for baf in baf_list:
                plot_info.write(0, col, label='BA(baf=' + str(baf) + ')')
                #plot_info.write(0, col+1, label='In Tree Num')
                col += 1 #col += 2

            for i in range(img_length):
                plot_info.write(i + 1, 0, img_data['img_id'][i])
                plot_info.write(i + 1, 1, img_data['img_name'][i])
                col = 2
                for j, value in enumerate(img_data['baf_num_ba'][i]):
                    plot_info.write(i + 1, col + j, value)
                app.update_progress(10 + 30 * i / img_length)

            # tree_info
            tree_data = db.get_tree_info_all()
            tree_length = len(tree_data['tree_id'])
            tree_title = ['Tree ID', 'Image ID', 'Tree Width Pixel', 'Max BAF']
            for i, name in enumerate(tree_title):
                tree_info.write(0, i, label=name)
            for i in range(tree_length):
                tree_info.write(i + 1, 0, tree_data['tree_id'][i])
                tree_info.write(i + 1, 1, tree_data['img_id'][i])
                tree_info.write(i + 1, 2, tree_data['width'][i])
                tree_info.write(i + 1, 3, tree_data['max_baf'][i])
                app.update_progress(40 + 30 * i / tree_length)

            # click_info
            click_data = db.get_click_info_all()
            click_length = len(click_data['click_id'])
            click_title = ['img_id', 'click_id', 'x', 'y', 'BAF']
            for i, name in enumerate(click_title):
                click_info.write(0, i, label=name)
            for i in range(click_length):
                click_info.write(i + 1, 0, click_data['click_id'][i])
                click_info.write(i + 1, 1, click_data['img_id'][i])
                click_info.write(i + 1, 2, click_data['x'][i])
                click_info.write(i + 1, 3, click_data['y'][i])
                click_info.write(i + 1, 4, click_data['baf'][i])
                app.update_progress(70 + 25 * i / click_length)

            wb.save(save_path)
            app.update_progress(100)
            showinfo('Success', 'Successfully export result into ' + save_path)


class ScrolledCanvas(Frame):
    add_tree = False
    add_tree_lock = False
```

```
zoom_ratio = 1.0
mouse_in_canvas = False
shift_hold = False
move_point = False
zooming = False
reference_bar = False

# default, point1 is left, point2 is right, r is id for reference bar
## edge mode
shape_ids = {'point1': [], 'line': [], 'point2': [], 'text': [], 'canvas_img': None, 'r': None}
moving = {'fixed_p': [0, 0], 'line': 'line_id', 'move_p': 'point_id',
          'text': 'text_id', 'tree_row': 0, 'which': 0}
## click mode
click_ids = {'point':[], 'text':[], 'canvas_img':None, 'r':None}
moving_cmode = {'move_p':'point_id', 'text':'text_id', 'tree_row':0}

# record current img
img_id = -1
img_dir = ''
baf = 2
img_width = 1000
img_height = 800
save_image = None  # preprocess photos = PIL.Image()
save_photo = None  # zoomed photo shows in canvas = tk.PhotoImage()

min_width = in_tree_pixel(1, img_width) * zoom_ratio
r_pixel = (in_tree_pixel(baf, img_width) * zoom_ratio) / 2

def __init__(self, parent=None):
    Frame.__init__(self, parent)

    self.canvas = Canvas(self, relief='sunken')
    self.vbar = Scrollbar(self)
    self.hbar = Scrollbar(self, orient='horizontal')

    self.canvas.config(borderwidth=0, bg='white')
    self.vbar.config(command=self.canvas.yview, bg='white')  # scroll steps
    self.hbar.config(command=self.canvas.xview, bg='white')
    self.canvas.config(yscrollcommand=self.vbar.set)  # canvas steps
    self.canvas.config(xscrollcommand=self.hbar.set)
    self.canvas.bind('<ButtonPress-1>', self.left_click)
    self.canvas.bind('<B1-Motion>', self.hold_move_mouse)
    self.canvas.bind('<Motion>', self.move_mouse)
    self.canvas.bind('<ButtonRelease-1>', self.left_loose)
    self.canvas.bind('<MouseWheel>', self.xbar_scroll)
    self.canvas.bind('<Control-MouseWheel>', self.zoom)
    self.canvas.bind("<Enter>", self.on_enter)
    self.canvas.bind("<Leave>", self.on_leave)
    self.canvas.bind('<Lock-KeyPress>', Pano2BA.show_capslock_warning)

    self.vbar.pack(side='right', fill='y')
    self.hbar.pack(side='bottom', fill='x')
    self.canvas.pack(side='top', fill='both', expand='yes')

    imarray = ones((10, 10, 3)) * 255
    im = Image.fromarray(imarray.astype('uint8')).convert("RGBA")
    photo_im = PhotoImage(im)
    self.shape_ids['canvas_img'] = self.canvas.create_image(0, 0, image=photo_im, anchor='nw')
    self.shape_ids['r'] = self.canvas.create_rectangle(0, 0, 5, 5, fill='white',
                                                        outline='black', state='hidden')
    self.click_ids['r'] = self.canvas_create_octagon(self.img_width / 2, self.img_height / 2,
                                                      fill='white', outline='yellow',
                                                      stipple='gray12', state='hidden')

# ========================
#  functions used outside
# ========================
def initialize(self, clean_canvas=False):
    # functions used to clear trees or background image (if clean_canvas =True)
    self.add_tree = False
    self.add_tree_lock = False
    if clean_canvas:
        self.zoom_ratio = 1.0
    self.mouse_in_canvas = False
    self.shift_hold = False
    self.move_point = False

    self.reference_bar = False
    if self.shape_ids['r'] is not None:
        self.canvas.itemconfig(self.shape_ids['r'], state='hidden')
    if self.click_ids['r'] is not None:
        self.canvas.itemconfig(self.click_ids['r'], state='hidden')
    self.add_tree = False
    self.config(cursor='arrow')

    self._update_r_pixel()

    # clear canvas trees record
    self._clear_canvas_all_trees()
    if app.mode.get() == 0:
        self.shape_ids['point1'] = []
        self.shape_ids['point2'] = []
        self.shape_ids['line'] = []
        self.shape_ids['text'] = []
    else:
        self.click_ids['point'] = []
        self.click_ids['text'] = []


    if clean_canvas:
        self.img_id = -1
        self.img_dir = ''
        self.baf = 2
        self.img_width = 1000
        self.img_height = 800
        self.save_image = None
        self.save_photo = None

        imarray = ones((10, 10, 3)) * 255
        im = Image.fromarray(imarray.astype('uint8')).convert("RGBA")
        self.save_photo = PhotoImage(im)
        self._update_img()

def open_img(self, reload=True, recenter=True):
    # step0: clear canvas
    # step1: load image and image equalization
    # step2: draw dealt image
    # step3: draw trees and update self.shapes_ids; init moving and other ctrl params
    self.initialize(clean_canvas=False)
    app.update_progress(45)

    # step 0
    if reload:
        self._preprocess_img()
        app.update_progress(60)
        self._resize_img()
        app.update_progress(70)
        self._update_img()

    if recenter:
        self.change_canvas_position(0, self.save_photo.height() / 2)

    # step 1
    app.update_progress(80)

    # step 3: draw trees
    if app.mode.get() == 0:
        tree_num = len(app.tree_info['tree_id'])
        for tree_row in range(tree_num):
            x1, y1 = app.tree_info['left'][tree_row]
            x2, y2 = app.tree_info['right'][tree_row]
            x1 *= self.zoom_ratio
            y1 *= self.zoom_ratio
            x2 *= self.zoom_ratio
            y2 *= self.zoom_ratio
            if app.tree_info['state'][tree_row] == 'out':
                line = self.canvas.create_line(x1, y1, x2, y2, fill='red', width=3)
            else:
                line = self.canvas.create_line(x1, y1, x2, y2, fill='blue', width=3)
            point1 = self.canvas.create_oval(x1 - 5, y1 - 5, x1 + 5, y1 + 5, fill='yellow', outline='black')
            point2 = self.canvas.create_oval(x2 - 5, y2 - 5, x2 + 5, y2 + 5, fill='yellow', outline='black')
            text_x = (x1 + x2) / 2
            text_y = (y1 + y2) / 2
            text = self.canvas.create_text(text_x, text_y, text=str(tree_row+1),
                                           fill='yellow', font=('Times', '12', 'bold'))

            self.shape_ids['point1'].append(point1)
            self.shape_ids['point2'].append(point2)
            self.shape_ids['line'].append(line)
            self.shape_ids['text'].append(text)

            progress = 20 * (tree_row / tree_num)
            app.update_progress(80 + progress)
    else:
        # tree_info = {'click_id': [], 'x':[], 'y':[], 'width':[], 'state':[]}
        tree_num = len(app.tree_info['click_id'])
        for tree_row in range(tree_num):
            x = app.tree_info['x'][tree_row] * self.zoom_ratio
            y = app.tree_info['y'][tree_row] * self.zoom_ratio

            octagon = self.canvas_create_octagon(x, y, fill='white', outline='black')
            text = self.canvas.create_text(x, y, text=str(tree_row + 1), fill='black',
                                           font=('Times', '12', 'bold'))

            # click_ids = {'point':[], 'text':[], 'canvas_img':None, 'r':None}
            self.click_ids['point'].append(octagon)
            self.click_ids['text'].append(text)

            progress = 20 * (tree_row / tree_num)
            app.update_progress(80 + progress)


def change_canvas_position(self, center_x=None, center_y=None):
    canvas_width = self.canvas.winfo_width()
    canvas_height = self.canvas.winfo_height()
    img_width = self.save_photo.width()
    img_height = self.save_photo.height()

    if center_x is not None:
        x = (center_x - 0.5 * canvas_width) / img_width
        final_x = min(max(0, x), 1)
        self.canvas.xview_moveto(final_x)

    if center_y is not None:
        y = (center_y - 0.5 * canvas_height) / img_height
        final_y = min(max(0, y), 1)
        self.canvas.yview_moveto(final_y)

def open_create_tree_mode(self, event):
    # press 'space' changing to adding tree mode
    if app.del_img_btn['state'] == 'normal':  # ensure have img data
        if not self.add_tree:  # not in add tree mode
            self.add_tree = True
            if app.mode.get() == 1:  # click mode show reference ball
                self.reference_ball_display(event)
            if self.mouse_in_canvas:
                self.config(cursor='tcross')
        else:
            if not self.add_tree_lock:  # not in the second tree
                self.add_tree = False
                self.config(cursor='arrow')
                if app.mode.get() == 1:
                    self.reference_ball_display(event)

# =======================
#  functions used inside
# =======================
@staticmethod
def top_iteration(n, x, y, r):
    angle = [pi / 16 + 2 * pi * (i / n)  for i in range(n)]
    for a in angle:
        yield x + r * cos(a)
        yield y + r * sin(a)

def canvas_create_octagon(self, x, y, fill='white', outline='yellow', stipple='', state='normal', mode='oct'):
    #      H--|--A
    #   G /   |o  \ B
    #  --|----|----|--
    #   F \   |   / C
    #      E--|--D
    #
    # O (x, y)

    r = self.r_pixel

    if mode == 'oct':
        e = 2 / (sqrt(2) + 1) * r
        xa = xd = x + 0.5 * e
        ya = yh = y + r
        xb = xc = x + r
        yb = yg = y + 0.5 * e
        yc = yf = y - 0.5 * e
        yd = ye = y - r
        xe = xh = x - 0.5 * e
        xf = xg = x - r
```

```
            oct = self.canvas.create_polygon(xa, ya, xb, yb, xc, yc, xd, yd, xe, ye, xf, yf, xg, yg, xh, yh, xa, ya,
                                             fill=fill, outline=outline, state=state, stipple=stipple)
        else:
            R = r / cos(pi / 16)
            top = list(self.top_iteration(16, x, y, R))
            oct = self.canvas.create_polygon(*top, fill=fill, outline=outline, state=state, stipple=stipple)
            #oct = self.canvas.create_oval(x - r, y - r, x + r, y + r, fill='LightBlue',
            #                              outline='yellow', state=state, stipple="gray12")

        return oct

    def canvas_coords_octagon(self, oct_id, x, y, mode="oct"):

        r = self.r_pixel

        if mode == 'oct':
            e = 2 / (sqrt(2) + 1) * r
            xa = xd = x + 0.5 * e
            ya = yh = y + r
            xb = xc = x + r
            yb = yg = y + 0.5 * e
            yc = yf = y - 0.5 * e
            yd = ye = y - r
            xe = xh = x - 0.5 * e
            xf = xg = x - r

            self.canvas.coords(oct_id, [xa, ya, xb, yb, xc, yc, xd, yd, xe, ye, xf, yf, xg, yg, xh, yh, xa, ya])
        else:
            R = r / cos(pi / 16)
            top = list(self.top_iteration(16, x, y, R))
            self.canvas.coords(oct_id, top)

    # --------------
    #  mouse events
    # --------------
    def left_click(self, event):
        if app.mode.get() == 0:   # edge mode
            if self.add_tree:
                x = self.canvas.canvasx(event.x)
                y = self.canvas.canvasy(event.y)
                app.make_unsaved()
                if not self.add_tree_lock:  # click for the first time
                    number = len(self.shape_ids['point1'])

                    line = self.canvas.create_line(x, y, x, y, fill='red', width=3)
                    point1 = self.canvas.create_oval(x - 5, y - 5, x + 5, y + 5,
                                                     fill='yellow', outline='black')
                    point2 = self.canvas.create_oval(x - 5, y - 5, x + 5, y + 5,
                                                     fill='yellow', outline='black')
                    text = self.canvas.create_text(x, y, text=str(number + 1),
                                                   fill='yellow', font=('Times', '12', 'bold'))

                    self.moving['fixed_p'] = [x, y]
                    self.moving['line'] = line
                    self.moving['move_p'] = point2
                    self.moving['text'] = text

                    self.shape_ids['point1'].append(point1)
                    self.shape_ids['point2'].append(point2)
                    self.shape_ids['line'].append(line)
                    self.shape_ids['text'].append(text)

                    self.add_tree_lock = True
                else:  # click for the second time
                    x0, y0 = self.moving['fixed_p']
                    self._update_shape_info(x, y)
                    self.add_tree_lock = False
                    self.add_tree = False
                    self.config(cursor='arrow')

                    if not self.shift_hold:  # horizontal lock
                        y = y0

                    self._update_tree_infos(self.img_id, x0, y0, x, y)
        else:   # click mode
            if self.add_tree:
                x = self.canvas.canvasx(event.x)
                y = self.canvas.canvasy(event.y)
                app.make_unsaved()

                number = len(self.click_ids['point'])
            point = self.canvas_create_octagon(x, y, fill='white', outline='black',
                                               state='normal', stipple='')
            text = self.canvas.create_text(x, y, text=str(number + 1), fill='black',
                                          font=('Times', '12', 'bold'))

            self.click_ids['point'].append(point)
            self.click_ids['text'].append(text)

            self._update_tree_infos_cmode(self.img_id, x, y)


    def move_mouse(self, event):
        x = self.canvas.canvasx(event.x)
        y = self.canvas.canvasy(event.y)
        if app.mode.get() == 0:   # edge mode
            if self.add_tree_lock:  # draw lines follow mouse, only works when clicking the second point
                self._update_shape_info(x, y)
            else:  # make a minimum bar follow mouse
                if self.reference_bar:
                    self.canvas.coords(self.shape_ids['r'],
                                       [x, y - 5, x + self.min_width * self.zoom_ratio, y])
        else:   # click mode
            self.canvas_coords_octagon(self.click_ids['r'], x, y)


    def hold_move_mouse(self, event):
        # only activated when press left and not loose
        x = self.canvas.canvasx(event.x)
        y = self.canvas.canvasy(event.y)
        if not self.add_tree:  # make sure not in adding tree mode
            if not self.move_point:  # find new points
                id_touched = event.widget.find_closest(x, y, halo=5)
                if id_touched:  # except canvas empty get nothing
                    if app.mode.get() == 0:  # edge mode
                        ## not touch the line and text item
                        if id_touched[0] in self.shape_ids['point1'] or id_touched[0] in self.shape_ids['point2']:
                            [center_x, center_y] = self._get_shape_center(id_touched[0])
                            if (center_x - x) ** 2 + (center_y - y) ** 2 <= 25:  # make sure touch in points
                                # find which tree record it belongs to
                                self._pick_moving_ids(id_touched[0])
                                self._update_shape_info(x, y)
                                self.move_point = True
                    else:    # click mode
                        if id_touched[0] in self.click_ids['point']:
                            self.canvas.itemconfigure(id_touched[0], outline='yellow', stipple='gray12')
                            self._pick_moving_ids(id_touched[0])
                            self._update_shape_info_cmode(x, y)
                            self.move_point = True

            else:  # is moving former points, keep updating is enough
                if app.mode.get() == 0:
                    self._update_shape_info(x, y)
                else:
                    self._update_shape_info_cmode(x, y)

    def left_loose(self, event):
        # update tree info if in edit mode
        if self.move_point:  # finish moving
            x0, y0 = self.moving['fixed_p']
            x = self.canvas.canvasx(event.x)
            y = self.canvas.canvasy(event.y)
            if app.mode.get() == 0:
                self._update_tree_infos(app.tree_info['tree_id'][self.moving['tree_row']],
                                        x0, y0, x, y, mode='edit')
            else:
                self._update_tree_infos_cmode(app.tree_info['click_id'][self.moving_cmode['tree_row']],
                                              x, y, mode='edit')
                self.canvas.itemconfigure(self.moving_cmode['move_p'], outline='black', stipple='')
            self.move_point = False
            app.make_unsaved()

    def on_enter(self, event):
        self.mouse_in_canvas = True
        if self.add_tree:
            self.config(cursor='tcross')
            if app.mode.get() == 0:
                if self.reference_bar:
                    self.canvas.itemconfig(self.shape_ids['r'], state='normal')
            else:
                if self.reference_bar:
                    self.canvas.itemconfig(self.click_ids['r'], state='normal')
```

```
def on_leave(self, event):
    self.mouse_in_canvas = False
    self.config(cursor='arrow')
    if app.mode.get() == 0:
        if self.reference_bar:
            self.canvas.itemconfig(self.shape_ids['r'], state='hidden')
    else:
        if self.reference_bar:
            self.canvas.itemconfig(self.click_ids['r'], state='hidden')

def press_shift(self, event):
    if not self.shift_hold:
        self.shift_hold = True

def release_shift(self, event):
    self.shift_hold = False

def press_r(self, event):
    if app.del_img_btn['state'] == 'normal':
        x = self.canvas.canvasx(event.x)
        y = self.canvas.canvasy(event.y)
        if app.mode.get() == 0:
            if not self.reference_bar:
                self.reference_bar = True
                self.min_width = in_tree_pixel(1, self.img_width)
                self.canvas.coords(self.shape_ids['r'],
                                   [x, y - 5, x + self.min_width * self.zoom_ratio, y])
                self.canvas.itemconfig(self.shape_ids['r'], state='normal')
            else:
                self.reference_bar = False
                self.canvas.itemconfig(self.shape_ids['r'], state='hidden')

def reference_ball_display(self, event):
    x = self.canvas.canvasx(event.x)
    y = self.canvas.canvasy(event.y)
    if not self.reference_bar:
        self.reference_bar = True
        self.canvas_coords_octagon(self.click_ids['r'], x, y)
        self.canvas.itemconfig(self.click_ids['r'], state='normal')
    else:
        self.reference_bar = False
        self.canvas.itemconfig(self.click_ids['r'], state='hidden')

def xbar_scroll(self, event):
    scroll = -1 if event.delta > 0 else 1
    self.canvas.xview_scroll(scroll, 'units')

def zoom(self, event):
    if app.del_img_btn['state'] == 'normal':  # ensure open a image
        if not self.add_tree_lock:
            rate = 0.2 if event.delta > 0 else -0.2
            zoom_rate = round(self.zoom_ratio + rate, 1)
            if zoom_rate + 0.2 > 2.5:
                self.zoom_ratio = 2.4
                app.update_title()
            else:
                canvas_width = self.canvas.winfo_width()
                canvas_height = self.canvas.winfo_height()
                img_width, img_height = self.save_image.size
                if img_width * zoom_rate < canvas_width or img_height * zoom_rate < canvas_height:
                    # can't small any more
                    app.update_title()
                else:  # proper zoom operation
                    app.update_progress(10)
                    self.zooming = True
                    self.zoom_ratio = zoom_rate
                    self._update_r_pixel()
                    app.update_title()

def refresh_zoomed_image(self, event):
    if self.zooming:
        self._resize_img()
        app.update_progress(50)
        self._update_img()
        app.update_progress(80)
        self._zoom_shapes()
        app.update_progress(90)
        app.update_title()
        app.update_progress(100)
        self.change_canvas_position(center_y=self.img_height / 2 * self.zoom_ratio)
        self.zooming = False
```

```
# ------------------
#  reused functions
# ------------------
def _update_r_pixel(self):
    self.r_pixel = (in_tree_pixel(self.baf, self.img_width) * self.zoom_ratio) / 2

def _update_tree_infos(self, tree_img_id, x0, y0, x, y, mode='add'):
    # functions to update img_table and tree_table when adding and editing tree points
    # x0, y0 is the fixed points position
    fx = x0 / self.zoom_ratio  # fixed_x
    fy = y0 / self.zoom_ratio
    mx = x / self.zoom_ratio  # moved_x
    my = y / self.zoom_ratio
    if not self.shift_hold:
        my = fy
    if mode == 'add':
        # consider zoom_ratio
        tree_id, width, baf_max = db.add_tree(img_id=tree_img_id, lx=fx, ly=fy, rx=mx, ry=my, return_value=True)
        if baf_max >= self.baf:
            state = 'in'
        else:
            state = 'out'

        # add records to tree_table
        app.tree_info['tree_id'].append(tree_id)
        app.tree_info['left'].append([fx, fy])
        app.tree_info['right'].append([mx, my])
        app.tree_info['width'].append(width)
        app.tree_info['state'].append(state)

        length = len(app.tree_info['tree_id'])

        if app.del_tree_btn['state'] == 'disabled':  # tree exist
            app.del_tree_btn.config(state='normal')

        tree_values = [length, width, state]
        app.tree_table.insert('', 'end', iid=str(tree_id), values=tree_values)

    else:  # mode=='edit'
        tree_row = self.moving['tree_row']
        if self.moving['which'] == 1:  # move the left(point1)
            app.tree_info['left'][tree_row] = [mx, my]
            width, baf_max = db.edit_tree(tree_id=tree_img_id, lx=mx, ly=my, rx=fx, ry=fy, return_value=True)
        else:  # move the right(point2)
            app.tree_info['right'][tree_row] = [mx, my]
            width, baf_max = db.edit_tree(tree_id=tree_img_id, lx=fx, ly=fy, rx=mx, ry=my, return_value=True)

        if baf_max >= self.baf:
            state = 'in'
        else:
            state = 'out'

        app.tree_info['width'][tree_row] = width
        app.tree_info['state'][tree_row] = state

        tree_values = [tree_row + 1, width, state]
        app.tree_table.item(str(app.tree_info['tree_id'][tree_row]), values=tree_values)

    app.local_refresh_img_table(self.baf)

def _update_tree_infos_cmode(self, tree_img_id, x, y, mode='add'):
    mx = x / self.zoom_ratio  # moved_x
    my = y / self.zoom_ratio

    if mode == 'add':   # add click point mode
        click_id, width = db.add_click(img_id=tree_img_id, x=mx, y=my, return_value=True)

        # add records to tree_table
        app.tree_info['click_id'].append(click_id)
        app.tree_info['x'].append(mx)
        app.tree_info['y'].append(my)
        app.tree_info['width'].append(width)
        app.tree_info['state'].append('in')

        if app.del_tree_btn['state'] == 'disabled':  # tree exist
            app.del_tree_btn.config(state='normal')

        length = len(app.tree_info['click_id'])

        click_values = [length, width, 'in']
        app.tree_table.insert('', 'end', iid=str(click_id), values=click_values)
    else:   # edit exists point mode
        tree_row = self.moving_cmode['tree_row']
        db.edit_click(click_id=tree_img_id, x=mx, y=my)
        app.tree_info['x'][tree_row] = mx
        app.tree_info['y'][tree_row] = my

    app.local_refresh_img_table(self.baf)

def _update_shape_info(self, x, y):
    # when adding and dragging tree points, line and points follow mouse
    x0, y0 = self.moving['fixed_p']
    line = self.moving['line']
    move_p = self.moving['move_p']
    text = self.moving['text']

    if not self.shift_hold:  # horizontal lock
        y = y0
    tree_width = db.length_calculator(x0, y0, x, y) / self.zoom_ratio
    baf_max = max_baf(self.img_width, tree_width)

    text_x = (x0 + x) / 2
    text_y = (y0 + y) / 2
    self.canvas.coords(line, [x0, y0, x, y])
    self.canvas.coords(move_p, [x - 5, y - 5, x + 5, y + 5])
    self.canvas.coords(text, [text_x, text_y])

    # change line colors
    if baf_max >= self.baf:
        # in tree
        self.canvas.itemconfigure(line, fill='blue')
    else:
        # out tree
        self.canvas.itemconfigure(line, fill='red')

def _update_shape_info_cmode(self, x, y):
    octagon_id = self.moving_cmode['move_p']
    text_id = self.moving_cmode['text']

    self.canvas_coords_octagon(octagon_id, x, y)
    self.canvas.coords(text_id, [x, y])

def _get_shape_center(self, shape_id):
    # return the tree edge points (oval) center coordinate as a fixed point
    x1, y1, x2, y2 = self.canvas.coords(shape_id)
    center_x = (x1 + x2) / 2
    center_y = (y1 + y2) / 2
    return [center_x, center_y]

def _pick_moving_ids(self, shape_id):
    # functions to update self.moving dictionary
    if app.mode.get() == 0:
        if shape_id in self.shape_ids['point1']:
            row_num = self.shape_ids['point1'].index(shape_id)
            line_id = self.shape_ids['line'][row_num]
            fixed_id = self.shape_ids['point2'][row_num]
            text = self.shape_ids['text'][row_num]
            self.moving['line'] = line_id
            self.moving['move_p'] = shape_id
            self.moving['fixed_p'] = self._get_shape_center(fixed_id)
            self.moving['tree_row'] = row_num
            self.moving['text'] = text
            self.moving['which'] = 1
        if shape_id in self.shape_ids['point2']:
            row_num = self.shape_ids['point2'].index(shape_id)
            line_id = self.shape_ids['line'][row_num]
            fixed_id = self.shape_ids['point1'][row_num]
            text = self.shape_ids['text'][row_num]
            self.moving['line'] = line_id
            self.moving['move_p'] = shape_id
            self.moving['fixed_p'] = self._get_shape_center(fixed_id)
            self.moving['tree_row'] = row_num
            self.moving['text'] = text
            self.moving['which'] = 2
    else:
        # moving_cmode = {'move_p':'point_id', 'text':'text_id', 'tree_row':0}
        row_num = self.click_ids['point'].index(shape_id)
        text_id = self.click_ids['text'][row_num]
        self.moving_cmode['move_p'] = shape_id
        self.moving_cmode['text'] = text_id
        self.moving_cmode['tree_row'] = row_num
```

```python
def _zoom_shapes(self):
    # functions changing points positions after zooming
    if app.mode.get() == 0:
        length = len(app.tree_info['tree_id'])
        if length > 0:  # not empty tree
            for i in range(length):
                lx, ly = app.tree_info['left'][i]
                rx, ry = app.tree_info['right'][i]
                lx *= self.zoom_ratio
                ly *= self.zoom_ratio
                rx *= self.zoom_ratio
                ry *= self.zoom_ratio
                center_x = (lx + rx) / 2
                center_y = (ly + ry) / 2
                p1_id = self.shape_ids['point1'][i]
                p2_id = self.shape_ids['point2'][i]
                l_id = self.shape_ids['line'][i]
                t_id = self.shape_ids['text'][i]
                self.canvas.coords(l_id, [lx, ly, rx, ry])
                self.canvas.coords(p1_id, [lx - 5, ly - 5, lx + 5, ly + 5])
                self.canvas.coords(p2_id, [rx - 5, ry - 5, rx + 5, ry + 5])
                self.canvas.coords(t_id, [center_x, center_y])
    else:
        length = len(app.tree_info['click_id'])
        if length > 0:
            for i in range(length):
                x = app.tree_info['x'][i] * self.zoom_ratio
                y = app.tree_info['y'][i] * self.zoom_ratio
                octagon_id = self.click_ids['point'][i]
                t_id = self.click_ids['text'][i]

                self.canvas_coords_octagon(octagon_id, x, y)
                self.canvas.coords(t_id, [x, y])

def _clear_canvas_all_trees(self):
    # edge mode
    for i in range(len(self.shape_ids['point1'])):
        self.canvas.delete(self.shape_ids['point1'][i])
        self.canvas.delete(self.shape_ids['point2'][i])
        self.canvas.delete(self.shape_ids['line'][i])
        self.canvas.delete(self.shape_ids['text'][i])
    # click mode
    for i in range(len(self.click_ids['point'])):
        self.canvas.delete(self.click_ids['point'][i])
        self.canvas.delete(self.click_ids['text'][i])


def _update_img(self):
    self.canvas.itemconfig(self.shape_ids['canvas_img'], image=self.save_photo)
    width = self.save_photo.width()
    height = self.save_photo.height()
    self.canvas.config(scrollregion=(0, 0, width, height))

def _preprocess_img(self):
    image = Image.open(self.img_dir)
    image = equalize(image)
    # draw center reference line
    draw = ImageDraw.Draw(image)
    draw.line([0, image.size[1] / 2, image.size[0], image.size[1] / 2], fill=(255, 255, 0))

    self.save_image = image
    del image, draw

def _resize_img(self):
    if self.zoom_ratio == 1.0:
        self.save_photo = PhotoImage(self.save_image)
    else:
        width, height = self.save_image.size
        if self.zoom_ratio < 1.0:
            img_zoom = self.save_image.resize((int(width * self.zoom_ratio),
                                               int(height * self.zoom_ratio)), Image.ANTIALIAS)
        else:
            img_zoom = self.save_image.resize((int(width * self.zoom_ratio),
                                               int(height * self.zoom_ratio)), Image.BICUBIC)
        try:
            self.save_photo = PhotoImage(img_zoom)
            del img_zoom
        except (MemoryError, TclError):
            showwarning('Warning', 'Not enough memory to support zoom in this size, please try another one')
            self.zoom_ratio = 1.0
            self.save_photo = PhotoImage(self.save_image)
```

```
class TkErrorCatcher:
    # In some cases tkinter will only print the traceback.
    # Enables the program to catch tkinter errors normally
    # To use
    # import tkinter
    # tkinter.CallWrapper = TkErrorCatcher

    def __init__(self, func, subst, widget):
        self.func = func
        self.subst = subst
        self.widget = widget

    def __call__(self, *args):
        try:
            if self.subst:
                args = self.subst(*args)
            return self.func(*args)
        # except SystemExit as msg:
        #    raise SystemExit(msg)
        except Exception as err:
            raise err


if __name__ == '__main__':
    import tkinter
    tkinter.CallWrapper = TkErrorCatcher
    app = Pano2BA()
    db = DataBase('~$default.sqlite')
    try:
        app.mainloop()
    except Exception as e:
        exc_type, exc_value, exc_traceback = sys.exc_info()
        lines = traceback.format_exception(exc_type, exc_value, exc_traceback)
        error_info = ''.join(line for line in lines)
        print(error_info)
        showerror('Error', error_info)
```

ba.py

```
from math import sin, asin, sqrt, pi


def in_tree_pixel(baf, img_width):
    # baf is the Basal Area factor
    # tree_width is the app measured tree pixel width

    theta = 2 * asin(sqrt(baf) / 100)  # radians
    min_tree_width = theta / (2*pi) * img_width  # also use rad(360) = 2 pi

    return min_tree_width


def max_baf(img_width, tree_width):

    return (100 * sin((pi * tree_width) / img_width)) ** 2


def plot_ba_calculator(baf, in_tree_num):

    return baf * in_tree_num
```

db.py

```
import os
import sqlite3
from math import sqrt
from PIL import Image
from ba import plot_ba_calculator, max_baf, in_tree_pixel


class DataBase:

    db_path = 'test.sqlite'

    def __init__(self, db_path='test.sqlite'):
        if not os.path.exists(db_path):
            self.create_db(db_path)
        else:  # open a table
            self.conn = sqlite3.connect(db_path)
        self.curs = self.conn.cursor()

    def create_db(self, db_path):
        self.conn = sqlite3.connect(db_path)
        self.curs = self.conn.cursor()

        self.curs.execute('''
            CREATE TABLE ImageInfo (
                img_id INT NOT NULL PRIMARY KEY,
                img_dir CHAR(256) NOT NULL,
                img_name CHAR(64) NOT NULL,
                width INT NOT NULL,
                height INT NOT NULL,
                default_baf REAL NOT NULL DEFAULT 2,
                mode INT NOT NULL DEFAULT 0)''')
        self.curs.execute('''
            CREATE TABLE TreeInfo (
                tree_id INT NOT NULL PRIMARY KEY,
                img_id INT NOT NULL,
                lx REAL NOT NULL,
                ly REAL NOT NULL,
                rx REAL NOT NULL,
                ry REAL NOT NULL,
                max_baf REAL NOT NULL,
                    FOREIGN KEY (img_id) REFERENCES ImageInfo(img_id))''')
        self.curs.execute('''
            CREATE TABLE ClickInfo (
                click_id INT NOT NULL PRIMARY KEY,
                img_id INT NOT NULL,
                x REAL NOT NULL,
                y REAL NOT NULL,
                baf REAL NOT NULL,
                    FOREIGN KEY (img_id) REFERENCES ImageInfo(img_id))''')
        self.conn.commit()
        self.db_path = db_path


    def change_db(self, db_path):
        self.conn.close()
        self.conn = sqlite3.connect(db_path)
        self.curs = self.conn.cursor()
        self.db_path = db_path

    def update_db(self):
        # add a ref.ball mode here, fit to previous database
        self.curs.execute('''
            CREATE TABLE IF NOT EXISTS ClickInfo (
                click_id INT NOT NULL PRIMARY KEY,
                img_id INT NOT NULL,
                x REAL NOT NULL,
                y REAL NOT NULL,
                baf REAL NOT NULL,
                    FOREIGN KEY (img_id) REFERENCES ImageInfo(img_id))''')
        try:
            self.curs.execute('''
                ALTER TABLE ImageInfo ADD COLUMN mode INT NOT NULL DEFAULT 0''')
        except:
            pass

        self.commit()

    def add_img(self, img_path, mode=0):
        im = Image.open(img_path)
        width, height = im.size
        img_name_ext = os.path.basename(img_path)
        img_name = os.path.splitext(img_name_ext)[0]

        self.curs.execute('select MAX(img_id) from ImageInfo')
        max_id = self.curs.fetchone()[0]
        if max_id is None:
            img_id = 0
        else:
            img_id = max_id + 1

        self.curs.execute('insert into ImageInfo values (?,?,?,?,?,?,?)',
                          (img_id, img_path, img_name, width, height, 2, mode))

    def rm_img(self, img_id):
        self.curs.execute('delete from ImageInfo where img_id = ?', [img_id])
        self.curs.execute('delete from TreeInfo where img_id = ?', [img_id])

    def edit_img_mode(self, img_id, mode=0):
        self.curs.execute('update ImageInfo set mode = ? where img_id = ?', [mode, img_id])

    def edit_img_baf(self, img_id, baf):
        self.curs.execute('update ImageInfo set default_baf = ? where img_id = ?', [baf, img_id])

    def edit_img_baf_all(self, baf):
        self.curs.execute('update ImageInfo set default_baf = ?', [baf])

    def get_img_info(self):
        self.curs.execute('select img_id, img_dir, img_name, width, height, default_baf, mode from ImageInfo')
        img_info = {'img_id': [], 'img_dir': [], 'img_name': [],
                    'width': [], 'height': [], 'baf': [], 'mode':[], 'in_num': [], 'ba': []}
        for r in self.curs.fetchall():
            img_info['img_id'].append(r[0])
            img_info['img_dir'].append(r[1])
            img_info['img_name'].append(r[2])
            img_info['width'].append(r[3])
            img_info['height'].append(r[4])
            img_info['baf'].append(r[5])
            img_info['mode'].append(r[6])

        for i, img_id in enumerate(img_info['img_id']):
            baf = img_info['baf'][i]
            mode = img_info['mode'][i]
            if mode == 0:
                self.curs.execute('select tree_id from TreeInfo where img_id = ? and max_baf >= ?', [img_id, baf])
                in_num = len(self.curs.fetchall())
            else:
                self.curs.execute(('select click_id from ClickInfo where img_id = ? and baf = ?'), [img_id, baf])
                in_num = len(self.curs.fetchall())

            ba = plot_ba_calculator(baf, in_num)
            img_info['in_num'].append(in_num)
            img_info['ba'].append(ba)

        return img_info

    def get_img_info_baf_range(self, baf_list):
        img_info_all = {'img_id':[], 'img_name':[], 'baf_num_ba':[]}
        self.curs.execute('select img_id from ImageInfo')

        img_info_all['img_id'] = [r[0] for r in self.curs.fetchall()]

        for img_id in img_info_all['img_id']:
            self.curs.execute('select img_name from ImageInfo where img_id = ?', [img_id])
            img_info_all['img_name'].append(self.curs.fetchone()[0])
            baf_num_ba = []
            for baf in baf_list:
                self.curs.execute('select tree_id from TreeInfo where img_id =? and max_baf >= ?', [img_id, baf])
                in_num = len(self.curs.fetchall())
                ba = plot_ba_calculator(baf, in_num)
                baf_num_ba.append(ba)
                #baf_num_ba.append(in_num)

            img_info_all['baf_num_ba'].append(baf_num_ba)

        return img_info_all

    def add_tree(self, img_id, lx, ly, rx, ry, return_value=False):
        self.curs.execute('select MAX(tree_id) from TreeInfo')
        max_id = self.curs.fetchone()[0]
        if max_id is None:
            tree_id = 0
        else:
            tree_id = max_id + 1

        self.curs.execute('select width from ImageInfo where img_id = ?', [img_id])
        img_width = self.curs.fetchone()[0]
        baf_max = self.max_baf_calculator(lx, ly, rx, ry, img_width)

        self.curs.execute('insert into TreeInfo values (?,?,?,?,?,?,?)',
                          (tree_id, img_id, lx, ly, rx, ry, baf_max))
        width = self.length_calculator(lx, ly, rx, ry)
        if return_value:
            return tree_id, width, baf_max  # same order as get_tree_info

    def add_click(self, img_id,  x, y, return_value=False):
        self.curs.execute('select MAX(click_id) from ClickInfo')
        max_id = self.curs.fetchone()[0]
        if max_id is None:
            click_id = 0
        else:
            click_id = max_id + 1

        self.curs.execute('select default_baf from ImageInfo where img_id = ?', [img_id])
        baf = self.curs.fetchone()[0]

        self.curs.execute('select width from ImageInfo where img_id = ?', [img_id])
        img_width = self.curs.fetchone()[0]

        diameter_pixel = int(in_tree_pixel(baf, img_width))

        self.curs.execute('insert into ClickInfo values (?,?,?,?,?)', [click_id, img_id, x, y, baf])

        if return_value:
            return click_id, diameter_pixel

    def rm_tree(self, tree_id):
        self.curs.execute('delete from TreeInfo where tree_id = ?', [tree_id])

    def rm_click(self, click_id):
        self.curs.execute('delete from ClickInfo where click_id = ?', [click_id])

    def edit_tree(self, tree_id, lx, ly, rx, ry, return_value=False):
        self.curs.execute('select img_id from TreeInfo where tree_id = ?', [tree_id])
        img_id = self.curs.fetchone()[0]
        self.curs.execute('select width from ImageInfo where img_id = ?', [img_id])
        img_width = self.curs.fetchone()[0]

        width = self.length_calculator(lx, ly, rx, ry)
        baf_max = self.max_baf_calculator(lx, ly, rx, ry, img_width)

        self.curs.execute('update TreeInfo set lx = ?, ly = ?, rx = ?, ry = ?, max_baf = ? where tree_id = ?',
                          [lx, ly, rx, ry, baf_max, tree_id])
        if return_value:
            return width, baf_max

    def edit_click(self, click_id, x, y, return_value=False):
        self.curs.execute('update ClickInfo set x=?, y=? where click_id = ?', [x, y, click_id])

    def get_tree_info(self, img_id):
        self.curs.execute('select default_baf from ImageInfo where img_id = ?', [img_id])
        default_baf = self.curs.fetchone()

        tree_info = {'tree_id': [], 'left': [], 'right': [], 'width': [], 'state': []}

        if default_baf is not None:
            default_baf = default_baf[0]
            self.curs.execute('select tree_id, lx, ly, rx, ry, max_baf from TreeInfo where img_id = ?', [img_id])

            for ti in self.curs.fetchall():
                tree_info['tree_id'].append(ti[0])
                tree_info['left'].append([ti[1], ti[2]])
                tree_info['right'].append([ti[3], ti[4]])
                tree_info['width'].append(self.length_calculator(ti[1], ti[2], ti[3], ti[4]))
                if ti[5] >= default_baf:
                    state = 'in'
                else:
                    state = 'out'
                tree_info['state'].append(state)

        return tree_info

    def get_click_info(self, img_id):
        self.curs.execute('select default_baf from ImageInfo where img_id = ?', [img_id])
        default_baf = self.curs.fetchone()

        self.curs.execute('select width from ImageInfo where img_id = ?', [img_id])
        img_width = self.curs.fetchone()[0]

        diameter_pixel = int(in_tree_pixel(default_baf[0], img_width))

        click_info = {'click_id':[], 'x':[], 'y':[], 'width':[], 'state':[]}

        if default_baf is not None:
            default_baf = default_baf[0]
            self.curs.execute('select click_id, x, y from ClickInfo where img_id = ? AND baf=?', [img_id, default_baf])

            for ci in self.curs.fetchall():
                click_info['click_id'].append(ci[0])
                click_info['x'].append(ci[1])
                click_info['y'].append(ci[2])
                click_info['width'].append(diameter_pixel)
                click_info['state'].append('in')
        return click_info


    def get_tree_info_all(self):
        self.curs.execute('select img_id, tree_id, lx, ly, rx, ry, max_baf from TreeInfo order by img_id')
        tree_info_all = {'img_id':[], 'tree_id':[], 'width':[], 'max_baf':[]}
        for item in self.curs.fetchall():
            tree_info_all['img_id'].append(item[0])
            tree_info_all['tree_id'].append(item[1])
            tree_info_all['width'].append(self.length_calculator(item[2], item[3], item[4], item[5]))
            tree_info_all['max_baf'].append(item[6])

        return tree_info_all

    def get_click_info_all(self):
        self.curs.execute('select img_id, click_id, x, y, baf from ClickInfo order by img_id, baf')
        click_info_all = {'img_id':[], 'click_id':[], 'x':[], 'y':[], 'baf':[]}
        for item in self.curs.fetchall():
            click_info_all['img_id'].append(item[0])
            click_info_all['click_id'].append(item[1])
            click_info_all['x'].append(item[2])
            click_info_all['y'].append(item[3])
            click_info_all['baf'].append((item[4]))

        return click_info_all

    def commit(self):
        self.conn.commit()

    def max_baf_calculator(self, lx, ly, rx, ry, img_width):
        diameter_pixel = self.length_calculator(lx, ly, rx, ry)
        baf_max = max_baf(img_width, diameter_pixel)
        return baf_max

    @staticmethod
    def length_calculator(lx, ly, rx, ry):
        return int(sqrt((lx - rx) ** 2 + (ly - ry) ** 2))


if __name__ == '__main__':
    # testing
    if os.path.exists('test.sqlite'):
        os.remove('test.sqlite')
    db = DataBase()
    # testing add img
    db.add_img(r'..\images\examples\COR R1 S00 0 16.JPG')
    db.add_img(r'..\images\examples\COR R1 S00 1 16.JPG')
    # testing remove img
    db.rm_img(0)
    # testing add img to discontinuous img_id
    db.add_img(r'..\images\examples\COR R1 S12 0 16.JPG')
    db.add_img(r'..\images\examples\COR R1 S12 1 16.JPG')
    # testing edit baf info without trees
    db.edit_img_baf(img_id=1, baf=3)
    # try to update non exist img
    db.edit_img_baf(0, 3.4)
    # add trees to test
    db.add_tree(img_id=1, lx=360, ly=720, rx=658, ry=720)
    db.add_tree(img_id=1, lx=360, ly=720, rx=358, ry=720)  # lx < rx
    db.add_tree(img_id=2, lx=390, ly=720, rx=458, ry=770)  # not horizontal
    db.add_tree(img_id=2, lx=380, ly=720, rx=489, ry=720)
    db.add_click(img_id=1, x=300, y=500)
    db.add_click(img_id=1, x=500, y=765)
    db.add_click(img_id=2, x=5640, y=725)
    # test delete tree
    db.rm_tree(tree_id=0)
    db.rm_click(click_id=1)
    # test update tree info
    db.edit_tree(tree_id=3, lx=240, ly=430, rx=261, ry=430)
    db.edit_click(click_id=2, x=430, y=370)
    # test getting info from db for gui.py
    print(db.get_img_info())
    print(db.get_tree_info(img_id=2))
    print(db.get_click_info(img_id=2))
    # testing edit baf info and change tree info at the same time
    db.edit_img_baf(img_id=2, baf=300)
    print(db.get_tree_info(img_id=2))
    print(db.get_click_info(img_id=2))
    db.commit()
```

Appendix B: Plant Fraction Calculation Code

All the following codes in this appendix can be download from: https://github.com/HowcanoeWang/Spherical2TreeAttributes/tree/master/Plant%20Fraction

config.py (HSV Threshold)

```
hsv_version = 190410
hsv_threshold = {'sky':{'min':[(0, 0, 0.88), (175/360, 0.15, 0.85), (180/360, 0.45, 0.75)],
                        'max':[(1, 0.15, 1), (220/360, 0.45, 1),    (245/360, 1,    1)  ]},
                 'leaf':{'min':[(60 / 360, 0.15, 0.2)],
                         'max':[(170 / 360, 1, 1)]}}

femel_path = r'D:\OneDrive\Documents\3_UNB\3_Graduate\[Data].FieldPhoto\Femel_Data\Femel_Panorama'
nl_path = r'D:\OneDrive\Documents\3_UNB\3_Graduate\[Data].FieldPhotos\Newfoundland_Data\Newfoundland_Panorama'
```

Hemispherical/converse.py

```
import os
import time
import numpy as np
import pandas as pd
from PIL import Image, ImageDraw
from scipy import interpolate
from skimage import filters
from skimage.morphology import disk, binary_dilation
import multiprocessing

import scipy.interpolate as spint
import scipy.spatial.qhull as qhull
import itertools

# =================  Three main functions ================
def pano2fisheye(pil_img, model='equal_width', inter_method='linear', log='off', multi='off'):
    if log == 'on':
        print('|- Start conversing...')
    img_df, shape = img2dataframe(pil_img)
    if log == 'on':
        print('|-  Image DataFrame initialized')
    img_conv, fisheye_shape = coordinate_converse(img_df, shape, model=model)
    if log == 'on':
        print('|-  New pixel positions calculated')
    img_cali = unique_points(img_conv)
    if log == 'on':
        print('|-  Duplicated pixels removed')
    if log == 'on':
        print('|-  Start fixing holes')
    red, green, blue = interpolate_img(img_cali, fisheye_shape, method=inter_method, multi=multi, log=log)
    fisheye_img = merge_layers(red, green, blue)
    if log == 'on':
        print('|-  Image combined')
    return fisheye_img


def fisheye_correction(img, center_radius, model='equidistant', vision_angle=50, inter_method='linear',  multi='off',
log='off'):
    x, y, r = center_radius
    if log == 'on':
        print('- Start conversing...')
    img_df, shape = img2dataframe(img, center_radius)
    if log == 'on':
        print('|-  Image DataFrame initialized')
    img_df = calculate_radius_calibrated(img_df, r, model=model)
    if log == 'on':
        print('|-  New radius calculated')
    img_df, r_new = zenith_filter(img_df, r, vision_angle)
    if log == 'on':
        print('|-  Vision angle filtered')
    img_df = calculate_new_xy(img_df, r, r_new)
    if log == 'on':
        print('|-  New pixel positions calculated')
    df_cali = unique_points(img_df)
    if log == 'on':
```

```python
        print('|-  Duplicated pixels removed')
        print('|-  Start fixing holes')
    length = int(np.ceil(r_new * 2))
    red, green, blue = interpolate_img(df_cali, (length, length), method=inter_method, multi=multi)
    corrected_img = merge_layers(red, green, blue)
    if log == 'on':
        print('|-  Image combined')
    return corrected_img


def pano2fisheye_correction(pil_img, trans_model='equal_width', cali_model='equisolid', vision_angle=50,
                            inter_method='linear', multi='off', log='off'):
    if log == 'on':
        print('- Start conversing...')
    img_df, shape = img2dataframe(pil_img)
    del pil_img
    if log == 'on':
        print('|-  Image DataFrame initialized')
    img_conv, fisheye_shape = coordinate_converse(img_df, shape, model=trans_model)
    if log == 'on':
        print('|-  New pixel positions calculated')
    img_cali = unique_points(img_conv)
    if log == 'on':
        print('|-  Duplicated pixels removed')
    del img_conv

    r = int(fisheye_shape[0] / 2)

    img_df = calculate_radius_calibrated(img_cali, r, model=cali_model)
    del img_cali

    if log == 'on':
        print('|-  New radius calculated')
    img_df, r_new = zenith_filter(img_df, r, vision_angle)
    if log == 'on':
        print('|-  Vision angle filtered')
    img_df = calculate_new_xy(img_df, r, r_new)
    if log == 'on':
        print('|-  New pixel positions calculated')
    df_cali = unique_points(img_df)

    if log == 'on':
        print('|-  Start fixing holes')
    length = int(np.ceil(r_new * 2))
    red, green, blue = interpolate_img(df_cali, (length, length), method=inter_method, multi=multi)
    del df_cali

    fisheye_cali_img = merge_layers(red, green, blue)
    if log == 'on':
        print('|-  Image combined')

    return fisheye_cali_img


# =============== The modules that used for previews three main functions =====================
def img2dataframe(img, center_radius=None):
    '''
    if img is a fisheye image, (x, y, r) is required to crop fisheye edge.
    '''
    if type(center_radius) == tuple and len(center_radius) == 3:
        # fisheye image
        x, y, radius = center_radius
        img_crop = img.crop((x - radius - 1, y - radius - 1, x + radius - 1, y + radius - 1))

        mask = Image.new('RGBA', (2 * radius, 2 * radius))
        draw = ImageDraw.Draw(mask)
        draw.ellipse((0, 0, 2 * radius, 2 * radius), fill='blue', outline='blue')
        # overlay mask on image
        img_out = Image.new('RGBA', (2 * radius, 2 * radius))
        img_out.paste(img_crop, (0, 0), mask)
    else:
        # panorama image need crop half
        width, height = img.size
        img_out = img.crop((0, 0, width, int(height / 2)))

    '''PIL.img.size = (w, h)'''
    w, h = img_out.size
    np_img = np.asarray(img_out)
    '''
    numpy.ndarray:
     ┌→ y
     │  np.asarray(img).shape = (h, w, d)
    x↓
    '''
    x_grid, y_grid = np.mgrid[0:h, 0:w]
    red = np_img[:, :, 0]
    green = np_img[:, :, 1]
    blue = np_img[:, :, 2]
    if np_img.shape[2] == 4:
        alpha = np.asarray(img_out)[:, :, 3]
        img_df = pd.DataFrame({'x': x_grid.flatten(), 'y': y_grid.flatten(),
                               'red': red.flatten(), 'green': green.flatten(), 'blue': blue.flatten(),
                               'alpha': alpha.flatten()},
                              columns=['x', 'y', 'red', 'green', 'blue', 'alpha'])
        # remove alpha layer
        img_df = img_df.loc[img_df['alpha'] == 255]
        img_df = img_df.drop(['alpha'], axis=1)
    else:
        img_df = pd.DataFrame({'x': x_grid.flatten(), 'y': y_grid.flatten(),
                               'red': red.flatten(), 'green': green.flatten(), 'blue': blue.flatten()},
                              columns=['x', 'y', 'red', 'green', 'blue'])
    np_shape = (h, w)
    return img_df, np_shape


def unique_points(img_df):
    '''
    remove duplicate points which overlay one the same pixel
    x: conversed x (float)
    y: conversed y (float)
    shape: (height, width)

    return x, y , v_new
    '''
    x_int = img_df['x_cali'].astype(int)
    y_int = img_df['y_cali'].astype(int)
    df_cali = pd.DataFrame(
        {'x': x_int, 'y': y_int, 'red': img_df['red'], 'green': img_df['green'], 'blue': img_df['blue']})
    df_cali = df_cali.groupby(['x', 'y'], as_index=False).mean()

    return df_cali


def interpolate_img(img_df, shape, method='none', log='off', multi='off'):
    '''
    shape: (height, width)

    method: using griddata.linear to interpolate, this is very slow and time consuming
    return 2D.ndarray of that layer
    '''
    xi, yi = np.mgrid[0:shape[0], 0:shape[1]]
    if method == 'none':
        red = np.zeros(shape)
        green = np.zeros(shape)
        blue = np.zeros(shape)

        red[img_df['x'], img_df['y']] = img_df['red']
        green[img_df['x'], img_df['y']] = img_df['green']
        blue[img_df['x'], img_df['y']] = img_df['blue']
        if log == 'on': print('| |- no interpolate method applied')

        return red, green, blue

    if method == 'linear':

        if multi == 'on':
            key_words = ['red', 'green', 'blue']
            multiprocessing.freeze_support()
            pool = multiprocessing.Pool(processes=3)
            pool_list = {}
            for channel in key_words:
                pool_list[channel] = pool.apply_async(interpolate.griddata,
                                                      args=((img_df['x'], img_df['y']), img_df[channel], (xi, yi)))

            result_list = {key:value.get() for key, value in pool_list.items()}

            pool.close()
            pool.join()
            return result_list['red'], result_list['green'], result_list['blue']
        else:
            mask_hole = np.zeros(shape)
            mask_hole[img_df['x'], img_df['y']] = 1
            mask_circ = createCircularMask(*shape)
            mask = (mask_hole==0) * mask_circ
            if log == 'on': print('| |- mask generated')

            red = np.zeros(shape).astype(np.uint16)
            green = np.zeros(shape).astype(np.uint16)
            blue = np.zeros(shape).astype(np.uint16)

            red[img_df['x'], img_df['y']] = img_df['red']
            green[img_df['x'], img_df['y']] = img_df['green']
            blue[img_df['x'], img_df['y']] = img_df['blue']

            red_filter = filters.rank.mean(red, disk(1),mask=mask_hole==1)
            green_filter = filters.rank.mean(green, disk(1),mask=mask_hole==1)
            blue_filter = filters.rank.mean(blue, disk(1),mask=mask_hole==1)
            if log == 'on': print('| |- filter generated')

            #mask_deli = binary_dilation(mask)

            red[mask] = red_filter[mask]
            green[mask] = green_filter[mask]
            blue[mask] = blue_filter[mask]
            '''
            t = time.time()
            red = interpolate.griddata((img_df['x'], img_df['y']), img_df['red'], (xi, yi))
            if log == 'on':
                print(f'| |- [red] channel finished, {time.time() - t}s spend')
            tr = time.time()
            green = interpolate.griddata((img_df['x'], img_df['y']), img_df['green'], (xi, yi))
            if log == 'on':
                print(f'| |- [green] channel finished, {time.time() - t}s spend')
            tr = time.time()
            blue = interpolate.griddata((img_df['x'], img_df['y']), img_df['blue'], (xi, yi))
            if log == 'on':
                print(f'| |- [blue] channel finished, {time.time() - t}s spend')
            '''
            return red, green, blue


def merge_layers(r, g, b):
    img = np.zeros((r.shape[0], r.shape[1], 3))
    img[:, :, 0] = r
    img[:, :, 1] = g
    img[:, :, 2] = b
    img[np.isnan(img)] = 0
    img = img.astype('uint8')
    pil_img = Image.fromarray(img)

    return pil_img


def coordinate_converse(img_df, panorama_size, model='equal_width'):
    '''
    panorama size = (h, w)
        h: panorama image height
        w: panorama image width
    model
    'equal_width': assume height of one pixel in panorama = the distance to circle center in fisheye
    'projection': assume height of panorama = height of hemisphere of fisheye ghostball,
                  which the radius of ghostball (r), height of pixel in panorama (h),
                  distance to circle center of fisheye for that pixel(d) satisfy:
                  r^2 = h^2 + d^2
    '''
    h, w = panorama_size
    r = h
    fisheye_size = (2 * r, 2 * r)
    theta = (img_df['y'] + 0.5) / w * 360  # +0.5 is to mark pixel center
    sin_theta = np.sin(np.deg2rad(theta))
    cos_theta = np.cos(np.deg2rad(theta))
    if model == 'equal_width':
        img_df['x_cali'] = r + sin_theta * img_df['x']
        img_df['y_cali'] = r + cos_theta * img_df['x']
    if model == 'projection':
        d = np.sqrt(abs(2 * (img_df['x'] + 0.5) * r - (img_df['x'] + 0.5) ** 2))
        img_df['x_cali'] = r + sin_theta * d
        img_df['y_cali'] = r + cos_theta * d

    return img_df, fisheye_size


def calculate_radius_calibrated(img_df, img_radius, model='equidistant', log='off'):
    '''
    img_radius: half of fisheye width or height
    models:
```

```python
        'equidistant'
        'equidolid'
        'orthographic'
        'stereographic'
    '''
    if model == 'equidistant':
        f = img_radius * 2 / np.pi  # the radius of fake sphere
        d = np.sqrt((img_df['x'] - img_radius) ** 2 + (img_df['y'] - img_radius) ** 2)
        img_df['r_cali'] = f * np.tan(d / f)
    elif model == 'equisolid':
        f = img_radius / np.sqrt(2)
        d = np.sqrt((img_df['x'] - img_radius) ** 2 + (img_df['y'] - img_radius) ** 2)
        img_df['r_cali'] = f * np.tan(2 * np.arcsin(d / (2 * f)))
    elif model == 'orthographic':
        f = img_radius
        d = np.sqrt((img_df['x'] - img_radius) ** 2 + (img_df['y'] - img_radius) ** 2)
        img_df['r_cali'] = d / np.sqrt(1 + (d / f) ** 2)
    elif model == 'stereographic':
        f = img_radius / 2
        d = np.sqrt((img_df['x'] - img_radius) ** 2 + (img_df['y'] - img_radius) ** 2)
        img_df['r_cali'] = f * np.tan(2 * np.arctan(d / (2 * f)))
    else:
        d = np.sqrt((img_df['x'] - img_radius) ** 2 + (img_df['y'] - img_radius) ** 2)
        if log == 'on': print('no input [' + model + '] model, please choose another one!')
        img_df['r_cali'] = d

    return img_df


def zenith_filter(img_df, img_radius, filter_degree=50):
    f = img_radius * 2 / np.pi
    if filter_degree <= 70:
        threshold = f * np.tan(np.deg2rad(filter_degree))
        img_df = img_df.loc[np.abs(img_df['r_cali']) <= threshold]

        return img_df, threshold
    else:
        return img_df, False


def calculate_new_xy(img_df, img_radius, cali_radius):
    rad_theta = np.arctan2((img_df['x'] - img_radius), (img_df['y'] - img_radius))
    rad_theta += (img_df['x'] <= img_radius) * 2 * np.pi
    img_df = img_df.assign(x_cali=cali_radius + np.sin(rad_theta) * img_df['r_cali'])
    img_df = img_df.assign(y_cali=cali_radius + np.cos(rad_theta) * img_df['r_cali'])

    return img_df


def createCircularMask(h, w, center=None, radius=None):
    if center is None: # use the middle of the image
        center = [int(w/2), int(h/2)]
    if radius is None: # use the smallest distance between the center and image walls
        radius = min(center[0], center[1], w-center[0], h-center[1])

    Y, X = np.ogrid[:h, :w]
    dist_from_center = np.sqrt((X - center[0])**2 + (Y-center[1])**2)

    mask = dist_from_center <= radius
    return mask
```

Hemispherical/plant_fraction_hemi.py

```python
import numpy as np
import pandas as pd
from PIL import Image, ImageDraw
from skimage.color import rgb2hsv
from math import floor

import sys
sys.path.insert(0, '..')
import config

class PF:

    def __init__(self, img_path, threshold):
        img = Image.open(img_path)
        self.img = np.asarray(img)

        self.threshold = threshold
        self.img_data = rgb2hsv(self.img)
        #self.binary = self._in_range(threshold['min'], threshold['max'])
        #self.overlay, self.pai = self.count_pai(self.binary)
        self.kind = self._classify()
        self.kind_ref = {'plant': self.kind != 2,
                         'stem': self.kind == 0,
                         'leaf': self.kind == 1,
                         'sky': self.kind == 2}


    def _in_range(self, lower, upper):
        '''
        input a image and threshold, give a classified binary image (m*n booleans ndarray)
        Image out is binary w*h matrix, T is in threshold (sky), F is out of threshold (plant)
        '''
        img_data = self.img_data

        mask = np.zeros(img_data.shape[0:2], dtype=bool)

        for min, max in zip(lower, upper):
            mask_0 = (img_data[:, :, 0] >= min[0]) * (img_data[:, :, 0] <= max[0])
            mask_1 = (img_data[:, :, 1] >= min[1]) * (img_data[:, :, 1] <= max[1])
            mask_2 = (img_data[:, :, 2] >= min[2]) * (img_data[:, :, 2] <= max[2])

            mask_all = mask_0 * mask_1 * mask_2
            mask += mask_all

        return mask

    def _classify(self):
        threshold = self.threshold
        self.sky_mask = self._in_range(threshold['sky']['min'], threshold['sky']['max'])
        self.leaf_mask = self._in_range(threshold['leaf']['min'], threshold['leaf']['max'])

        kind = np.zeros(self.img_data.shape[0:2], dtype=int)
        # stem = 0, leaf = 1, sky = 2
        kind[self.leaf_mask] = 1
        kind[self.sky_mask] = 2

        return kind

    @staticmethod
    def createCircularMask(h, w, center=None, radius=None):
        if center is None: # use the middle of the image
            center = [int(w/2), int(h/2)]
        if radius is None: # use the smallest distance between the center and image walls
            radius = min(center[0], center[1], w-center[0], h-center[1])

        Y, X = np.ogrid[:h, :w]
        dist_from_center = np.sqrt((X - center[0])**2 + (Y-center[1])**2)

        mask = dist_from_center <= radius
        return mask

    '''
    def count_pai(self, binary_img):
        h, w = binary_img.shape
        r = w / 2
        mask = self.createCircularMask(h, w)
        overlay = binary_img * mask

        u_img, counts_img = np.unique(overlay, return_counts=True)
        u_mask, counts_mask = np.unique(mask, return_counts=True)

        sky_percent = counts_img[1] / counts_mask[1]
        pai = 1-sky_percent
        return overlay, pai

    def write_result(self, result_dir, mode='binary'):
        h, w, d = self.img.shape

        rua = np.zeros((h, w, 3))
        if mode=='colored'
            rua[:, :, 0] = self.img[:,:,0] * abs(self.overlay - 1)
            rua[:, :, 1] = self.img[:,:,1] * abs(self.overlay - 1)
            rua[:, :, 2] = self.img[:,:,2] * abs(self.overlay - 1)
            # merge img|classified
            img_comb = Image.fromarray( np.hstack((self.img, rua)).astype('uint8'))
            img_comb.save(result_dir)
        else:
            for i in range(0,3):
                rua[:,:,i] = self.binary * 255
            rua.save(result_dir)
    '''
    def pf_value(self, kind='plant', zenith_angle=57.5):
        h, w = self.kind.shape
        r = w / 2
        mask = self.createCircularMask(h, w)

        binary_img = self.kind_ref[kind]
        overlay = binary_img * mask

        u_img, counts_img = np.unique(overlay, return_counts=True)
        u_mask, counts_mask = np.unique(mask, return_counts=True)

        percent = counts_img[1] / counts_mask[1]

        return percent
```

Hemispherical/classify_all_fisheye.py

```
import os
import pandas as pd
from plant_fraction_hemi import PF

import sys
sys.path.insert(0, '..')
import config

g = os.walk(r'Conversed_57.5/')

# plant fraction, leaf fraction, stem Fraction sky fraction
pai_data = pd.DataFrame(columns=['File_name', 'PlantFrac', 'LeafFrac', 'StemFrac', 'SkyFrac'])

'''
write_dir = f'./Classified_57.5_ver.{config.hsv_version}/'
if not os.path.exists(write_dir):
    os.mkdir(write_dir)
'''


for path, dir_list, file_list in g:
    for file_name in file_list:
        if file_name[-4:] == '.JPG':

            img_path = os.path.join(path, file_name)
            img = PF(img_path, config.hsv_threshold)

            result_list = [file_name,
                           img.pf_value('plant', 57.5),
                           img.pf_value('leaf', 57.5),
                           img.pf_value('stem', 57.5),
                           img.pf_value('sky', 57.5)]

            #img.write_result(write_dir + file_name)

            #result_list.append()

            pai_data.loc[len(pai_data)] = result_list

            print(str(result_list))


pai_data.to_csv(f'pf57.5_3classes_fisheye_ver.{config.hsv_version}.csv', index=False)
```

Cylindrical/plant_fraction_cyli.py

```
import numpy as np
import os
import pandas as pd
from PIL import Image, ImageDraw
from skimage.color import rgb2hsv
from math import floor

import sys
sys.path.insert(0, '..')
import config


class PF:
```

```
def __init__(self, img_path, threshold):
    img = Image.open(img_path)
    self.img_name = os.path.basename(img_path)

    w, h = img.size
    self.h_half = int(h / 2)

    self.threshold = threshold

    self.img = np.asarray(img.crop((0, 0, w, self.h_half)))
    self.img_data = rgb2hsv(self.img)
    self.height = self.radius = self.h_half
    self.width = w

    self.aw = self._angle_weight()
    self.kind = self._classify()
    self.row_percent = self._percent_each_row()
    self.ring_s = self._ring_area(calibration=True)

def _classify(self):
    threshold = self.threshold
    self.sky_mask = self._in_range(threshold['sky']['min'], threshold['sky']['max'])
    self.leaf_mask = self._in_range(threshold['leaf']['min'], threshold['leaf']['max'])

    kind = np.zeros(self.img_data.shape[0:2], dtype=int)
    # Stem = 0, leaf = 1, sky = 2, plant =0 +1
    kind[self.leaf_mask] = 1
    kind[self.sky_mask] = 2

    return kind


def _in_range(self, lower, upper):
    '''
    input a image and threshold, give a classified binary image (m*n booleans ndarray)
    Image out is binary w*h matrix, T is in threshold (sky), F is out of threshold (plant)
    '''
    img_data = self.img_data

    mask = np.zeros(img_data.shape[0:2], dtype=bool)

    for min, max in zip(lower, upper):
        mask_0 = (img_data[:, :, 0] >= min[0]) * (img_data[:, :, 0] <= max[0])
        mask_1 = (img_data[:, :, 1] >= min[1]) * (img_data[:, :, 1] <= max[1])
        mask_2 = (img_data[:, :, 2] >= min[2]) * (img_data[:, :, 2] <= max[2])

        mask_all = mask_0 * mask_1 * mask_2
        mask += mask_all

    return mask

def _percent_each_row(self):
    stem_num = (self.kind == 0).sum(axis=1)
    leaf_num = (self.kind == 1).sum(axis=1)
    plant_num = stem_num + leaf_num
    sky_num = (self.kind == 2).sum(axis=1)

    stem_percent = stem_num / self.width
    leaf_percent = leaf_num / self.width
    plant_percent = plant_num / self.width
    sky_percent = sky_num / self.width

    return {'plant':plant_percent, 'leaf':leaf_percent, 'stem':stem_percent, 'sky':sky_percent}

def _ring_area(self, calibration=False):
    r_range = np.arange(0, self.radius + 1)

    if calibration:
        f = self.radius / np.sqrt(2)
        r_new = f * np.tan(2 * np.arcsin(r_range / (2 * f)))
    else:
        r_new = r_range

    self.r_in = r_new[:-1]
    self.r_out = r_new[1:]

    s = np.pi * self.r_out ** 2 - np.pi * self.r_in ** 2

    return s

def _angle_weight(self):
    line_id = np.arange(0, self.h_half, step=1)
    angle_weight = np.cos(line_id / self.h_half * np.pi / 2)

    return angle_weight

# TODO
def write_output(self, result_dir='outputs/', return_jpg=True, return_csv=False, merge=False):

    if return_jpg:
        rua = np.zeros((self.height, self.width, 3))

        #sky:   white R=255, G=255, B=255
        #plant: blue  R=0,   G=0,   B=255
        #leaf:  green R=0,   G=255, B=0

        # Red Channel
        rua[:, :, 0] = (self.kind == 2) * 255   # only sky = 255
        # Green Channel
        rua[:, :, 1] = ((self.kind == 1) | (self.kind == 2)) * 255  # sky & leaf = 255
        # Blue Channel
        rua[:, :, 2] = ((self.kind == 0) | (self.kind == 2)) * 255  # sky & plant = 255

        img_class = Image.fromarray((rua).astype('uint8'))

        d = ImageDraw.Draw(img_class)
        d.text((10,10), str(self.threshold), fill=(0,0,0))

        img_class.save(f'{result_dir}/class/{self.img_name}_class.jpg')
        if merge:
            # merge img|classified|leaf|plant|sky
            img_comb = Image.fromarray(np.vstack((np.asanyarray(self.img), rua)).astype('uint8'))
            d = ImageDraw.Draw(img_comb)
            d.text((10, 10), str(self.threshold), fill=(0,0,0))
            img_comb.save(f'{result_dir}/merge/{self.img_name}_merge.jpg')

    if return_csv:
        np.savetxt(f'{result_dir}/csv/{self.img_name}.csv', self.kind.astype(int), fmt='%i', delimiter=',')


def pf_value(self, kind='plant', zenith_angle=57.5):
    # zenith_angle should < 80 to be more precious
    line_num = floor(self.height * zenith_angle / 90) - 1

    percent = self.row_percent[kind][:line_num]
    #aw = self.aw[:line_num]
    r_max = self.r_in[line_num]

    s_max = np.pi * r_max ** 2
    ring_s = self.ring_s[:line_num]
    weight = ring_s / s_max

    pf_row = percent * weight# * aw

    return pf_row.sum()
```

Cylindrical/classify_all_cylindrical.py

```
import os
import pandas as pd
from plant_fraction_cyli import PF

import sys
sys.path.insert(0, '..')
import config

paths = [r'D:\OneDrive\Documents\3_UNB\3_Graduate\[Data].FieldPhoto\Newfoundland_Data\Newfoundland_Panorama',
         r'D:\OneDrive\Documents\3_UNB\3_Graduate\[Data].FieldPhoto\Femel_Data\Femel_Panorama']

# plant fraction, leaf fraction, stem Fraction sky fraction
pai_data = pd.DataFrame(columns=['File_name', 'PlantFrac', 'LeafFrac', 'StemFrac', 'SkyFrac'])

'''
write_dir = f'./Classified_57.5_ver.{config.hsv_version}/'
if not os.path.exists(write_dir):
    os.mkdir(write_dir)
'''

for path in paths:
    g = os.walk(path)
    for path, dir_list, file_list in g:
        for file_name in file_list:
            if file_name[-4:] == '.JPG':

                img_path = os.path.join(path, file_name)
                img = PF(img_path, config.hsv_threshold)

                result_list = [file_name,
                               img.pf_value('plant', 57.5),
                               img.pf_value('leaf', 57.5),
                               img.pf_value('stem', 57.5),
                               img.pf_value('sky', 57.5)]

                #img.write_result(write_dir + file_name)

                #result_list.append()

                pai_data.loc[len(pai_data)] = result_list

                print(str(result_list))


pai_data.to_csv(f'pf57.5_3classes_matrix_ver.{config.hsv_version}.csv', index=False)
```

Appendix C: Individual Tree Extraction Software Code

All the following codes in this appendix can be download from: https://github.com/HowcanoeWang/Spherical2TreeAttributes/tree/master/Individual%20Tree

app.py

```
import sys
import os
import numpy as np
from PyQt5.QtWidgets import *
from PyQt5.QtGui import *
from PyQt5.QtCore import *

from PIL import Image, ExifTags

from scipy import ndimage
from scipy.interpolate import interp1d
import imageio
from skimage.exposure import equalize_hist

from ba import in_tree_pixel

baf20 = in_tree_pixel(baf=20, img_width=5376)

class MainWindow(QMainWindow):
    keyPressed = pyqtSignal(QEvent)
    vLocked = pyqtSignal(int)


    def __init__(self, parent=None):
        super().__init__(parent)

        self.coordinate = '(x, y)'

        self.setWindowTitle('IndividualDemo')
        self.setupUI()
        self.functionConnector()

        self.initPlot()
        self.initTree()

        self.addTree = -1  # No add

        self.e1 = 1.6
        self.e2 = 2.6

    def setupUI(self):
        self.mainWidget = QWidget()

        self.panel16 = ImgPanel(self, 1.6)
        self.panel26 = ImgPanel(self, 2.6)

        self.line = QFrame()
        self.line.setFrameShape(QFrame.VLine)
        self.line.setFrameShadow(QFrame.Sunken)

        self.wl = QHBoxLayout(self.mainWidget)

        self.wl.addWidget(self.panel16)
        self.wl.addWidget(self.line)
        self.wl.addWidget(self.panel26)

        self.setCentralWidget(self.mainWidget)

    def functionConnector(self):
        self.panel16.xScrollChanged.connect(self.panel26.setXScroll)
        self.panel26.xScrollChanged.connect(self.panel16.setXScroll)
        self.panel16.yScrollChanged.connect(self.panel26.setYScroll)
        self.panel26.yScrollChanged.connect(self.panel16.setYScroll)

        self.panel16.exifData.connect(self.updatePlot)
        self.panel26.exifData.connect(self.updatePlot)
        self.keyPressed.connect(self.panel16.imgShow.changeDirection)
        self.keyPressed.connect(self.panel26.imgShow.changeDirection)

        self.panel16.imgShow.emitPoint.connect(self.addTree)
        self.panel26.imgShow.emitPoint.connect(self.addTree)

        self.vLocked.connect(self.panel16.imgShow.changeVLock)
        self.vLocked.connect(self.panel26.imgShow.changeVLock)

    def keyPressEvent(self, event):
        if event.key() == Qt.Key_L:
            v, okPressed = QInputDialog.getInt(self, "Get integer","Y pixel", 6000, 0, 13000, 1)
            if okPressed:
                self.vLocked.emit(v)
        elif event.key() == Qt.Key_U:
            self.vLocked.emit(-1)
        elif event.key() == Qt.Key_N:   # Add tree easy mode
            self.addTree = 0
            self.initTree()
            self.changeDirection('NE')
            self.showStep('[S1:1.6Base]')
        else:
            self.keyPressed.emit(event)

    def initPlot(self):
        self.plot = {'GCP16':0,
             'LatDeg16':0, 'LatMin16':0, 'LatSec16':0.0,
             'LonDeg16':0, 'LonMin16':0, 'LonSec16':0.0,
             'Altitude16':0.0, 'North16':0.0,
             'GCP26':0,
             'LatDeg26':0, 'LatMin26':0, 'LatSec26':0.0,
             'LonDeg26':0, 'LonMin26':0, 'LonSec26':0.0,
             'Altitude26':0.0, 'North26':0.0}

    def updatePlot(self, ht, data_list):
        if ht == 1.6:
            self.plot['GCP16']      = data_list[0]
            self.plot['LatDeg16']   = data_list[1]
            self.plot['LatMin16']   = data_list[2]
            self.plot['LatSec16']   = data_list[3]
            self.plot['LonDeg16']   = data_list[4]
            self.plot['LonDeg16']   = data_list[5]
            self.plot['LonDeg16']   = data_list[6]
            self.plot['Altitude16'] = data_list[7]
            self.plot['North16']    = data_list[8]
        else:
            self.plot['GCP26']      = data_list[0]
            self.plot['LatDeg26']   = data_list[1]
            self.plot['LatMin26']   = data_list[2]
            self.plot['LatSec26']   = data_list[3]
            self.plot['LonDeg26']   = data_list[4]
            self.plot['LonDeg26']   = data_list[5]
            self.plot['LonDeg26']   = data_list[6]
            self.plot['Altitude26'] = data_list[7]
            self.plot['North26']    = data_list[8]

        print(self.plot)

    def initTree(self):
        self.tree = {'16BX':0, '16BY':0, '16TX':0, '16TY':0,
             '26BX':0, '26BY':0, '26TX':0, '26TY':0,
             '16LX':0, '16LY':0, '16RX':0, '16RY':0,
             '26LX':0, '26LY':0, '26RX':0, '26RY':0,
             'Dist':0.0, 'DeltaH':0.0, 'HT':0.0, 'DBH':0.0, 'Gamma':0.0, 'Altitude':0.0}

    def addTree(self, x, y):
        # 0: Add 16Base
        # 1: Add 26Base => Calculate Dist, DeltaH, Altitude, Gamma, 1.3m, set panel16, panel 26
        # change direction to "W"
        # 2: Add 16Left => change direction to "E"
        # 3: Add 16Right => change direction to "W"
        # 4: Add 26Left => change direction to "E"
        # 5: Add 26Right => calculate DBH
        # 6: Add 16Top
        # 7: Add 26Top => calculate HT, change to -1
        if self.addTree == 0:
            self.tree['16BX'] = x
            self.tree['16BY'] = y
            self.addTree += 1
            self.showStep('[S2: 2.6Base]')
        elif self.addTree == 1:
            self.tree['26BX'] = x
            self.tree['26BY'] = y

            k1 = np.tan(-self.zenithRadians(self.tree['16BY']))
            k2 = np.tan(-self.zenithRadians(self.tree['26BY']))
            ix, iy = self.interactBase(k1, self.e1, k2, self.e2)
            self.tree['Dist'] = -ix
            self.tree['DeltaH'] = iy

            self.tree['Altitude'] = (self.plot['Altitude16'] + self.plot['Altitude26']) / 2 + iy
            gamma1 = self.horizonAngle(self.tree['16BX'], self.plot['GCP16'], self.plot['North16'])
            gamma2 = self.horizonAngle(self.tree['26BX'], self.plot['GCP26'], self.plot['North26'])
            self.tree['Gamma'] = (gamma1 + gamma2) / 2

            dbh16pos = self.getDBHPosition(self.e1, ix, iy)
            dbh26pos = self.getDBHPosition(self.e2, ix, iy)

            self.panel16.imgShow.changeVLock(int(dbh16pos))
            self.panel26.imgShow.changeVLock(int(dbh26pos))

            self.changeDirection('NW')
            self.showStep('[S3:1.6Left]')
            self.addTree += 1
        elif self.addTree == 2:
            self.tree['16LX'] = x
            self.tree['16LY'] = y
            self.changeDirection('NE')
            self.showStep('[S4:1.6Right]')
            self.addTree += 1
        elif self.addTree == 3:
            self.tree['16RX'] = x
            self.tree['16RY'] = y
            self.changeDirection('NW')
            self.showStep('[S5:2.6Left]')
            self.addTree += 1
        elif self.addTree == 4:
            self.tree['26LX'] = x
            self.tree['26LY'] = y
            self.changeDirection('NE')
            self.showStep('[S6:2.6Right]')
            self.addTree += 1
        elif self.addTree == 5:
            self.tree['26RX'] = x
            self.tree['26RY'] = y
            self.changeDirection('NW')

            dbh16 = self.getDBH(self.tree['16LX'], self.tree['16RX'], self.tree['Dist'])
            dbh26 = self.getDBH(self.tree['26LX'], self.tree['26RX'], self.tree['Dist'])
            self.tree['DBH'] = (dbh16 + dbh26) / 2

            self.panel16.imgShow.changeVLock(-1)
            self.panel26.imgShow.changeVLock(-1)
            self.showStep('[S7:1.6Top]')

            self.addTree += 1
        elif self.addTree == 6:
            self.tree['16TX'] = x
            self.tree['16TY'] = y
            self.showStep('[S8:2.6Top]')
            self.addTree += 1
        elif self.addTree == 7:
            self.tree['26TX'] = x
            self.tree['26TY'] = y

            k1 = np.tan(-self.zenithRadians(self.tree['16TY']))
            k2 = np.tan(-self.zenithRadians(self.tree['26TY']))
            ht1 = - self.tree['Dist'] * k1 + self.e1 - self.tree['DeltaH']
            ht2 = - self.tree['Dist'] * k2 + self.e2 - self.tree['DeltaH']

            self.tree['HT'] = (ht1 + ht2) / 2
            self.showStep('[Done&Paste]')

            text = ''
            for key, value in self.tree.items():
                text += f'{value}\t'

            self.cb = QApplication.clipboard()
            self.cb.clear(mode=self.cb.Clipboard)
            self.cb.setText(text[:-1], mode=self.cb.Clipboard)

            print(text)
            self.addTree = -1
```

```
    def changeDirection(self, direct='NE'):
        self.panel16.imgShow.corner = direct
        self.panel26.imgShow.corner = direct
        self.panel16.imgShow.update()
        self.panel26.imgShow.update()

    def showStep(self, string):
        self.panel16.updateProgress(string)
        self.panel26.updateProgress(string)

    @staticmethod
    def interactBase(k1, b1, k2, b2):
        x = (b2-b1)/(k1-k2)
        y = k1*x + b1
        return x, y

    @staticmethod
    def zenithRadians(ypos):
        return np.radians((1344 - (ypos - 1))/2688*180)

    @staticmethod
    def horizonAngle(xpos, gcp, north):
        gamma = (xpos+gcp) / 5376 * 360 - north
        if gamma < 0:
            gamma += 360
        if gamma > 360:
            gamma -= 360
        return gamma

    @staticmethod
    def getDBHPosition(e, bx, by):
        angles = -np.degrees(np.arctan((e-1.3-by)/(0-bx)))
        pos = 1344 - angles / 180 * 2688
        return pos

    @staticmethod
    def getDBH(lx, rx, dist):
        omiga = np.radians(abs(rx-lx) / 5376 * 360)
        sin_half_omiga = np.sin(omiga / 2)
        dbh = 2 * sin_half_omiga * dist / (1 - sin_half_omiga) * 100
        return dbh


class ImgPanel(QWidget):
    xScrollChanged = pyqtSignal(int)
    yScrollChanged = pyqtSignal(int)
    exifData = pyqtSignal(float, list)

    def __init__(self, parent=None, ht=1.6):
        super().__init__(parent)
        self.refX = 0
        self.refY = 0

        self.scrollX = 0
        self.scrollY = 0

        self.ht = ht

        self.converter = Converter(self)

        self.setupUI(ht)
        self.functionConnector()

    def setupUI(self, ht):
        self.layout = QVBoxLayout(self)
        self.infoLayout = QHBoxLayout()

        self.htName = QLabel(f"[{ht}m]:")
        self.imgName = QLabel('D:/xxx.Jpg')
        self.infoBtn = QPushButton('Info')
        self.changeImgBtn = QPushButton('OpenImg')
        self.convertBtn = QPushButton('Convert')
        self.saveImgBtn = QPushButton('save')

        self.imgShow = ImgShow(self)
        #self.scrollArea = QScrollArea()
        self.scrollArea = Scroller()
        self.scrollArea.setWidget(self.imgShow)

        self.hBar = self.scrollArea.horizontalScrollBar()
        self.vBar = self.scrollArea.verticalScrollBar()
        self.scrollX = self.hBar.value()
        self.scrollY = self.vBar.value()

        self.infoLayout.addWidget(self.htName)
        self.infoLayout.addWidget(self.imgName)
        self.infoLayout.addStretch(0)
        self.infoLayout.addWidget(self.infoBtn)
        self.infoLayout.addWidget(self.changeImgBtn)
        self.infoLayout.addWidget(self.convertBtn)
        self.infoLayout.addWidget(self.saveImgBtn)

        self.layout.addLayout(self.infoLayout)
        self.layout.addWidget(self.scrollArea)

    def functionConnector(self):
        self.imgShow.mouseClicked.connect(self.updateRef)
        self.infoBtn.clicked.connect(self.showInfo)
        self.changeImgBtn.clicked.connect(self.loadImg)
        self.convertBtn.clicked.connect(self.convertImg)
        self.saveImgBtn.clicked.connect(self.imgShow.saveImg)
        self.hBar.valueChanged.connect(self.emitX)
        self.vBar.valueChanged.connect(self.emitY)
        self.converter.sigOut.connect(self.updateProgress)
        self.imgShow.saver.sigOut.connect(self.updateProgress)

    def emitX(self):
        self.xScrollChanged.emit(self.hBar.value())

    def emitY(self):
        self.yScrollChanged.emit(self.vBar.value())

    def setXScroll(self, value):
        self.hBar.setValue(min(self.hBar.maximum(),value))

    def setYScroll(self, value):
        self.vBar.setValue(min(self.vBar.maximum(),value))

    def wheelEvent(self, event):
        if event.modifiers() == Qt.ShiftModifier:
            self.hBar.wheelEvent(event)
        else:
            self.vBar.wheelEvent(event)

    def getExifInfo(self):
        self.show_str = ''
        self.clip_str = ''
        # gcp, lat.D, lat.M, lat.S, Lon.D, Lon.M, Lon.S, Altitude, North
        # 0,   1,     2,     3,     4,     5,     6,     7,        8
        self.data_list = [0, 0, 0, 0.0, 0, 0, 0.0, 0.0, None]

        if self.imgShow.img_path is not None:
            img = Image.open(self.imgShow.img_path)
            exif_human = {ExifTags.TAGS[k]: v for k, v in img._getexif().items() if k in ExifTags.TAGS}
            gps_info = exif_human['GPSInfo']

            self.data_list[0] = self.refX
            lat_label = gps_info[1] # N
            lat_exif = gps_info[2] # ((45, 1), (56, 1), (4682, 100))
            self.data_list[1] = lat_exif[0][0]
            self.data_list[2] = lat_exif[1][0]
            self.data_list[3] = lat_exif[2][0]/lat_exif[2][1]
            self.show_str += f"{lat_exif[0][0]}°{lat_exif[1][0]}’{self.data_list[3]}” {lat_label}\n"

            lon_label = gps_info[3] # W
            lon_exif = gps_info[4] # ((66, 1), (38, 1), (3938, 100))
            self.data_list[4] = lon_exif[0][0]
            self.data_list[5] = lon_exif[1][0]
            self.data_list[6] = lon_exif[2][0]/lat_exif[2][1]
            self.show_str += f"{lon_exif[0][0]}°{lon_exif[1][0]}’{self.data_list[6]}” {lon_label}\n"

            alt_exif = gps_info[6] # (3512, 100)
            self.data_list[7] = alt_exif[0]/alt_exif[1]
            self.show_str += f"altitude:{self.data_list[7]}\n"

            if 17 in gps_info.keys():
                north_angle = gps_info[17] # (1125, 10)
                self.data_list[8] = north_angle[0]/north_angle[1]
                self.show_str += f"north:{self.data_list[8]}°"
            else:
                self.show_str += f"north: missing"

            for i in self.data_list:
                self.clip_str += f'{i}\t'
    def showInfo(self):
        self.getExifInfo()
        try:
            QMessageBox.information(self, "GPS Info", self.show_str)
            self.cb = QApplication.clipboard()
            self.cb.clear(mode=self.cb.Clipboard)
            self.cb.setText(self.clip_str[:-1], mode=self.cb.Clipboard)
        except:
            QMessageBox.information(self, "GPS Info", "Please use raw images!")

    def loadImg(self, choose=True):
        if not isinstance(choose, str):
            options = QFileDialog.Options()
            fileName, _ = QFileDialog.getOpenFileName(self, 'QFileDialog.getOpenFileName()', '',
                                                      'Images (*.png *.jpeg *.jpg *.bmp *.gif)', options=options)
            self.convertBtn.setEnabled(True)
        else:
            fileName=choose

        if fileName:
            image = QImage(fileName)
            if image.isNull():
                QMessageBox.information(self, "Image Viewer", "Cannot load %s." % fileName)
                return

            self.imgName.setText(fileName[:10]+'...'+fileName[-20:])
            self.imgShow.img_path = fileName
            self.imgShow.addImg = True
            self.imgShow.update()
            if 'converted_imgs/' not in fileName:
                self.getExifInfo()

    def convertImg(self):
        if self.imgShow.img_path is not None:
            self.converter.set_param(self.imgShow.img_path,append=self.ht,
                                     zenith=89, equalize=False, gcp=self.refX)
            self.data_list[0] = self.refX
            self.exifData.emit(self.ht, self.data_list)
            self.converter.start()
        else:
            print('empty img')

    def updateRef(self, X, Y):
        self.refX = X
        self.refY = Y

    def updateProgress(self, percent):
        if isinstance(percent, str):
            self.htName.setText(percent)
        else:
            # finished processing
            base = os.path.basename(self.imgShow.img_path)
            file, ext = os.path.splitext(base)
            #self.loadImg(f'converted_imgs/{file}_M{self.refX}{ext}')
            self.loadImg(f'converted_imgs/{file}_D{self.refX}{ext}')
            self.htName.setText(f"|{self.ht}m|:")
            self.convertBtn.setEnabled(False)


class Scroller(QScrollArea):

    def __init__(self):
        QScrollArea.__init__(self)

    def wheelEvent(self, ev):
        if ev.type() == QEvent.Wheel:
            ev.ignore()

class Converter(QThread):
    sigOut = pyqtSignal(object)

    def __init__(self, parent=None):
        super().__init__(parent)
        self.img_path = None
        self.mode = 'direct'
        self.append = 1.6
        self.zenith = 85
        self.equalize = False
        self.gcp = 0
```

```python
def set_param(self, img_path, append=1.6, zenith=85, equalize=False, gcp=0, mode='direct'):
    self.img_path = img_path
    self.append = append
    self.zenith = zenith
    self.equalize = equalize
    self.gcp = gcp
    self.mode = mode

def run(self):
    '''Document see mercator.py'''
    img = imageio.imread(self.img_path)
    h, w, d = img.shape
    self.sigOut.emit('[10%..]')

    if self.mode == 'mercator':
        if self.equalize:
            img = equalize_hist(img)
            self.sigOut.emit('[20%..]')

        h_id = np.arange(h)
        w_id = np.arange(w)
        self.sigOut.emit('[30%..]')

        angle_id = h/2 - h_id - 0.5
        angle = angle_id / angle_id.max() * 90 # degree
        self.sigOut.emit('[40%..]')

        select = abs(angle) <= self.zenith
        select_angle = angle[select]
        self.sigOut.emit('[45%..]')

        select_img = img[select, :, :]
        select_h, _, _ = select_img.shape  # (2538, 5376, 3)
        self.sigOut.emit('[50%..]')

        mecator_coord = h / 2 * np.log(np.tan(np.deg2rad(45 + select_angle / 2)))
        mecator_coord_zero = mecator_coord.max() - mecator_coord
        self.sigOut.emit('[55%..]')

        f = interp1d(mecator_coord_zero, np.arange(select_h), fill_value="extrapolate")
        self.sigOut.emit('[60%..]')
        xnew = np.arange(0, np.ceil(mecator_coord.max())*2, 1)
        mecator_id = f(xnew)  # related img_h id in raw image (85 degree selected)
        self.sigOut.emit('[65%..]')

        # table to refer mecator_id -> zenith angle
        f_angle = interp1d(mecator_coord_zero, select_angle, fill_value="extrapolate")
        mecator_angle = f_angle(xnew)
        self.sigOut.emit('[70%..]')

        ww, hh = np.meshgrid(w_id, mecator_id) # shape (8404, 5376)
        self.sigOut.emit('[75%..]')

        img_out = np.zeros((*hh.shape, 3))
        for i in range(0 ,3):
            img_out[:,:,i] = ndimage.map_coordinates(select_img[:,:,i],
                                                     np.array([hh,ww]),output=float,order=1)
            self.sigOut.emit(f'[{70 + 9*(i+1)}%..]')

        img_out = np.hstack((img_out[:,self.gcp:, :], img_out[:,0:self.gcp, :]))
        self.sigOut.emit('[98%..]')

        base = os.path.basename(self.img_path)
        file, ext = os.path.splitext(base)
        imageio.imwrite(f'converted_imgs/{file}_M{self.gcp}{ext}', img_out)

        self.m2a = mecator_angle

    else:
        self.sigOut.emit('[40%..]')
        img_out = img_out = np.hstack((img[:,self.gcp:, :], img[:,0:self.gcp, :]))
        self.sigOut.emit('[60%..]')
        base = os.path.basename(self.img_path)
        file, ext = os.path.splitext(base)
        self.sigOut.emit('[80%..]')
        imageio.imwrite(f'converted_imgs/{file}_D{self.gcp}{ext}', img_out)
        self.sigOut.emit('[99%..]')

    self.sigOut.emit(True)
```

```
class ImgShow(QWidget):
    mouseClicked = pyqtSignal(object, object)
    emitPoint = pyqtSignal(object, object)

    def __init__(self, parent=None):
        super().__init__(parent)
        self.x = 0
        self.y = 0
        self.w = self.frameGeometry().width()  # 100
        self.h = self.frameGeometry().height()  # 30

        self.corner = 'NE' # North East(default)
        self.vLock = -1

        self.img_path = None
        self.addImg = False
        self.isMoving = True
        self.leftPressed = False

        self.setMinimumSize(5376, 2000)

        self.tempPix = QPixmap(5376, 2000)

        self.pix = QPixmap(5376, 2000)
        self.pix.fill(Qt.white)

        self.saver = Saver(self)

        self.setMouseTracking(True)
        self.setCursor(Qt.BlankCursor)

        self.functionConnector()

    def functionConnector(self):
        pass

    def paintEvent(self, event):
        painter = QPainter(self)

        if self.addImg:
            imgPixmap = QPixmap.fromImage(QImage(self.img_path))

            imgH = imgPixmap.height()
            imgW = imgPixmap.width()

            self.pix = QPixmap(imgW, imgH)
            self.tempPix = QPixmap(imgW, imgH)
            self.resize(imgW, imgH)

            p = QPainter(self.pix)
            p.setPen(QColor(255, 255,0))
            p.drawPixmap(0, 0, imgPixmap)
            p.drawLine(0, imgH/2, imgW, imgH/2)
            self.addImg = False

        fm = QFontMetrics(QFont('SimSun', 10))
        pw = fm.width(f'{self.x},{self.y}')
        ph = fm.height()
        if self.corner == 'NE':
            text_x, text_y = self.x, self.y
            rect_x, rect_y = self.x-baf20, self.y-20
        elif self.corner == 'NW':
            text_x, text_y = self.x-pw, self.y
            rect_x, rect_y = self.x, self.y-20
        elif self.corner == 'SE':
            text_x, text_y = self.x, self.y+ph
            rect_x, rect_y = self.x-baf20, self.y-20
        else:
            text_x, text_y = self.x-pw, self.y+ph
            rect_x, rect_y = self.x-baf20, self.y-20

        if self.isMoving:
            # 把以前的pix 复制一遍(相当于清空)
            self.tempPix = self.pix.copy()

            qp = QPainter(self.tempPix)
            qp.setPen(QColor(255, 0,0))
            qp.setFont(QFont('SimSun', 10))

            qp.drawLine(self.x, 0, self.x, self.h)
            qp.drawLine(0, self.y, self.w, self.y)
            qp.drawText(text_x, text_y, f'{self.x},{self.y}')

            qp.drawRect(rect_x, rect_y, baf20, 20)

            painter.drawPixmap(0, 0, self.tempPix)
        else:
            qp = QPainter(self.pix)
            qp.setPen(QColor(255, 0,0))
            qp.setFont(QFont('SimSun', 10))

            qp.drawLine(self.x, self.y-20, self.x, self.y+20)
            qp.drawLine(self.x-20, self.y, self.x+20, self.y)
            qp.drawText(text_x, text_y, f'{self.x},{self.y}')

            painter.drawPixmap(0, 0, self.pix)

    def saveImg(self):
        if self.img_path is not None:
            self.saver.set_param(self.img_path, self.pix.toImage())
            self.saver.start()

    def mousePressEvent(self, event):
        if event.button() == Qt.LeftButton:
            self.leftPressed = True
            self.x = event.x()
            if self.vLock == -1:
                self.y = event.y()
            else:
                self.y = self.vLock
            self.mouseClicked.emit(self.x, self.y)

            self.w = self.frameGeometry().width()  # 100
            self.h = self.frameGeometry().height()  # 30
            self.isMoving=False
            self.update()

    def mouseMoveEvent(self,event):
        if not self.leftPressed:
            self.x = event.x()
            if self.vLock == -1:
                self.y = event.y()
            else:
                self.y = self.vLock
            self.w = self.frameGeometry().width()  # 100
            self.h = self.frameGeometry().height()  # 30
            self.update()

    def mouseReleaseEvent(self, event):
        if event.button() == Qt.LeftButton:
            self.leftPressed = False
            self.isMoving=True
            if window.addTree == -1:
                self.copy2Clipboard()
            else:
                self.emitPoint.emit(self.x, self.y)

    def changeDirection(self, event):
        if event.key() == Qt.Key_W:
            if 'S' in self.corner:
                self.corner = self.corner.replace('S', 'N')
        elif event.key() == Qt.Key_S:
            if 'N' in self.corner:
                self.corner = self.corner.replace('N', 'S')
        elif event.key() == Qt.Key_A:
            if 'E' in self.corner:
                self.corner = self.corner.replace('E', 'W')
        elif event.key() == Qt.Key_D:
            if 'W' in self.corner:
                self.corner = self.corner.replace('W', 'E')
        self.update()

    def changeVLock(self, value):
        self.vLock = value
        self.update()

    def copy2Clipboard(self):
        text = f'{self.x}\t{self.y}'
        self.cb = QApplication.clipboard()
        self.cb.clear(mode=self.cb.Clipboard)
        self.cb.setText(text, mode=self.cb.Clipboard)
```

```
class Saver(QThread):
    sigOut = pyqtSignal(object)

    def __init__(self, parent=None):
        super().__init__(parent)
        # https://stackoverflow.com/questions/46945997/creating-qpixmaps-in-a-thread
        # that *QPixmaps* cannot be created outside the main thread.
        # But it's pretty straightforward to instead use an image loader object,
        # move it to one or more background threads, in which it loads a QImage,
        # and then sends that to the main thread for later use
        self.qimage = QImage()
        self.img_path = 'result_imgs/rua.png'

    def set_param(self, img_path, qimage):
        self.img_path = img_path
        self.qimage = qimage

    def run(self):
        self.sigOut.emit('[20%..]')
        base = os.path.basename(self.img_path)
        self.sigOut.emit('[40%..]')
        file, ext = os.path.splitext(base)
        self.sigOut.emit('[60%..]')
        #self.pix.save(f"result_imgs/{file}_C{ext}", "PNG")
        self.qimage.save(f"result_imgs/{file}_C{ext}", "PNG")
        self.sigOut.emit('[Saved]')


if __name__ == '__main__':
    app = QApplication(sys.argv)
    window = MainWindow()
    window.showMaximized()
    sys.exit(app.exec_())
```

Curriculum Vitae

Candidate's full name: Haozhou WANG

Universities attended:

Nanjing Forestry University (2013-2017)

Bachelor of Science in Forestry

Articles published in or submitted to refereed journals:

Wang, H., D. Han, Y. Mu, L. Jiang, X. Yao, Y. Bai, Q. Lu, and F. Wang. 2019. Landscape-level vegetation classification and fractional woody and herbaceous vegetation cover estimation over the dryland ecosystems by unmanned aerial vehicle platform. Agricultural and Forest Meteorology 278:107665.

Wang, H., J. A. Kershaw, T.-R. Yang, Y.-H. Hsu, X. Ma, and Y. Chen. Under review. An Integrated System for Estimating Forest Basal Area from Spherical Images. Mathematical and Computational Forestry & Natural-Resource Sciences.

Dong, H., W. Haozhou, Z. Bangyou, and W. Feng. 2018. Vegetation type classification and fractional vegetation coverage estimation for an open elm (Ulmus pumila) woodland ecosystem during a growing season based on an unmanned aerial vehicle platform coupled with decision tree algorithms. Acta Ecologica Sinica 38.

Selected non-refereed contributions (posters, presentations):

WANG, H., and J. A. Kershaw. 2017. Extracting DBH Measurements from RGB Photo Images. Oral, The Northeastern Mensurationists Annual Meeting, New York, U.S.

WANG, H., and J. A. Kershaw. 2018. Measuring Plant Area Index (PAI) from panorama photo images. Oral, The 25th Annual UNB Graduate Research Conference (GRC), New Brunswick, Canada.

WANG, H., and J. A. Kershaw. 2019. Estimating Forest Attributes from Spherical Images. Oral, The 26th Annual UNB Graduate Research Conference (GRC), New Brunswick, Canada.

WANG, H., F. WANG, X. YAO, Y. MU, Y. BAI, and Q. LU. 2017. UAV-HiRAP: A novel method to improve landscape-level vegetation classification and coverage fraction estimation with unmanned aerial vehicle platform. Oral, The 12th International Congress of Ecological (INTECOL), Beijing, China.